Study of underlying mechanisms of NK cell impairment in B-CLL patients

By

MUSTAFA EMHEMED FARHAT

A thesis submitted to the University of Birmingham
for the degree of
DOCTOR OF PHILOSOPHY

Institute of Immunology and Immunotherapy
College of Medical and Dental Sciences
University of Birmingham
November 2021

Impact of COVID-19 statement

This work has been performed under difficult circumstances as the COVID-19 pandemic started during the third year of my PhD. The biggest disruption is the sample collection from the patients and healthy donors as well due to the situation of hospital and appointment being online which affected the level of work.

For scRNA seq experiment, we managed to perform the sequencing on 2 donors, which was planned to be done at least three donors. For ATAC seq, we only managed to do the ATAC seq with one patients high PD-1 NK to allow the comparison of PD-1pos and PD-1neg NK cells. In addition, CYTOF experiment, we would also like to perform it with more donors.

Due to the availability of the clinicians in the middle of pandemic, it was not possible to collect clinical data for further clinical correlation analysis.

ABSTRACT

Despite the potent role of NK cells in eliminating the tumor and leukemic cells, NK cells in B-CLL patients are dysfunctional and impaired, which contributes to the disease progression and B-CLL patients' mortality. NK cell impairment has been linked at least to the downregulation of activating receptors on NK cells in B-CLL patients. The first part of this study has investigated further the phenotype of NK cells and detailed functionality of NK cells from B-CLL patients. The data showed that the expression of checkpoint receptors on NK cells were significantly upregulated, including PD-1,CTLA-4, LAG-3 and CD96. Also, NK cells from B-CLL patients demonstrated reduced cytokine production and impaired DNAM-1 dependent NK cell cytotoxicity compared to age-matched healthy controls. In addition, TIGIT and/or CD96 blockades can robustly reverse the DNAM-1 dependent NK cytotoxicity against tumor cell lines. The second part of this study focused on PD-$1^{positive}$ NK cells. At first, scRNA-seq analysis revealed that PD-1^{pos} NK cells have differentiated transcription profile compared to PD-1^{neg} NK cells, which can be used to identify new potential therapeutic targets to reverse anti-tumor functions of PD-1^{pos} NK cells. Secondly, the functionality of PD-1pos NK cells was compared with PD-1neg NK cells using primary NK cells and NK cell line models. The function of PD-1^{pos} NK cells were significantly impaired compared to PD-1^{neg} counterparts, including lower expression of cytokine and cytotoxicity against tumor cell lines. Interestingly, blocking of PD-1/PD-1Ls interactions have partially reversed the anti-tumor activity of PD-1^{pos} NK cells. This study revealed for the first time that the checkpoint receptors expression on NK cells from B-CLL are upregulated and blocking PD-1 or TIGIT/CD96 receptors might be potential novel strategies for NK cell based immunotherapy for B-CLL patients.

ACKNOWLEDGEMENT S

I would firstly like to express my greatest thanks to my main supervisor, Dr Jianmin Zuo for his continuous support during challenging times, encouragement, guidance, study design and valuable knowledge to be a good scientist throughout my PhD journey. Also, I would like to thank my second supervisor Professor Paul Moss who has always given me a confidence and motivation and for giving me this valuable opportunity to join his group.

Special thanks to Dr Wayne Croft and David Bone for helping me with R analysis. I also would like to thank Dr Kriti Verma for her valuable advice and giving me excellent support in carrying out ATAC-seq experiments. I am also very grateful to Dr Francesca Kinsella and Dr Samantha Drennan for their great feedback and suggestions on my data analysis. In addition, I also would like to thank all the past and present members of the Moss group and friends, especially Jusnara Begum, Jimmy Van and Dr Guido Fermento for the useful discussion and overall helping, and of course to the guys who agreed to participate in this study as healthy donors.

My greatest gratitude extends to the Libyan Ministry of Higher Education for the financial support for this study. Last but not least, I am extremely grateful to my family, my wife, my children and parents for endless support and understanding all the time.

Thank you all

TABLE OF CONTENTS

TABLE OF FIGURES

LIST OF TABLES

CHAPTER 1: GENERAL INTRODUCTION

1.1 The immune system

The defense system of the human body is complex and has evolved to efficiently protect the host against wide range of invasive pathogenic microorganisms. The immune system is an integrated partnership of many organs, specialised cells, and soluble factors, which work collectively to defend the body from endogenous and exogenous threats (Georgountzou & Papadopoulos, 2017). All immune cells originate from the same progenitor cells in the bone marrow, where many of them mature and migrate to the circulation and lymphatic system. The immune cells are able to discriminate self (self-tolerance) from non-self, thereby only targeting invasive bodies and avoiding host's own cells, unless these undergo alterations as in cancer (Chaplin, 2010). The immune system is classically divided into two lines of defense, the innate immunity which is the first line and the adaptive immunity the second line of defense against non-self pathogens. Both parts of the immune system work together to achieve rapid and effective elimination of invading pathogens (**Figure 1.1**)

1.1.1 Innate Immunity

The innate immune system is the first line of defense against pathogens. It comprises of barrier surfaces and a broad and extending range of myeloid and lymphoid cell types including phagocytes, dendritic cells (DCs) and Natural Killer (NK) cells. The innate immune responses are not specific to a particular pathogen which adaptive immune responses are, they lack somatically recombined specific antigen receptors and conventional immunological memory. In turn, innate immune cells sense the host-environment and distinguish between self and non-

self through germ-line encoded pattern recognition receptors (PRR) such as toll-like receptors (TLRs) (Alberts et al., 2002).

The innate immune cells provide rapid responses within hours of first exposure to the pathogen, which are mediated through cell dependent phagocytosis and cytotoxicity or secreted factors such as cytokines and chemoattractants. In response to pathogen, innate immune cells secrete chemoattractants and inflammatory cytokines such as IL-8 (CXCL-8) and interleukin (IL)-12, tumor necrosis factor (TNF) that recruit other innate cells to the site of inflammation and provide activation signals to other innate and adaptive cells. Neutrophils are the first innate cells recruited to the site of inflammation followed by monocytes and DCs which interact with tissue-resident lymphoid cells such as NK cells (Gasteiger et al., 2017). As NK cells are the focus of this project, they are discussed in more details in the subsequent sections.

1.1.2 Adaptive Immunity

The development of adaptive immune response is initiated and facilitated by the actions of innate immunity and can take several days to take a place, thus it is critical when innate immunity fails to eliminate pathogens or transformed cells. The hallmark of adaptive response is antigen-dependence and antigen-specificity and is characterised by its ability to generate immunological memory which enables the immune system to respond more rapidly and effectively to the pathogen if re-encountered. The specificity and selective feature of adaptive immune response is acquired from the vast repertoire of receptors that are somatically generated during cell development (Marshall et al., 2018). When a naïve lymphocyte recognises foreign antigen for the first time, it proliferates and creates clones of specific lymphocytes to attack that particular antigen. Furthermore, adaptive immunity is further subdivided into humoral and cell-mediated immunity based on the type of the immune response

they provide (Weinmann, 2021). Cell-mediated immunity (CMI) is an immunological response that relies on the antigen-specific cytotoxic T cells against target cells, which release various cytokines following activation, but not antibodies. Cell-mediated immunity is very important in recognizing and destroying cancerous and tumor cells (Vesely et al., 2011). Instead, humoral immunity is triggered by B cells that produce antibodies which occurs in the blood and lymph nodes. The circulating antibodies are the main mechanism of the humoral immunity to offer immunity of the body against extracellular pathogens, therefore humoral immunity does not offer protection against the cancer and will not be studied here. (Tan & Coussens, 2007). However, the hyperactivity of B cells such as in autoimmune disorders and rheumatoid arthritis are associated with tumor incidences, particularly non-Hodgkin's lymphoma. (Bernatsky et al., 2006).

As the main focus of this study is NK cells, they will be discussed in more details below including phenotype, function, and their latest involvement in cancer immunotherapy.

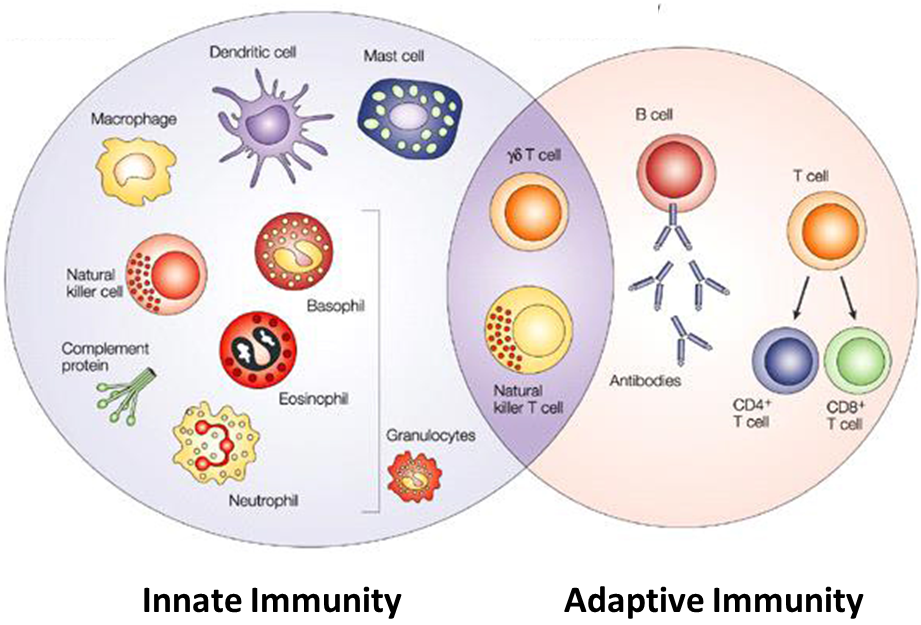

Figure 1.1 Innate and adaptive immunity.

The innate immune response is the first line of defense amounted against pathogens and provide a rapid response to these invasive pathogens through a variety of different cells, including granulocytes such as neutrophils, basophils and eosinophils, and natural killer cells, macrophages, mast cells and dendritic cells. Whilst adaptive immunity response develops slowly (within days from infection) but demonstrates increased antigenic specificity and memory. This slower process results from the combination of effector lymphocytes, including T cells ($CD4^+$ and $CD8^+$ T cells) and B cells. The overlap between innate and adaptive immunity involves the γδ T cells and more recently NK cells. Adapted and modified from (Dranoff, 2004).

1.2 Natural Killer cell overview

1.2.1 Natural killer cells development and differentiation

Natural Killer cells (NK cells) were first identified in the mid of 1970s, then recently were further classified as a type of lymphocyte that belong to the type 1 innate lymphoid cells (ILC1s), which have the ability to recognize and kill certain tumour cells and virally infected cells without pre-activation (Caligiuri, 2008). NK cells normally constitute about 5–15% of circulating lymphocytes and this proportion varies with the age (Yu et al., 2013). Like other lymphocyte lineages such as B and T cells, NK cells develop primarily in the bone marrow (BM) through different sequential stages, originating from $CD34^+$ hematopoietic stem cells (HSC) through common lymphoid progenitor (CLPs) cells. CLPs in turn give rise to innate lymphoid cells (ILCs) and other lineages such as pro-B and pre-T lineages. Interleukin-7 (IL-7) expression in Lin^- CD244 cells is considered mark of early step of CLP transition into lymphoid lineage. A subset of this early CLP transition defined as pre-NK cell precursors (Pre-NKPs) that express high IL-2 receptor β chain which further differentiate to become NKPs. NKP progress to immature NK population (iNK) that express activating receptor complex NKG2D and activating protein DAP-10. By this stage iNK population express lineage receptors of mature NK cells including NKG2A, DNAM-1, natural cytotoxicity receptors NCRs and adhesion molecules (Abel et al., 2018). Moreover, NK cells can also develop and differentiate in other multiple tissues including, lymph nodes, liver, uterus, and thymus (Geiger & Sun, 2016). In mice, the early stage of NK cell development and functional maturation is characterised by expression of IL-15 receptor (IL-15R) β chain (CD122) which is important step in NK cell differentiation. It has been shown that IL-15 selectively enhances NK differentiation, functional maturation, and survival (Rosmaraki et al., 2001). In response to IL-15, CLP differentiates into another population called NK cell precursors (NKP) that express CD122 and CD132 and lack other lineage markers (Lin^{neg}), including CD3, CD19 and CD14

(Fathman et al., 2011). NKPs further develop into immature NK cells (iNK) by losing CD127 and expressing NK1.1. Before leaving the BM, Mature NK cells (mNK) acquire CD43, CD11b, CD49b and Ly49 with functional specialization in cytotoxicity and IFN-γ production (Rosmaraki et al., 2001).

Mature NK cells are phenotypically defined by expressing CD56 and lacking the T cell receptor CD3 (Romee et al., 2013). NK cells are classified based on their cell surface expression of CD56 into $CD56^{dim}$ and $CD56^{bright}$, and further divided based on CD56 and CD16 density on the cell surface to another four NK subsets $CD56^{dim}$ $CD16^{pos}$, $CD56^{dim}$ $CD16^{neg}$, $CD56^{bright}$ $CD16^{pos}$ and $CD56^{bright}$ $CD16^{neg}$. NK cell subsets display functional differences in their cytotoxicity capacity, cytokine production and homing (Moretta et al., 2008). $CD56^{dim}$ NK subsets have high cytotoxic activity and comprise about 90% of total NK cells circulating in the blood and these subsets have low receptor affinity to constant region of immunoglobulin G, FC γ. Whilst, $CD56^{bright}$ NK subset consists approximately 10% of total NK cells in the peripheral blood but are dominant in the lymph nodes (LN). The function of $CD56^{bright}$ NK subsets are mostly involved in the production of cytokines. $CD56^{bright}$ NK subsets are known to be more proliferative than $CD56^{dim}$ subsets (Mandal & Viswanathan, 2015). Studies suggest that $CD56^{bright}$ NK cells are the immature NK cells they can further differentiate to become mature $CD56^{dim}$ NK cells (Wodnar-Filipowicz & Kalberer, 2006). Immature $CD56^{bright}$ NK cells can be characterised by the absent or low perforin and granzyme-B and acquire a distinct surface phenotype of $CD56^{bright}CD16^{neg}KIR^{neg}CD57^{neg}NKG2A^{pos}NCR^{neg}$. Over time this subset develops gradually to become more mature NK cells and acquire potent cytotoxicity by

expressing more lytic granules and can be characterized by $CD56^{dim}CD16^{pos}CD57^{pos}$ $NKG2A^{neg}KIR^{pos}NCR^{pos}$ phenotype (**Figure 1.2**) (Wodnar-Filipowicz & Kalberer, 2006).

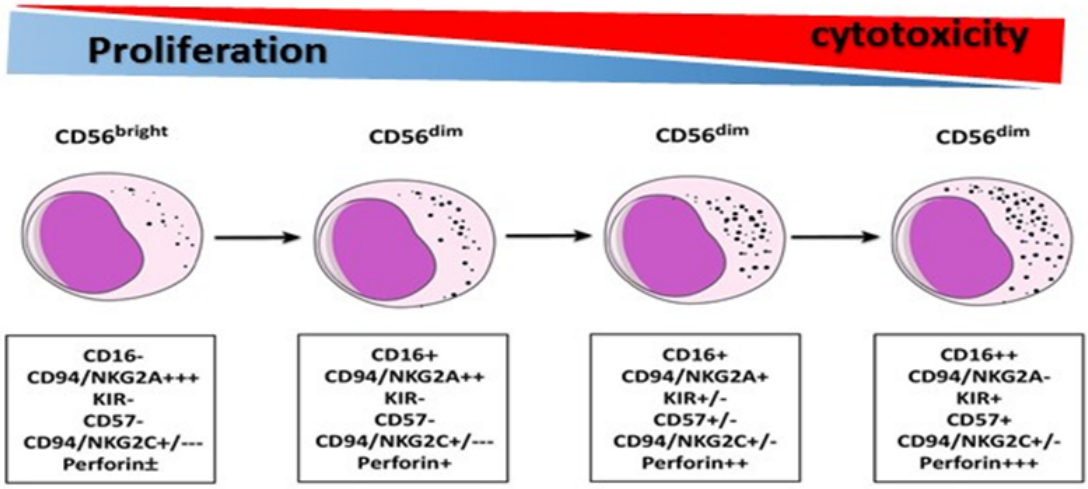

Figure 1.2 Schematic diagram of NK cells differentiation from CD56bright to CD56dim.

As $CD56^{bright}$ differentiate to $CD56^{dim}$, they gain mature phenotype and become more cytotoxic NK cells. adapted from Montaldo E., et al (2013)

1.2.2 NK cell receptors and target cell recognition

NK cells response is mediated through receptors expressed on their surfaces, which can be activating or inhibitory receptors. Unlike T and B cells, NK cells do not undergo gene rearrangement coding for antigen specific receptors, instead the activating and inhibitory receptors are germ line encoded (Carrillo-Bustamante et al., 2016). NK cells express variety of activating and inhibitory receptors including Natural Cytotoxic Receptors (NCRs), Such as NKp30, NKp44 and NKp46, NK group 2, member D (NKG2D), DNAX accessory molecule (DNAM-1/CD226), in addition to co-stimulatory molecules NKp80, CD244 and LFA-1. The Killer Inhibitory Receptors (KIRs) and NKG2A are the classic inhibitory receptors that specifically bind to Major Histocompatibility complex (MHC) class I molecules. KIRs and NKG2A function in context of cancer immunotherapy are being under investigation to restore antitumor activity of NK cells. The activation of NK cells and their cytotoxicity functions are regulated mainly by the balance between expression of activating and inhibitory receptors on their surface. NK cells recognise target cells by the alterations in the target cell phenotype, such as reduction in the expression of inhibitory ligands (MHC-I) or expression of activating ligands on their surface (Pegram et al., 2011).

NK cell receptors are clustered in to two groups based on the type of encoding gene, the immunoglobulin superfamily and natural killer complex (NKC) encoding C-type Lectin-like molecules. They have similar extracellular domains, so they might recognise the same ligands, but differ in intracellular domains, where inhibitory isoforms have long intracellular domains containing immunoreceptor tyrosine-based inhibitory motifs (ITIM), whereas activating isoforms have short cytoplasmic tails (Kelley et al., 2005).

1.2.2.1 NK cell activating receptors

NK cells express several activating receptors that initiate and transduce activating signals to the NK cells (**Table 1.2**). These receptors can recognise ligands expressed by tumour and virally infected cells in a non-MHC class-I restricted recognition manner, which means that triggering these receptors will overcome even the inhibitory signals induced by inhibitory receptors and MHC class-I binding, leading to NK cell activation (Barrow et al., 2019). Activating NK cell receptors include but are not limited to natural cytotoxicity receptors (NCRs), NKG2D, NK group 2 member C (NKG2C), DNAM-1/CD226, activating human killer immunoglobulin-like receptor (KIR).

Natural cytotoxicity receptors (NCRs) are type I transmembrane proteins and member of immunoglobulin superfamily that are almost exclusively expressed on NK cells and play a fundamental role in triggering their activation and regulate cytokine production (Moretta et al., 2001). NCRs have one or two extracellular domains that interact and bind to cellular and exogenously derived ligands, and short cytoplasmic domain that is associated with appropriate adaptor proteins via charged amino acid in their transmembrane domain. There are three NCRs, first discovered being expressed on human NK cells: NKp30, NKp46 and NKp44, which have similar expression density on NK cells and ability to trigger the killing of target cells (Terra Junior et al., 2016). NKp30 and NKp46 are constitutively expressed on resting and activated NK cells, while NKp44 expression is induced following the activation of NK cells, but their concerted action with other triggering receptors such as NKG2D, NKp80 and 2B4 induces a strong activation of NK cell-mediated cytolysis (Moretta et al., 2001). Some pathogen-associated ligands of NCRs have been identified, but most tumour-associated ligands for NCRs are still unknown (Memmer et al., 2016). NKp30 recognizes the B7-H6 and BAG6, which are

expressed on membrane of multiple tumour cells lines and trigger NK cell cytotoxicity, while galectin-3 released by many tumour cells is thought to be an inhibitory ligand for NKp30 (Rosental et al., 2011). So far, two activating tumour-associated ligands were reported for NKp44, the nuclear protein proliferating cell nuclear antigen (PCNA) and the isoform of mixed lineage of leukemia-5 (MLL-5), while no cellular ligands for NKp46 have been discovered yet (Parodi et al., 2019). NKp44 with the other NCRs play a crucial role in mediating NK killing of tumor and viral infected cells, therefore in context of tumor conditions the expression pattern of NCRs is altered on the immune cells including NK cells. The effect of NCRs expression on NK cells is thought to be induced by many factors including tumor microenvironment such as TGF-β that can induce NK cells to down regulate expression of activating receptors, and the direct effect of the tumor cells themselves (Huergo-Zapico et al., 2018).

NKG2D is another main surface activating receptor expressed on NK cells, and also on NKT and $CD8^+$ T cells. However, its activation signal slightly distinct from other activating receptors on NK cells, as its intracellular segment does not have signalling element. In addition, there are two forms of NKG2D, short isoform (NKG2D-S) and long isoform (NKG2D-L) that are created from different splicing. Both isoforms interact with the adapters transmembrane DAP10 or DAP12 to activate downstream intracellular signalling pathways inducing a series of NK cytotoxic responses when stimulated (H. Liu et al., 2019). NKG2D recognises and binds to the ligands including MHC class-I related chain molecules A and B (MIC-A and MIC-B), and UL16-binding proteins (ULBPs), that their expression can be induced in response to variety of cell stress such as viral infection, DNA damage and proinflammatory signals (Zafirova et al., 2011). Notably, NKG2D ligands are also expressed on many tumors and precancerous lesions, which thought to be induced by the effect of the oncogenic process itself. Importantly, expression of NKG2D ligands on the tumor cells render them more susceptible to $NKG2D^+$ lymphocytes including NK cells. This play a crucial role in NK immune surveillance,

elimination of tumor cells and disease progress (Chitadze et al., 2013). However, in many tumors particularly in B-CLL disease, shedding NKG2D ligands from the surface of tumor cells (soluble NKG2D ligands) counteracts the immune surveillance mediated by $NKG2D^+$ NK cells and T cells. This can in turn reduce their effector function by down-regulation of NKG2D expression. Moreover, low expression of NKG2D ligands on the tumor cells render them less susceptible to be eliminated by NK cells. Soluble NKG2D ligands can be found in the sera of tumor patients such as in Multiple myeloma (MM), and is associated with metastasis, advanced disease and poor prognosis (Nückel et al., 2010; Rebmann et al., 2007).

NK cell function is also controlled by another activating receptor DNAM-1 (CD226), which is important in controlling NK cell cytotoxicity and IFN-γ production. DNAM-1 recognises a wide range of cancer target cells through its well know ligands the poliovirus receptor (PVR) CD155 and Nectin-2 CD112 (Fuchs & Colonna, 2006). DNAM-1 receptor is indispensable to NK cell dependent antitumor activity, and other pathological conditions such as infection and autoimmunity disease (de Andrade et al., 2014). DNAM-1 receptor consists of two extracellular domains (Ig like domains) with another transmembrane and cytoplasmic domain, that contains three phosphorylation sites. DNAM-1 binds less efficiently to CD112 than CD155, which is suggested due to the homophilic interaction of CD112 (Tahara-Hanaoka et al., 2004). Like most activating receptors on NK cells, DNAM-1 signalling cascade starts upon engagement with its ligands on the target cells, ITAM motifs are phosphorylated by Src kinases and then recruit other tyrosine kinases such as Syk and ZAP-70 which in turn transmit downstream signalling of Vav and PLC-γ leading to activation of PI3K and mitogen kinase signalling pathways. Ligation of DNAM-1 with its ligands is essential for NK dependent anti-tumor immunity and susceptibility of tumor and viral infected cells to NK cell killing (Cifaldi et al., 2019).

In particularly, DNAM-1 dependent NK cell function is counterbalanced by two inhibitory receptors, CD96 and TIGIT that belong to the same family of immunoglobulin-like receptor of DNAM-1. In contrast to DNAM-1, CD96 and TIGIT compete with DNAM-1 for binding to the same ligands, which can reduce NK cell activation (**Figure 1.3**). CD96 particularly binds to CD155, whilst TIGIT binds to both CD155 and CD112 ligands with more affinity, therefore the expression and ability of CD96 and TIGIT receptors to compete with DNAM-1 for binding to cognate ligands are crucial for determining the outcome of NK cells in mediating anti-tumor and anti-viral responses (Georgiev et al., 2018; Q. Zhang et al., 2018).

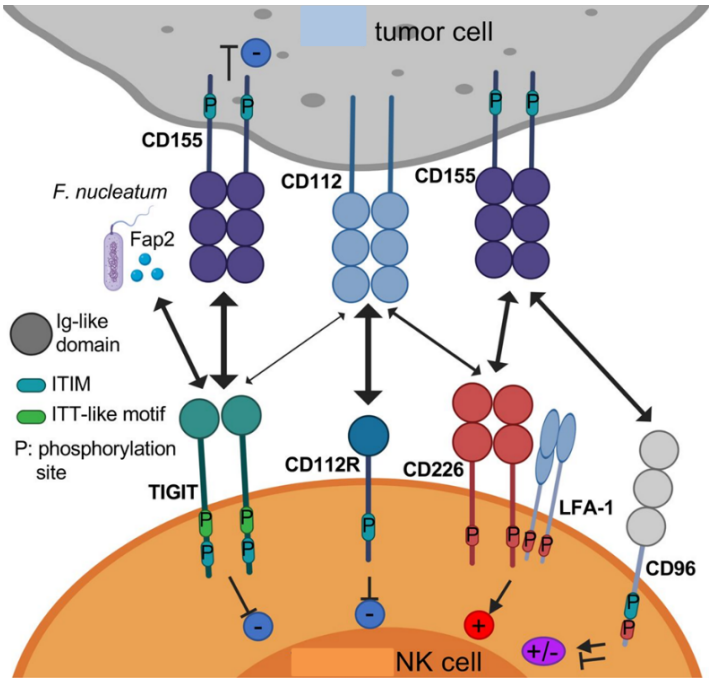

Figure 1.3 DNAM-1/TIGIT/CD96 axis on activated NK cells.

DNAM-1 is expressed on NK cells and bind to CD155 to deliver an activating signal to NK cell. TIGIT and CD96 are expressed on activated NK cells as well and they compete with DNAM-1 to bind to CD155 counterpart DNAM-1 function by delivering inhibitory signals through ITIM and ITT like motif on their cytoplasmic tails shifting NK cell to inhibitory function. TIGIT followed by CD96 has higher affinity to bind to CD155 ligand on the target cells. Adapted from (Chauvin & Zarour, 2020).

1.2.2.2 Inhibitory receptors

In NK cells, inhibitory receptors including inhibitory KIRs (iKIRs) and CD94/NKG2A are primarily involved in regulating NK cell function and protecting healthy cells from NK cell-mediated damage (Kumar, 2018). iKIRs are a member of immunoglobulin superfamily expressed on NK cells and some subsets of T cells. Each KIR consists of two (KIR2D) or three (KIR3D) extracellular Ig-domains. These domains are encoded by different regions of KIR genes located on chromosome 19q13.4. The membrane distal domain (D0) is encoded by exon 3, middle membrane (D1) is encoded by exon 4, while (D2) by exon 5 (Kusnierczyk, 2013). Most KIR molecules have inhibitory function through long (L) cytoplasmic tails (KIR2DL and KIR3DL) possessing immunoreceptor tyrosine-based inhibitory motifs (ITIM). Moreover, these receptors have a potential activating function through short (S) cytoplasmic tails (KIR2DS and KIR3DS) that lack a signalling motifs, instead they exert their activating function by connecting with adapter molecule, DAP12 homodimer with an immunoreceptor tyrosine-based activating motifs (ITAM) (Long, 2008).

In human, iKIRs regulate NK cell activity predominantly by recognizing and binding to MHC class I molecules (HLA-A, HLA-B, HLA-C and HLA-E). KIRs recognise the amino acid-binding groove of HLA molecules, therefore each KIR binds to different HLA molecule. For example, KIR2DL1, KIR2DL2 and KIR2DL3 receptors recognize all HLA-C allotypes such as HLA-Cw1, HLA-Cw2 and HLA-Cw3, whereas KIR3DL1 and KIR3DL2 bind HLA-B and HLA-A alleles (Thielens et al., 2012).

CD94/NK group 2 member A (NKG2A) inhibitory receptor, which belongs to C-type Lectin superfamily (Ly49) have the similar regulatory mechanism as KIRs (Petrie et al., 2008). NKG2A is considered to be one of the major inhibitory receptors expressed on NK cells, that

binds to the non-classical MLA- class I (HLA-E) molecule on the candidate target cells (**Table 1.1**). Once binding to its cognitive ligand, NKG2A transduces strong inhibitory signals through (ITIM) to suppress NK cytotoxicity and cytokines production (Kamiya et al., n.d.). Ligation of KIRs and NKG2A with their ligands are important in sparing healthy cells from being attacked, which results in a transient suppression of NK activation but not anergy or apoptosis of NK cells, termed with 'dominant inhibition' to keep healthy cells safe (Long, 1999). However, in context of cancer and viral infection diseases, increased expression of NKG2A on NK cells contributes to NK cell exhaustion and dysfunctional, which reduces the ability of NK cells to clear virally infected cells and decreases their cytotoxicity against tumor cells in human and mouse models (F. Li et al., 2013; C. Sun et al., 2016).

Table 1.1 Human NK cell activating and inhibitory receptors and their ligands

Type	Receptor	Ligand
Activating	NKG2D	MIC-A/B, ULBP1-4
	CD94-NKG2C	HLA-E
	DNAM-1	CD155, CD112
	KIR2DL4	HLA-G
	KIR2DS1	HLA-C2
	KIR2DS2	HLA-C1
	KIR2DS3	Unknown
	KIR2DS4	HLA-A11
	KIR2DS5	Unknown
	KIR3DS1	HLA-Bw4
	NKp30	BAT3, B7H6, pp65 of HCMV
	NKp44	Viral HA and HN, PCNA
	NKp46	Viral HA and HN
Inhibitory	KIR2DL1	HLA-C2
	KIR2DL2	HLA-C1
	KIR2DL3	HLAC1
	KIR3DL1	HLA-Bw4
	KIR3DL2	HLA-A3, HLA-A11
	CD94/NKG2A	HLA-E
	CD85 (ILT2)	HLA-A,B,C, HLA-G1
	CD244 (2B4)	CD48

Adapted from (Paul & Lal, 2017)

1.2.2.3 Immune checkpoint receptors

Immune checkpoint molecules or co-inhibitory receptors are expressed on the activated immune cells and have a critical role in the maintenance of immune homeostasis and tolerance to self-antigens. In addition, checkpoint receptors modulate the size and magnitude of immune response (J. Li et al., 2017). However, this inhibitory mechanism is exploited by cancer cells to protect themselves from eradication by the immune system (Vinay et al., 2015). The number of immune checkpoints is steadily increasing and most of these receptors are expressed on the adaptive immune cells, in particularly activated T cells. Increased expression of checkpoint receptors such as but not limited to programmed cell death-1 (PD-1), cytotoxic T lymphocyte-

associated antigen-4 (CTLA-4), lymphocyte activation gene-3 (LAG-3), T cell immunoglobulin-and mucin-domain 3 (TIM-3) and T cell immunoreceptor with Ig and ITIM domains (TIGIT) has been found to largely decrease T cell functions and lead to exhausted immune cells (Beldi-Ferchiou & Caillat-Zucman, 2017). Their expression and functional consequences on NK cells are much less explored. Targeting immune checkpoints with specific blocking antibodies has been very successful in clinical setting for a number of cancers, which aim to reverse the immune cells exhaustion and recover their function capacity (Wolchok et al., 2017). Here, I am going to give a brief overview on the best known immune checkpoints in terms of their expression and function in cancer settings.

Programmed cell Death-1 (PD-1), inhibitory receptor belongs to a type I membrane protein and is a member of CD28/CTLA-4 family. Upon binding to its ligands PD-L1 (B7-H1; CD274) or PD-L2 (B7-DC; CD273) can transmit a potent inhibitory signal to many immune cells including NK cells. PD-L1 is very broadly expressed on different immune cells and non-immune cells and has a higher affinity to PD-1 compared to PD-L2, which expressed in a restricted pattern to antigen presenting cells (APCs) including monocytes, macrophages dendritic cells (Quatrini et al., 2020). PD-1 signal transduction starts when binding to its ligands and phosphorylation of a tyrosine residue in the immunoreceptor tyrosine-based switch motif (ITSM) of PD-1, which leads to a recruitment of SH-2-domain containing tyrosine phosphate 2 (SHP-2) to the cytoplasmic domain of PD-1 (**Figure 1.4**). This in turn down-regulates CD28 mediated PI3K activity leading to less activation of Akt (R. V. Parry et al., 2005). PD-1 expression is well established on many immune cells such as T cells, NK cells, B cells, macrophages, and subsets of DCs. PD-1 expression and function in T cells have been well studied in physiological and pathological contexts, whilst the knowledge of the role of PD-1 on NK cells and the rest of immune cells is still limited. PD-1 expression is up-regulated on activated T cells, and its inhibitory signalling counterpart the activating signalling mediated

through TCR. In addition, the level of PD-1 expression is associated with the strength of TCR signalling (Pauken et al., 2020). In cancer context, PD-1/PD-L1 pathway has an inhibitory role of NK and T cells function, when they bind to cancer cell expressing PD-L1 or/and PD-L2. PD-1 signalling negatively regulate cytokine production and expression of transcription factors such as IFN-γ, TNF-α, IL-2, and Tbet, Eomes respectively. PD-1 can also reduce T cell proliferation, differentiation, and survival (Latchman et al., 2001; Y. Liu et al., 2017). In contrast, blockade of PD-1 or PD-L1 using MoAbs can significantly reverse the function of exhausted T cells and markedly enhance cytokine production, degranulation and reduce the apoptosis of NK cells in many tumor types (Judge, Murphy, et al., 2020; Quatrini et al., 2020). However, PD-1 expression and its consequences on NK cell function on B-CLL patients is still unknown.

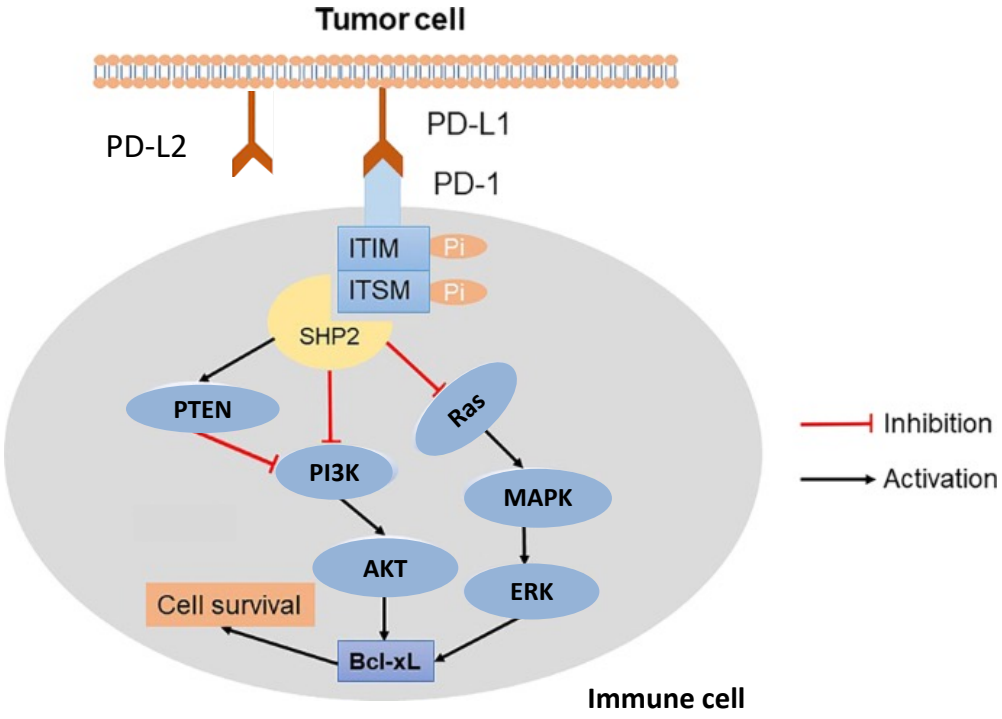

Figure 1.4 Programmed cell death (PD-1) signalling pathway

Major signalling pathways of PD-1 receptor in the immune cells. Interaction of PD-1 expressed on immune cells with its ligands (PDL1 and PDL2) that up-regulated on the target cells, promotes inhibition of both innate and adaptive immune response. Upon interaction of PD-1/PDLs, the tyrosine residues in both ITIM and ITSM domines of PD-1 become phosphorylated and recruit SHP2 which is a key step for modulating the downstream molecular pathways. SHP2 can block activation of PI3K and Ras, that in turn suppress signals of MAP kinase pathways. These inhibitory signals together modulate metabolic programming and dampen cell proliferation, differentiation, and survival. Adapted and modified from Wu., et al 2020.

Cytotoxic T-lymphocyte-associated antigen 4 (CTLA-4) also known as CD152 is another main co-inhibitor molecule that belongs to immunoglobulin (Ig) family, is normally expressed on activated T cells and functions as a negative regulator of their activation (Rudd et al., 2009). CTLA-4 expression is largely expressed as intracellular molecular, in addition to cell surface on T cells. CTLA-4 exerts its inhibitory function by competitively binding to B7 ligands B7-1 (CD80) and B7-2 (CD86) expressed on antigen presenting cells (APCs) with CD28 co-stimulatory molecule. Previous studies by Chiossone et al and Terme et al have demonstrated that CTLA-4 transcripts were detected in mouse NK cells using whole-genome microarray analysis (Stojanovic et al., 2014). Same study showed that IL-2 activated mouse NK cells express both CD28 and CTLA-4, where CTLA-4 inhibits IFN-γ production, while CD28 induces NK cell activation and proliferation. This indicates that CTLA-4 might also be expressed on human NK cells. Co-expression of these receptors in mouse models have been detected in tumour infiltrating NK cells which indicates their involvement in NK cell mediated antitumor responses (Stojanovic et al., 2014).

T cell immunoglobulin-and mucin-domain 3 (Tim-3) is one member of TIM gene family, which includes Tim-1, Tim-3, and Tim-4 in humans. The most recent ligand identified for Tim-3 is Ceacam-1 in addition to galectin-9 and both are thought to have inhibitory function after binding to Tim-3. Tim-3 is expressed on the most suppressed or dysfunctional populations of $CD4^+$ and $CD8^+$ T cells in both solid and haematological malignancies (Das et al., 2017). Tim-3 expressing $CD4^+$ and $CD8^+$ T cells produce lower amounts of cytokines and are less proliferative than Tim-3 negative T cells when stimulated with specific antigen such as in chronic virus infection (Golden-Mason et al., 2009). In cancer and virally infected cells, the overexpression of Tim3 is related to inhibition in the immune response. Tim3 expression has been identified on NK cells from patients with metastatic melanoma, and its upregulation is

correlated with the progression of melanoma and poor prognosis (da Silva et al., 2014). In contrast, NK cells with high Tim3 levels attributed to the most cytotoxic cells with highest production of IFN-g. Overall, study concluded that Tim-3 expression is not solely marker for NK cell activation but also limit the duration and magnitude of response and prevent NK cell over activation.

Lymphocyte activation gene-3 (LAG-3) first identified on activated T cells and a subset of NK cells, binds with high affinity to MHC class II. In addition, another LAG-3 ligand has been suggested to be LSECtin (Liver Sinusoidal Endothelial Lectin) which is expressed on many tumour cells, providing a potential regulatory mechanism of LAG-3 expressing $CD8^+$ T cells and NK cells (Anderson et al., 2016). In addition, LAG-3 expression is shown to inhibit the effector $CD4^+$ T cell cytotoxicity and promote the suppression role of Treg cells and has an impact on the function of $CD8^+$ T cells and NK cells. In murine cancer models, co-expression of LAG-3 and PD-1 has been documented on $CD4^+$ and $CD8^+$ in infiltrating lymphocytes (TILs), and co-blockade of LAG-3 and PD-1 pathways has been shown to improve the cytotoxicity of $CD8^+$. In human follicular lymphoma and murine ovarian cancer, co-expression of LAG-3 and PD-1 has also been identified on exhausted $CD8^+$ T cells, and co-blockade of LAG-3 and PD-1has improved cytokine production and proliferation of $CD8^+$ T cells (Huang et al., 2015; Yang et al., 2017).

As mentioned previously (section 1.1.3.2.1), It has been shown that NK cells can be regulated by another checkpoint receptor named T-cell immunoglobulin and ITIM domain (TIGIT), which is also expressed on T cells and Treg cells. TIGIT has an immunoglobulin tail tyrosine (ITT) like phosphorylation motif and ITIM. TIGIT receptor competes with activating DNAM-

1 receptor to bind to its physical ligand CD155 (PVR), which is expressed mainly on the target cells. But, TIGIT has higher affinity than DNAM-1 to bind to CD155. The interaction of TIGIT/CD155 leads to inhibition of activation and function of effector T cells and on another hand enhance the suppressive function of Tregs (F. Wang et al., 2015). Recently, it has been shown that TIGIT activation can reduce the cytokines production and cytotoxicity of both human and mouse NK cells (Luo et al., 2018). The inhibitory intracellular signalling of TIGIT starts by recruiting Grb2 and SHIP1 to bind to ITT like motif to initiate negative signalling that suppresses the granule polarisation and cytotoxicity of NK cells (M. Li et al., 2014). TIGIT expression on NK cells varies between healthy individuals and its expression is associated with the functional heterogeneity of NK cells in different individuals. NK cells with low TIGIT expression have stronger cytokines, degranulation, and potential cytotoxicity than NK cells comparing with high levels TIGIT expression. This explains the different capacity of NK cell function and susceptibility to infection and cancer (F. Wang et al., 2015). TIGIT has several mechanisms in mediating an inhibitory signals to T and NK cells. TIGIT acts through extrinsic or intrinsic manner as a ligand for CD155 by either interfering with DNAM-1 or directly mediating inhibitory signals to the effector immune cells (Harjunpää & Guillerey, 2020). In cancer context, TIGIT is considered to be an immune checkpoint that inhibits immune cell responses against tumor cells. T cell priming by dendritic cells (DCs) is inhibited by TIGIT and also TIGIT can mediate tumor killing escape by NK cells. TIGIT expression has been reported to be increased on T cells and NK cells in addition to Tregs in many cancer types including multiple myeloma (MM), melanoma, acute myeloid leukaemia and breast cancer (Chauvin et al., 2015; Guillerey et al., 2015, 2018). Therefore, TIGIT may become a major target in cancer immunotherapy to restore the anti-tumor cell response.

In addition, CD96 which is a novel immune checkpoint receptor belongs to the same superfamily of immunoglobulin (Ig) that TIGIT and DNAM-1 belong. CD96 shares the same ligands with TIGIT and DNAM-1 from target cells. CD96 and TIGIT act as co-inhibitory receptors whilst DNAM-1 as co-stimulatory receptors. However, CD96 and TIGIT have higher affinity to bind to CD155 (F. Liu et al., 2020). CD96 is expressed on a proportion of T cells during late activation, NK cells and Tregs. Study (Fuchs et al., 2004) reported that CD96 promotes NK cell-target cell adhesion whilst inhibits cytokines production by NK cells through competing with DNAM-1 interaction with CD155. Also, mice lacking CD96 expression ($CD96^{-/-}$ mice) induced increase in NK cell mediated control of metastasis, which is due to enhanced interaction of DNAM-1/CD155 (Mittal et al., 2019). DNAM-1/TIGIT/CD96 pathway has been elucidated in many reviews, discussing the important role of these dual receptors in many cancer types. TIGIT and CD96 can suppress the anti-tumor immune responses by dampening the co-stimulatory signal of DNAM-1. **Figure 1.5** summarises the inhibitory and checkpoint receptors expressed on NK cells and their respective ligands on the target cells.

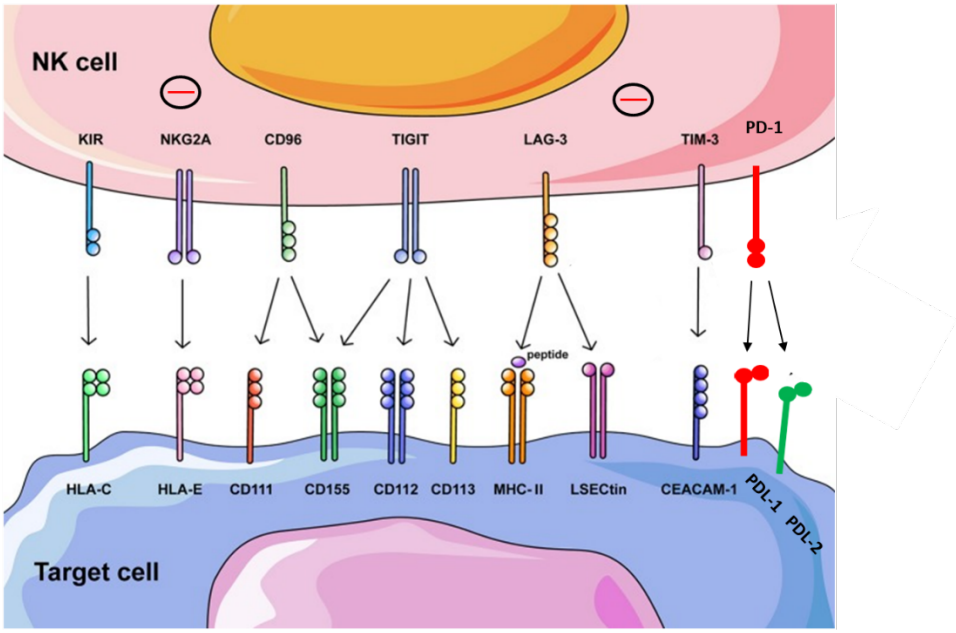

Figure 1.5 Inhibitory and checkpoint receptors expression on NK cells and their respective ligands on the target/cancer cells.

Detection and elimination of tumor cells by NK cells are regulated by engagement of activating and inhibitory receptors on NK cells with their respective ligands on tumor cells. Thus, increased expression of inhibitory ligands on tumor cells induces changes in expression of inhibitory receptors on NK cells which increase negative regulation resulting in functionally exhausted NK cells. The figure was adapted and modified from (H. Sun & Sun, 2019).

1.2.2.4 NK cell adhesion molecules (CAMs)

Adhesion molecules are generally classified based on the structural into five groups: Integrins, Selectins, cadherins, immunoglobulin superfamily (IgSF), and conventional adhesion molecules such as vascular adhesion molecules-1 (VAP-1). However apart from structural differences, we will discuss them below based on the function and binding ligands. As integrins typically bind to extracellular matrix, while selectins, IgSF and cadherins are associated with cell to cell contact.

1.2.2.4.1 Integrins

NK cells can be defined by surface receptors including integrins. The differential expression of integrins indicates the environmental adaption, development, and functional processes. Integrins mediate communications of cell to extracellular matrix (ECM) and cell to cell contact. Multiple ECM ligands for integrins have been identified including different isoforms of fibronectin, collagen, selectins, and cell adhesion molecules (CAMs). Integrins form island of nanometer-scale signalling 'nano adhesion' that can be defined as clusters of integrins, adaptors, scaffolds, kinases, phosphatases, and actin linkers. Nano-adhesions form the functional unit on lymphocytes to fulfil cell migration and behaviour, and they have short lifespan due to fast cell migration and adhesion turnover (Humphries et al., 2006).

Integrins in immunology are often described as single subunits which are heterodimers composed of α and β subunit. To date, there are 18 known integrins of α and β subunits that can differentially pair to form 24 heterodimer integrins (Shannon & Mace, 2021). Integrins follow three affinity models: low affinity bent closed confirmation, an intermediate affinity

extended closed confirmation, and high affinity extended open confirmation which is thought to be formed only after extracellular receptor interaction. αLβ2 (CD11a/CD18, LFA-1) heterodimer adopt both bent and extended confirmation up on binding to ICAM-1ligand. The majority of cytoplasmic β integrin tails are 40 -70 residual long and their structure depends on what intermediate they bind which form helices or pack close to the membrane (Moore et al., 2018).

Integrin β subunits have been used to classify and identify the integrin functions on NK cells, **Table 1.2** lists common β integrins and their known ligands and functions on NK cells. The β1 subunit can bind to 12 α subunits generating heterodimers that bind to collagen, laminin, fibronectin, and VCAM-1. In general, β1 heterodimers are often associated with tissue homing as they serve as a " bar code" for cells in various tissue niches. β1 heterodimers function as cell adhesion as well as transmigration during tissue entry and exit (K. Zhang & Chen, 2012). Although β1 integrins are not specific to leukocytes, they are abundantly expressed on lymphocytes, and play a key role in tissue microenvironment migration. In particular, α1β1, α2β1, α4β1, and α5β1 are critical components of tissue resident signatures that are commonly expressed on NK cells (Shannon & Mace, 2021).

More importantly, the β2 subunit, which is specific for leukocytes generates heterodimers with 4 α subunits (αL, αM, αX, and αD), each of them binds to ICAM-1 and fibrinogen. The function of β2 integrins is to mediate leukocyte recruitment from peripheral blood to tissues. In addition, they mediate target cell killing, particularly αLβ2 integrins (LFA-1), which can initiate cell polarisation through actin remodelling during development of an immunological

synapse (IS) between NK cells and target cells (Mace et al., 2009). Other integrins such as αDβ2 (CD11d/CD18) and αMβ2 (CD11b/CD18,Mac-1) are important for NK cell movement and residency. Overall, β2 integrins are involved in the ability of cells to move and communicate, and they are mainly related to tissue recruitment rather than residency.

Integrins are not always active and able to bind to their ligands, instead their activity is regulated through a mechanism known as inside-out signalling within the cell. Through this process, cell signalling induced by other cell surface receptors such as chemokine receptors, Toll-like receptors (TLRs), and selectins, trigger integrin activation in the immune cells Eventually, in response to inside-out signalling, integrin activation is achieved by interaction of cytoplasmic factors with integrin β-chin cytoplasmic proteins (Rose et al., 2003). The most well-known integrin activator is Talin, which binds to the membrane of proximal NPXY motif in the integrin β-chain cytoplasmic domain. This process leads to destabilises transmembrane connection between the α and β chain of the integrins and facilitate integrin activation (Harjunpää et al., 2019).

Downregulation of adhesion molecules van be found in patients with leukocyte adhesion deficiency type I (LAD-I) who either have missing or diminished expression of β-2 integrins on their leukocytes, and these patients are prone to recurrent infections. Whilst, in leukocyte adhesion deficiency type III (LAD-III) the integrins are expressed at normal level but dysfunctional due to kindlin-3 mutation or completely absent (Etzioni, 2009). This indicates that β-2 integrins are important components for immunity.

Table 1.2 Integrins on NK cells, their function and known ligands

Alpha/beta name	Alternative name	Ligand	Migration type	Activity level
β1; CD29				
α1; CD49a	VLA-1	Collagen IV (high affinity)	ECM residency	trNKs with baseline activation
α2; CD49b	VLA-2	Collagen IV, III and I (low affinity)	Migration from circulation to tissue	cNK/trNK switchable
α3; CD49c	VLA-3	Collagen, laminin, fibrinogen	Blood and ECM adhesion	cNK cells
α4; CD49d	VLA-4	Collagen, laminin, VCAM-1, Fibrinogen	Blood and ECM adhesion	cNK cells
α5; CD49e	VLA-5	Fibrinogen, ADAM	Blood and ECM adhesion	cNK cells
α6; CD49f	VLA-6	Laminin, ADAM	Blood and ECM adhesion	cNK cells
αv; CD51		Fibrinogen (RGD), vitronectin	Blood and ECM adhesion	cNK cells
α10;		Collagen, Laminin	Blood and ECM adhesion	cNK cells
α11;		Collagen, Laminin	Blood and ECM adhesion	cNK cells
β2; CD18				
αL	LFA-1	ICAM-1,2,3,4	Fast cell migration within blood and LN	cNKs, migration in lymph nodes, synapse formation
αM	Mac-1	ICAM-1,4. Fibrinogen	Cell migration	cNKs, migration in lymph nodes, synapse formation
αD		ICAM-3, fibrinogen, vitronectin	Cell migration	cNKs, migration in lymph nodes, synapse formation
αX	CR4		Cell migration	cNKs, migration in lymph nodes, synapse formation

***trNK** are tissue residence NK cells, **cNK** cells are conventional NK cells present in the peripheral blood. Adapted from (Shannon & Mace, 2021).

1.2.2.4.2 Selectins

Selectins are further classified based on the cell type that they bind, into P-selectin (platelets), E-selectin (endothelial cells), and L-selectin (leukocytes). Selectins have different kinetic expression upon cell activation, as P-selectins are expressed shortly within minutes of activation whilst E-selectins are expressed within hours. Selectins play a crucial role in leukocyte trafficking, lymphocyte migration through peripheral, lymph nodes and to the skin. The most important function of selectins is initiating the first step of the rolling cell adhesion cascade in which selectins binding induce cell to roll (McEver & Zhu, 2010). Moreover, selectin binding in combination with chemokine receptor activation triggers the subsequent integrin-dependent step of inside-out signalling that leads to integrin activation and slow cell rolling and cell arrest. In brief, selectin interaction with its ligand leads to rolling of NK cells endothelial cells which in turn activates the chemokine receptor by endothelial cells. This step leads to activation of integrins on the surface of NK cells, allowing to NK cells to spread or transcellular extravasation and migrate into lymph nodes or tissues (Harjunpaa et al., 2019). Several selectin ligands have been identified, such as P-selectin glycoprotein ligand 1(PSGL-1) which is considered the main ligand for all three different selectins, mucosal addressin cell adhesion molecule -1 (MAdCAM-1), and peripheral node addressin (PNAd) (Perez-Vilar & Hill, 1999). Over expression of mucins, particularly (MUC-1) have been reported in many tumors and is thought to promote cancer cell growth and survival.

Cadherins are involved mainly in cell to cell adhesion in solid tissues, which is calcium dependent cell to cell adhesion. Cadherins play essential roles in tissue morphogenesis and homeostasis by controlling both cell to cell adhesion and cell signalling. Conventional cadherins are primarily responsible for translating intercellular contact signals which is

important in cellular organisation. This process in mediated mainly by membrane undercoat proteins that link the cytoplasmic tail of cadherins.

1.2.2.4.3 Expression of adhesion molecules on immune cells in tumors

T cells particularly $CD8^+$ T cells and NK cells are important components in recognizing and killing tumor cells. Therefore, they have been shown to be crucial in protecting the host from cancer. In different human malignancies the increase in infiltrated $CD8^+$ T cells in the tumor microenvironment has been correlated to the better prognosis. Indeed, CD8+ T cells and NK cells must come in to contact with the malignant cells in order to mediate tumor cell killing. T and NK cells, however frequently fail to enter the tumor tissue, posing a significant obstacle for successful immunotherapy of cancer patients (Melero et al., 2014). T cells homing to healthy and infected tissues are well recognised, however this pathway may be changed in cancer. In mouse models, T cell infiltration into tumors is influenced by the expression level of both integrin ligands on the tumor cells and integrin molecules on T cells, for example ICAM-1 deficiency or blockade substantially decreases CD8+ T cell infiltration into melanoma or colon carcinoma tumors. On the other hand, T cell mediated immunosurveillance is better in the presence of tumor cells expressing ICAM-1 compared to ICAM-1 deficiency mice (Fisher et al., 2011; Sartor et al., 1995).

In human, high expression of integrin ligands including ICAM-1, VCAM-1, and MAdCAM-1 has been linked to a high lymphocytes infiltration in colorectal cancer (CRC), and in human hepatocellular carcinoma (HCC) tumors, as well as a longer disease-free survival. At the same time, higher proportions of tumor infiltrating T cells in both tumor types expressed LFA-1 and VLA-4 compared to peripheral T cells (Mlecnik et al., 2010). Therefore, integrins and their

ligands may influence T and NK cell priming and effector functions, in addition to cell recruitment into tumors which increase anti-tumor immune response.

1.2.3 NK cell function

As mentioned earlier, NK cells have inherent ability to recognise and specifically eradicate transformed and virally infected cells. The key effector functions of NK cells are cytokines secretion and cytolytic granule-mediated cell lysis (Wodnar-Filipowicz & Kalberer, 2006). Upon recognition of infected or neoplastic cells, NK cells are able mediate instant killing to appropriate target cells by releasing cytotoxic granules containing perforin and granzymes and secreting inflammatory cytokines and chemokines (Fauriat et al., 2010). Perforin pathway and its lytic capacity have been well studied in cytotoxic T lymphocytes (CTLs), which has similar properties as in NK cells. NK cells use perforin/granzymes cooperatively as a fast killing mechanism and the major pathway to induce target cell apoptosis. Perforin known as a membrane-disrupting protein involved in causing a pores in the target cell membrane and this allow granzymes mainly granzyme B to enter target cells and trigger caspases activation such as caspase-3, caspase-8 or BH3- interacting domain death agonist (BID) (Hassin et al., 2011; Stanley & Lacy, 2010).

Another major function of NK cells is secreting inflammatory cytokines. Cytokine molecules secreted from NK cells allow other cells in the immune system to communicate indirectly to each other to generate a coordinated and robust response against target cells (Vivier & Ugolini, 2011). The most prominent cytokines produced by NK cells are interferon γ (IFN-γ) and tumour necrosis factor-α (TNF-α) in addition to other immunoregulatory cytokines such as, growth factors and chemokines, including interleukin-5 (IL-5), IL-10, IL-13, GM-CSF and

MIP-1α, MIP-1β, IL-8 and RANTES respectively (Raulet, 2004). The generation of immunoregulatory cytokines production is dependent on the type of stimulation and the time course after activation. Cytokines produced by NK cells not solely augment NK cell function, but also have various effectors towards other immune cells, dendritic cells (DCs), macrophages, T and B cells, including enhanced phagocytosis, production of antimicrobial peptides and initiate the signals for T cell activation (Vivier & Ugolini, 2011).

The recognition system of NK cells includes a number of cell surface activating and inhibitory receptors that engagement of these receptors with their ligands control NK cell activity. As a result, the dynamic balance of these receptors governs NK cell activation and determines whether or not NK cells are triggered to destroy target cells during interaction with surrounding cells (Vivier et al., 2004). NK cell effector function depends on the integration of signals received from two types of receptors. MHC class I molecules are expressed on the surface of healthy cells and act as ligands for inhibitory receptors and contribute to NK cell self-tolerance. On the other hand, tumor cells and viral infected cells lack or reduce surface expression of MHC-I (missing self), which results in a reduction of inhibitory signals in NK cells. Cellular stress associated with tumorigenesis or viral infected cells such as DNA damage and tumor suppressor genes, induce upregulation of ligands for activating receptors. As such, the activating signals from NK cell activating receptors shift the balance promoting NK activation (**Figure 1.6**) (Lanier, 2008).

The strength and quality of NK cell function is influenced by the cytokine microenvironment and the interactions with other immune cells such as T cells and DCs. It is well known that IFN type I, IL-12, IL-18, and IL-15 are potent activators for NK cell function. In addition, IL-2 induces NK proliferation, cytotoxicity and less extend cytokines production. In human and

mice, NK cell function can be regulated by transforming growth factor (TGF-β) produced by regulatory T cells (Vivier et al., 2008).

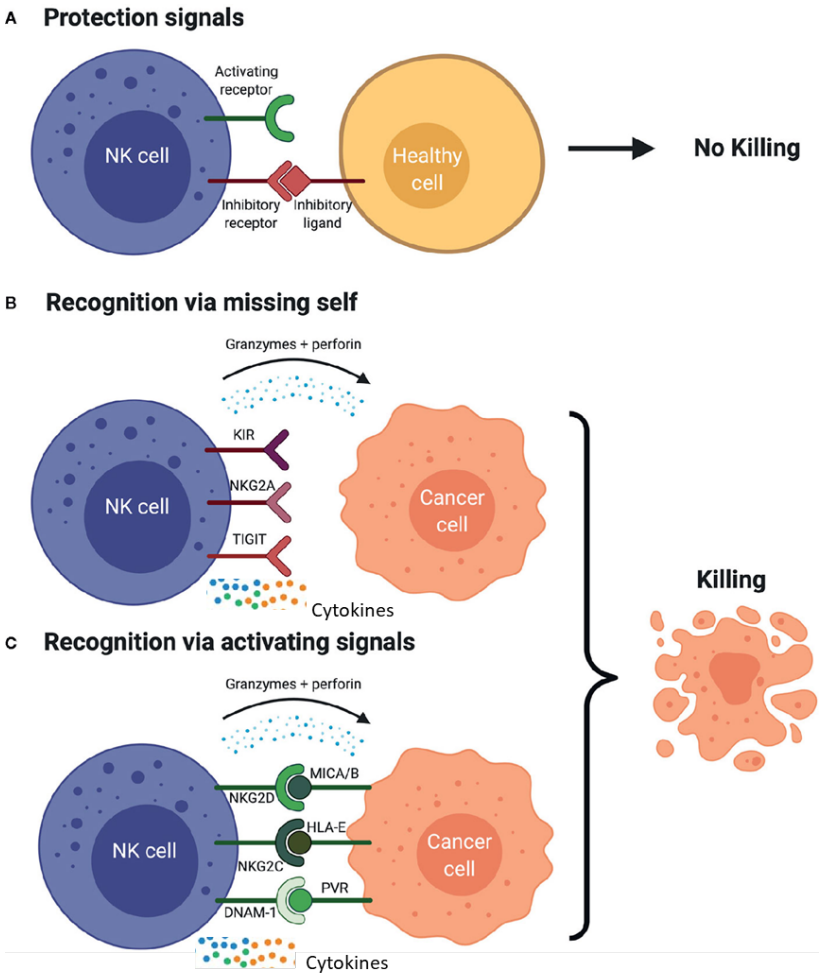

Figure 1.6 NK cell-mediated surveillance and killing of cancer cells.

(**A**) The absence of activating signals and presence of inhibitory signals inhibit NK cell activation, preventing the lysis of healthy cells. (**B**) Due to the lack of human leukocyte antigens (HLAs) on cancer cells (missing self-hypothesis) results in NK cell activation and cytokines production (IFN-γ and TNF-α), cytolytic granules (perforin and granzyme B) that mediate cancer cell lysis. In this scenario activation signals are required to induce NK cell activation as loosing inhibitory signals alone is usually insufficient for NK cell activation. (**c**) The presence of activating signals through engagement of activating receptors with their cognitive ligands on cancer cells and absence of inhibitory signals strongly activate NK cells and induces the secretion of cytokines and cytolytic granules which ultimately result in cancer killing**.** Adapted from (Alfarra et al., 2020)**.**

1.2.3.1 Cytotoxicity of NK cells

The fundamental process of NK cytotoxicity is embedded with exocytosis of preformed lytic granules (perforin and granzymes). Perforin is a multi-domain pore-forming protein that target cell membrane, whilst granzymes are serine proteases that function together with perforin to induce programmed cell death cascades (Young et al., 1986). NK cell cytotoxicity response undergoes four steps. The first step is the formation of immunological synapse between NK and target cells, which is accompanied by actin cytoskeleton rearrangement. The next step is the polarization of microtube organizing centre (MTOC) and followed by lysosome move toward the lytic synapse. At last, the lysosome from NK cells will be fused into target cell plasma membrane (Topham & Hewitt, 2009). This process results in release of cytotoxic granules including perforin and granzymes which known as NK degranulation. This NK degranulation is commonly used to test cytotoxic capacity of NK cells. Through degranulation process, lysosomal-associated membrane protein-1 (LAMP-1/CD107a) and (LAMP-2/CD107b) emerge transiently on the surface of degranulating NK cells. The expression level of CD107a on the surface of NK cells is used as indirect way to measure the cytotoxicity capacity of NK cells (Alter et al., 2004). Perforin infused in the target cells polymerises and generates holes in their cell membrane facilitating the entry of granzymes into target cells, which in turn activates the caspase molecules causing target cell apoptosis (Martínez-Lostao et al., 2015).

NK cells can mediate target cell killing by other mechanisms that involves death receptor-induced target cell apoptosis. TNF-related apoptosis induced ligand (TRAIL), in addition to FAS ligand (FASL) are all expressed on NK cells. These receptors mediate NK cell cytotoxicity through interaction with their respective ligands on the target cells, including death

receptor DR4 (TRAIL-RI) and DR5 (TRAIL-RII) or CD95 respectively (**Figure 1.7**) (Sonar & Lal, 2015).

1.2.3.2 Antibody-dependent cell-mediated cytotoxicity (ADCC)

ADCC is another mechanism utilised by NK cells to mediate a cytotoxicity against IgG coated target cells. Human NK cells express FcγRIIC/CD32c and FcγRIIA/CD16a, which bind to the Fc fragment of an antibody molecules. This ligation induces phosphorylation of homodimers or heterodimers of ζ and γ chains that have immune tyrosine-based activating motif (ITAM) in their cytoplasmic tails (W. Wang et al., 2015). Upon ITAM phosphorylation, the subsequent signal transduction activates PI3K, NF-kb, and ERK pathways which induce NK cell degranulation, cytokines secretion and ultimately target cell death (**Figure 1.7**) (Smyth et al., 2005; Du and Wei 2019).

NK ADCC mediates tumor killing through several pathways, including exocytosis of cytotoxic granules, TNF death receptor signalling, and secretion of pro-inflammatory cytokines in particular IFN-γ. The first two pathways are involved directly in target cell apoptosis, whilst IFN-γ produced by NK cells activates the surrounding immune cells such as DCs to promote antigen presentation and eventually stimulate the adaptive immune response (Srivastava et al., 2013). Although, IFN-γ production and cytotoxicity were previously thought to be two separate functions from different NK subsets, however, studies show that the major cytotoxicity NK subset ($CD56^{dim}$ $CD16^{pos}$), that is responsible in ADCC, can also produce considerable amount of IFN-γ following activation (De Maria et al., 2011).

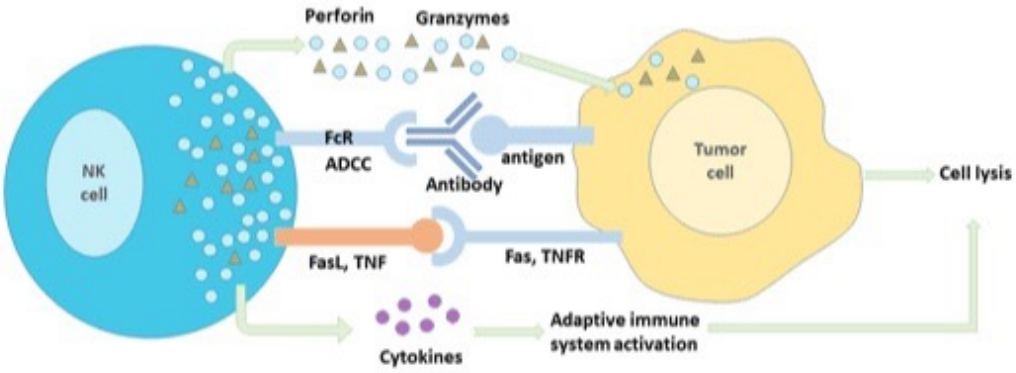

Figure 1.7 NK cell mediates cytotoxicity through ADCC and FasL mechanisms.

NK cell targets tumor cells by antibody-dependent cell-mediated cytotoxicity (ADCC). This mechanism involves CD16A binds specifically to tumor-bound IgG resulting in phosphorylation of adaptor proteins that initiate intracellular signals, activating NK cells to release perforin, granzymes, and cytokines to lyse target cell. In addition, activated NK cells express FasL which binds to its receptor CD95 on the surface of tumor cells to initiate apoptosis pathways led to tumor cell lysis. Adapted from Du and Wei 2019.

1.2.4 NK cells in cancer and immunosurveillance

Since discovered in the early of 1970s, NK cells have been shown to actively prevent the development of neoplastic cells by cancer immunosurveillance process. First discovery of NK cell involvement in host immunity against cancer was established when investigations revealed the effector lymphocytes from athymic nude mice had antitumour reactivity, which was not dependent on T cells (Lancet, 2000). NK cells can recognise malignant and virally transformed cells through the losing expression of MHC class I on their surfaces (missing self) and expression of ligands for activating receptors, which gains NK cells a potent function to kill susceptible cells without pre-activation. NK cells can directly contact target cells and mediate cellular cytotoxicity, and cytokine secretion such as IFN-γ and TNF-α. However, tumour cells have developed multiple mechanisms for evading immunosurveillance including modification of surface antigens and alteration of their surrounding microenvironments (Bachanova & Miller, 2014). There are two main mechanisms that tumor microenvironment uses to facilitate tumor escape from NK mediated cytotoxicity: suppression of effector NK cell function and evasion through the alteration of surface antigens on tumor cells (Vesely et al., 2011). Increased levels of various cytokines and enzymes in the tumor microenvironment has been demonstrated, which modulate NK cell function. For example, TFG-β produced by Tregs and MDSCs, inhibits the expression of the main activating receptors on NK cells NKp30 and NKG2D that are important for recognition and killing of tumor cells (Bellora et al., 2010). In addition, Chronic NK exposure to tumor cells may induce the tumor cells to alter the expression of either inhibitory or activating ligands for NK receptors. For example, melanoma cells can upregulate inhibitory total HLA-I molecule and become resistance to NK cell lysis. Moreover, tumor cells can evade NK cell recognition by downregulating surface expression of NKG2D and NKp44 ligands (El-Gazzar et al., 2013). In breast cancer, the upregulation of PDL1 on tumor cells and PD-1 expression on NK cells and cytotoxic T cells have been found to impair

NK cell function, and inhibit the activation of T cells (M. Wang et al., 2017). In addition, myeloid cells can highly suppress the immune cells by up-regulation of Arginase-1 (Arg -1), iNOS inhibits the phosphorylation of tyrosine residuals leading to blockade of T cell and NK cell activation, whereas Arginine promotes tumour progression (Noonan & Borrello, 2011). Recent investigations have identified several classes of anticancer agents that specifically target these suppressive molecules to reverse the impaired immune cells and have less side effects compared to standard treatment such as chemotherapy, radiation, and surgery. One such agent that acts against PD-1 immune checkpoints is nivolumab and pembrolizumab, and atezolizumab that blocks PDL1 ligand. These drugs are treatment for many cancers including lymphoma, melanoma, breast cancer and small lung cancer (Robert., 2020).

1.3 B cell Chronic lymphocytic leukaemia (B-CLL)

1.3.1 Disease overview

B cells Chronic lymphocytic leukaemia B-CLL is the most common type of leukaemia in western counters. B-CLL typically affects elderly people aged between 60 and 72 years, as the incidence rates increase with age and the disease is more common in males than females (1.7:1) (Matutes & Polliack, 2000). Approximately 15,000 diagnosed with B-CLL and about one-third of patients die each year. Due to demographic changes the incidence and mortality of B-CLL are expected to rise further in forthcoming decades (Marionneaux et al., 2014). CLL is characterized by the clonal proliferation and gradual accumulation of mature $CD5^+$ B cells in the bone marrow, peripheral blood, lymph nodes, liver, and spleen. Therefore, the clinical symptoms of advanced disease are bone marrow failure and other consequences resulting from enlargement of liver and lymph nodes (Lens et al., 1997).

The exact cause of the disease is still unknown. However, Kikushige et al have reported that in B-CLL disease the generation of clonal malignant B cells might be acquired at the hematopoietic stem cells (HSC) stage, which implies that the leukemogenic event might involve multipotent, self-renewing HSCs (Faria et al., 2000). Researchers have demonstrated many genetic differences between normal lymphocytes and B-CLL cells and these genetic aberrations are detected in over 80% of B-CLL cases. Recent study has characterized the comprehensive genomic landscape in large cohort of B-CLL patients using whole exome sequencing, it showed that the disease might occur due to inherited mutations, where deletion or addition in large chromosome materials. The loss of part of chromosome 13 (del 13q), deletion of (11q) and (trisomy 12) are the most common deletions that have been observed in B-CLL patients. In addition, over 50% of cases show hypermutated immunoglobulin variable region (IgV) (Uhm, 2020).

1.3.2 Diagnosis and staging

B-CLL has been defined and classified by the world health organisation (WHO) as a disease of neoplastic B cells and is only distinguishable from small lymphocytic lymphoma (SLL) by its clinical appearance, as at the diagnosis stage the lymph nodes in SLL appear to be swollen (Hallek et al., 2008). Thus, it is important to distinguish between B-CLL and other lymphoproliferative diseases such as prolymphocytic leukaemia (PLL), hairy cell leukaemia (HCL), mantle cell lymphoma and marginal zone lymphoma during diagnosis and confirm that the patient has B-CLL no other type of leukaemia mentioned earlier. In addition to clinical manifestations, the accurate diagnosis of B-CLL requires immunophenotyping by flow cytometry (IFC) and other examinations such as evaluation of blood count and blood film (Binet et al., 1981).

There is no single marker exclusively expressed on B-CLL cells, but a combination of different B cell markers can help to diagnose B-CLL. The co-expression profile of B-CLL cells includes T cell antigen CD5, B cell surface antigens CD19, CD20, CD23 and surface immunoglobulin (sIg) with light chain restriction, as majority of B-CLL cases lack the expression of kappa and lambda light chains (Hallek et al., 2008). In all cases, the diagnosis of B-CLL should be considered when the circulating lymphocytes are greater than 5×10^9/L (5000/µl). Nevertheless, the confirmation of B cell clonality with a mild lymphocytosis is an important test to confirm the diagnosis and rule out other disorders such as a reactive B or T lymphocytosis (Catovsky et al., 2007). Morphologically, careful analysis of cytoplasmic morphology of lymphocytes using fresh peripheral blood films is the best. Where there are two distinct subgroups of B- CLL, typical CLL (tCLL) and atypical CLL (aCLL). Approximately 80% of cases are tCLL. In this CLL subtype the majority of lymphocytes are small to medium in size with constant cytoplasm and regular border. However, the cytoplasm is usually scanty, and the nuclear chromatin is characteristically clumped in regular nuclear membrane. In aCLL subgroup which represents about 25% of B-CLL cases, lymphocytes show less condensed nuclear chromatin with nuclear irregularities (Rodrigues et al., 2016).

For most cancers, staging is a process used to find out how far the cancer has spread, and it is a useful tool for guiding treatment and determining a patient's outlook. In B-CLL, the staging classifications of Rai and Binet are widely accepted and have been in use for many years. Both systems estimate three major prognostic groups based on the extent of lymphadenopathy, splenomegaly and hepatomegaly measured by palpitation and anaemia and thrombocytopenia measured by blood cell count. These staging systems are simple and inexpensive and rely solely on physical examinations and standard laboratory tests (Rodrigues et al., 2016).

Rai staging system, which is more widely used in the United States, considers B-CLL disease is at low risk (stage 0) if a patient has lymphocytosis with leukaemia cells in the blood or bone

marrow. Intermediate disease (stage I) is defined when the patient has lymphocytosis, enlarged nodes and splenomegaly. While high risk disease (stage II, III) includes patients with anaemia haemoglobin (Hb) <11 g/dl and platelets count <100 × 10^9 /L (Hallek et al., 2008). Binet staging system which is more often applied in Europe relies on the number of involved areas that have enlarged nodes, and whether there is anaemia or thrombocytopenia. Binet system defined stage A as Hb ≥10 g/dl and platelets count ≥100 × 10^9 /l, stage B as stage A with organomegaly greater than in stage A, while stage C as Hb <10 g/l and platelets <100 × 10^9 /L (Letestu et al., 2010).

Table 1.3 Binet staging system and Ria classification of B-CLL disease

Binet staging system		
Stage	**Risk**	**Characteristics**
A	Low	Less than three enlarged node sites, without anaemia or thrombocytopenia
B	Intermediate	More than three enlarged node sites, without anaemia or thrombocytopenia
C	High	Presence of anaemia and/or thrombocytopenia
Rai staging system		
Stage	**Risk**	**Characteristics**
0	Low	Lymphocytosis
I	Intermediate	Lymphocytosis with node enlargement
II	Intermediate	Lymphocytosis with palpable spleen and/or liver
III	High	Lymphocytosis with anaemia
IV	High	Lymphocytosis with thrombocytopenia

Adapted from (Gribben, 2010).

1.3.3 Treatment

Patients with early stages of B-CLL (stage A in Binet or stage 0 in Rai systems) typically do not require treatment. Clinical studies have shown that early treatment does not prolong survival, rather than put the patients through side effects and complications of treatment. Because B-CLL usually progress very slowly for months or years, patient are monitored regularly (wait and watch period) for any symptoms or indications for treatment (Jaglowski, 2014). Patients with active or symptomatic disease require treatment, and the treatment aims to reduce the number of tumor B-CLL cells to the lowest possible, so the patient have normal live with no symptoms which called remission. The International Workshop on CLL (iwCLL) guidelines are recommended for indications of treatment and evaluation of therapy (Jakšić et al., 2018). There are some treatment indications that the physician can rely on to establish the initiation of treatment such as evidence of bone marrow failure manifested by anaemia or thrombocytopenia, massive splenomegaly and/or lymph node and progressive lymphocytosis with increase more than 50% within two months (Jakšić et al., 2018).

1.3.3.1 Chemotherapy

Chemotherapy can be a single drug or a combination of drugs, it depends on the overall health and patient's fitness. The first-line standard chemotherapy in fit patients who require a therapy is fludarabine, cyclophosphamide and in combination with rituximab (FCR). This combination of drugs has high rates of response with 40 to 50% of complete response (CR). However, FCR has side effects and not tolerant for many of b-CLL patients due to the age, decreased fitness and renal function, therefore other treatment regimens which are more tolerant should be administrated (Eichhorst et al., 2016).

1.3.3.2 Monoclonal antibodies therapy

Monoclonal antibodies (mAb) are agents having high affinity and specificity to target antigens expressed on B-CLL cells. There are a number of monoclonal antibodies such as rituximab, ofatumumab and obinutuzumab. Rituximab is the most common monoclonal antibody used in CLL therapy, which can recognise CD20 antigen on the normal and malignant B cells (Ferrajoli et al., 2006). Generally, single agent therapy is less effective compared to combined therapy. For example, when rituximab is combined with chemotherapeutic agents, the cancer cell apoptosis is enhanced in synergic manner. In addition, rituximab in combination with idelalisib and ibrutinib (BCR signalling inhibitors) and venetoclax (BCL2 antagonist) showed spectacular efficacy and favourable tolerability compared to chemoimmunotherapy (Chow et al., 2002).

1.3.3.3 Stem cell transplantation

Allogeneic hematopoietic stem cell transplantation (allo HSCT) is thought the only curative potential therapy for appropriate B-CLL patients. European blood and marrow transplant group has demonstrated that allo-HSCT is a feasible treatment option for younger patients who relapsed within 12 months or non-responsive to other options of treatments and relapse within 24 months of treatment with purine analogue based combination therapy or patients with genetic abnormalities such as p53 (Dreger et al., 2007). However, the application of allo-HSCT is limited by its toxicity and more than 70% of patients develop acute or chronic graft-versus-host disease (GvHD) (Burger et al., 2020).

1.4 Immune system landscape in B-CLL patients

Generally speaking, compromised immune system is the main problem in cancer patients. The impairment of immune function leads to more complications and reduce the treatment efficacy, which in turn results in disease progression, high risk of infections and poor prognosis. The dysfunction of immune system in human involves multiple mechanisms and is characterized by a reduction in innate immune cells function such as monocytes, DCs, macrophages and NK cell activity (Costello et al., 2012). In B-CLL patients, changes in T cell composition has been extensively documented, but the specific impact of these alterations on disease onset and progression is still unknown. The first T cell aberration in B-CLL patients was the discovery of increased number of T cells in the peripheral blood, which was mostly due to $CD8^+$ T cell expansion resulting in an inversion of the normal $CD4^+/CD8^+$ T cells ratio (Scrivener et al., 2003). In addition, increased expression of exhaustion markers such as PD-1, CD244 and CD160 has been documented on $CD8^+$ and $CD4^+$ T cells, where these molecules are highly expressed on the effector T cells. The investigation of gene expression profile of T cells has revealed down regulations in genes involved in vesicle transport and cytoskeletal regulation leading to functional defects in immunologic synapse formation with APCs. Several profound defects in T cell functions that reduced their capacity of antitumour activity including impairment in proliferation, cytotoxicity, and immune synapse formation resulting in disease progress and increase the susceptibility to infection (Vlachonikola et al., 2021).

Despite the potent role of NK cells in immunosurveillance and defence against tumors and leukemic cells, studies showed that NK cells in B-CLL patients are dysfunctional. Impaired cytolytic activity of NK cells was first reported in B-CLL patients in 1980's and was primarily attributed to the substantial abnormalities in the cytotoxic machinery (Kay & Zarling, 1984).

Further studies revealed that autologous NK cells are unable to kill B-CLL cells not only due to their impaired cytotoxicity but also due to immune escape mechanism developed by B-CLL cells (Reiners et al., 2013). However, contrast studies have revealed that NK cells from B-CLL patients have an intact on phenotype with normal degranulation, cytokine production, and ADCC (Kay & Zarling, 1987). One of the key explanations for NK dysfunction in B-CLL patients could be the dysregulation and imbalanced expression of activating and inhibitory receptors. Several studies have demonstrated that NK cells from B-CLL patients had lower expression of activating receptors such as NKG2D, DNAM-1 and NKp30, and NKp46 compared with healthy donors. This phenotype alteration is associated with poorer cytotoxic activity, degranulation, and killing of target cells (Hadadi et al., 2019; Hofland, Endstra, et al., 2019). Moreover, NK cells in B-CLL patients express high levels of CD27 which is a marker for less mature NK cells. These NK subsets display marked reductions in cytokines production and degranulation in response to B cell line 721.221 (MacFarlane et al., 2017). In parallel with previous studies, recent findings from our group (Parry H, et al 2016) demonstrated that NK cells from B-CLL patients displayed an impaired cytotoxic activity *in vivo* (mice models) and *in vitro* assays. Impaired NK cells characterized by reduction in expression of several activating receptors including NKG2D, DNAM-1 and NCRs. Cytotoxicity assay was carried out using K562 cell line, target cell lysis was reduced 40% after incubation with NK cells from B-CLL patients compared to healthy donors (**Figure 1.8**).

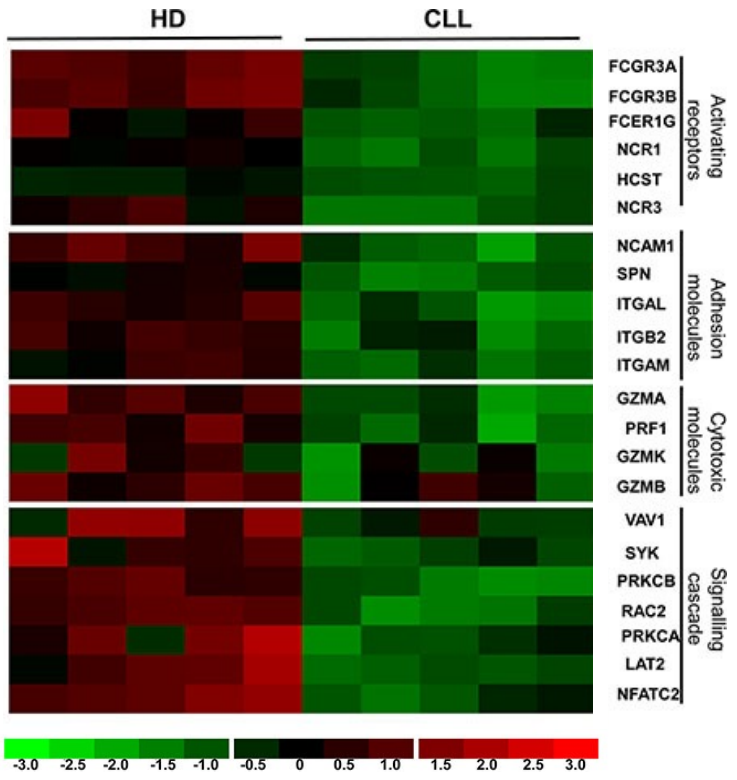

Figure 1.8 Impairment of Cytotoxicity pathways of NK cells in B-CLL patients.

The intensity profile of genes related to NK cytotoxicity are downregulated in NK cells from B-CLL patients compared to HCs, including genes coding for activating receptors, adhesion molecules and effector molecules such as perforin and granzymes (Parry H, et al 2016).

Regarding NK cell inhibitory receptors, CD94/NKG2A has been found to suppress NK cytokines production and cytotoxicity against CLL cells by binding to its respective ligand HLA-E molecule, which is upregulated on the surface of CLL cells (McWilliams et al., 2016). According to studies on expression of inhibitory KIRs (iKIRs) on NK cells from B-CLL patients, KIRD2L2/3 and KIRD3L1 that recognise and bind to HLA-C and HLA-B allotypes respectively, have been reported to be similar to that from healthy individual. However, a slight decrease in KIRD2L1 expression which bind to group 2 HLA-Cw alleles has been found on NK cells from B-CLL patients (Le Garff-Tavernier et al., 2011; Veuillen et al., 2012).

Similar to T cells, NK cells express variety of inhibitory checkpoints that keep NK cells in check. In line with evidence obtained from conventional T cells, inhibitory checkpoints expression on NK cells can be an additional mechanism that may impact anti-tumor activity of NK cells in B-CLL patients. For example, immune checkpoint TIM-3 was observed to be upregulated on NK cells from B-CLL patients, combined with the high mRNA levels of its ligand galectin-9 in CLL cells and increased galectin-9 itself in B-CLL patients serum. This was related with unfavourable prognostic factors of B-CLL disease, as dysregulation of expression of TIM-3 and NKp30 receptor confirms the exhausted state of NK cell in B-CLL which in turn leads to tumor cell escape from NK cells and disease progression (Hadadi et al., 2019). In addition, sustained expression of TIM-3 on NK cells in other malignancies has been demonstrated to cause an exhausted/dysfunctional NK cells which can be restored by TIM-3 blockade (Gallois et al., 2014). It is well known that interaction of PD-1 expressed on T cells with its ligand PDL1 expressed on CLL cells severely inhibits T cell function, resulting in an exhausted T cell phonotype (Brusa et al., 2013). Despite all evidence that PD-1 expression on NK cells and PDL1 on tumor cells in other cancers results in functional impairment of NK cells (Beldi-Ferchiou et al., 2016), the impact of PD-1/PD1Ls ligation in regulation of NK cell

activity in B-CLL patients still need to be investigated, as CLL cells express high levels of PDL1 (Taghiloo et al., 2017). Therefore, the major part of this study will address this mechanism in detail.

1.5 NK cell-based immunotherapy in B-CLL patients

Despite the advances in various of cancer therapies, cancer remains incurable with standard therapies. A growing number of scientific reports and clinical studies have shown promising anti-tumour effects when using NK cell-based therapy, due to their selective ability to distinguish between healthy and cancer cells in addition to their instant killing (Kwon et al., 2017). Previous data suggests that peripheral CLL-derived NK cells retain fundamental functionality, which can be restored by appropriate activating signals including cytokines such as IL-2, IL-15 (Le Garff-Tavernier et al., 2011). In B-CLL disease and other tumors, the aim of therapeutic strategy based NK cells is to strengthen and/or recover NK cell activity against tumor cells, or to infuse patients with functional NK cells that are able to eliminate tumor cells (Sportoletti et al., 2021). These goals can be met through variety of methods which are summarised in (**Figure 1.9**).

Enhancement of NK cell-mediated ADCC: Therapeutic strategies that are based on the advantage of NK cell-mediated ADCC in B-CLL patients can be achieved using tumor-specific monoclonal antibodies (mAbs) or bispecific and trispecific killer engagers. The ability of NK cells to kill tumor B cells is opsonised with mAbs by ADCC, a mechanism dependent on the engagement of CD16 receptor on NK cells with Fc region of IgG bond to the tumor cells, which is one of the important NK-based therapeutic strategies in B-CLL (Ochoa et al., 2017). Various humanised mAbs that target multiple B-CLL surface antigens, such as CD20, CD19, and

recently CD37 can promote therapeutic activation of NK cell-mediated ADCC. Anti-CD20 Rituximab (RTX) was the first to be approved (1998) to induce NK ADCC and complement-dependent cytotoxicity (CDC). Despite the fact that Rituximab had limited success as a single agent therapy, it was found to be more effective when combined with chemotherapy such as fludarabine and cyclophosphamide (FCR) (Boross & Leusen, 2012; Jaglowski et al., 2010). More recently, a new form of anti-CD20 mAbs, ofatumumab has been approved, which is Fc-engineered mAb targeting different epitopes than RTX (van der Horst et al., 2020). CD19 is another target for mAbs-based therapy in B-CLL. The anti-CD19, afucosylated mAbs inebilizumab and Fc-engineered mAbs tafasitamab have been also demonstrated to boost NK cell-mediated ADCC against B-lymphoma and leukaemia cell line. In addition, trial studies showed that inebilizumab and tafasitamab are well tolerant and have preliminary efficacy in pre-treated and relapsed B-CLL patients (Jurczak et al., 2018; Ohmachi et al., 2019). CD37 is another potential target for B-CLL immunotherapy that is under investigation at the moment (Phase II trials) (Payandeh et al., 2018). Among these CD37 mAbs, BI836826 (Mab 37.1), an Fc-engineered mAb that has the ability to induce apoptosis and NK cell-mediated ADCC (Betrian et al., 2016).

In addition, Bispecific and trispecific killer engagers (BiKEs and TriKEs) are new potential therapeutic approaches to augment NK cell activation at the tumor site by targeting CD16. BiKE construct consists of a single-chain variable fragment (scFv), that is specific for tumor antigen and a second scFv which is specific for activating receptors on NK cells, which can bring the tumor cells and NK cells together to form an immunological synapse and trigger NK cytotoxicity response (Labrijn et al., 2019). TriKEs construct has enhanced ability and specificity to bind to the target cells by recognising and binding to two different tumor antigens which will allow recognition of cancer cells even when one antigen is lost or downregulated.

To date, BiKEs, and TriKEs to activate NK cells have only been studies at pre-clinical settings. However, the results demonstrate that these constructs have a high therapeutic potential for B-CLL. The BiKE construct for example anti-CD19/CD16 can induce NK based ADCC against primary tumor B cells. The TriKEs, like anti-CD16/CD19/CD22 can also directly induce NK cell activation through CD16 and increase NK cytotoxicity and IFN-γ production against tumor B cells (Bruenke et al., 2004; Kellner et al., 2011).

Immune checkpoint blockade: Blocking immune checkpoints on NK cells is one possible approach for B-CLL NK-based immunotherapy. However, in B-CLL, the main focus of releasing anti-tumor immune responses with immune checkpoints blockade has been on T cells using PD-1 blockade (Palma et al., 2017; Taghiloo et al., 2017). PD-1 blockade in B-CLL showed an acceptable response rate whether used as a single therapy or in combination with ibrutinib, particularly in B-CLL patients with high levels of PDL1 and PD-1 expression in tumor microenvironment (Ding et al., 2017). In addition to PD-1, other inhibitory receptors expressed on NK cells have been evaluated in B-CLL including iKIRs and CD94/NKG2A. The first human clinical trials using full human IgG4 mAb lirilumab (IPH2102) against shared epitope of KIR2DL1/2/3 has determined that the dose that can fully saturate KIRs showed no clinical or immunological side effects, indicating the safe and well tolerant does to induce prolonged KIRs blockade in B-CLL patients (Vey et al., 2018). Furthermore, overexpression of HLA-E on tumor B cells, a major ligand for CD94/NKG2A has supported the rationale of using humanised IgG4 mAb monalizumab (IPH2201) for B-CLL immunotherapy (André et al., 2018). Ex vivo study has shown that monalizumab is able to restore direct cytotoxicity of NK cells from B-CLL patients while having no effect on NK cell-mediated ADCC (McWilliams et al., 2016). The functional consequence of *in vitro* blocking of LAG-3 in B-CLL has been mainly investigated on T cells. However, very recent *in vitro* work using LAG-

3 blocking mAb relatlimab (MBS-986016) demonstrated an increase in NK cell proliferation and anti-tumor activity (Sordo-Bahamonde et al., 2021).

Allogeneic NK cell therapy: Allogeneic hematopoietic stem cell transplantation (allo-HSCT) is believed to be the only curative option for advanced B-CLL patients, especially those patients with relapsed or refractory disease. However, allo-HSCT treatment decreased after the discovery of BCR and Bcl-2 inhibitors which are effective in treatment of high risk B-CLL patients, as allo-HSCT cause graft-versus host disease (GvHD) mediated by T cells and treatment is limited by donors (Burger et al., 2020). *In vitro* studies have shown that expanded/activated allogeneic NK cells using optimal protocol are able to kill B-CLL cells in independent manner of KIR-HLA molecule mismatch (Calvo et al., 2020). Thus, they are attractive and safe option for adaptive immunotherapy of B-CLL patients.

CAR-NK cell therapy: A new strategy of adaptive cellular immunotherapy in B-CLL is transfusing T or NK cells engineered with chimeric antigen receptors (CARs) (CAR-T cells or CAR-NK cells), which can detect a specific epitope on tumor cells to induce activation and anti-tumor activity of modified T or NK cells, However, due to the risk of GvHD associated with CAR-T cells, CAR-NK cells have emerged as a prospective source for CAR-based therapy due to their availability, do not induce GvHD and safe profile (Rafei et al., 2021). CD19 directed CAR-T cells was the first CAR-based therapy in refractory/relapsed B-CLL patients. But due to the low efficacy and excessive toxicity mediated by CAR-T cells including cytokine release syndrome (CRS) and neurotoxicity, CAR-T cell therapy in B-CLL is discouraged. The low efficacy of CAR-T cell therapy compared to other B cell malignancies is mainly due to T cell exhaustion and T cell terminal differentiation (Magalhaes et al., 2018).

Given the poor efficacy of CAR-T cell therapy in B-CLL patients, in addition to their complex and costly donor-patient based manufacturing, there is a growing interest in CAR-NK cells as an alternative tool CAR based therapy due to their availability, do not induce GvHD and safe profile.

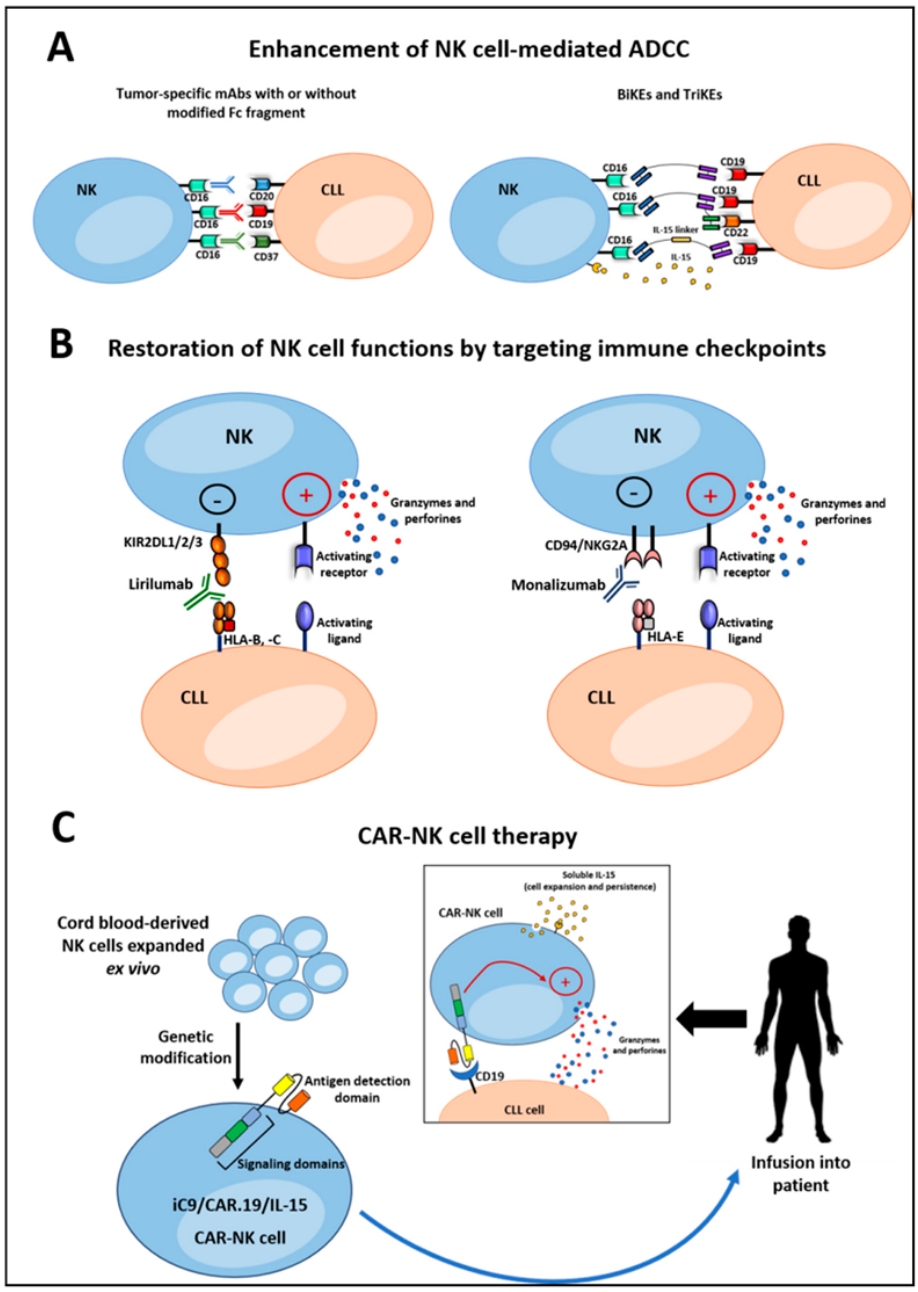

Figure 1.9 NK cell based immunotherapy in B-CLL patients.

To exploit NK activity against CLL cells, many approaches have been developed. (A) Enhancement of NK cell-mediated ADCC using tumor specific monoclonal antibodies (mAbs) (left diagram) or bispecific and trispecific killer engagers (right diagram). (B) Blocking inhibitory immune checkpoints using mAbs to restore anti-tumor NK cell function. (C) CAR-NK cell based adaptive immune therapy. Adapted from (Sportoletti et al., 2021).

1.6 Hypothesis and objectives

Previous studies, including our own study have shown that NK cells in B-CLL patients are functionally impaired, which is attributed partially to the low expression of activating receptors on NK cells. This study aims to explore even further this function impairment of NK cells in B-CLL patients, including the detailed phenotype using high dimensional flow cytometry and detailed functionality study.

One particular interest in this study is the immune checkpoint expression on NK cells, which has not been explored in B-CLL disease setting. Similar to T cells, NK cells express several immune checkpoints on their surfaces that inhibit the activation of NK cells. Blocking of these inhibitory checkpoints receptors on T cells has been successful in reinvigorating anti-tumor T cell function. Therefore, this study will investigate the expression pattern of all the known inhibitory checkpoint receptors on NK cells in B-CLL patients and also the transcription profile of those NK cells expressing checkpoint receptors. In addition, the hypothesised of the potential that the immune checkpoint blockade may restore anti-tumor function of NK cells will be tested. Eventually, this study can discover or improve the NK cell-based immunotherapy for B-CLL patients.

1.7 Aims of this work

The main aims of this study were:

- To investigate the phenotype of NK cells from B-CLL patients, focusing on the expression of immune checkpoint receptors and adhesion molecules.
- To assess the functional capacity of NK cells in B-CLL patients, particularly cytokine production and DNAM-1 dependent NK cytotoxicity.

- To investigate the effect of TIGIT or/and CD96 blockade in restoring the DNAM-1 based NK cytotoxicity.

- To characterise the phenotype of PD-1^{pos} NK cells compared to PD-1^{neg} NK cells and investigate the co-expression of PD-1 with other checkpoint markers.

- To investigate the functional capacity of PD-1^{pos} NK cells in comparison to PD-1^{neg} NK cells, and the possibility of reversing the anti-tumor activity of PD-1^{pos} NK cells by blocking PD-1/PDL1s interactions using primary PD-1^{pos} NK cells from B-CLL patients

- The PD-1^{pos} NK cell lines *in-vitro* model using NK-92 and NKL lines will be used to explore the phenotype and functionality of PD-1^{pos} NK cells.

- To study the gene expression profile of PD-1^{pos} NK cells vs PD-1^{neg} NK cells using scRNA-seq and chromatin accessibility using ATAC-seq.

CHAPTER 2: MATERIALS AND METHODS

2.1 Materials and reagents

2.1.1 Materials

Materials and kits used in this study are summarised in **Table 2.1** and **Table 2.2** respectively.

Table 2.1 lists the materials used in this study

Materials	Source
Tissue flasks 25 and 75cm^2	Corning, Sigma-U.K
Multi-wells plates (6, 12, 24)	Corning, Sigma-USA
96 well flat bottom micro plates	Corning, Sigma-USA
96 well round bottom micro plates	Corning, Sigma-USA
96 well PCR plates	Bio-Rad Laboratories, U.S.A
24 Trans-well plates	Corning, sigma-USA
1and 2ml Cryovials	Alpha Laboratories, UK
Mr-Frosty™ Freezing Container	Thermo Fisher Scientific, U.K
15ml falcon tubes	Sarstedt Inc Fisher Scientific-U.S.A
50ml conical tubes	Corning, Sigma-U.K
5ml polypropylene and Polystyrene FACS tubes	BD Biosciences, U.S.A
5ml polystyrene FACS tubes with strainer cap	Corning, Sigma-U.K
FastRead Counting Slides	Immune Systems, U.K
Pipette 5, 20, 25, 50ml	CELLSTAR®

Table 2.2 A list of Kits used in this study

Kit	Source
EasySepTM Human NK cell Enrichment Kit	Stemcell Technologies
EasySepTM Human B cell Enrichment Kit	Stemcell Technologies
TGF-beta Human ELISA kit	Thermo Fisher Scientific-UK
QIAquick^{R} PCR Purification Kit	Qiagen
KAPA Library Quant kit	Illumina
Nextera® DNA library prep kit	Illumina
AMPure XP PCR purification beads	Beckman coulter-USA
VersaComp Antibody Capture Beads Kit	Beckman Coulter, Inc.
CountBrightTM beads	Thermo Fisher Scientific-UK

2.1.2 Buffers and reagents

Prepared buffers and reagents used to set up the experiments in this study are listed in **Table 2.3**, **Table 2.4,** and **Table 2.5**. Also, Cell culture media used throughout this study are listed in **Table 2.6.**

Table 2.3 List of reagents and manufactures used in this study

Reagent	Source
RPMI-1640 medium	Sigma-Aldrich-UK
F-12 Nut mix	gibco-uk
Lympholyte®	CEDARLANE, Canada
Pen Strep	Gibco Thermo Fisher Scientific-USA
Glutamine	Gibco Thermo Fisher Scientific-USA
670 dye	Gibco Thermo Fisher Scientific-USA
CFSE	eBioscience Thermo Fisher Scientific-U.K
Trypsin enzyme	gibco-USA
PBS	Sigma-Aldrich-UK
DMSO	Sigma-Aldrich-USA
Paraformaldehyde	Sigma-Aldrich-Germany
Recombinant Human IFN-α	PeproTech-U.S.A
Recombinant Human IL-2	PeproTech-U.S.A
Human serum	Invitrogen Thermo Fisher Scientific-U.K
Hours serum	Invitrogen Thermo Fisher Scientific-U.K
Propidium Iodide	Miltenyi Biotec-Germany
DEPC-Treated water	Ambion-USA
Fetal Bovine serum (FBS)	Signa-Aldrich-USA
Fast SYBER Green master mix	Biosystem- Thermo Fisher- Lithuania
Live/DEADTM Fixable dye	Thermo Fisher-USA
Brefeldin A	Sigma-Aldrich-USA
Saponin	Sigma-Aldrich-UK
Maxpar Cell staining buffer	FLUDIGM-USA

Table 2.4 list of buffers and their preparation in the lab

Buffer	Preparation
1x Phosphate Buffered saline (1x PBS)	1 tablet PBS 100ml distilled H_2O
CMV-Coating buffer	1 capsule Carbonate-Bicarbonate Buffer 25ml distilled H_2O
CMV-dilution buffer	0.05% Tween20 1% BSA 1X PBS
Wash buffer	0.05% Tween20 1x PBS
Paraformaldehyde PFA	4.0% FPS distilled H_2O
0.1X TE buffer	9.9ml 10mM Tris-HCL 2ml 5mM EDTA 88ml distilled H_2O

Table 2.5 List of anti-human blocking antibodies

Blocking antibody	Manufacturer	Clone	Cat#
Purified anti human PDL1	BioLegend	29E2A3	329710
Purified anti human PDL2	BioLegend	M1H18	345504
Purified anti human CD226	BioLegend	11A8	338302
Purified anti human TIGIT	BioLegend	A15153G	372702
Purified anti human CD96	BioLegend	NK92.39	338402
Purified anti human CD155	BioLegend	SKP4	337602

Table 2.6 list of cell culture media used to maintain and grow up cells

Culture media	Components
Growth media (GM)	RPMI-1640 10% Fetal Calf Serum (FCS) 1% Penicillin/streptomycin 1% L-glutamine
NK-92 cells culture media	RPMI-1640 10% Fetal Calf Serum (FCS) 1% Penicillin/streptomycin 1% L-glutamine 5% human serum 10% hours serum 400IU/ml rhIL-2
NKL cells culture media	RPMI-1640 10% Fetal Calf Serum (FCS) 1% Penicillin/streptomycin 1% L-glutamine 400IU/ml rhIL-2
CHO cells culture media	F-12 Nut mix medium 10% Fetal Calf Serum (FCS) 1% Penicillin/streptomycin 1% L-glutamine
Freezing medium	90% FCS 10% DMSO

2.1.3 Cell lines

Suspension and adherent cell lines used for experiments in this study were cultured in 25cm^2 and 75cm^2 flasks in humidified incubator at 37°C, 5% CO_2 and these are listed with more information in **Table 2.7**

Table 2.7 List of suspension and adherent cell lines used in this study

Suspension cell line	Source
WTNK-92	Dr Jianmin Zuo (purchased from ATCC)
PD-1^{pos} NK-92	Generated by Dr Jianmin Zuo
WT-NKL	Gifted by University of Cardiff
PD-1^{pos} NKL	Generated by Dr Jianmin Zuo
K562 target cells	Dr Amandeep Kaur (purchased from ATCC)
721.221 target cells	Dr Amandeep Kaur (purchased from ATCC)
Adherent cell line	**Source**
WT-CHO cells	Dr Jianmin Zuo (purchased from ATCC)
CD155-CHO cells	Generated by Dr Jianmin Zuo

2.2 Study design and donors recruitment

2.2.1 B-CLL patient cohort

About 9ml of heparinised whole blood received from 75 untreated and Binet stage A, B-CLL patients from outpatient haematology clinics at Queen Elizabeth Hospital Birmingham (QEHB), and Heartlands Hospital Birmingham (HHB) following written informed consent form (REC no 10/H1206/58) with the median age of 65 years. Unfortunately, due to the pandemic and the subsequent circumstances, the patients' clinical data was not collected. The CMV sero-statues of those patients were determined within this study using in house CMV serum IgG ELISA which is showed in detail in this chapter.

2.2.2 Healthy controls

Age-matched healthy volunteers were recruited among staff over 50 years from Medical and Dental science college – University of Birmingham, with written and informed consent form (REC no 2002/073). 9ml of heparinised whole blood were collected from volunteers by trained phlebotomist. Also, some healthy donors were obtained from platelet donors attending NHS Blood and Transplant Services Birmingham as fresh blood (cones). Healthy volunteers were used as controls in this study.

2.3 Processing of peripheral blood samples

2.3.1 Peripheral Blood Mononuclear cells (PBMCs) isolation

Heparinised whole blood received from patients and healthy controls were processed within 24 hours of collection. The work was achieved under sterile condition (inside hood) and the isolation was performed using density gradient centrifugation method. Using 50ml conical sterile tubes, peripheral blood was diluted 1:1 with RPMI media and gently layered over 15ml Lymphoprep™ (2:1 ratio). Tubes spun down at 645x g without brake for 25 minutes at room temperature. The second layer (buffy coat layer) containing PBMCs was gently removed using transfer pipette into new 50ml tube and washed with 50ml RPMI media at 523x g for 10 minutes to remove the plasma and proteins residuals (**Figure 2.1**). Cell pellet was resuspended in RPMI media, and the cell count was determined by disposable haematocytometer chamber (Fast-Read 102®, Kova International). PBMCs were then centrifuged at lower speed 316x g for 5 minutes to get rid of remaining platelets. The fresh PBMCs were either used straightway in daily experiments or prepared for cryopreservation at -80 or liquid nitrogen (described below). Meanwhile, 2 ml of plasma (top layer) was saved in 2ml cryovials in -20 which is used later for CMV ELISA test.

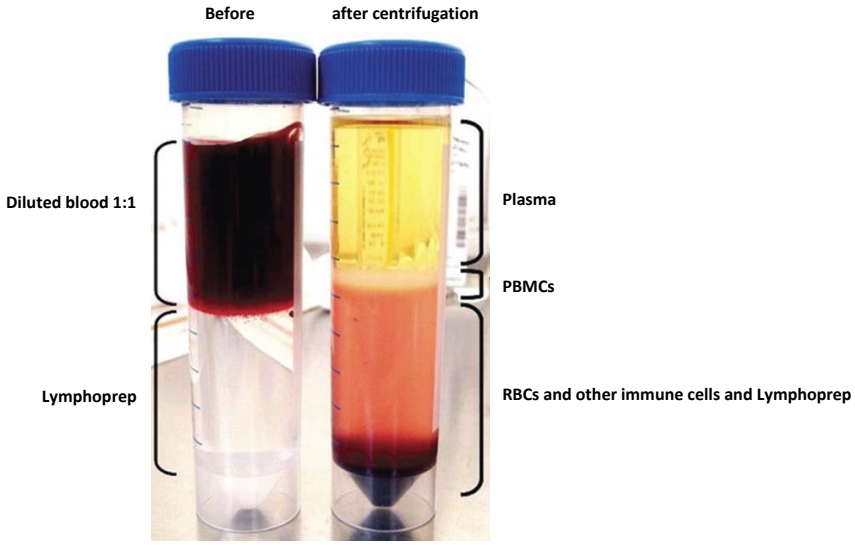

Figure 2.1 Peripheral blood mononuclear cells isolations from the whole blood

2.3.2 PBMCs cryopreservation and storage

After the final wash of PBMCs isolation processing, cell pellet was resuspended in appropriate cold freezing media (1 to 2ml). Freezing media was added in dropwise with gentle swirling the tube. PBMCs were aliquoted in 1 or 2 cryovial tubes no more than $20x10^6$ PBMCs/vail, and immediately transferred to Mr-Frosty^{TM} freezing container containing Isopropanol (Fisher Scientific, Cat #10674732), which allows cells to cool at gradual and constant degree 1°C/minute. Mr-Frosty was then placed overnight at -80 before freezer transferred to liquid nitrogen for longer storage.

2.3.3 Thawing cryopreserved PBMCs

PBMCs were brought from -80 freezer or liquid nitrogen in dry ice and immediately recovered rapid thawing at 37°C water bath for 2 minutes. Pre-warmed growth media was added gradually and slowly to the cells to provide high level of cell viability and functionality during assays. Meanwhile, cell clumps were filtered if necessary, using 5ml FACS tubes with strainer cap (EASY strainer^{TM} cells Sieves). The cells were washed with 20ml of growth media at 363x g for 5 minutes. The cell pellet was then resuspended in appropriate volume of PBS or growth media for assays.

2.4 Maintenance of NK cells and cell lines

All cells were maintained and grown in tissue culture flasks of 25cm^2 and 75cm^2 at 37°C, 5% CO_2 humidified incubator. Primary NK cells isolated from PBMCs were maintained and activated overnight in general growth media. NKL cell lines were grown in tissue culture flasks and maintained in general growth media supplemented with 400IU rhIL-2 (NKL media). NK-92 cell lines were grown with NK-92 media, which is supplemented with 10% hours and 5% human serum and rhIL-2. NK cell lines were passaged/used when 80% confluent by removing old media and replacing it with new at 1/3 dilution. K562 and 721.221 target cells were also grown and maintained in general growth media and were passaged twice a week when 80% confluent. CHO cell lines were grown in Ham's F12K media supplemented with 10% FBS. CHO cells were passaged three times a week by removing old media and washing cells with PBS and detached from the flask by trypsinising with trypsin for 3 to 5 minutes at 37°C, 5%CO_2. Trypsin was neutralised with fresh growth media and a fraction of cells were transferred to new culture flask and topped with appropriate volume with growth media.

2.5 Absolute count of NK cells and tumor B-CLL cells

Fresh heparinised blood samples from B-CLL patients were received from the Queen Elizabeth hospital-Birmingham and were prepared immediately. The volume of the blood was measured for each patient (tube) and PBMCs were isolated as described in section 2.3.1. PBMCs of each patient were washed once with PBS and resuspended in appropriate volume of PBS (5ml) depends on the number of the PBMCs. 100µl of cell suspension (1:50) was transferred to a new FACS tube and stained with adding 5µl of the following antibodies CD56-PE-Cy7, CD3-Perp.cy5.5, CD19-PB, CD5-FITC and CD16 and incubated for 20 to 25 minutes at 4°C. Cells were washed once with 2ml PBS at 413x g for 5 minutes and resuspended in 300µl PBS with gentle mix. CountBright beads were vortexed for 30sec and 10µl was added to the cell suspension with pipetting up and down for mixing. 2µl PI was added just before cell acquisition on Gallios^{TM}. Cells were run on Gallios^{TM} for fixed period (3 minutes). Data were analysed offline on Kaluza software where total NK cells $CD56^{pos}$ $CD3^{neg}$ and four NK subsets $CD56^{bright}$ $CD16^{neg}$, $CD56^{bright}$ $CD16^{pos}$, $CD56^{dim}$ $CD16^{neg}$, $CD56^{dim}$ $CD16^{pos}$ were identified and gated. Also, Tumor B-CLL cells $CD19^{pos}$ $CD5^{pos}$ and CountBright beads were identified and gated. Cell concentration was calculated using the following equation:

$$\left(\frac{\text{Cell events}}{\text{Beads events}}\right) x \left(\frac{\text{Assigned beads concentration}}{\text{Sample volume 300ul}}\right) = \text{X cells/ul}$$

$$\text{X cells } x \text{ 50 (dilution factor) } x \text{ 9 (blood volume) } x \text{ 2 (blood dilution)}$$

$$= \text{concentration of cell/µl}$$

2.6 In House CMV IgG ELISA assay

CMV sero-status of B-CLL patients and HCs was established in the lab using in house CMV IgG Enzyme Linked Immunosorbant Assay (ELISA) to detect plasma IgG. This was carried out in two days length as following.

2.6.1 Coating the plate with CMV Lysate

Day1, mock and lysate (UV-inactivated, from CMV infected fibroblasts) were diluted with coating buffer at 1/4000 (1µl/4ml). Using 96 well plate (Plates MAXISORP^{TM}, Cat #44-2404-21) 50µl of diluted mock or lysate were plated in corresponding wells in duplicate after washing the plate once with 200µl washing buffer. The plate was sealed and left overnight at fridge 4°C. Mock lysate served as negative fraction, while lysate as positive fraction.

2.6.2 setting up the experimental plate

On day 2, using spare 96-well plate plasma samples of B-CLL and HCs were diluted in at 1/60 with dilution buffer. Also, serial dilutions were prepared for the standard wells by adding 80µl dilution buffer to the first two wells (duplicate) of first column and 75µl for the remining wells to make 7 serial dilutions. 20µl of the standard was added to the first well, mixed well and then 25µl was transferred to the next well and carried out until final well (well 7). As 25µl was disposed, this leaves 75µl solution in each standard well.

The MaxiSorp plate coated with lysate was washed 3 times with 200µl /wash by wash buffer. 90µl dilution buffer were added into each well of the plate and 10µl of serial standards or

diluted plasma were added in duplicate into corresponding wells (standard/sample dilution is 1/600). The plate was covered and incubated for 1 hour at room temperature, then the plate was washed 3 times (200µl/wash) with wash buffer. Conjugate antibody (goat anti-human IgG-HRP) was vortexed and prepared by diluting 1.25µl in 10ml of dilution buffer (1:8000) and then 100µl was added into test/standard wells. The plate was covered and incubated again for another hour. After the incubation the plate was washed 3 times with wash buffer and 100µl of TMB solution (1 Step™ Ultra TMB-ELISA) was added to the plate wells. The plate was covered and incubated for 15 minutes at room temperature in dark place. After yellow colour developed 100µl of 1M HCL was added into each well to stop the reaction. Plate was read immediately (within 15 minutes) by ELISA plate reader at 450nm (Bio-Rad, iMark™ Microplate Reader) and data was exported and analysed by Excel.

In Excel sheet, data was analysed by calculating the average values of duplicated mock and lysate. For both samples and standard, the average of mock values was subtracted from the average values of lysate. The generated values were transferred to GraphPad prism and standard values were transformed using X=logX. After generating the standard curve, CMV IgG titration of samples were determined from standard curve. Titres over 10U/ml are considered positive. Representative example is shown in (**Figure 2.2**).

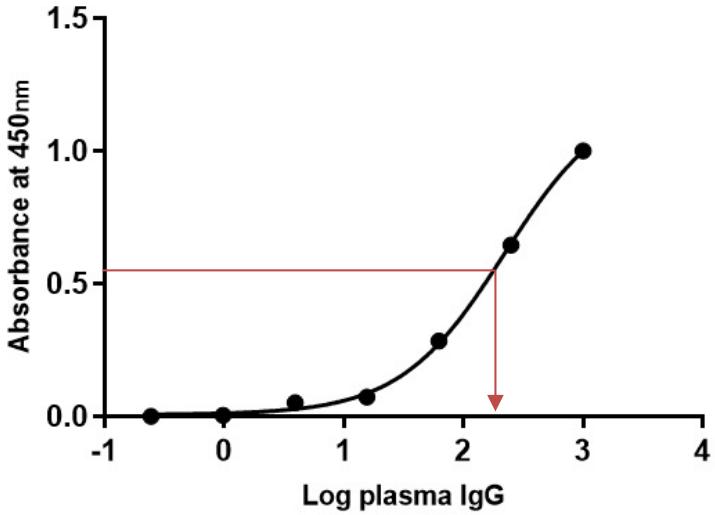

	Mock1	Mock2	Average	Lysate1	Lysate2	Average	L-M	IgG titre
Positive	0.166358	0.16731	0.166834	0.580446	0.556595	0.568521	0.401687	107.5581
Negative	0.200595	0.200371	0.200483	0.203305	0.385251	0.294278	0.093795	0.0187

Figure 2.2 An example of CMV plasma IgG ELISA calculations.

Patient/Hc plasma IgG titration was determined from the standard curve (top graph) as IgG titration >10U/ml is considered positive and <10U/ml is negative (lower table). The table shows an example of ELISA readings of mock/lysate and the calculations for CMV positive vs CMV negative.

2.7 TGF-b (LAP) ELISA assay

Plasma samples of B-CLL patients and HCs were prepared prior starting the procedure. The plasma samples were diluted 1:10 with assay buffer, and 20µl 1N HCL was added to 200µl prediluted samples, mixed and incubated to 1 hour at room temperature. Samples were neutralized with 20µl 1N NaOH. 7 serial dilutions from standard were prepared. The number of microwell stripes needed for the assay was determined and washed with 400µl wash buffer. Microwell strips were taped and stripped on pad towel to remove excess wash buffer. 100µl of assay buffer (1x) was added into standard wells in duplicate and topped with 100µl of prepared serial standards. Another 100µl of assay buffer (1x) was added to the blank wells, and 60µl to sample wells in duplicate. 40µl of each prepared plasma was added into sample wells. All wells were vortexed and covered with adherent film and incubated at room temperature on a microplate shaker for 2 hours. The cover was removed, liquid discarded, and microwell was washed with 400µl wash buffer 5 times. After taping and stripping the microwell on pad towel, 100µl of Biotin Conjugate was added to all wells, covered, and incubated for 1hour at room temperature on microplate shaker. Cover was removed and wells was emptied, washed, and followed by adding 100µl of streptavidin HRP to all wells and incubated for another hour on the shaker. Microwell was washed 5 times and 100µl of TMB substrate solution was added to all wells and incubated at room temperature for about 30 minutes in the dark. Once the blue colour developed, 100µl stop solution was added to all wells and microwell was read on ELISA reader at 620nm.

2.8 Flow cytometry analysis

Flow cytometry with ten channels (Gallios^{TM} Flow cytometry Backman Coulter, Inc.) with four lasers (Blue, Red, Violet and Green) was used in this study as a major read out and analysis tool. Flow cytometry was used to study the phenotype and functions of primary NK cells and NK cell lines including cytokines production and cytotoxicity. Data analysis was performed offline using Kalusa flow analysis software version 2.1a (Backman Coulter Inc). The use of multicolour flow cytometry requires compensation. In this section, setting up flow cytometry, antibody panels and protocols used for cell surface staining are described.

2.8.1 Compensation of flow cytometry

Before performing the compensation, panels were set up on Gallios^{TM} with optimal voltages for each fluorescence channel using unstained cells for each antibody panel. The compensation was performed to correct the fluorescence signal and to minimise the fluorochromes spillover between channels. Following setting up the panel, a compensation protocol from VersaComp Antibody Capture beads kit (Beckman Coulter, Inc) was performed. One drop of each negative and positive beads was added into labelled 5ml polypropylene FACS tubes (the number of tubes are equal to the number of fluorochromes used in the antibody panel) and 100µl of PBS was added to each tube and spun down for a minute at 363x g to bring the tube content to the tube bottom. 5µl of a single fluorochrome-antibody conjugates were added into corresponding individual tubes containing beads, vortexed and incubated for 30 minutes at room temperature and in the dark place. Tubes were then washed with 2ml PBS and centrifuged at 645x g for 10 minutes. The supernatant was aspirated carefully using transfer pipette leaving beads with approximately 200µl of supernatant, this is to avoid disturbing the beads pellet. Beads were resuspended in PBS to bring the total volume to 400µl then vortexed.

The compensation tubes were made freshly prior acquisition on the Gallios™ and stored at 4°C for one week for re-use. The compensation was performed according to the manufacturer's instruction and compensation matrix was analysed by Kaluza software, then applied to the data acquired using the same antibody panel on Gallios™.

2.8.2 NK cell surface staining

Fresh or frozen PBMCs form B-CLL patients or HCs were used to analyse NK cell surface expression. About $1x10^6$ PBMCs were washed with 2ml PBS at 413x g for 5 minutes and supernatant was discarded. Cells were resuspended in the residual supernatant (about 50µl) and co-incubated with the relevant antibodies panel at 4°C for 20 to 25 minutes in the dark. 2ml PBS was added to each tube and centrifuged at 413x g for 5 minutes. The supernatant was discarded, and cells were resuspended in the residual and topped with 200µl PBS. 1µl/200µl cell suspension of PI was added to each tube just prior sample acquisition on the Gallios™.

The antibodies panel used for analysing NK cell differentiation in B-CLL patients and HCs including CD56, CD57, NKG2A, CD16 and analysing PD-1 expression is shown in **Table 2.8.**

The antibodies panel analysing immune checkpoint expression on NK cells is described in **Table 2.9**.Also, adhesion molecule and CD96 expressions on NK cells was studied using

Table 2.8 Antibodies panel for NK cell differentiation and PD-1 expression

Channel	Antibody	Fluorochrome	Manufacturer	Clone	Cat. No.
FL1	TNF-a	AF-488	BioLegend	MAB11	502915
FL2	PD-1	PE	BioLegend	EH12.2H7	329906
FL4	CD3	PerCP/Cy5.5	BioLegend	HIT3a	300328
FL5	CD56	PE-Cy7	BioLegend	HCD56	318318
FL7	IFN-g	AF-700	BioLegend	4S.B3	502520
FL9	CD19	Pacific blue (PB)	BioLegend	SJ25C1	363036

Table 2.9 Antibodies panel for checkpoints expression on NK cells

Channel	Antibody	Fluorochrome	Manufacturer	Clone	Cat. No.
FL1	CD16	AF-488	BioLegend	3G8	302019
FL2	Siglec-7	PE	BioLegend	6-434	339204
FL3	CD19 CD14	ECD ECD	Beckman coulter	HD237 RMO52	6604551 IM2707U
FL4	CTLA-4	PerCP/Cy5.5	BioLegend	L3D10	349928
FL5	LAG-3	PE/Cy7	BioLegend	11C3C65	369310
FL6	TIGIT	APC	BioLegend	A15153G	372706
FL7	CD3	AF-700	BioLegend	HIT39	300324
FL8	CD56	APC-Cy7	BioLegend	HCD56	318332
FL9	Tim-3	PB	BioLegend	F38-2E2	345042
FL10	PD-1	Brilliant violet 510	BioLegend	EH12.2H7	329932

Table 2.10 Antibodies panel for adhesion molecules and other important markers on NK cells

Channel	Antibody	Fluorochrome	Manufacturer	Clone	Cat. No.
FL1	CD162	AF-488	BioLegend	AK4	304916
FL2	CD95	PE	BioLegend	DX2	305608
FL3	CD16	PE-Dazzle	BioLegend	3G8	302054
FL4	CD18	PerCP/Cy5.5	BioLegend	CBR.LFA-12	366315
FL5	CD49a	PE/Cy7	BioLegend	TS2/7	328312
FL6	CD95L	APC	BioLegend	MFL3	106610
FL7	CD3	AF-700	BioLegend	HIT39	300324
FL8	CD56	APC-Cy7	BioLegend	HCD56	318332
FL9	CD19 CD14	PB PB	BioLegend BioLegend	SJ25C1	363036
FL10	CD49d	Brilliant violet 510	BioLegend	9F10	304318

Table 2.11 Antibodies panel for adhesion molecules and other important markers on NK cells

Channel	Antibody	Fluorochrome	Manufacturer	Clone	Cat. No.
FL1	CD11b	AF-488	BioLegend	CBRM1/5	301404
FL2	NKG2C	PE	BioLegend	S19005E	375004
FL3	CD16	PE-Dazzle	BioLegend	3G8	302054
FL4	CD11a	PerCP/Cy5.5	BioLegend	HI111	301230
FL5	CD43	PE/Cy7	BioLegend	CD43-10G7	343208
FL6	CD96	APC	BioLegend	NK92.39	338410
FL7	CD3	AF-700	BioLegend	HIT39	300324
FL8	CD56	APC-Cy7	BioLegend	HCD56	318332
FL9	CD19 CD14	PB PB	BioLegend BioLegend	SJ25C1	363036
FL10	CD11c	Brilliant violet 510	BioLegend	3.9	301634

2.8.3 Surface staining of NK cell lines

The phenotype of NK cell lines (NK-92 and NKL cells) was studied using Gallios^{TM} flow cytometry. Similar staining protocol was applied as in primary NK cells. Approximately $0.5x10^6$ each of NK cell lines were washed separately and resuspended in the residual and co-incubated with 5µl of single fluorochrome conjugated antibodies at 4°C for 20 to 25 minutes. Cells were washed with 2ml PBS and centrifuged at 363x g for 5 minutes. The supernatant was discarded, and cells were resuspended in 200µl PBS prior running on Gallios^{TM}.

The antibodies panel for NK cell line phenotype focused on the expression of activating receptors on wt-NK cell line versus PD-1 transduced NK cell lines which is shown in **Table 2.12**

Table 2.12 Antibodies panel for activating receptors on NK cell lines

Channel	Antibody	Fluorochrome	Manufacturer	Clone	Cat. No.
FL1	CD16	AF-488	BioLegend	3G8	302019
FL2	NKG2D	PE	BioLegend	1D11	320806
FL3	DNAM-1	PE-Dazzle	BioLegend	11A8	338318
FL5	NKp46	PE/Cy7	BioLegend	9E2	331916
FL6	CD28	APC	BioLegend	CD28.2	983406
FL8	CD56	APC-Cy7	BioLegend	HCD56	318332
FL9	CD57	PB	BioLegend	HNK-1	359608
FL10	PD-1	Brilliant violet 510	BioLegend	EH12.2H7	329932

2.8.4 Fluorescence Minus One (FMO) control

Fluorescence Minus One (FMO) controls were performed throughout the surface staining of NK cells, particularly for markers that up-regulated on NK cells. FMO controls is involved in identifying the background staining due to fluorescence spillover, therefore determining the cut-off point between fluorescence background and the actual positive population. The FMO FACS tube contains NK cells stained with all fluorochrome-conjugated antibodies except one that need to be tested in the specific antibody panel. Below is some examples of FMO controls for PD-1,CTLA-4 and CD18.

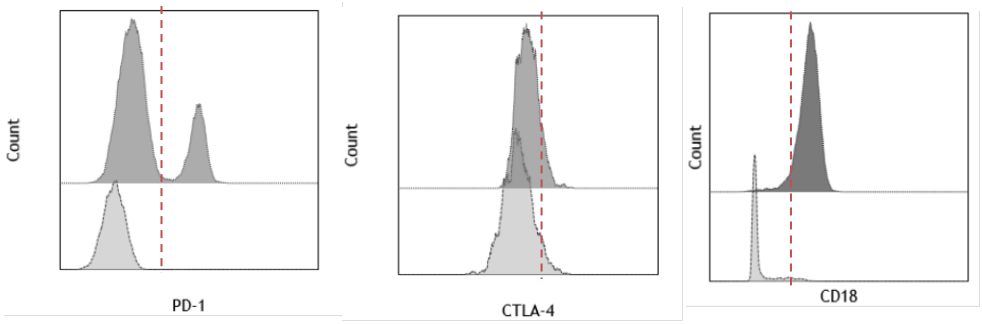

Figure 2.3 Examples of FMO staining for PD-1, CTLA-4 and CD18.

NK cells were stained with all antibody panel except one and acquired by flow cytometry.

2.9 Intracellular cytokine staining of NK cells

2 x 10^6 PBMCs were co-cultured with K562 target cells overnight in the presence of Brefeldin A in a total volume of 0.5ml growth media, at 1:1 ratio at 37°C, 5% CO_2. Next day, cells were washed with PBS and resuspended in the residual buffer and stained with appropriate surface antibodies panel (**Table 2.13**) with live dye 1µl/100µl cell suspension for 30 minutes at 4°C. Cells were then washed with 2ml PBS and supernatant was discarded. Cells were resuspended and vortexed in100µl of 4% paraformaldehyde (PFA) for 15 minutes for fixation. Cells were washed with 4ml PBS at 2000rpm/645g for 10 minutes, resuspended in the residual volume and permeabilised in 100µl of 0.5% Saponin for 5 minutes in the dark at room temperature with gentle mixing. In the presence of saponin, cytokines antibodies panel was added subsequently and incubated for 30 minutes at room temperature in the dark. Cells were then washed with PBS and resuspended in 200µl PBS buffer for flow cytometry acquisition.

Table 2.13 Antibodies panel for NK cell intracellular cytokine staining

Channel	Antibody	Fluorochrome	Manufacturer	Clone	Cat. No.
FL1	TNF-a	AF-488	BioLegend	MAB11	502915
FL2	IL-10	PE	BioLegend	JE53-19F1	506804
FL3	CD16	PE-Dazzle	BioLegend	3G8	302054
FL4	CD3	PerCP/Cy5.5	BioLegend	HIT3a	300328
FL5	CD56	PE/Cy7	BioLegend	HCD56	318318
FL6	IL-5	APC	BioLegend	TRFK5	504306
FL7	IFN-g	AF-700	BioLegend	4S.B3	502520
FL8	IL-4	APC-Cy7	BioLegend	MP4-25D2	500834
FL9	CD19	PB	BioLegend	SJ25C1	363036
FL10	IL-2	Brilliant violet 510	BioLegend	MQ1-17H12	500338

2.10 PD-1 ligands blockade and degranulation and cytokines secretion of PD-1^{pos} NK cells

Fresh or frozen PBMCs from B-CLL patients with high percentage of PD-1^{pos} NK cells were used in this experiment. Frozen PBMCs were taken out from liquid nitrogen and thawed immediately as indicated earlier. The degranulation assay was set up using purified NK cells, whilst cytokines assay using whole PBMCs. In the degranulation assay, NK cells were enriched using a negative selection EasySep^{TM} Haman NK cell Enrichment Kit (**described in detail in the section 2.9.1**). Purified NK cells were counted and washed in 2ml PBS at 413x g for 5 minutes. NK cells were resuspended at concentration of 2x10^6 NK cells/ml in growth media. 1ml of each K562 or 721.221 (express PDL1 and PDL2) target cells were taken from culture flask, counted and washed with growth media and resuspended at concentration of 5x of NK

cell concentration (E:T ration 1:5). Target cell lines were resuspended in growth media at $1x10^7$ cells/ml. Using sterile round well 96 well plate, 100µl each of target cell line suspension was plated separately and in duplicate (2 wells for no PD-1 ligands blocking and another 2 wells set up for PD-1 ligands blockade for each type of target cell line). 9µl each of anti PDL1 and PDL2 blocking antibodies were added into blocking wells for both cell lines in duplicate, mixed well and incubated for 40 to 60 minutes at 37°C, 5% CO_2 to allow blocking antibodies binding to their ligands on target cells. 100µl of NK cell suspension was topped on each of well containing target cells and mixed gently by pipetting up and down and incubated for 5 hours at 37°C, 5% CO_2. After one hour of incubation 7µl of anti CD107a-FITC antibody was added into all wells with gentle mix to capture the CD107a molecules on the surface of degranulating NK cells. Another 4 wells were set up using only 100µl NK suspension with 100µl growth media with and without 7µl of anti CD107a-FITC antibody as a controls.

After 5 hours incubation, cells were transferred to labelled 5ml FACS tubes, washed with PBS at 363x g for 5 minutes. Supernatant was discarded and cells resuspended in the residual volumes and stained with antibody panel (**Table 2.14**) for 30 minutes at ice and in dark to prevent photobleaching. Tubes were then washed with 2ml PBS at 363x g for 5 minutes, supernatant was discarded, and cells resuspended in residual volumes and 200µl of PBS was added to each tube. 1µl of PI was added to all tubes just prior sample acquisition on Gallios™.

Cytokines production assay (IFN-γ and TNF-α) was set up as described earlier in **Section 2.7** but K562 and 721.221 target cells were co-incubated with anti PDL-1 and PDL-2 blocking antibodies for 40 to 60 minutes at 37°C 5% CO_2 followed by adding PBMCs (1:1ratio) and in the presence 0.5µl Brefeldin A. PBMCs were incubated only with growth media and Brefeldin

A as a negative control. All conditions were set up in duplicate. Tubes were then incubated overnight at 37°C 5% CO_2. Next day cells were washed, and intracellular cytokines staining was performed as described earlier in section 2.7 (**Table 2.15**).

Table 2.14 Antibodies panel for CD107a expression on NK cells before and after PDL-1 blocking

Channel	Antibody	Fluorochrome	Manufacturer	Clone	Cat. No.
FL1	CD107a	FITC	BioLegend	EBIOH4A3	4312979
FL2	PD-1	PE	BioLegend	EH12.2H7	329906
FL5	CD56	PE-Cy7	BioLegend	HCD56	318318

Table 2.15 Antibodies panel for intracellular cytokines staining before and after PDL-1 blocking

Channel	Antibody	Fluorochrome	Manufacturer	Clone	Cat. No.
FL1	TNF-a	AF-488	BioLegend	MAB11	502915
FL2	PD-1	PE	BioLegend	EH12.2H7	329906
FL4	CD3	PerCP/Cy5.5	BioLegend	HIT3a	300328
FL5	CD56	PE-Cy7	BioLegend	HCD56	318318
FL7	IFN-g	AF-700	BioLegend	4S.B3	502520
FL9	CD19	PB	BioLegend	SJ25C1	363036

2.11 DNAM-1 dependent NK cytotoxicity

To determine the capacity of DNAM-1 dependent NK cytotoxicity in B-CLL patients, an optimised 3-day assay was performed using purified NK cells from B-CLL patients and age-matched healthy controls and Chinese hamster ovary cells (CHO cells). As detailed below the experiments were set up using different E:T ratios by co-culturing CD155 transduced CHO cells (CD155-CHO cells) and wt-CHO cells as a control with pre-activated NK cells using IFN-α.

2.11.1 NK cell enrichment and activation

The negative selection EasySep™ Haman NK cell Enrichment Kit (STEMCELL™ Technology, Cat #19055) was used to isolate NK cells from frozen or fresh PBMCs of both B-CLL patients and HCs. According to the manufactures' instructions, about $25x10^6$ PBMCs were used in 15 ml falcon tube for each enrichment. Cells were washed in PBS at 413x g for 5 minutes. $1x10^6$ PBMCs were spared in 5 ml polypropylene FACS tube for purity test after isolation.

Using polystyrene round bottom FACS tube, PBMCs were resuspended in 0.5ml of sterile PBS at a maximum concentration of $5x10^7$ cells/ml ($25x10^6/5x10^7$= 0.5ml). To get rid of unwanted cells (except NK cells), 25µl of EasySep™ human NK cell enrichment cocktail (50µl /ml of cell suspension) were added to the cell suspension with mixing. The enrichment cocktail contains antibodies that can bind to the surface markers of all non-NK cells. The mixture was incubated for 10 minutes at room temperature. EasySepTM D magnetic particles was vortexed for 30 seconds and 50µl (100µl/ml) were added to the mixture and mixed well and incubated for 5 minutes at room temperature. The cell suspension was topped up to 2.5ml of PBS with a

gentle mix up and down. Tubes were then placed in an EasySepTM magnet and left for 2 to 5 minutes at room temperature. Unwanted cells (non-NK cells) attached with antibodies and magnetic particles were separated from NK cells to the side of 5ml tube that touching the magnet. While the tube in the magnet, NK cells in the suspension were transferred by pipette to a new 5ml FACS tube and NK cell count was performed. NK cells were washed with PBS to remove the residual antibodies/particles at 363x g for 5 minutes and resuspend in the desired concentration with growth media. Also, about $1x10^5$ NK cells were spared to test the purity of purification by flow cytometry.

For NK cell activation, 1 x 10^6 NK cells were resuspended in 0.5ml of growth media and plated in 48 well plate, followed by adding 20ug/ml of IFN-α for overnight activation at 37°C, and 5% CO_2.

2.11.2 High purity of enriched NK cells

The purity of NK cell isolation from PBMCs was carried out using flow cytometry. PBMCs and purified NK cells were incubated with anti CD3-FITC, CD56-PE/Cy7 and CD19-EDC antibodies for 20 minutes at 4°C. Cells were then washed with 2ml PBS at 413x g for 5 minutes and supernatant was discarded. The cell pellets were resuspended in appropriate volume of PBS and just before acquiring the samples on flow cytometry 1µl of PI was added to the 200 µl of cell suspension. The purity of NK cells $CD56^+$ $CD3^-$ was always > 98%.

2.11.3 Labelling of CHO target cells

$2.0x10^6$ each of CHO cell type were used to set up this experiment. Wt-CHO and CD155-CHO cells were labelled separately with different dyes. Wt-CHO cells were labelled with 670 dye and CD155-CHO cells with CFSE dye. Cells were washed twice with sterile PBS and centrifuged at 413x g for 5 minutes. After the second wash all supernatant was removed leaving cell pallet at the bottom of the 15ml falcon tube which were then resuspended in 200µl PBS. 5µM of CFSE and 670 dyes were diluted at 1/50 (1µl o 49ml PBS) and 10µl of diluted CFSE or 670 dye were added to 200µl of cell suspension, mixed well and incubated in 37°C and 5% CO_2 for 10 minutes. Cells were washed twice with 10% FCS RPMI at 413x g for 5 minutes and resuspended in 10ml of the same media and incubated again for 15 minutes at 37°C, 5% CO_2. Meanwhile labelled wt-CHO cells and CD155-CHO cells were counted and diluted to the concentration of $5x10^5$ cells/ml. The number of wells needed to set up the experiment with different conditions was calculated to triplicate every condition.

2.11.4 Set up the ratios of effector NK cells to target CHO cells

A 50:50 mixture of CD155 transduced CHO cells and wt-CHO cells at concentration of $5x10^5$ cells/ml was prepared in 15ml falcon tube. After they were mixed well, 100µl of cell mixture was transferred to each well in 96 U bottom well plate ($5x10^4$ cells per well). The well plate was gently mixed to give a homogenous mixture of cells. Plate was covered and incubated overnight at 37°C and 5% CO_2 incubator to allow cells to settle and adhere to the bottom of the well. On the following day, IFN-α activated NK cells were harvested, counted again, and washed with growth media at 363x g for 5 minutes and resuspended in growth media at concentration of $5x10^5$ NK cells/ml. After discarding all old medium from CHO wells, 100µl of NK cell suspension ($5x10^4$ NK cells per well) were added to each well of CHO cells except

the control well that topped up with 100µl of growth media to make up the final volume to 200µl. This will make an E:T ration 1:1 and further ratios 0.25:1 and 4:1 were made as well. Cell mixture in wells were mixed by gently pipetting up and down 3 times and then incubated overnight 17 hrs in 37°C and 5% CO_2 incubator.

For the TIGIT and CD96 blockades, the experiments were set up alongside and in the same previous plate. 8µl of each anti-TIGIT and/or anti-CD96 antibodies were added to the corresponding wells in triplicates to give a final concentration of 40ug/ml.

On the third day, the supernatant was taken out from the wells, and each well washed once with 100ul PBS. 30 to 40µl of Trypsin were added to each well and incubated for 3 to 5 minutes at 37°C to release the CHO cells from the bottom of wells. 200µl PBS were added to each well, mixed gently and all suspension in each well were transferred to one FACS tube and then analysed by Gallios™

Table 2.16 shows diagram of experiment plate

Condition	Well-1	Well-2	Well-3
Control	Wt-CHO+CD155-CHO cells	Wt-CHO+CD155-CHO cells	Wt-CHO+CD155-CHO cells
HD-NK cells	Wt-CHO+CD155-CHO+HD-NK cells	Wt-CHO+CD155-CHO+HD-NK cells	Wt-CHO+CD155-CHO+HD-NK cells
CLL-NK cells	Wt-CHO+CD155-CHO+CLL-NK cells	Wt-CHO+CD155-CHO+CLL-NK cells	Wt-CHO+CD155-CHO+CLL-NK cells

2.11.5 Percentage of DNAM-1 dependent NK killing calculation

After the cells were analysed by flow cytometry, the average ratios of CFSE negative (670 positive) to CFSE positive (670 negative) was calculated for all condition of control, B-CLL and HCs to determine the percentage of specific DNAM-1 dependent NK killing before and after TIGIT and CD96 blockades. wt-CHO cells (CFSE negative) serves as an internal control, as NK cells are supposed to only kill the CD155-CHO cells (CFSE positive). To compare the ratio changes from control wells, we can calculate the percentage of CD155-CHO cells being killed. And this killing is dependent on the DNAM-1/TIGIT/CD96 interaction with CD155. The specific lysis was calculated using the following equation:

% of specific lysis = 100x{1-(average of control ratio/average of experimental ratio)}.

The control ratio refers to the CFSE negative/CFSE positive CHO cells without NK cells. Whilst the experimental ratio refers to the CFSE negative/CFSE positive CHO cells in the presence of effector NK cells as shown in **Figure 2.4**. This experiment was validated by blocking DNAM-1 receptor using anti-DNAM-1 antibody.

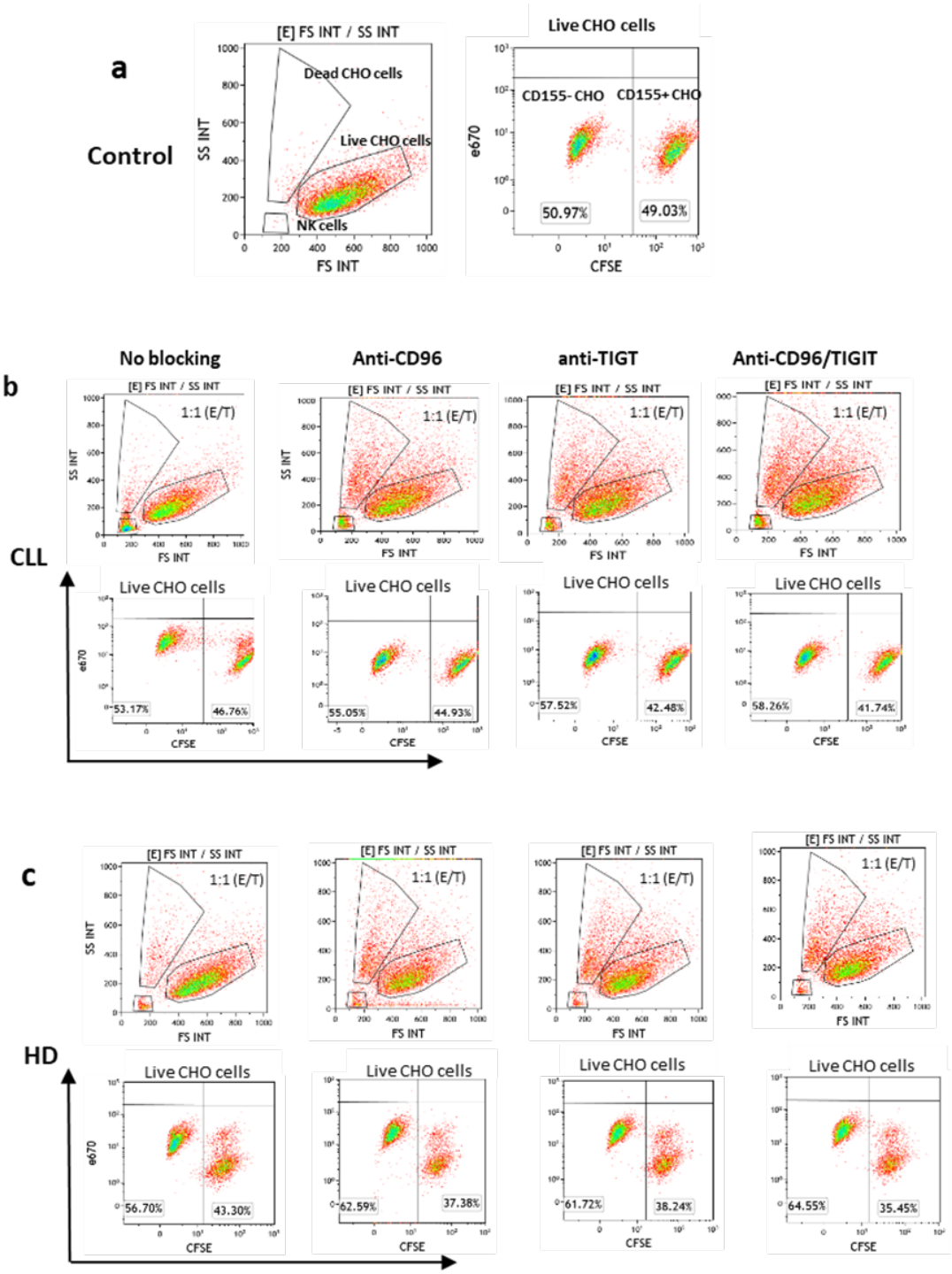

Figure 2.4 Gating strategy and representative examples of optimised DNAM-1 dependent NK cytotoxicity assay.

(a) Shows the gating of mixture (50:50) live wt-CHO and CD155-CHO cells without adding effector NK cells (control). Representative flow plots of DNAM-1 dependent NK killing before and after TIGIT and or CD96 blockade (1:1 ratio) in B-CLL patients (**b**) compared with HCs (**c**).

2.12 In-vitro migration of NK cells assay

The migration assay was achieved using polycarbonate membrane trans-well plate with 6.5mm diameter and 5um pore size (Corning Costar, US). This experiment was performed in sterile environment and aimed to assess the potential migration capacity of NK cells from B-CLL patients compared to NK cells from HCs.

2.12.1 NK cell enrichment

NK cells were enriched from fresh or frozen PBMCs of B-CLL patients and HCs using negative selection EasySep^{TM} Haman NK cell Enrichment Kit as described earlier in **section 2.9.1.** The purity of NK cell enrichment was >95% every time. After washing NK cells with 2ml PBS, NK cells were counted and $5x10^5$ NK cells from each donor were resuspended in 100µl growth media.

2.12.2 setting up trans-well plate

The inserts (upper chamber) of Trans-well plate was pre-soaked in growth media for 10 to 15 minutes. K562 target cell lines were taken out from cell culture and $5x10^5$ cells were washed with PBS at 413x g for 5 minutes and resuspended in 600µl growth media and transferred to bottom chamber. NK cell suspension (100µl) was then added to the inserts after discarding the old media. Inserts were then placed inside the bottom chamber in right position. For control, 100µl of NK suspension was placed on 600µl growth media without K562 target cells. Trans-well plate was covered and incubated for overnight (~ 16hours) in humidified incubator at 37°C, 5% CO_2. Each well was set up in duplicate.

In the next day, media from the upper and lower chambers were harvested in separate FACS tubes with PBS wash to make sure no NK cells leftover. Tubes were spun down at 363x g for 5 minutes and supernatant was aspirated carefully by transfer pipette. Cells were resuspended in the residuals and stained with anti CD3 FITC and anti CD56 PE-Cy7 antibodies for 20 to 25 minutes.

2.12.3 NK cell counting

After the staining, cells were washed with PBS and resuspended 300µl PBS. Counting beads (Count Bright^{TM} life technology) was vortexed for 30 sec and 10µl was added to the cell suspension just prior acquisition on Gallios^{TM}.

Data was analysed by Kalusa software and migrated NK cell population (lower chamber) and counting beads were identified and gated on. Also, non-migrated NK cell population (upper chamber) with counting beads were identified and gated on. The number of migrated and non-migrated NK cells was calculated using this equation:

Number of migrated NK cells. = (NK cell events / beads events) x number of added beads (105000)

% migrated NK cells = (number of migrated NK cells /total number of NK cells) x 100

2.13 PD-1^{pos} NK cell line cytotoxicity assay

The cytotoxicity of PD-1 transduced NK cells lines (PD-1^{pos} NK-92 and PD-1^{pos} NKL cell lines) were investigated against K562 and PDL1/L2 expressing 721.221 target cells and compared with their corresponding wild type NK-92 and NKL cell lines. Both effector cells and target cells were maintained in appropriate media at 37°C, 5% CO_2 incubator. The flow cytometry-based assay was used to measure the capacity of cytotoxicity of PD-1pos versus PD-1neg NK cell lines by quantifying the number of viable CFSE-labelled target cells following overnight co-incubation. This *in vitro* model was modified to assess the effect of blocking PD-1 signalling on the cytotoxicity activity of PD-1^{pos} NK cells. This experiment was achieved at 5 times independently.

2.13.1 PD-1^{pos} NK-92 versus wt-NK-92 cytotoxicity assay

PD-1^{pos} NK-92 and wt-NK-92 cell lines were harvested from culture media and were washed in 15ml tube with growth media and resuspended at concentration 1x10^6 cells/ml.

2.13.2 K562 and 721.221 target cell CFSE-labelling

5mM CFSE dye was diluted to 1uM (1µl was added to 5ml PBS). 2x10^6 each of K562 and 721.221 cells were harvested and prepared separately in 15ml tube, washed with growth media and cell pellet was resuspended in 200µl of diluted PBS-CFSE solution with pipetting to mix. Tubes were incubated for 15 minutes at 37°C in 5% CO_2. 10ml of growth media was added to each tube to quench the staining and spun down at 363x g for 5 minutes. The supernatant was discarded, and cells were resuspended at concentration of 2x10^5/ml and incubated further at 37°C for 15 minutes to quench the dye. Using sterile 96 well plate, 100µl each of K562 and

721.221 target cells ($0.2x10^5$ cells) were plated in duplicate (10 wells needed for each target cell type) and topped up with 100µl ($1x10^5$ cells) of either PD-1^{pos} NK-92 or wtNK-92 to achieve 5:1 E/T ratio. Other E/T ratios, including 2.5:1 and 10:1 were set up. To assess the effect of blocking PD-1 signalling, 9µl of each anti PDL1 and anti-PDL2 blocking antibodies was added in the corresponding wells with pipetting up and down gently for 3 times to mix. Plate incubated at 37°C in 5% CO_2 for overnight (16 hours). The controls were only set up with 100µl of target cells (K562 and 721.221) 100µl growth media in duplicate.

In the next day, cells were transferred to labelled 5ml FACS tubes without wash, and 10µl of vortexed CountBright beads was added to each tube. Tubes were topped up with PBS to 300µl and 2µl PI was added to each tube just prior cell acquisition on Gallios™. All tubes were run on Gallios™ with equal time (2 minutes) at high flow rate. Data was analysed on Kalusa software. To calculate viable target cells, $CFSE^{positive}$ $PI^{negative}$ cells and CountBright beads were gated. Example of wt-NK-92 and PD-1^{pos}NK-92 killing is shown in **Table 2.18** and **Table 2.19** respectively. The following equation was used to calculate the percentage of Killing:

(Average number of live cell events/average number of beads events) x (count of added beads in 10µl / sample volume) = concentration of live K562 or 721.221 cells/ul in the sample.

Percentage of NK killing = (Average of target cell concentration in sample/ control) x 100

2.13.3 PD-1^{pos} NKL versus wt-NKL cytotoxicity assay

This is another *in vitro* cell line model used to study the cytotoxicity of PD-1^{pos} NK cells. The protocol and steps are similar to that with NK-92 discussed last section. The only difference is replacing wt-NK-92 and PD-1^{pos} NK-92 effector cells with wt-NKL and PD-1^{pos} NKL cells.

Table 2.17 A representative example of calculating the concentration of live 721.221 cells/µl for all ratios in duplicate after co-incubation with wt-NK92, with and without PDL1/2 blockade.

Replication	Ratios	PDL1/2 blockade	No of live 721.221 cell events (A)	No of Beads events (B)	(A)/(B) = X	Assigned beads count in 10ul (c)	Sample volume/ul (D)	(C)/(D) = Y	(X) X (Y)	Mean of 721.221/ul
1	Control	-	6519	3533	1.8	105000	300	350	630	665
2		-	7023	3447	2.0	105000	300	350	700	
1	2.5:1	-	2857	3591	0.8	105000	300	350	280	280
2		-	3174	3573	0.8	105000	300	350	280	
1	2.5:1	Yes	3228	2932	1.1	105000	300	350	385	367
2		Yes	3028	2943	1.0	105000	300	350	350	
1	5:1	-	2156	3035	0.7	105000	300	350	245	245
2		-	2224	2996	0.7	105000	300	350	245	
1	5:1	Yes	2189	2713	0.8	105000	300	350	280	262
2		Yes	2051	2707	0.7	105000	300	350	245	
1	10:1	-	1850	3058	0.6	105000	300	350	210	210
2		-	1793	2836	0.6	105000	300	350	210	
1	10:1	Yes	1531	2917	0.5	105000	300	350	175	175
2		yes	1540	2913	0.5	105000	300	350	175	

Table 2.18 Representative example of calculating the percentage cytotoxicity of 721.221 target cells mediated by wt-NK-92 before and after PDL1/2 blockade

Ratios	PDL1/2 blockade	Mean of live 721.221 (sample)	Mean of live cells (control)	Sample/control	%	% of Killing
Control	-	-	6771	-	-	-
2.5:1	-	3015	6771	0.44	44	56
2.5:1	Yes	3128	6771	0.46	46	54
5:1	-	2190	6771	0.32	32	68
5:1	Yes	2120	6771	0.31	31	69
10:1	-	1821	6771	0.26	26	74
10:1	yes	1535	6771	0.22	22	78

Table 2.19 Representative example of calculating the percentage cytotoxicity of 721.221 target cells mediated by PD-1^{pos} NK-92 before and after PDL1/2 blockade

Ratios	PDL1/2 blockade	Mean of live 721.221 (sample)	Mean of live cells (control)	Sample/control	%	% of Killing
Control	-	-		-	-	-
2.5:1	-	7265.5	7304.5	0.99	99	1
2.5:1	Yes	6977	7304.5	0.95	95	5
5:1	-	6304.5	7304.5	0.86	86	14
5:1	Yes	5587.5	7304.5	0.76	76	24
10:1	-	7014	7304.5	0.96	96	4
10:1	yes	6594	7304.5	0.90	90	10

2.14 Mass cytometry (CyTOF) analysis

Mass cytometry assay was performed to study the phenotype of PD-1^{pos} NK cells compared to PD-1^{neg} NK cells from B-CLL patients. Particularly, the co-expression of PD-1 with other immune checkpoints and the expression of PD-1 ligands on the immune cells were the main focus. Frozen PBMCs from 3 B-CLL patients with high PD-1^{pos} NK cells (279KB, 111AD and 351MB) were used in this experiment. CyTOF uses antibodies that conjugated with heavy metals rather than fluorochromes used in conventional flow cytometry. In addition, CyTOF panel has more than 40 parameters that provides a chance to investigate more markers at once compared to flow cytometry that has limited parameters up to 10.

2.14.1 Sample preparation and staining

Frozen PBMCs from 3 B-CLL patients with high PD-1^{pos} NK cells (>10% PD-1^{pos} NK cells of total NK population) were taken out from liquid nitrogen. After defrosting PBMCs separately, cells were washed with 3ml PBS at 363x g for 5 minutes and resuspended in the residuals. Due to the high prevalence of malignant B cells in those samples, and to get enough NK cells for the analysis, some of malignant B cells were depleted using positive selection of CD19 cells EasySepTM kit. PBMCs were washed in PBS at 363x g for 5 minutes and resuspended in 1ml MAX-per staining buffer and transferred into 3 individual labelled FACS polypropylene tubes. PBMCs were then filtered using polypropylene FACS tubes with filter cups followed by cell counting. $3x10^6$ PBMCs from each individual sample were transferred into new 5ml polypropylene FACS tubes and spun down at 363x g for 5 minutes. As CD16 marker is not our interest here, PBMCs were resuspended in 5µl FC receptor blocking solution and incubated for 10 to 15 minutes at room temperature. 22.5µl of antibody master mix (**Table 2.21**) to each sample tube and 75µl of MAX-per buffer was added to each tube so that the total volume in

each tube is 100µl. Tubes were incubated for 30 minutes at room temperature with mixing by pipette halfway through. After 30 minutes incubation and to identify cells (cell-ID), 10µl of 50uM cisplatin (pt 194) (2µl 1mM pt 194 was diluted by 38µl of sterile PBS to achieve 50uM) was added to the suspension and cells were incubated further for 3 minutes at room temperature. This step is to label the viable cells. Tubes were washed twice with 3ml MAX-per buffer and spun 5 minutes at 363x g. Supernatants were completely removed leaving pellets on the bottom of the tubes. Cell pellets were disrupted thoroughly using pipette and 1ml of 1.6% of paraformaldehyde (PFA) solution was added to each tube with mixing well and incubated for 10 minutes at dark room temperature. This step is for cell fixation. Cells were spun at 645x g for 5 minutes and resuspended in 1ml of 62.5nM of cell-ID intercalator-Ir solution with good mixing by pipetting up and down. Cells were incubated overnight at 4°C and transferred next day morning to the University of Birmingham Mass Cytometry services for analysis using CyTOF-Helios Mass Cytometry. The normalisation beads were added to the cell suspension immediately prior to run on a CyTOF. The cell concentration was slightly low therefore samples were run on CyTOF at a low EPS (avg. EPS 157 and 171) and acquired cells was around 500,000 events per sample. The quality of data was good with minimal doublets. Samples were prepared individually so the barcode antibodies have not been used in this experiment. Data was produced by CyTOF as FCS files that can be directly and manually analysed using Flowjo and Cytobank software.

2.14.2 Gating scheme and clustering analysis for Mass cytometry data

After acquiring data from CyTOF, FCS files of 3 individual B-CLL patients were concatenated by Flowjo and transferred to Cytobank premium software https://premium.cytobank.org/cytobank/login . The initial gating was on the dense cluster of

events. Different parameters vs time were used to reduce background and gate cells. Normalisation beads Ce140+ were subsequently excluded, and intact cells were identified by gating on the strong staining of two isotopes of Ir intercalators (191Ir DNA and 193Ir DNA). Further gating on cell-length parameter was used to eliminate some residual aggregates and events within this gate referred as 'intact-singlets'. Using Cisplatin 194Pt-cell ID which labels cells with compromised cell membrane greater than live cells, live immune cells were identified based on expression of CD45 with non/low 194Pt-cell ID. No barcoding was used in this experiment, samples were run individually. As our main interest is NK cells, the initial gating was based on CD56 vs CD3 to separate NK cells ($CD56^{pos}$ $CD3^{neg}$) from other immune cells. (**Figure 2.5**).

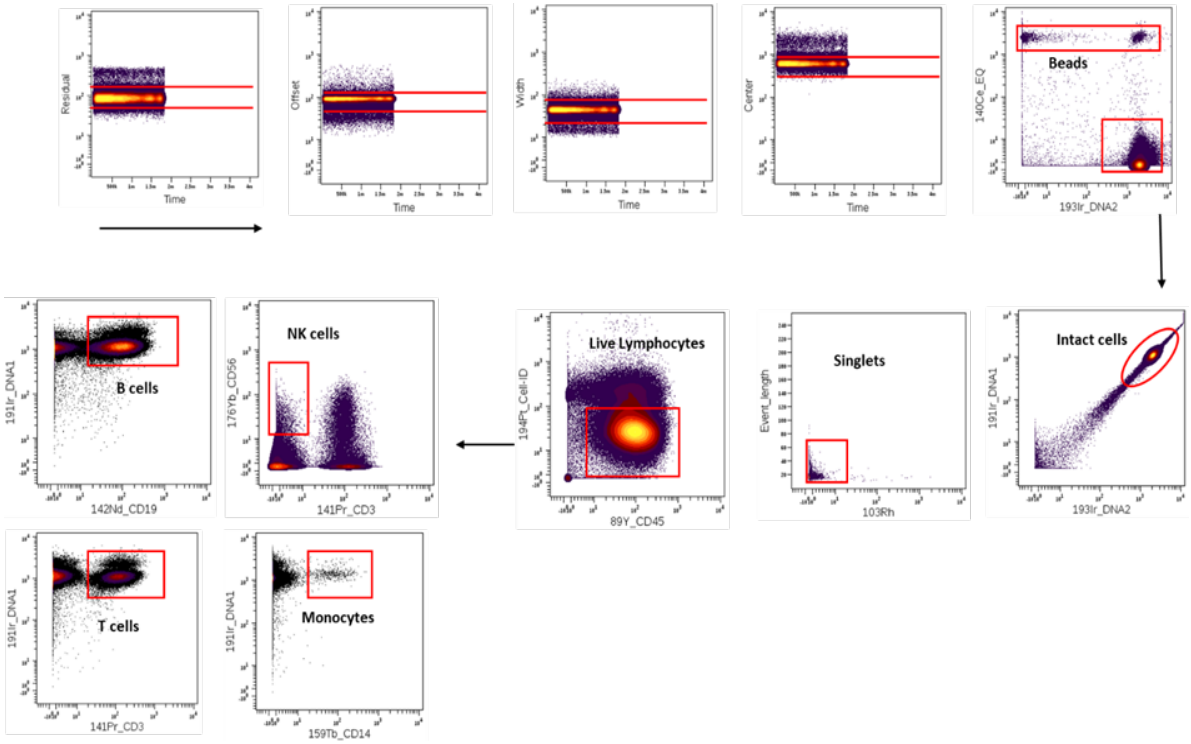

Figure 2.5 Gating scheme of CyTOF analysis

Using 3 concatenated B-CLL samples to identify NK and other immune cells. The gating and down-stream analysis was performed by Cytobank premium software version 8.0

Table 2.20 CyTOF antibodies panel purchased from Fluidigm

Metal conjugate	Target	Clone	Cat#
141Pr	CD3	UCHTI	3141019B
142Nd	CD19	HIB19	314200B
143Nd	CD127 (IL-7Ra)	A019D5	3143012B
144Nd	CD31/PECAM-1	WM59	3144023B
145Nd	CD4	RPA-T4	3145001B
146Nd	IgD	1A6-2	3146005B
147Sm	CD11c	Bu15	314708b
148Nd	CD274 (PD-L1)	29E.2A3	3148017B
149Sm	CD25 (IL-2R)	2A3	3149010B
150Nd	HLA-DR, DP	Tu36	3150028B
151Eu	CD70	EPR8569	3171024D
152Sm	TCRgd	11F2	315008B
153Eu	NKG2C	HP-3D9	3174015B
154Sm	TIGIT	MBSA43	3154016B
155Gd	CD27	L128	3155001B
156Gd	CD86	IT2.2	3156008B
158Gd	CD10	H110a	3158011B
159Tb	CD14	M5E2	3151009B
160Gd	CD39	A1	3160004B
161Dy	CD117 (ckit)	I04D2	3143001B
162Dy	CD335 (NKp46)	BAB281	3162021B
163Dy	CD33	WM53	3163023
164Dy	CD96	DX2	3164008B
165Ho	CD11b (Mac-1)	EPR1344	3149028D
166Er	CD34	581	3166012B
167Er	CD197 (CCR7)	GO43H7	3167009A
168Er	CD8a	SK1	3168002B
169Tm	CD159a (NKG2A)	Z199	3169013B
170Er	CD45RA	HI100	3170010B
171Yb	CD226	DX11	3171013B
172Yb	CD273 (PD-L2)	24F.10C12	3172014B
173Yb	CD141	1A4	3173002B
174Yb	CD279 (PD-1)	EH12.2H7	3174020B
175Lu	CD184 (CXCR4)	12G5	3175001B
176Yb	CD56 (NCAM)	N901	3176009B
209Bi	CD16	3G8	3209002B
89Y	CD45	HI30	3089003B

2.15 ATAC-seq experiment

Assay for Transposase Accessibility Chromatin (ATAC-seq) was used to study the potential differences in the open chromatin regions of the whole NK cells from B-CLL patients versus HCs, and PD-1^{pos} NK cells versus PD-1^{neg} NK cells from B-CLL. This method relies on library construction by hyperactive Tn5, and adapters loaded onto the transposase, which tags and fragments the accessible chromatin allowing adaptors to integrate into these open regions. The library generated can be sequenced by NGS and chromatin open regions can be analysed. FAST protocol with digitonin protocol was used to prepare NK cells for ATAC-seq, which has the beneficial of skipping the initial cell lysis step and reducing the number of read maps to mitochondrial DNA. This experiment was achieved on fresh PBMCs from 3 B-CLL patients (306BA, 368JR and 310AP), 3 age-matched healthy controls (101AK, 33GG and 84ABW), and 1 sample from B-CLL patients (279KB) with more than 20% PD-1^{pos} NK cells of the total NK population (sorted into PD-1^{pos} NK cells and PD-1^{neg} NK cells).

2.15.1 NK cell preparation and sorting

PBMCs were isolated from fresh heparinised whole blood from B-CLL patients and HCs as descripted in **section 2.3.1**, to retain the viability and to keep the DNA structure of NK cells intact. Using same NK isolation protocol and kit descried previously (EasySepTM human NK cell enrichment kit). 50x10^6 PBMCs from each donor were used for NK cells purification. After this initial enrichment step, one further FACS based sorting was performed to enhance the purity and get rid of dead cells. Purified NK cells from B-CLL and HCs were stained with anti-CD3-FITC, CD56-APC/Cy7 and viability dye. For B-CLL sample with high PD-1 NK cells, it was stained with anti-PD1-PE, CD3-FITC, CD56-APC/Cy7 and viability dye, sorting panel listed for 30 minutes on ice. NK cells were washed in 2ml PBS for 5 minutes at 363x g and cell

pellets were resuspended in appropriate volume of PBS and transferred in ice box to the cell sorter machine (BD FACSMelody^{TM} cell sorter). FACS sorted whole NK cells were collected in 1.5ml Eppendorf tubes with 400µl growth median. For PD-1^{pos} and PD-1^{neg} NK cells collected in two separated Eppendorf tubes with 400µl growth media. 50,000 NK cells in a single-cell suspension were successfully collected from each sample and each PD-1^{pos} and PD-1^{neg} NK cells

2.15.2 NK cell transposition and purification

FACS sorted NK cells are intact and in homogenous single-cell suspension. NK cells were kept all time in ice box to keep them intact and live. Immediately after the sorting, 50,000 NK cells from each Eppendorf tube were spun down at 500x g in 4°C for (The cell number at this stage is very crucial as the transposase to cell ratio determines the distribution of DNA fragment generated). Supernatant was removed and discarded using pipette leaving only the cell pellets at the bottom of the tube. Cells were immediately transposed using 50µl transposition reaction mix (25µl 2x TD buffer, 2.5µl Tn5 transposase enzyme, 1µl 0.5% Digitonin, 21.5µl Nuclease free H2O=50ul total). Gently pipette up/down to resuspend nuclei in the transposition reaction mix was followed by incubation for 30 minutes in gentle shaking 37°C incubator. The gentle shaking may increase the fragment yield. Immediately following transposition, the reaction was purified using a Qiagen MinElute PCR purification kit. Transposed DNA was eluted in 11µl of Elution buffer and stored at -20°C for PCR amplification and next preparation steps.

2.15.3 PCR amplification

Transposed DNA fragments were amplified by combining the following PCR materials in 0.2ml PCR tube with two adapters shown below (Ad1 and Ad2) and transferred on ice to the PCR machine.

10µl of transposed DNA

10µl of Nuclease free H2O

2.5µl 25uM PCR Primer 1

2.5µl 25uM PCR primer 2

25µl NEBNext High-Fidelity 2x PCR Master mix

Ad1 noMX: 5'AATGATACGGCGACCACCGAGAT CTACACTCGTCGGCAGCGTCAGATGTG 3'

Ad2 is changeable and a full list of primers 2 used in this experiment are available in the supplementary table 4.

Table 2.21 Thermal cycles for DNA amplification

Number of cycles	Temperature	Time
1 cycle	72°C	5 min
	98°C	30 sec
5 cycles	98°C	10 sec
	63°C	30 sec
	72°C	1 min

qPCR to determine the optimal number of PCR amplification cycles

qPCR was used to determine the appropriate additional number of PCR cycles needed to amplify the library prior reaching the saturation. Also, determining the optimal number of PCR cycles will reduce short oligonucleotides or primers, and the size bias of PCR amplification

which mostly comes from later PCR cycles that occur because of limited reagent/materials concentration . To run a qPCR the following materials were combined:

5µl of previously PCR amplified (5 cycles) DNA or water as a control
3.9µl of Nuclease free H2O
0.25µl of 25uM PCR primer 1
0.25µl of 25uM PCR primer 2
0.6µl of 10x SYBR Green I
5µl of NEBNext High-Fidelity 2x PCR master mix

The master mix of these materials was prepared separately for each adapter pair (each sample) x3 (1 with DNA , 1 without DNA as a negative control).

Table 2.22 qPCR run

Number of cycles	Temperature	Time
1 cycle	98°C	30 sec
29 cycles	98°C	10 sec
	63°C	30 sec
	72°C	1 min

After running the qPCR and exporting the raw data from qPCR machine, the optimal amplification cycle number (# cycle) of the remaining 45µl PCR reaction was determined by plotting linear Rn versus ct value of each cycle on a linear graph. The plateau value of sample (sample+primers, red line) reaction subtracted by the baseline value from the control (water+primers, blue line), the reaction was divided by 4 to get the optimal value which is used to decide the cycle number for amplification (**Figure 2.6**).

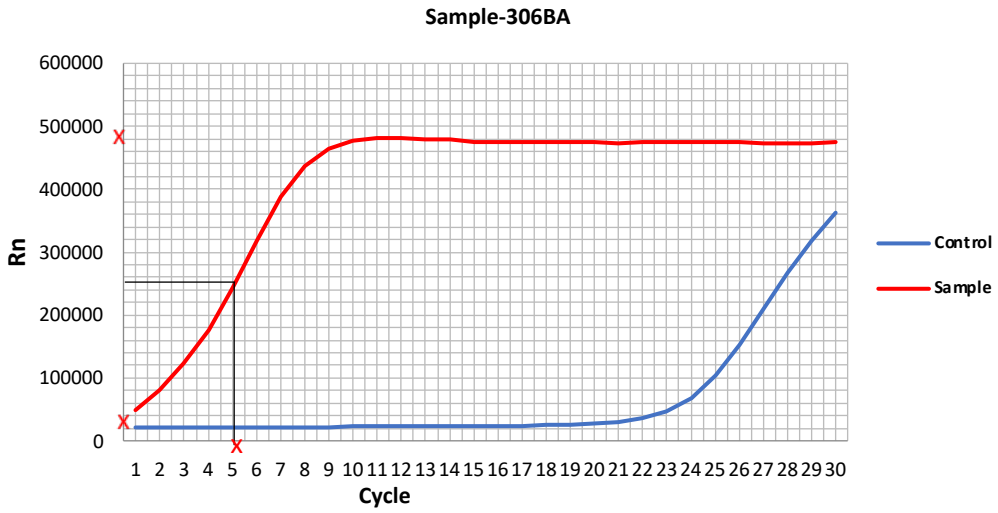

Figure 2.6 An example for qPCR amplification plot to determine # cycles required for PCR amplification

The remaining 45µl PCR reaction was amplified 6 cycles on PCR machine and stored at -20 for the next step (Library purification) as following:

Table 2.23 Final PCR amplification

Number of cycles	Temperature	Time
1 cycle	98°C	30 sec
6 cycles	98°C	10 sec
	63°C	30 sec
	72°C	1 min

2.15.4 Library purification using Ampure XP beads.

The generated library was thawed in ice box and cleaned up using Ampure beads. This step is to remove the adapter dimers and unwanted DNA fragments which are larger or smaller than optimal size (select predictable and consistent size of library fragments, between 100 to 500b p). 1.2 volume of Ampure beads was added to the generated library and pipetted up and down 10x for mixing, (24µl of Ampure beads was added to 20µl of library in 0.2ml PCR tube) and incubated 15 minutes at room temperature. The tube was placed on mini magnet for about 3 to 4 minutes until the suspension is clear and beads/DNA fragments attached to the sides of the tube. The liquid was discarded, and beads washed 2x with 100µl of fresh prepared 80% Ethanol alcohol (EtOH). The wash step was carried out while the tube still on the magnet. EtOH taken out by 50µl pipette, and the tube left with open cap for maximum 3 minutes to let the beads dry. The tube was taken out from magnet and 20µl of 0.1x TE was added with mixing up and down 10x, then incubated for 5 minutes to detach DNA fragments from beads. Tube was placed again on the magnet and set aside until the solution is clear and transferred carefully to a new PCR tube. 3µl from purified library was sent in ice for initial quality control (QC) and the rest 17µl was kept in -20°C for further steps.

2.15.5 Initial High sensitivity ScreenTape-QC

3µl of generated library was sent in ice for initial QC to CRUK Genomics Birmingham. The purpose of this QC is to check the size and concentration of DNA fragments as shown in **Figure 2.7** which showed a great concentration of desired size of DNA fragments, ranged between 180 to 600 bp.

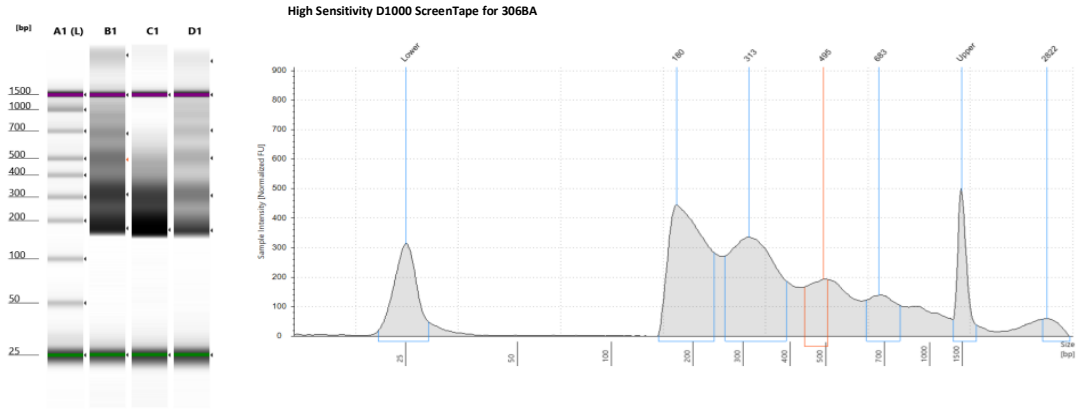

Well	Conc. (pg/ul)	Sample description
B1	2190	306BA

Size	Calibrated conc. (pg/ul)	Peak molarity (pmol/l)	% Integrated area	Observations
25	395	24300	-	Lower marker
180	879	7510	40.12	
313	846	4170	38.61	
495	207	643	9.43	
683	206	465	9.41	
1500	250	256	-	Upper marker
2822	53.2	92.0	2.43	

Figure 2.7 Example of High sensitivity ScreenTape QC report.

2.15.6 Validation qPCR

This step was performed to confirm that the majority >90% of our purified DNA is from open genes/regions. Therefore, the enrichment of TBP and β-Act versus human chr18 was measured. 50ng/ml of human genomic DNA was used in 5 serial concentrations as a standards. 50ng/ml gDNA was diluted with Nuclease free water to make 2.5, 0.5, 0.1, 0.02, 0.004ng using the equation C1V1=C2V2 . Also, library was diluted 1/100 with 0.1x TE. The following master mix was prepared for each gene Chr18, β-Act and TBP in triplicate and run on qPCR machine as descripted below **Table 2.24**:

5.0µl of 2x SYBR Green
0.03µl of 500nm Fwd primer
0.03µl of 500nm Rev primer
2.94µl of Nuclease free H2O
2.0µl of sample/standard gDNA into corresponding well

Table 2.24 qPCR validation cycles

Number of cycles	Temperature	Time
1 cycle	95°C	10 sec
40 cycles	95°C	15 sec
	60°C	1 min

The qPCR data was analysed on Excel, enrichment of Chr18, b-act and TBP were calculated from the standard curve and rations of Chr18/Chr18, TBP/Chr18 and β-ACT/Chr18 was calculated. β-Act and TBP were enriched in all libraries prepared from different donors (**Figure 2.8**), indicating that our libraries were made from open chromatin regions.

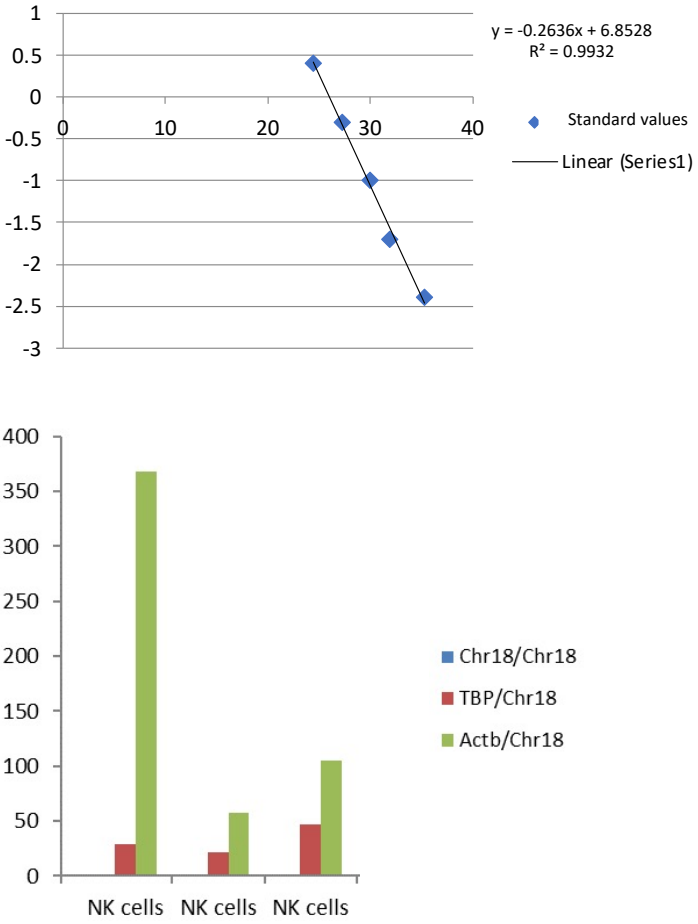

Figure 2.8 A representative example shows standard curve generated with qPCR validation (top graph), and TBP and b-Act gene enrichment within 3 generated libraries (bottom graph).

2.15.7 KAPA library quantification by qPCR based method

This final step before sequencing is to calculate the DNA concentration in each library (sample), so that we calculate how much volume needed from each library to pool them together in one PCR tube for sequencing as all libraries must be in the same concentration in the pool. KAPA Library Quantification kit Illumina® Platform was used in this assay which was performed in ice. Reagents and libraries were brought in ice box and 2µl from each libraries were serial diluted with 0.1x TE, 1:1000, 1:2000 and 1:4000. Using Kit protocol the mater mix was prepared by combining 5ml 2X KAPA SYBR® FAST with 1ml 10X primer Premix. 6µl of master mix were plated in 96 well plate followed by 4µl of each diluted library or standard and 4µl H2O in blank wells, all reactions were performed in duplicate. 96 Wells plate was then sealed and spun for 1 mint at 161X g for mixing and bringing the reaction materials together in wells. Plate was transferred in ice to qPCR machine and the cycles were set up as following:

Table 2.25 qPCR KAPA quantification cycles

Number of cycles	Temperature	Time
1 cycle	95°C	5 min
35 cycles	95°C	30 sec
	60°C	45 sec

qPCR data was exported from the machine and each library concentration was calculated based on the standard curve and from this the undiluted (original) libraries concentrations were calculated using Excel software. Equal concentrations were taken from each library to make a pool for final QC and sequencing as shown below **Tables 2.26 and 27**.

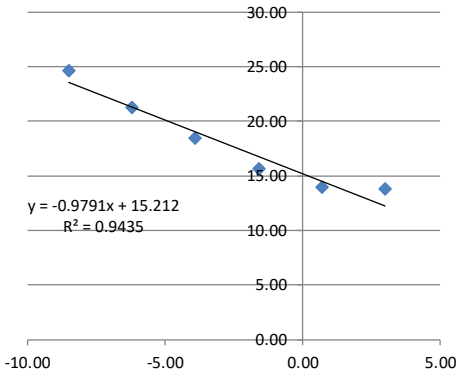

Standard values	Ct1	Ct2	Average	STDEV
20	13.4809	14.0012	13.74	0.3679
2	13.9964	13.8117	13.90	0.1306
0.2	15.6593	15.6246	15.64	0.0245
0.02	17.9196	18.8791	18.40	0.6785
0.002	21.3066	21.139	21.22	0.1185
0.0002	24.6838	24.4765	24.58	0.1466

log[C]	Average	STDEV
3.00	13.74	0.3679
0.69	13.90	0.1306
-1.61	15.64	0.0245
-3.91	18.40	0.6785
-6.21	21.22	0.1185
-8.52	24.58	0.1466

Slope	Intercept	R^2
-0.8451	15.2118	0.9435

dilutions	1000	2000	4000
	13.8314	15.3013	18.08
	13.7906	15.1311	17.85
Exp((ct-inter)/slop)	4.095008	0.912606	0.05
	4.26925	1.085864	0.07
Average	4.182129	0.999235	0.06
STDEV	0.123207	0.122512	0.01

	1000	2000	4000
size adjust concentration (pM)	7.16	1.7108	0.10
concentration of undiluted library stock pM	7160.31	3421.6233	413.01
average (pM)	3664.98		
average nM	3.66		
average size			
264.00			

Table 2.26 An example illustrates the sequential calculations for library KAPA quantification, performed by Excel software

samples	Source	Index - ID	Index-Sequence	KAPA [nM]	Volume (uL)	Concentration (nM)
297KB-PD1-	**Human**	**Ad2.22**	TGGTCACA	2.3489281	1.42	2.00
297KB-PD1+	**Human**	**Ad2.21**	TGGGTTTC	2.2716281	1.47	2.00
306BA-CLL	**Human**	**Ad2.20**	GTGTGGTG	3.6389816	0.29	2.00
AK-HD	**Human**	**Ad2.23**	TTGACCCT	23.063411	0.14	2.00
368JR-CLL	**Human**	**Ad2.24**	CCACTCCT	53.208528	0.06	2.00
310AP-CLL	**Human**	**Ad2.10**	CGAGGCTG	11.143957	0.30	2.00
84ABW-HD	**Human**	**Ad2.18**	GAGGGGTT	8.7314742	0.38	2.00
33GG-HD	**Human**	**Ad2.17**	TGCTGGGT	7.4414005	0.45	2.00
					Total vol=4.52	
					H20=5.49	
					Final vol= 10	Pool conc. 2nM

Table 2.27 KAPA quantifications.

Excel template shows libraries concentration (nM) from KAPA quantifications for each Library (brown column), and the volume required to make 2nM for each library (yellow column). Pool library was sent Genomic Birmingham in ice for final ScreenTape-QC and sequencing.

2.16 scRNA- seq of NK cells

scRNA seq experiment was performed to study the transcription profile of PD-1^{pos} versus PD-1^{neg} NK cells from B-CLL patients. PD-1^{pos} NK cells exhibited changed phenotype and function compared to PD-1^{neg} NK cells. Therefore, this experiment aims to investigate the possible underlying mechanisms of the altered phenotype and function of PD-1^{pos} NK cells. Also, this experiment aimed to identify the potential therapeutic targets to restore the anti-tumor activity of PD-1^{pos} NK cells in B-CLL patients. scRNA-seq was achieved using 2 fresh PBMCs from B-CLL patients with high percentage of PD-1^{pos} NK cells, 297BK patient with 22% PD-1^{pos} NK cells and 351MB patient with 13% PD-1^{pos} NK cells. 144x10^6 PBMCs and 640x10^6 PBMCs were isolated from about 25ml whole blood of B-CLL patients respectively. As the cell number in these samples are too much and to make FACS sorting quicker and faster, initially NK cells were quick enriched from both samples using negative selection EasySep™ Haman NK cell Enrichment Kit as described previously (**section 2.9.1**) to get rid of excessive load of other immune cells including malignant B cells and T cells. Enriched NK cells were stained with CD56-PE/Cy7, CD3-FITC, PD1-PE, CD19 and CD14-PB and viability dye (flour 506-PB) and incubated for 30 minutes in ice then washed with 3ml PBS and spun at 363x g for 5minutes. Cells were resuspended in 1 to 2ml PBS and FACS sorted as stated earlier. For each sample, PD-1^{pos} and PD-1^{neg} NK cells were collected separately in Eppendorf tubes containing 500µl of growth media. About 20x10^3 from each live NK cell type were collected form 297KB patients, and 60x10^3 of both live NK cell types from 351MB. NK cells were spun down at 363x g in 4°C and resuspended in growth media at 1000 cells/µl then sent for Genomic Birmingham-university of Birmingham to check the viability and sequencing . The viability of 297KB was 98%, and 58% for 351MB patient. The viability of last sample was improved by removing some of dead NK cells just before library preparation. The generated pool library passed the QC in terms of the library concentration and the fragment size, using Qubit and TapeStation

(**Figure 2.9**) and was sequenced using NextSeq 500 (Illumine) platform. The whole process is summarised in **Figure 2.10**.

Pool QC:

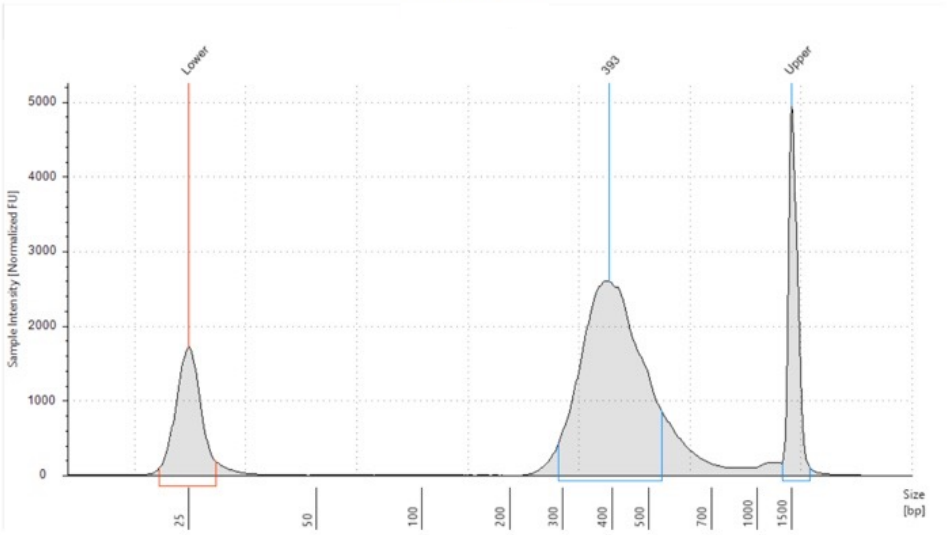

Pool Concentration (ng/µl)	Library Size (bp)	Molarity (nM)
29.0	393	113.7

Pool made to 4 nM for the sequencing.

Figure 2.9 QC for generated pool library demonstrates the library concentration and fragment size, which is made just before sequencing.

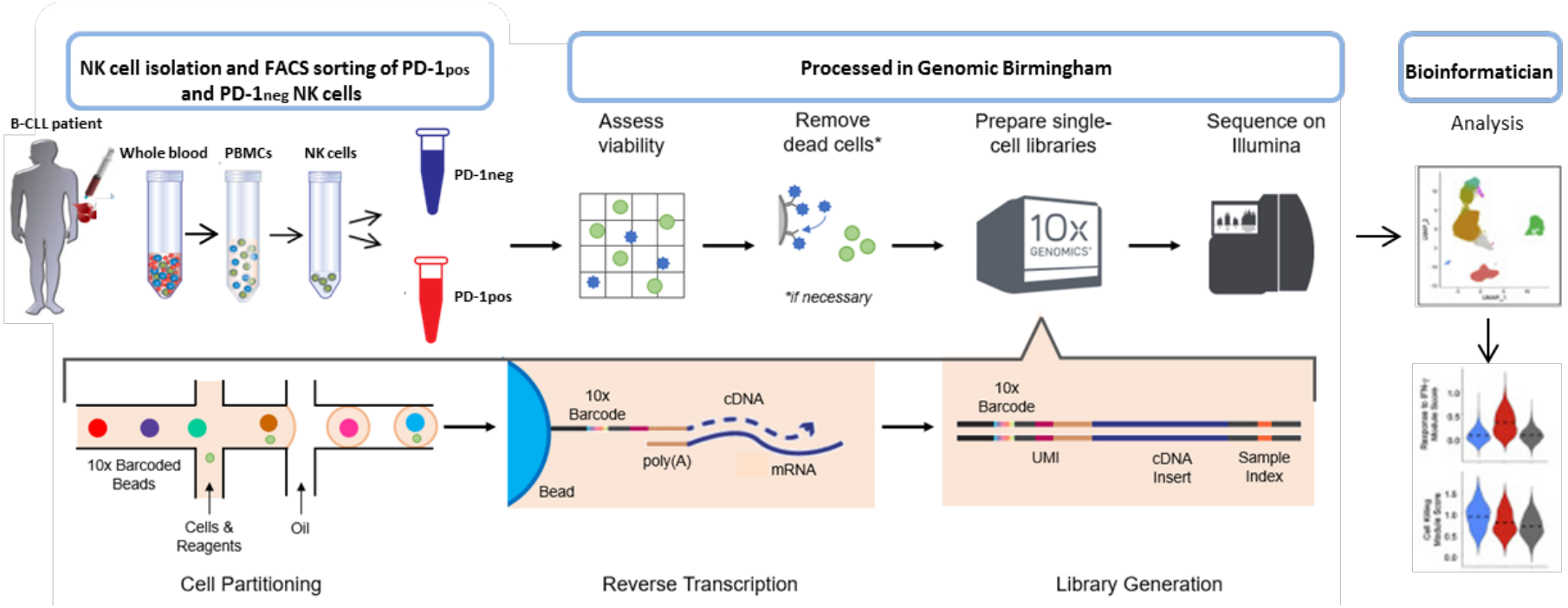

Figure 2.10 Diagram shows an overview of scRNA-seq from single cell isolation, library preparation, sequencing to Pipeline analysis.

CHAPTER3: FREQUENCY AND PHENOTYPE OF NK CELLS IN B-CLL PATIENTS

3.1 Introduction

As discussed in the previous chapter, NK cells are spontaneously able to recognise and kill various cancer cells particularly hematopoietic malignant cells. Many studies have shown that NK cells are phenotypically defective and functionally impaired in B-CLL patients. This includes downregulation of activating receptors such as NKG2D, DNAM-1, and NCRs on the surface of NK cells. However, the expression of immune checkpoints and adhesion molecules have not been studied thoroughly.

To further explore the modulation of NK cell population in patients with B-CLL, this chapter set to investigate the frequency and phenotype of NK cells from 75 untreated stage A B-CLL patients. This chapter focuses on the absolute count of NK cell population, frequency of different NK subsets, their correlation to the malignant B cells burden, and expression pattern of immune checkpoints, and adhesion molecules.

3.2 Results

3.2.1 Gating strategy for whole NK cell population and NK cell subsets

Following PBMCs isolation from heparinised whole blood of patients with B-CLL and healthy controls (HCs), PBMCs were stained with appropriate antibodies against cell surface antigens expressed on NK cells (**Chapter 2 Table 2.8**) and analysed by flow cytometry. Cells were first gated using FSC-H and FSC-A parameters to exclude doublet cells and gate only on single cells. Lymphocytes were then gated according to FCS-A and SSC-H and dead cells were excluded from analysis using Propidium Iodide (PI) alongside with unwanted cells (B cells and monocytes). At last, NK cells were identified within live population (PI negative staining) by their expression of CD56 and lacking CD3 expression ($CD3^{neg}$ $CD56^{pos}$) (**Figure 3.1**).

Subsequently, four NK cell subsets were identified from the total NK cells based on the density of surface expression of CD56 and CD16. These are $CD56^{brigh}$ $CD16^{neg}$, $CD56^{bright}$ $CD16^{pos}$, $CD56^{dim}$ $CD16^{dim}$ and $CD56^{dim}$ $CD16^{pos}$ subsets (**Figure 3.1**).

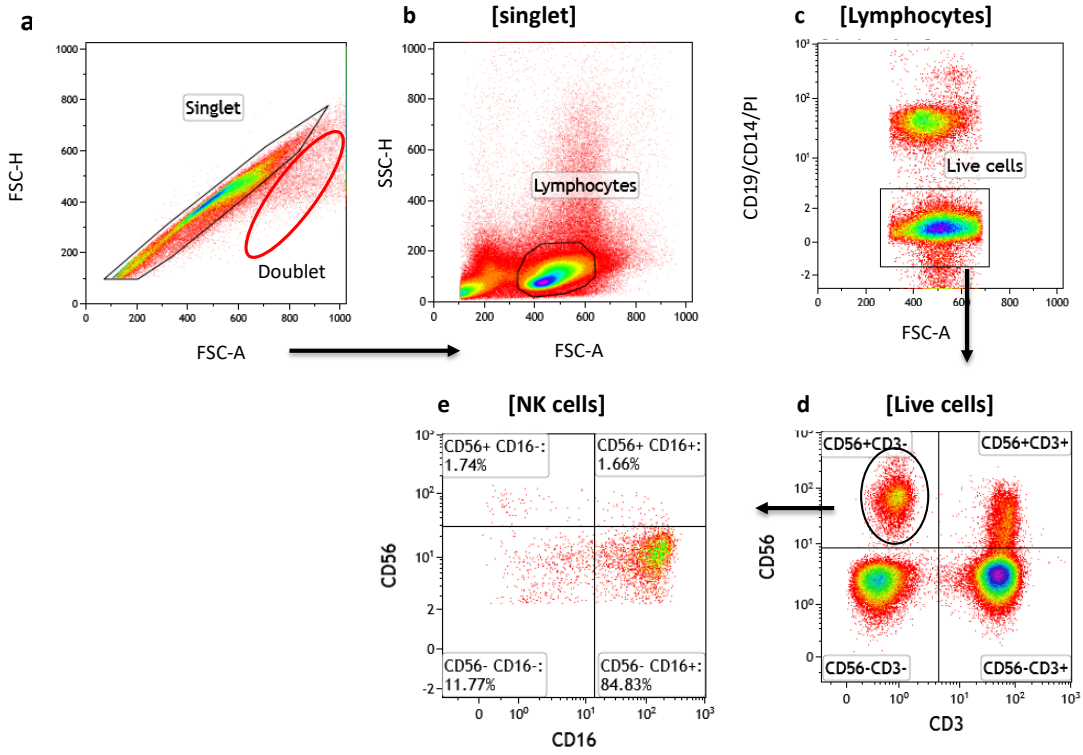

Figure 3.1 Gating strategy for identification of NK and NK cell subsets.

PBMC were first gated on singlet to remove doublet cells (**a**), lymphocytes were identified using FSC-A and SSC-H properties (**b**). Before gating on NK cells, live cells were identified as being PI negative cells, whilst dead cells (PI positive cells), B cells (including tumor B cells) and monocytes were excluded on dump channel (**c**). NK cells were identified from live population as CD56pos CD3neg PI- (**d**) and further classified into four different subsets according to the level of CD56 and CD16 expression (**e**). These flow plots represent an example of NK cell staining and identification of one individual of CLL patient and the same strategy is applied for healthy controls.

3.2.2 Different distribution of NK subsets in untreated B-CLL patients compared to HCs

Distribution of NK cells and their four subsets in 75 naïve treatment B-CLL patients has been investigated using flow cytometry. The percentage of total live NK cells $CD3^{neg}$ $CD56^{pos}$ out of lymphocytes and their subsets was compared to age-matched healthy controls. The distribution analysis showed that B-CLL patients had significantly lower NK cell frequency than healthy controls with 8.4±0.7% (Mean±SEM) compared to 19.6±2.1% (p=<0.0001, Mann-Whitney test) (**Figure 3.2 panel a**). SEM was used to indicate the precision of comparison of means and to estimates the mean for predicted data if the size of patients is increased. In addition, the frequency of mature $CD56^{dim}$ and immature $CD56^{bright}$ NK cells was analysed out of total live NK cells in B-CLL and HCs. $CD56^{dim}$ NK cells were significantly higher in B-CLL (95.3±0.2%) compared to (92.9±0.9%) in HCs (p=0.0161). Whilst $CD56^{bright}$ NK cells were significantly lower in B-CLL (4.6±0.3%) compared to HCs (7.5±4.5%) (p=0.0078).

Ultimately, the frequency of all different NK subsets (four NK subsets) was analysed in B-CLL and compared to HCs. **Figure 3.2 panels b and c** summarises the distribution of NK cell subsets in B-CLL and HCs with each bar represents an individual of patients/Healthy control and each colour represents one of NK subsets. The percentage of NK cell subsets with high cytotoxicity potential was higher in B-CLL compared to HCs. $CD56^{dim}$ $CD16^{pos}$ NK subsets (red) were significantly higher in B-CLL patients 88.5±0.7% compared to 82.3±1.5% (Mean ± SEM) healthy controls (p=0.0273), and $CD56^{bright}$ $CD16^{pos}$ NK subsets (blue) was also substantially higher in B-CLL (3.4±0.4%) compared to (1.9±0.2%) in HCs (p=0.0311). In contrast, non-cytotoxic NK subsets were significantly lower in B-CLL compared to HCs.

$CD56^{dim}$ $CD16^{neg}$ NK subsets (green) were significantly lower in CLL (5.7±0.5%) compared to HCs (8.7±1.2%) (p=0.0229), and $CD56^{bright}$ $CD16^{neg}$ NK subsets (purple) were also lower in B-CLL (3.4±0.6%) compared to HCs (5.6±0.8%) (p=0.0018) (**Figure 3.2 panel d**).

Overall, CLL patients have high percentage of mature cytotoxic NK cells and low immature/regulatory NK cells.

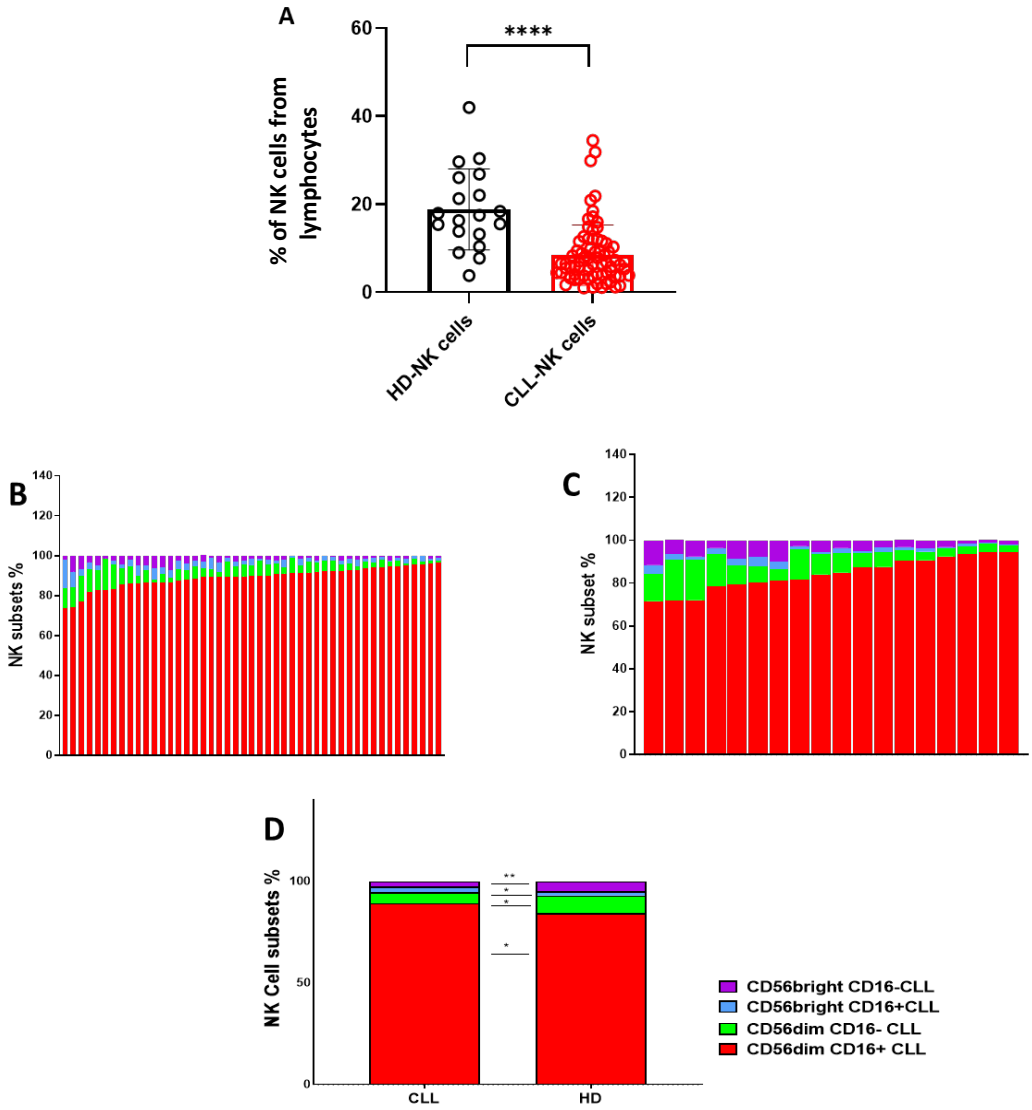

Figure 3.2 Percentage of NK cells of lymphocytes after excluding CD19$^+$ tumor B cells in naïve treatment B-CLL patients and age-matched healthy controls.

Percentage of total live NK cells out of lymphocytes determined as CD3$^-$ CD56$^+$ in CLL empty red circles compared to healthy controls empty black circles (**a**). Bar chart summarises the distribution of NK cell subsets out of total NK cells in CLL (**b**) and healthy controls (**c**), each bar represents an individual patient/healthy control. (**d**) is clustering graph depicts the distribution summary of NK cell subsets. The data shown are (Mean±SEM) and were analysed by Mann-Whitney nonparametric test (*p<0.05 and **p<0.01).

3.2.3 The impact of H-CMV infection on NK cells from B-CLL patients

As CMV infection is well known to leave imprint on NK cells and causes long-lived adaptive NK cells particularly during later stages of life. Here, we investigated whether CMV infection would influence the frequency and phenotype of total NK cells in B-CLL patients. First our CLL cohort has been divided into two groups based on HCMV serostatus (HCMV seropositive and HCMV seronegative). 58.7% of our cohort were HCMV seropositive and 41.3% were HCMV seronegative, which is not significantly different from HCs (Parry, Damery, et al., 2016). As such, HCMV seropositive patients had a significant higher proportion of NK cells compared to CMV seronegative patients 10.4±1.4% and 3.6±0.6% (Mean±SEM) ($p=0.0049$, Wilcoxon matched-pairs test) (**Figure 3.3 panel a**). NKG2C positive NK cells is a striking feature of CMV infection in healthy carriers (Malmberg et al., 2012), so the expression of NKG2C on NK cells was investigated by flow cytometry. Data showed that those B-CLL patients with HCMV seropositive had higher $NKG2C^+$ NK cell subset (HCMV associated NK cells) than HCMV seronegative patients 13.5±1.3% and 4.2±1.4% ($p=0.0156$) Wilcoxon matched-pairs test) (**Figure 3.3 panel b**).

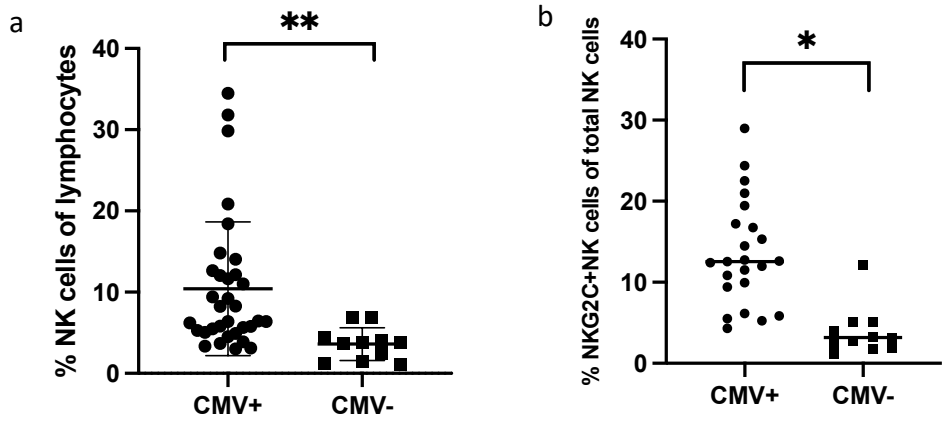

Figure 3.3 HCMV infection induced expansion of NKG2C expressing NK cells in CLL patients.

Percentage of total NK cells from lymphocytes were higher in CMV seropositive B-CLL patients compared to CMV seronegative B-CLL patients (a). CMV infection induced higher frequency of $NKG2C^{+}$ NK cells (CMV memory like NK cells) (b). Analysis was done by Wilcoxon matched-paired nonparametric tests (*$p<0.05$, **$p<0.01$).

Next, the four different NK subsets studied earlier was also compared between CMV seropositive and seronegative of B-CLL patients. NK subsets were identified in total PBMCs by gating on $CD3^{neg}$ $CD56^{pos}$, then divided into four subsets based on the density of their CD56 and CD16 expression. No changes were observed in the distribution of $CD56^{bright}$ $CD16^{neg}$, $CD56^{bright}$ $CD16^{pos}$ and $CD56^{dim}$ $CD16^{pos}$ NK subsets between CMV negative and CMV positive of B-CLL patients. Interestingly, there was a significant decrease in the frequency of $CD56^{dim}$ $CD16^{neg}$ NK subset in CMV seronegative compared to CMV seronegative of B-CLL patients 5.1±0.5% vs 5.9±0.6% (p=0.0290) (**Figure 3.4 panel b**). To further investigate this reduction in $CD56^{dim}$ $CD16^{neg}$ NK cells, age matched healthy controls were tested for the frequency of $CD56^{dim}$ $CD16^{neg}$ NK cells by flow cytometry based on HCMV serostatus. Unlike B-CLL patients, there was no significant difference in the frequency of $CD56^{dim}$ $CD16^{neg}$ between CMV seropositive and CMV seronegative in HCs (**Figure 3.4 panel b**). From **Figure 3.2 panel d**, the reduction in this NK population was observed in the whole B-CLL cohort compared to HCs. This data indicates that there is a combined reduction of $CD56^{dim}$ $CD16^{neg}$ NK cell subset between CMV infection and B-CLL disease, which needs further investigation.

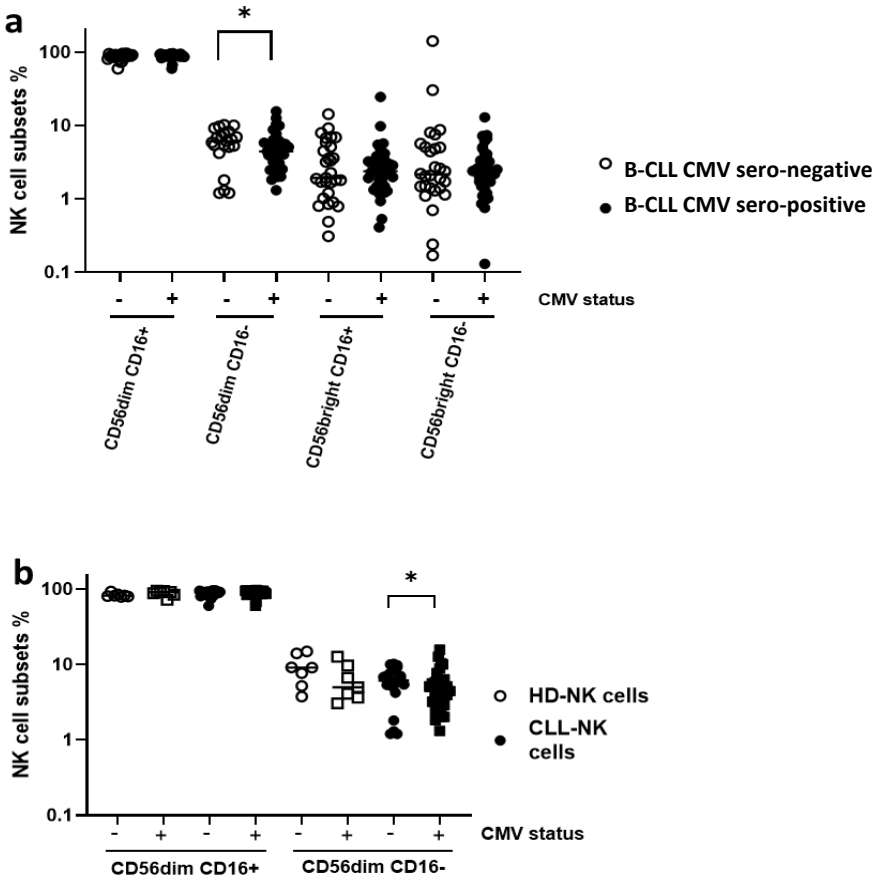

Figure 3.4 Percentages of NK cell subsets in CMV seropositive vs CMV seronegative.

(**a**)The percentage of $CD56^{dim}$ $CD16^{neg}$ NK subset out of the whole NK cell population was down regulated in CMV seropositive of B-CLL patients compared to CMV seronegative of B-CLL patients. (**b)** No changes in the percentage of this subset in CMV seropositive vs CMV seronegative of healthy controls. Statistical analysis performed by One way ANOVA with non-parametric data with paired for (a) and unpaired for (b) test (*$p<0.05$).

3.2.4 Absolute NK cell count in B-CLL patients and the correlation with tumor B cell burden

The previous data are based on the percentage of NK population. Also, it is important to study the absolute count of NK cells in B-CLL patients and its correlation to the tumor burden. To this end, the absolute count of whole NK, different NK subsets and B-CLL tumor cells were carried out using counting beads based flow cytometry (chapter 2, **section 2.3.5**). B-CLL disease is characterised by the clonal expansion of $CD5^+$ $CD19^+$ B-cells and in our cohort the average of this population constitutes about 71% of total circulating B cells with mean cell count (12535 cells/µl blood) (**Figure 3.5 panel a**) as an example of staining and gating of B CLL tumor cells). Previous studies have reported that untreated CLL patients have higher numbers of NK, $CD8^+$ and $CD4^+$ T cells compared to age-matched healthy controls, and this increase has been correlated with slower disease progression (Wang et al., 2018). As the focus of this work was NK cells, the influence of tumor B cell burden on NK cell expansion was assessed on fresh PBMCs from 21 untreated CLL patients. Due to time limitation and COVID pandemic, the absolute count of age-matched NK cells from HCs was not studied for comparison in this project. However, studies showed that the absolute count of NK cells was highly variable between healthy individuals ranged from 43 to 652 NK cells/µl with median180.5/µl (Merkt et al., 2021).

The median of NK cell absolute count of those 21 untreated B-CLL patients was 621.9 NK cells/µl blood. The median of absolute counts of four different NK subsets $CD56^{bright}$ $CD16^{neg}$, $CD56^{bright}$ $CD16^{pos}$, $CD56^{dim}$ $CD16^{neg}$ and $CD56^{dim}$ $CD16^{pos}$ were 13.5, 11.2, 28.3 and 444.2 NK subsets/µl blood, respectively. Interestingly, the absolute count of patient whole NK cells ($CD3^{neg}$ $CD56^{pos}$) was significantly correlated with the number of tumor B cells ($CD5^+$ $CD19^+$ B cells) (p=0.0289) (**Figure 3.5 panel b**). Looking at NK cell subsets, only the absolute count

of $CD56^{dim}$ $CD16^{neg}$ NK subset was significantly correlated with tumor B cells count (p=0.0434). There was no significant correlation for the absolute count of other NK subsets $CD56^{dim}$ $CD16^{pos}$, $CD56^{bright}$ $CD16^{neg}$ and $CD56^{bright}$ $CD16^{pos}$ in relation to tumor B cell count (**Figure 3.5 panel c**).

This result showed that the absolute count of whole NK cells significantly increased when tumor B cells count increases, which could possibly indicate that tumor B cells induce the proliferation of NK cells in B-CLL patients.

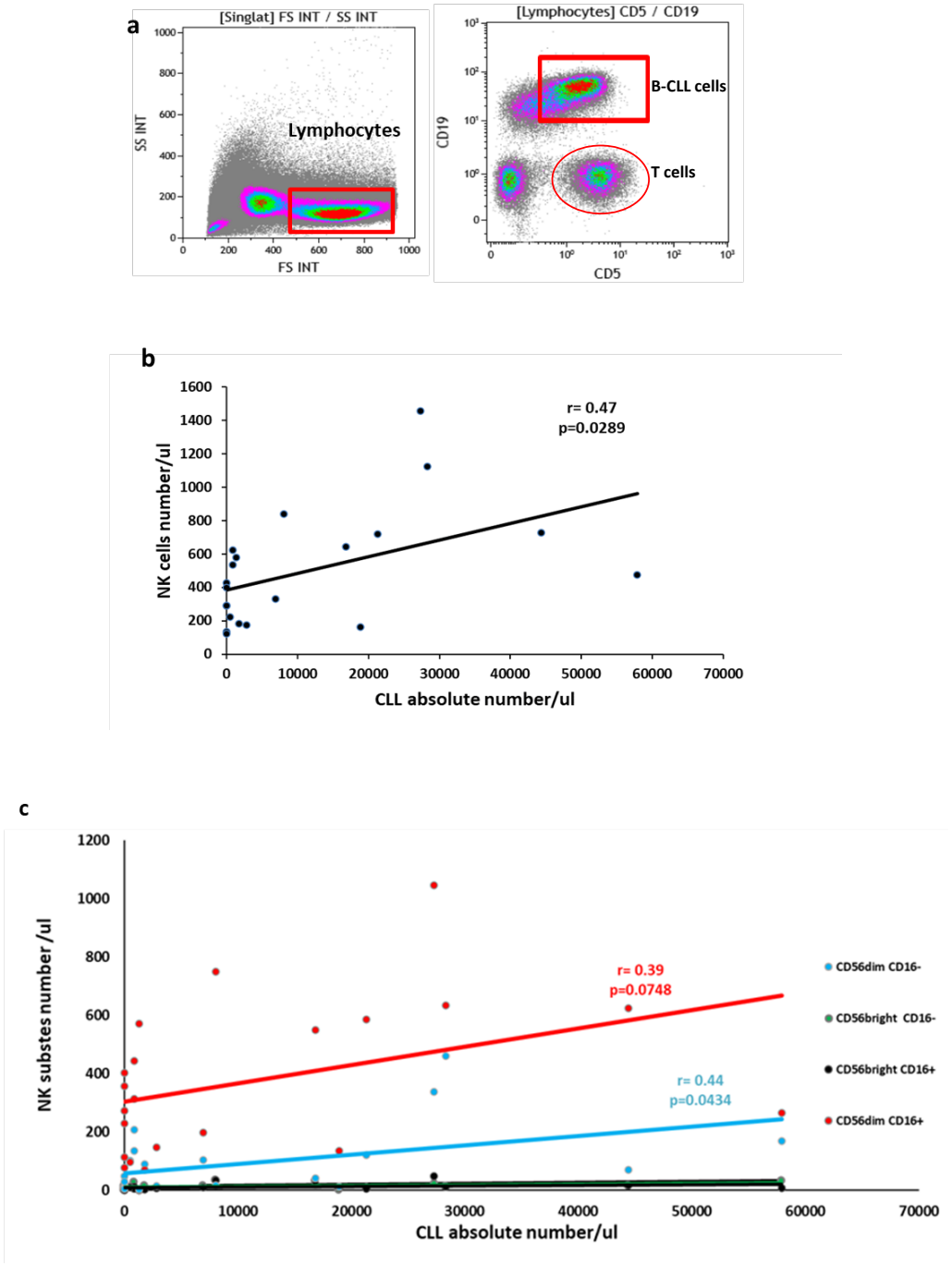

Figure 3.5 Correlation analysis of absolute number of NK and NK cell subsets vs tumor B cell number in CLL patients.

(**a**) Flow graphs show example of staining and gating of tumor B cells ($CD19^{+}$ $CD5^{+}$ cells) in B-CLL patients. NK cells and its subsets were gated as shown previously in this chapter. (**b**) The correlation was investigated between total NK cells count and tumor B cell count. Significant correlation was observed between NK cell subset ($CD56^{dim}$ $CD16^{neg}$) and tumor B cells. However, no significant correlation between cytotoxic NK cell subset ($CD56^{dim}$ $CD16^{pos}$) and tumor burden (**c**). Statistical analysis was performed by Pearson correlation coefficient using Excel.

3.2.5 The comparison of immune checkpoints expression on NK cells from B-CLL patients and healthy controls

The extensive phenotyping of NK cells from untreated CLL patients was performed using flow cytometry following specific antibodies staining. This section focused on the immune checkpoint expression on NK cells from B-CLL patients compared to age-matched healthy controls. To perform this analysis, NK cells ($CD3^{-}$ $CD56^{+}$) were gated from total lymphocytes and then the expression of immune checkpoints was measured on these cells, including PD1, TIGIT, CTLA-4, LAG3, CD96, TIM-3 and NKG2A (Chapter 2 table 2.9 and table 2.11). The expression level of these immune checkpoints was determined based on fluorescence minus one control (FMO) and compared to healthy controls (**Chapter 2 Figure 2.3**)

The expression of PD1 on NK cells in CLL patients has not been properly assessed before. Although there are some controversial reports about PD1 expression on NK cells (Judge et al., 2020; Dong et al., 2019), our findings showed that PD-1 expression was upregulated on NK cells from CLL patients compared to healthy controls 1.8±0.4% vs 0.5±0.1% ($p<0.0001$). In some CLL patients the expression of PD1 on NK cells reached up to 22% as shown in flow dot plot (**3.6 panel a**). In addition, this analysis showed a selective expression of PD1 on cytotoxic NK cell subset ($CD56^{dim}$ $CD16^{pos}$) but not on the other three NK subsets ($CD56^{dim}$ $CD16^{neg}$, $CD56^{bright}$ $CD16^{pso}$ and $CD56^{bright}$ $CD16^{neg}$). PD1 expression on NK cells in CLL patients might be a sign for exhaustion state of NK cells (chapter 5 discussed this in more details).

Not only PD1 expression was upregulated on NK cells from CLL patients, CTLA-4 checkpoint is another important inhibitory receptor that was also markedly upregulated on NK cells with 3.6±0.5% compared to 0.5±0.1% in healthy controls ($P<0.0001$) (**Figure 3.6 panel b**). Also,

the expression of CTLA-4 was more pronounced on $CD56^{dim}$ NK cells than $CD56^{bright}$ NK cells (p=0.0078).

Furthermore, expression of LAG-3 was assessed on NK cells from B-CLL patients, which is another co-inhibitory receptor that exerts differential inhibitory signals on various types of lymphocytes including NK cells (Narayanan et al., 2020). The findings showed that LAG-3 expression was significantly increased on NK cells from B-CLL patients compared to healthy controls with mean 3.4±0.9% and 0.7±0.09% (p=0.0164) (**Figure 3.7 panel a**). There was no difference in the expression level of LAG-3 on $CD56^{bright}$ and $CD56^{dim}$ NK cells.

In addition, expression of CD96 and TIGIT receptors that share the same ligands (CD155 and CD112) with DNAM-1 receptor, which has been shown to be downregulated on NK cells from B-CLL patients, was also evaluated on NK cells from B-CLL patients. After binding with the ligands, DNAM-1 receptor triggers an activation signal for NK cells, whilst CD96 and TIGIT instead inhibit NK cells functions. Interestingly, the frequency of CD96 expressing NK cells was significantly increased in CLL patients compared to healthy controls 4.0±0.6% vs 1.2±0.3% (p=0.0003) (**Figure 3.7 panel b**) and this was more evident on $CD56^{bright}$ NK cells. Whereas TIGIT expression level on NK cells from B-CLL patients was similar to its expression on NK cells from healthy controls 57.1±2.4% vs 57.3±2.2% (**Figure 3.8 panel c**).

No significant differences were seen in the expression of TIM3 and NKG2A on NK cells from CLL compared to healthy controls (**Figure 3.8 panels a and b**).

These data show that the expression of some immune checkpoints on NK cells from B-CLL patients was upregulated, including PD-1,CTLA-4, LAG-3 and CD96. The upregulation of these immune checkpoints indicates that they could contribute to the exhausted phenotype and function impairment of NK cells in B-CLL patients. PD-1 expression will be the focus in the coming chapters.

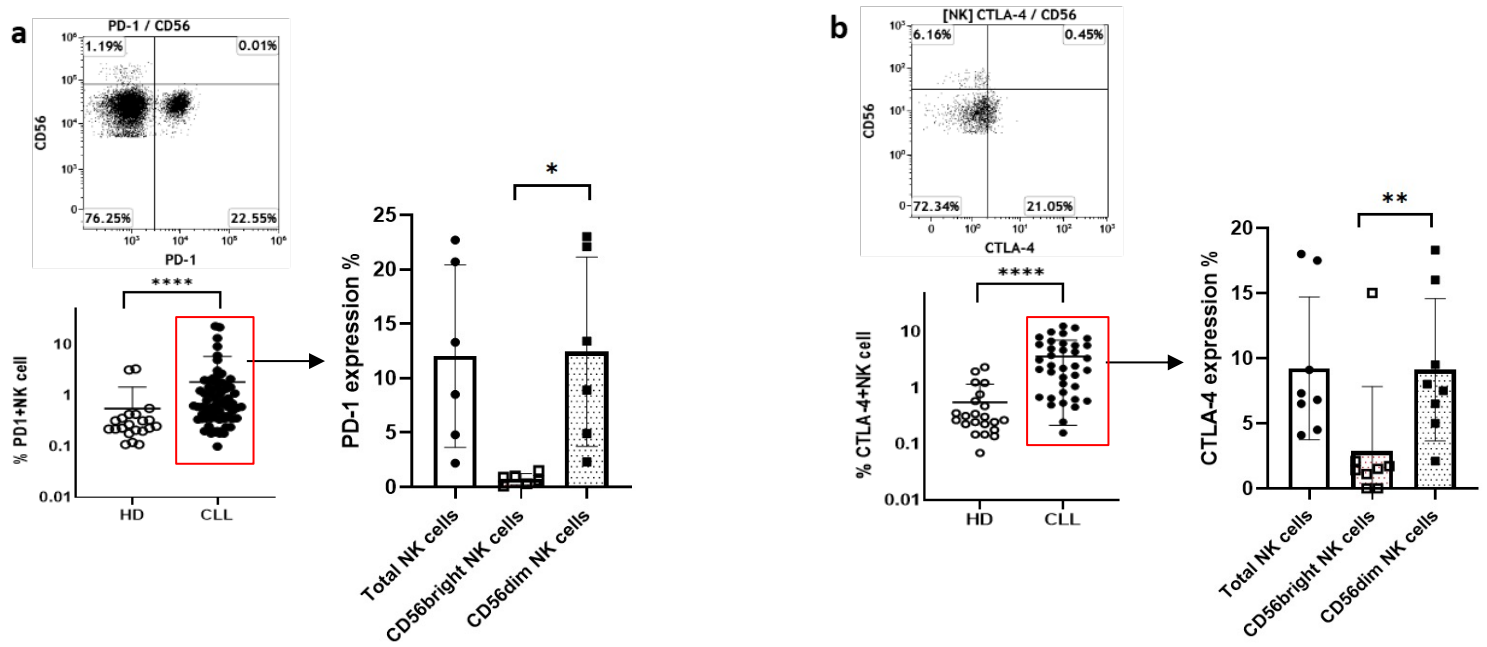

Figure 3.6 Surface expression of PD-1 and CTLA-4 checkpoints on NK cells from B-CLL versus HCs

Representative flow plots to demonstrate the PD-1 (a) and CTLA-4 (b) gating and expressions on NK cells from B-CLL patients. Dot graphs are comparisons of PD-1 and CTLA-4 expressions on total NK cells between B-CLL patients and HCs. Also, the differential expression of PD-1 and CTLA-4 on CD56 ^{bright} versus CD56^{dim} NK cells from B-CLL patients is shown in the bar charts. Analysis was performed using Mann-Whitney nonparametric test, and Wilcoxon matched-paired nonparametric tests (*p<0.01, **p<0.01 and****p<0.0001).

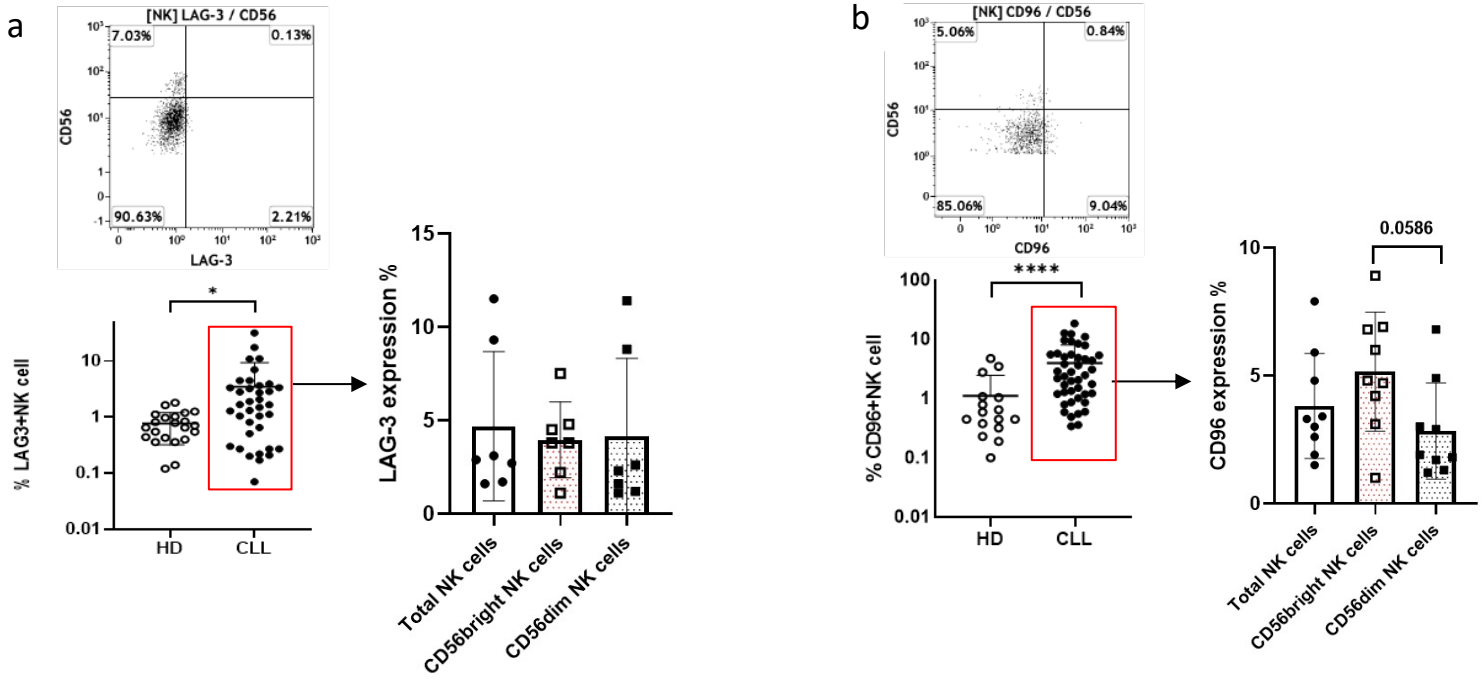

Figure 3.7 Surface expression of LAG-3 and CD96 receptors on NK cells from B-CLL versus HCs.

Flow plots are an examples to demonstrate the LAG-3 (**a**) and CD96. (**b**) gating and expression on NK cells from B-CLL patients. Dot graphs are comparisons of LAG-3 and CD96 expressions on total NK cells between B-CLL patients and HCs measured at different times/days. Also, the differential expression of LAG-3 and CD96 on CD56 ^{bright} versus CD56^{dim} NK cells from B-CLL patients is shown in the bar charts. The analysis was performed suing Mann-Whitney, and Wilcoxon matched-paired nonparametric tests (*p<0.01and****p<0.0001).

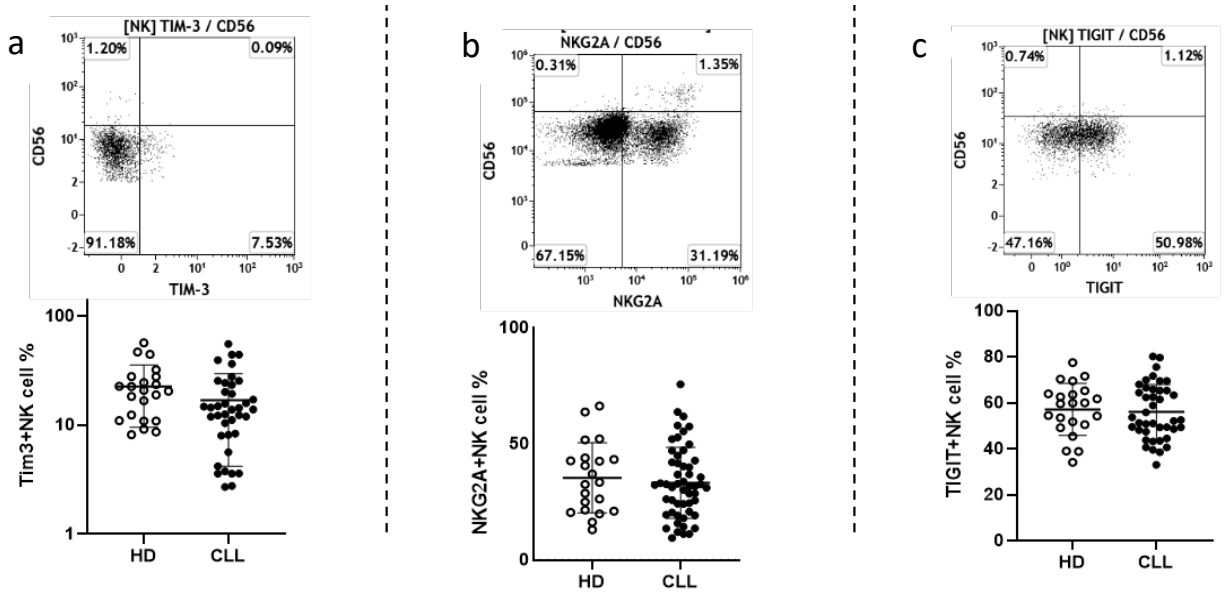

Figure 3.8 Surface expression of Tim-3, NKG2A and TIGIT on total NK cells from B-CLL versus HCs

Representative flow plots to demonstrate the gating and expression of Tim-3 (a), NKG2A (b), and TIGIT (c) on NK cells from B-CLL patients. Dot graphs are comparisons of Tim-3, NKG2A, and TIGIT expressions on total NK cells between B-CLL patients and HCs. Analysis was performed using Mann-Whitney nonparametric test.

3.2.6 Heterogeneity in expression of adhesion molecules on NK cells from CLL patients

Adhesion molecules play a fundamental role in leukocyte trafficking including NK cells, in addition to mediating cell to cell contacts that are important in the immune response against tumor and pathogens. For example, during cytolytic activity, integrins regulate the size and duration of lymphocyte degranulation and the rate of target cell lysis (Steblyanko et al, 2015). This part of NK cell phenotype has not been explored in B-CLL patients.

Initial study from our group has demonstrated that adhesion molecules, including NCAM-1, ITGAL, ITGB2, SPN, ITGAM are downregulated on NK cells from B-CLL patients at the transcription level (Parry, Stevens, et al., 2016) .Accordingly, we could reasonably hypothesise that the surface expression of adhesion molecules on NK cells are down regulated as well. Therefore, we investigated the surface expression of a panel of adhesion molecules (**Chapter 2 Table 2.10 and Table 2.11**) on total NK cells and differential expression on NK subsets from untreated CLL patients and age matched healthy controls using flow cytometry.

3.2.6.1 Expression of CD49a, CD49d and CD43 was downregulated on NK cells from B-CLL patients

Alpha 1 subunit (CD49a) and Alpha 4 subunit (CD49d) are both subunits of the integrins, which are transmembrane receptors that are important for cell to cell adhesion and critical for signalling and homeostasis (H. Sun, Liu, et al., 2019). Interestingly, the frequencies of CD49a and CD49d positive NK cells were both significantly decreased in CLL patients 1.53 ± 0.35% and 88.05 ± 2.34% compared to 1.90 ± 0.33% and 96.83 ± 0.59% (Mean ± SEM) on NK cells from healthy controls ($p = 0.0302$ and $p = 0.0090$ Mann-Whitney test), respectively (**Figure 3.9 a, b**). In CLL patients, CD49d is expressed almost at equal levels on different NK subsets,

except $CD56^{dim}$ $CD16^{neg}$ that showed significant decrease in expression of CD49d (p=<0.0001 one-way ANOVA nonparametric test). In addition, compared to $CD56^{dim}$ $CD16^{neg}$ subset from healthy controls CD49d was also significantly down regulated on the same NK subset from CLL patients (69.89±4.49 vs 86.74±2.77) (p=0.0267) (**Figure. 3.9a**).

Moreover, flow analysis showed that Sialophorin (CD43) adhesion molecule was significantly downregulated on total NK cells from CLL patients compared to NK cells from healthy controls (93.09±1.60 and 97.14±0.43) (p=0.0395) (**Figure 3.9 b**). CD43/SNP is one of the adhesion molecules that has been found downregulated in the microarray analysis in NK cells from B-CLL patients. SNP (sialophorin) is a surface glycoprotein on lymphocytes that is potentially important for proper immune function (Velázquez et al., 2016). In CLL patients, the expression of CD43 was significantly lower on non-cytotoxic potential NK subsets $CD56^{dim/bright}$ $CD16^{neg}$ particularly $CD56^{dim}$ $CD16^{neg}$ compared to cytotoxic NK subsets $CD56^{dim/bright}$ $CD16^{pos}$ (p<0.0001). This reduction was also pronounced on $CD56^{dim}$ $CD16^{neg}$ subset compared to $CD56^{dim}$ $CD16^{neg}$ subset from healthy controls, but this reduction was not statistically significant (**Figure 3.9 c**). No significant differences were seen in the expression of CD11a and CD11b between CLL and healthy controls.

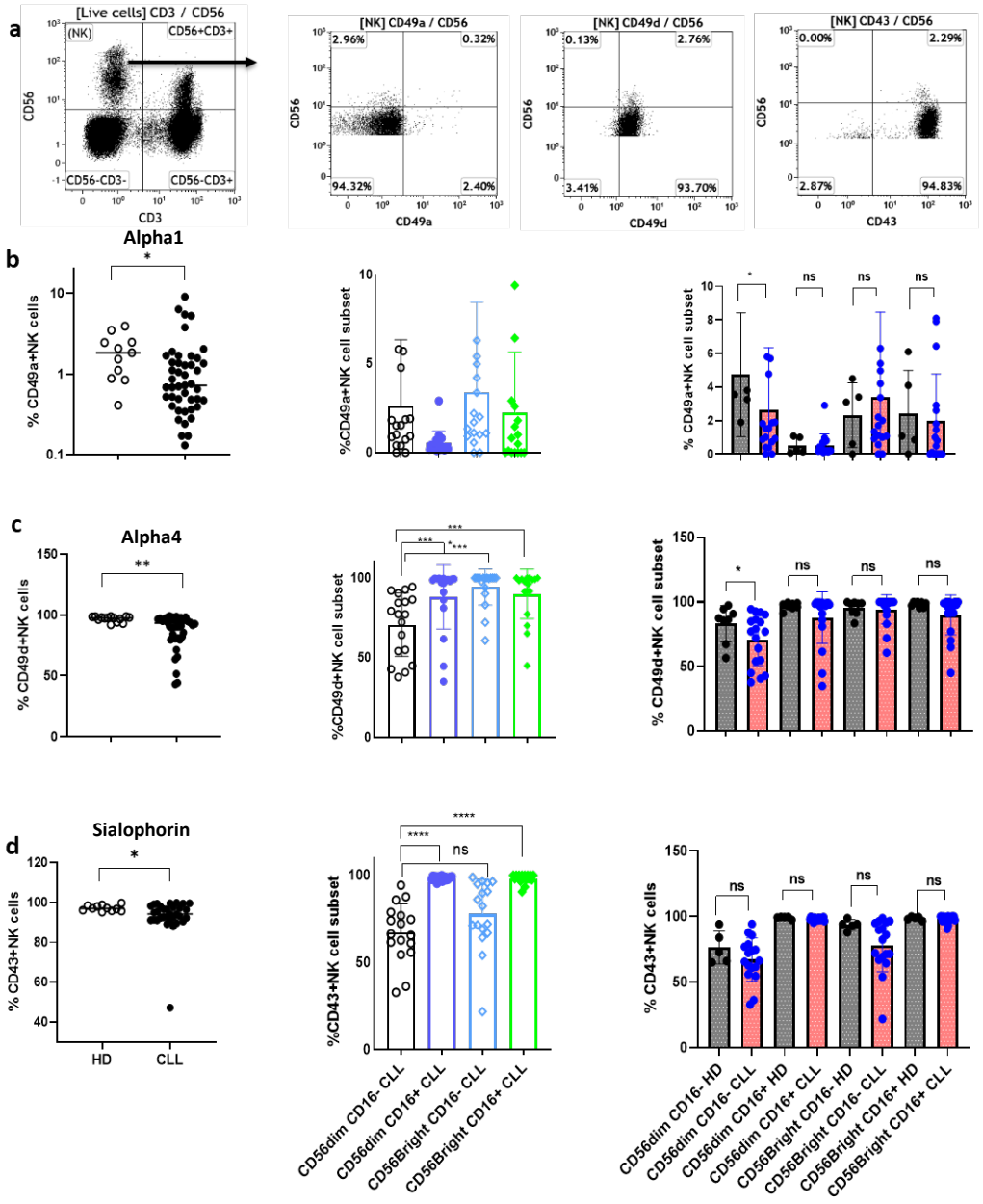

Figure 3.9 CD49a, CD49d and CD43 expression are significantly downregulated on NK cells from B-CLL patients compared to HCs.

Surface expression of alpha 1 CD49a, alpha 4 CD49d and Sialophorin CD43 was analysed using flow cytometry. Gating strategy and example of staining for each marker are shown in panel (**a**). Dot plot graphs to compare the expression of these three surface markers, each dot represents a single donor. The frequency of CD49a+ NK cells and CD49d+ NK cells were down regulated in B-CLL patients, and both were reduced on $CD56^{dim}$ $CD16^{neg}$ subset compared to healthy controls (b and c respectively). The frequency of CD43+ NK cells was also significantly down regulated in B-CLL patients, its lower frequency was more pronounced on $CD56^{dim/bright}$ $CD16^{neg}$ subsets (d). Each dot represent individual of eighter CLL patient or healthy control. Analysis was done by Mann Whitney and Wilcoxon matched-paired nonparametric tests (*p<0.05, **p<0.01, and ****p<0.0001).

3.2.6.2 Expression of CD18 and CD11c was upregulated on NK cells from CLL patients

Beta 2 integrin CD18 and alphaX CD11c can form a complement receptor CR4 (CD11c/CD18) which has an important role in immune response and participates in cell adhesion to fibrinogen (Sandor et al, 2016). Both molecules were upregulated on NK cells from CLL patients compared to NK cells from healthy controls 92.7±1.4 vs 89.9±1.3 and 5.65±1.27 vs 2.09±0.43 ($p=0.0183$ and $p=0.0104$) respectively **(Figure 3.10 b, c)**. In both CLL patients and healthy controls, potential cytotoxic NK subset $CD56^{dim}$ $CD16^{pos}$ expressed the highest level of CD18 compared to another three NK subsets ($p<0.0001$) (**Figure 3.10 c**). In comparison of four NK subsets, the increase of CD18 expression on NK cells from B-CLL patients was significant on both $CD56^{bright}$ NK subsets including $CD56^{bright}$ $CD16^{pos}$ and $CD56^{bright}$ $CD16^{neg}$ compared to HCs for $CD56^{bright}$ $CD16^{pos}$ 87.4±3.2% vs 76.8±5.8% ($p=0.0228$), and $CD56^{bright}$ $CD16^{neg}$ 62.6±5.8% vs 42.9±7.6% ($p=0.0479$).

CD11c has a different expression pattern compared to CD18, which was predominantly expressed on $CD56^{dim}$ $CD16^{neg}$ subset in both CLL and healthy controls, and the increased expression was more pronounced on cytotoxic NK subset $CD56^{dim}$ $CD16^{pos}$ in CLL patients compared to healthy controls (**Figure 3.10 c**).

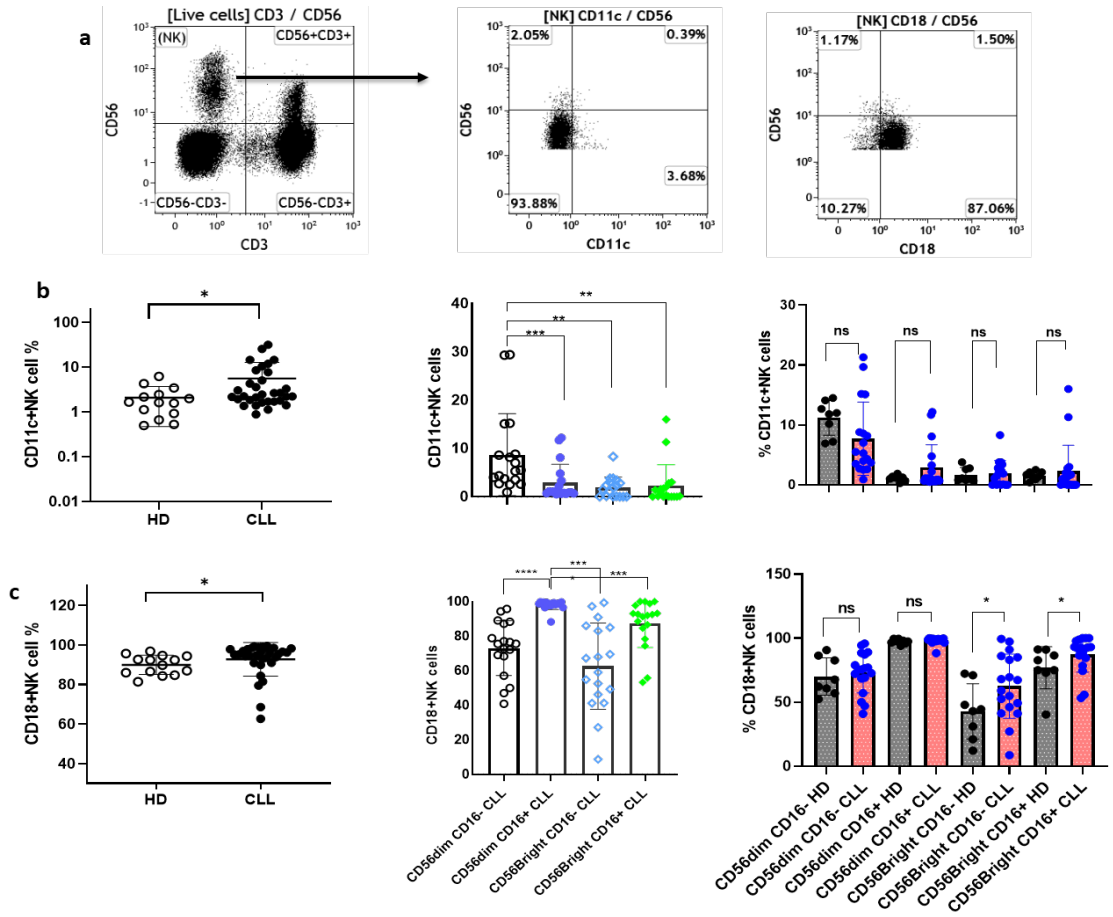

Figure 3.10 Expression of Beta 2 integrin CD18 and alphaX CD11c on NK cells and its subsets from B-CLL patients in comparison to NK cells from healthy controls.

Dot plots depict gating of NK cells and example of alphax CD11c and beta 2 integrin CD18 expression on NK cells (a). Dot plot to compare the expression of these two surface markers, each dot represents a single donor. The frequency of CD11c+NK cells and CD18+NK cells were markedly upregulated in B-CLL patients compared to healthy controls (b and c respectively). CD11c expression was predominant on $CD56^{dim}$ $CD16^{neg}$, compared to healthy NK cell subsets, the increased expression was mostly on cytotoxic NK subsets ($CD56^{dim}$ $CD16^{pos}$). Whilst CD18 expression was at highest level on cytotoxic NK subsets and also was increased on $CD56^{bright}$ NK subsets. Analysis was done by Mann Whitney and Wilcoxon matched-paired nonparametric tests (*p<0.05, **p<0.01, ***p<0.001 and ****p<0.0001).

3.2.6.3 PSGL-1 (CD162) homing receptor was downregulated on NK cells from CLL patients

P-selectin glycoprotein ligand -1 (CD162) is a member of selectins family known as homing receptor which mediates the first step of the immune cells entering into infected or tumor tissue from the blood. Although *in vitro* assays of NK cells from selectin-deficient mice showed normal function, they are impaired in *in vivo* assays (Sobolev et al, 2009). Accordingly, the surface expression of CD162 was measured on NK cells from CLL patients and compared to healthy controls. Flow dot blots show gating of NK cells and CD162 expression on NK cells (**Figure 3.11 a**). CD162 expression was higher on $CD16^{pos}$ NK cells compared with $CD16^{neg}$ NK cells. Interestingly, CD162 expression was markedly lower on NK cells from B-CLL patients compared to NK cells from healthy controls 77.03±2.74% vs 96.65±0.61% respectively, ($p<0.0001$) (**Figure 3.11 b**). To compare those four NK subsets, the data showed that the reduction of CD162 expression was more pronounced on $CD56^{dim}$ $CD16^{neg}$ and $CD56^{bright}$ $CD16^{neg}$ compared to healthy controls 51.81±4.19 vs 76.31±4.35 and 76.93 ± 4.87 vs 93.65 ± 1.64 ($P=0.0010$ and $P=0.0267$) respectively (**Figure 3.11 b**). However, CD162 expression was high (> 90%) and preserved on cytotoxic NK subsets $CD56^{dim/bright}$ $CD16^{pos}$ compared to healthy controls.

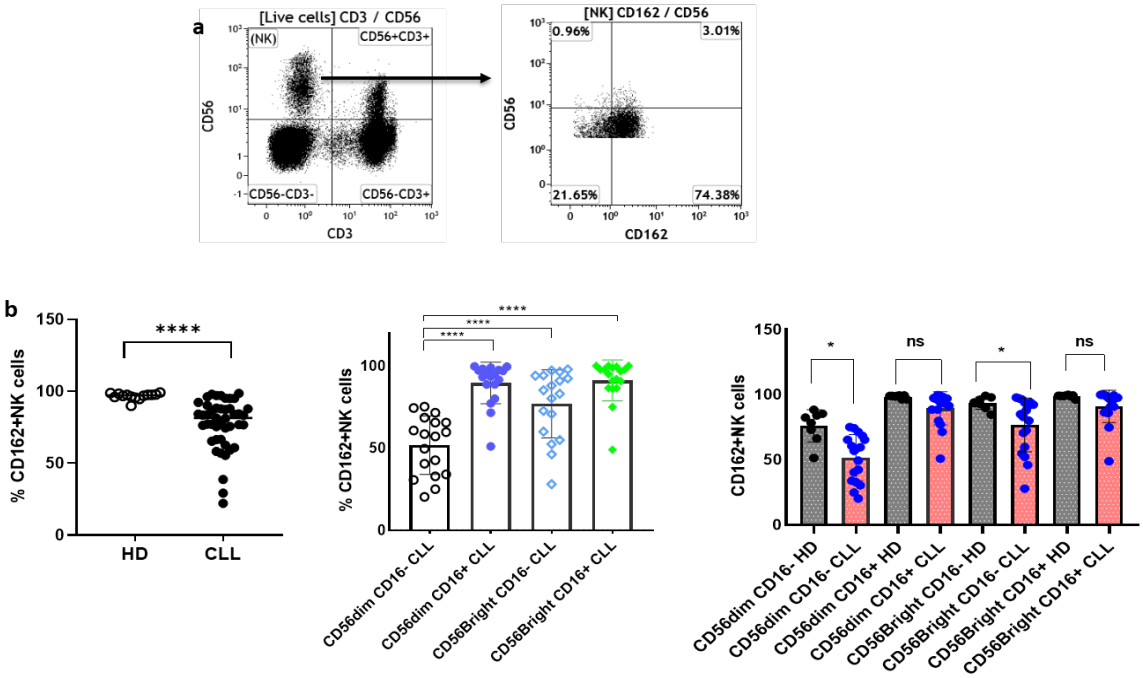

Figure 3.11 CD162 expression on NK cells from B-CLL patients was downregulated compared to NK from healthy controls.

Flow plots show gating strategy for NK cells and example of PSGL-1 CD162 expression on NK cells (**a**). The frequency of CD162+NK cells in B-CLL patients and HCs. Also, CD162 expression was compared between four different NK subsets within B-CLL patients and B-CLL vs HCs (**b**). Analysis was done by Mann Whitney and Wilcoxon matched-paired nonparametric tests (*p<0.05, **p<0.01, ***p<0.001).

3.3 Discussion

This chapter addressed the distribution and phenotype of NK cells from untreated CLL patients compared to age-matched healthy controls. The data showed that NK cell frequency was significantly lower in B-CLL patients compared to healthy controls. $CD56^{dim}$ $CD16^{pos}$ and $CD56^{bright}$ $CD16^{pos}$ NK subsets were considerably higher unlike $CD56^{dim}$ $CD16^{neg}$ and $CD56^{bright}$ $CD16^{neg}$ NK subsets in B-CLL patients compared to HCs. Also, the effect of HCMV infection on NK cell distribution and phenotype in B-CLL patients was studied. CMV infection drives the expansion of whole NK cells, particularly NKG2C positive NK cells in B-CLL patients (Sportoletti et al., 2021). Interestingly, although there was a significant decrease in the frequency of $CD56^{dim}$ $CD16^{neg}$ NK subset in CMV seropositive B-CLL patients compared to CMV seronegative patients, a positive correlation was found between the absolute count of NK cells and tumor B cells count, which indicates that tumor B cells play a role in NK cell expansion as well in B-CLL patients.

In addition, the immune checkpoints and adhesion molecules expression pattern was studied on NK cells from B-CLL patients. Expression of PD-1, CTLA-4, LAG-3 and CD96 was found to be significantly higher on NK cells from B-CLL patients compared to HCs. In contrast, there is no significant changes in expression of TIM-3, TIGIT and NKG2A. The expression of adhesion molecules has a mixed message. Where the expression of integrins including CD49a, CD49d and CD43 and homing receptor CD162 were markedly downregulated, but expression of CD18 and CD11c was significantly upregulated on NK cells from B-CLL patients compared to HCs.

3.3.1 Distribution of NK cells and NK subsets in peripheral blood of CLL patients

The immune system of previous diagnosed CLL patients characterised by expansion of $CD8^+$ T cells and NK cells coincided with tumor B cells evolution due to tumor microenvironment that tumor B cells created. The increase of $CD8^+$ T cells declines overtime with disease progression. In contrast, NK cell expansion remains high overtime in B-CLL patients (Huergo-Zapico et al., 2014), suggesting the potential antitumor role of NK cells against tumor B cells. Increased number of NK cells in CLL patients has been considered as a favourable marker and associated with better prognosis (Palmer et al., 2008).

In our study, the data showed that the percentage of total NK cells in CLL patients was significantly lower compared to healthy controls (**Figure 3.2 a**). This is probably due to the fact that most of our patients are at the early stage of their disease and $CD8^+$ T cell expansion overwhelms NK cell expansion (Roessner & Seiffert., 2020). Particularly, we have observed the different distribution of NK subsets. Percentages of NK cell subsets with potential cytotoxicity (highly differentiated/mature NK cells) $CD56^{dim}$ $CD16^{pos}$ and $CD56^{bright}$ $CD16^{pos}$ were significantly increased in peripheral blood of our CLL cohort compared to healthy controls (**Figure 3.2 d**). Whilst regulatory NK cell subsets $CD56^{dim}$ $CD16^{neg}$ and $CD56^{bright}$ $CD16^{neg}$ were markedly lower in B-CLL patients. This implies that NK cells have been stimulated to mature/highly differentiated stage in B-CLL patient, which could be due to either the tumor B cells themselves or/and the tumor microenvironment that tumor cells created.

On the other hand, there are other factors that can induce maturation and expansion of NK cells such as HCMV infection. Studies have described a specific NK cell subset with high differentiation phenotype $CD56^{dim}$ $NKG2C^+$ NK cells that expands in response to CMV

infection and also this NK population increased in peripheral blood of CLL (Hofland et al., 2019). As expected, our data showed that the percentage of total NK cells significantly increased in HCMV seropositive B-CLL patients compared to HCMV seronegative, and this expansion was coincided with the increase of proportion of $NKG2C^{+}$ NK cells. Combine our data with previous findings, it suggests that the expansion of high differentiated $NKG2C^{+}$ $CD56^{dim}$ NK cells are correlated with both CMV infection and tumor B cells.

Classically NK cells have been identified as two populations, $CD56^{dim}$ and $CD56^{bright}$. However, more and more studies point to that at least four different NK subsets can be identified according to the expression pattern of CD56 and CD16, which can serve different function (Amand et al., 2017; Michel et al., 2016). One interesting finding from our study is that the percentage of $CD56^{dim}$ $CD16^{neg}$ NK subset was significantly lower in B-CLL patients compared to HCs and was even lower in those CMV seropositive than CMV seronegative B-CLL patients. Our study with pancreatic cancer (PDAC) patients has shown that $CD56^{dim}$ $CD16^{pos}$ NK cells were enriched within tumor but depleted within peripheral blood, and it can help to control disease recurrence (Marcon et al., 2020).

In HIV-1 infection, study has shown that there is a reduction in $CD56^{dim}$ $CD16^{neg}$ subset but not other NK subsets, which can be partly reversed through antiretroviral treatment (Müller-Durovic et al., 2019; Amand et al., 2017). They hypothesized that this reduction of $CD56^{dim}$ $CD16^{neg}$ NK cells population contribute to the impairment of NK cell function in HIV-1 positive individuals. This subset normally carries less mature NK phenotype with high expression of NKG2A and low CD57. Altogether, these data suggest that comorbidity of CMV

and CLL disease can together modify $CD56^{dim}$ $CD16^{neg}$ NK subset and contribute to the NK function impairment.

3.3.2 NK cell count is correlated with tumor B cells count

The percentage of NK cells in B-CLL patients is substantially low compared to healthy controls. NK cell absolute count, however, is significantly higher in B-CLL patients and similar observation for T cells. Increased NK cell and T cell numbers has been shown to be related with the disease progress and increase of tumor B cells number in the blood of CLL patients (Le Garff-Tavernier et al., 2011).

To investigate this, absolute count of tumor B cells ($CD5^{+}$ $CD19^{+}$ B cells), NK cells ($CD3^{neg}$ $CD56^{pos}$) and its subsets were measured using flow cytometry. Interestingly, significant correlation was observed of total NK cell number vs tumour B cell burden. $CD56^{dim}$ $CD16^{neg}$ NK subset was the only subset that significantly correlated with tumor B cell burden. However, cytotoxic NK subset $CD56^{dim}$ $CD16^{pos}$ was not significantly correlated with tumour burden. This finding was in line with other reports that expansion of NK cells in parallel with high tumor burden, which is characterized by selective loss of most mature NK cells bearing $CD56^{dim}$ $NKG2D^{bright}$ $CD27^{dim}$ KIR^{+} (MacFarlane et al., 2017). This NK phenotype typically evokes antitumor response against tumour cells (Caligiuri, 2008). Taken together, B-CLL disease progress drives subpopulation of NK cell expansion, but not the cytotoxic NK subsets, and this contributed to the low antitumor activity of NK cells observed in CLL patients.

3.3.3 The immune checkpoints expression was upregulated on NK cells from B-CLL patients

In the absence of priming stage, NK cells demonstrate strong antitumor cell cytotoxicity against autologous and allogenic tumor cells and produce cytokines (D. Cho et al., 2010). This process is tightly regulated by the balance between activating and inhibitory receptors expressed on the surface of NK cells. Imbalance of immune regulatory receptors of NK cells has been reported in many cancer types such as Multiple myeloma, Hodgkin lymphoma and ovarian cancer (Cao et al., 2020; Guillerey et al., 2015; Souza-Fonseca-Guimaraes et al., 2019). Many studies have reported that NK cells express array of immune checkpoints similar to that expressed on T cells, for example but not limited to PD1, TIGIT,CTLA-4, CD96 and LAG-3 (Narayanan et al., 2020; H. Sun, Huang, et al., 2019). At present, PD1 and CTLA-4 are the most studied checkpoints, where blocking these immune checkpoints showed an incredible result in reversing T cell exhaustion and restoring antitumor capacity of T cells (Zou, 2018; Robert et al., 2015). In fact, upregulation of coinhibitory receptors on exhausted T cells such as PD1, LAG-3 and CTLA-4 has been demonstrated in B-CLL patients. As a result, this has led to the development of immune checkpoint blockade targeting T cells as a new strategy for CLL treatment (Ntsethe et al., 2020).

The expression and functionality of immune checkpoints on NK cells in B-CLL patients has not been evaluated. Therefore, this work investigated the expression of variety of immune checkpoint molecules on the surface of NK cells from untreated B-CLL patients by flow cytometry. Interestingly, our findings showed that NK cells from B-CLL patients express multiple immune checkpoints including PD1, CTLA-4, LAG-3 and CD96 (**Figures 3.6 and 3.7**). Most of these molecules, including PD-1, CTLA-4 and LAG-3 were highly expressed on

expanded cytotoxic NK cells .It's well established that the role of antitumor function of NK cells in cancer microenvironment is affected by increasing expression of inhibitory immune checkpoints and decreased activating receptors, which facilitates tumor immune escape and enables the development of different cancer types (Chiossone et al., 2017).

PD1 is expressed on activated NK cells (Pesce et al., 2017), and has recently been reported to be upregulated on NK cells in many cancer types including head and neck cancer, multiple myeloma, and Hodgkin lymphoma (Concha-Benavente et al., 2018; Giuliani et al., 2017). The ligands of PD1 (PDL1 and PDL2) are upregulated by many tumor and immune cells and their expression on tumor B-CLL cells are investigated in chapter 5. Their engagement with PD1 mediates potent inhibition of effector T cells and NK cells, allowing tumor cells to escape immunosurveillance (Taube et al., 2012). In vitro work has demonstrated that PD1 expression on NK cells from Lung cancer can be induced by high concentration of plasma IL-2 and is negatively regulated antitumor function of NK cell (Niu et al., 2020). Blocking PD1-PDL1/2 interaction can increase the antitumor activity of NK cells against both lung cancer and multiple myeloma cells (Benson et al., 2010; Niu et al., 2020). In this study, we have demonstrated for the first time that PD-1 expression is upregulated on NK cells from B-CLL patients. In a small group of patients, there are around 10 – 20% of NK cells with high PD-1 expression (**Figure 3.6**). In CLL, PDL1 was expressed by tumor B cells, upregulated on T cells, and expressed by monocytes as well (He et al., 2018; Xu-Monette et al., 2018). Thus, high PD1 NK cells in B-CLL patients might be functionally exhausted and blockade of PD1-PDL1/2 might be beneficial in restoring antitumor function of NK cells in B-CLL patients. However, the potential mechanism of how PD-1 effects NK cell phenotype and function still need more in-depth study. High PD-1 expression on NK cells in B-CLL patients creates a useful model for this study (PD-1 expressing NK cells will be investigated further in the next few chapters).

Likewise, CTLA-4, which is a key regulatory of T cell expansion, has been reported to be expressed on activated mouse NK cells. Its ligation with cognate ligands CD80 (B7-1) and CD86 (B7-2) inhibits cytokines production in response to dendritic cells (Stojanovic et al., 2014). Although expression level of CTLA-4 on NK cells from B-CLL patients was quite minor, and B7.1- CD28 interaction is not required to trigger NK cells activation, which render it uncertain what kind of role does CTLA-4 play in modulating NK cells function. But anti CTLA4 antibody has been shown to be able to enhance NK cell function, which can be due to the indirectly effect through blocking the suppressive CTLA-4^{+} Tregs (Hannani et al., 2015). Reports demonstrated that T regulatory cells are elevated in CLL patients, using anti CTLA-4 therapy for CLL patients might indirectly improve NK cell function by depleting Tregs.

CD96 and TIGIT are two novel immune checkpoint receptors expressed on NK cells. These inhibitory receptors compete with activating receptor DNAM-1 for binding to CD155 and CD112 ligands (Jin & Park, 2021). Engagement of CD96 and TIGIT to CD155 (main ligand for both receptors) counteract DNAM-1 mediating NK cell activation. TIGIT expression is conserved on resting NK cells but not mouse NK cells, and increased upon NK cell activation(Martinet & Smyth, 2015). Whereas CD96 is primely expressed on both human and mouse resting NK cells and found to inhibit mouse NK cells upon interaction with CD155 present on the target cells (Kim & Kim, 2018). Interestingly, our findings showed that CD96 expression was significantly upregulated on NK cells from B-CLL patients but not TIGIT. Both checkpoint molecules have role in modulating NK cells function, CD96 regulates IFN-γ production whilst TIGIT regulates NK cell cytotoxicity and cytokines production. However clinical results of blocking CD96 and/or TIGIT in human cancer patients remains under investigation (Blake et al., 2016). In our previous study (Parry, Stevens, et al., 2016), DNAM-1 expression has been shown to be downregulated on NK cells from B-CLL patients. This

upregulation of CD96 consolidates that DNAM-1/TIGIT/CD96 complex plays a role in NK cells function impairment in B-CLL patients. This will be investigated further in the next chapter.

Similar to the other checkpoint molecules mentioned above, LAG-3 is expressed on activated T and NK cells (Kisielow et al., 2005). Once binds to its ligand, LAG-3 inhibits anti-tumor function of $CD4^+$ T cells and involved in T cell exhaustion together with PD1. T cell function is enhanced by LAG-3 blockade, but LAG-3's role in regulating NK cell function still not well investigated. We found that LAG-3 expression was upregulated on NK cells from CLL patients, and this expression was pronounced in both $CD56^{dim}$ and $CD56^{bright}$ NK cells (**Figure 3.7**). Recent study has shown that there is an increase in LAG-3 expression in human NK cells following activation with IFN-α, and its expression was confined on high mature and cytotoxic NK subset. Blocking LAG-3 in NK cells by in vitro antibody led to dramatic increase in cytokines production, including IFN-γ and TNF-α but did not affect NK cytotoxicity capacity (Narayanan et al., 2020).

Altogether, NK cells from B-CLL patients showed upregulation of multiple immune checkpoint molecules that regulate cytokines production and cytotoxicity of NK cells, unveiling at least part of mechanisms mediating NK cell impairment in B-CLL patients. These immune checkpoints might be successful target in immunotherapy to restore antitumor function of NK cells in those patients.

3.3.4 Adhesion molecules were downregulated on NK cells from CLL patients

The expression of adhesion molecules has been extensively studied on both NK and T cells. Their role is fundamental in circulation and homing, cell interaction to extracellular and cell to cell contact (Robertson et al., 1990). IL-2 has been shown to modulate expression of adhesion molecules on NK cells. Indeed, IL-2 can significantly influence the expression of some integrins such as β1 integrins (CD49d and CD49f), β2 (CD11b and CD11c) and L-selectins (CD62L), but the effect can be upregulation or downregulation. Whilst some β1 and β2 integrins (CD11a and CD18) were increased upon culturing with IL-2, L-selectins expression was decreased (Mäenpää et al., 1993). This indicates that these changes of adhesion molecules induced by IL-2 facilitate cytotoxicity, but another hand decrease the migration capacity of NK cells.

Recent study has investigated the expression pattern of some genes coding for adhesion molecules of NK cells taken from B-CLL patients (Parry et al., 2016). Gene expression levels of some adhesion molecules has been significantly downregulated compared to healthy controls, particularly CD43 and CD11 isoforms. This work was performed to validate the surface expression of these adhesion molecules and to expand the panel of adhesion molecules on NK cells from B-CLL patients. Interestingly, our data showed that few integrins and P-selectin were markedly down regulated on NK cells from B-CLL patients compared to healthy controls including CD43, CD49d and CD49a. However, β2 integrins CD18 and CD11a were up regulated on NK cells from B-CLL patients. The active state of β2 integrins is involved in mediating the slow rolling of NK cells and killing of target cells (Fagerholm et al., 2019). Adhesion molecular profile of NK cells from B-CLL patients partially resembles to the NK

cells profile observed after IL-2 activation, indicating the possibility of activated state of NK cells in B-CLL patients.

P-selectin (CD162) is an adhesion molecule that is crucial in initiating extravasation of NK cells (Coupland et al., 2012) was also significantly down regulated on NK cells from B-CLL patients. However, adhesion molecules have variable effect on NK cell migration. Blocking CD162 and CD18 with antibodies had a minor effect on rolling adhesion of NK cells, whilst blocking CD49d and CD11a had a significant reduction on the static adhesion of NK cells by 60% and 47% respectively, and by 82% of blocking both CD49d and CD11a (Schneider et al., 2002). Since integrins mediate trafficking and rolling of NK cells through the extra cellular matrix and adhesion of NK cells to the target cell and the following cytotoxicity, the migration ability of NK cells from B-CLL patients might be reduced.

To conclude, the adhesion molecule profile of NK cells from B-CLL patients was different to NK cells profile from healthy controls. Adhesion molecules profile of NK cells from B-CLL resembles the NK cell profile after co-culture with IL-2, suggesting that changes in adhesion molecules expression of NK cells from B-CLL patients are reflection of highly differentiated/activated/exhausted phenotype of NK cells.

3.4 Conclusion

In conclusion, this chapter has investigated the distribution of NK cells and NK subsets in B-CLL patients, the potential effect of CMV serostatus and tumor B cell burden. Analysis showed that the percentage of cytotoxic NK subsets (CD16 expressing NK cells) were upregulated in B-CLL patients compared to healthy controls. In contrast, the percentage of noncytotoxic and less mature NK subsets (CD16 ^{negative} NK subsets) were down regulated in B-CLL, particularly $CD56^{dim}$ $CD16^{neg}$ subset was significantly lower in B-CLL patients than HCs, which might reflect the differentiation/activation state of NK cells in B-CLL patients. In addition, immune checkpoints and adhesion molecules expression were assessed. PD1, CTLA-4, LAG-3 and CD96 that regulate the cytotoxicity and cytokines production were significantly upregulated by NK cells from B-CLL patients. Furthermore, some adhesion molecules that mediate rolling migration and facilitate cytotoxicity of NK cells were lower on NK cells from B-CLL patients compared to NK cells from healthy controls. These findings might unveil part of mechanisms behind NK cell functional impairment in B-CLL patients. For new CLL therapy, these molecules might be potential therapeutic targets for restoring anti tumor function of NK cells in CLL patients.

CHAPTER 4: NK CELL FUNCTIONAL CAPACITY IN B-CLL PATIENTS

4.1 Introduction

NK cells from CLL patients have been shown to be dysfunctional, with reduced cytotoxicity capacity. NK cell dysfunction state increases the risk of infection and decreases antitumor surveillance leading to disease progression. However, the mechanism behind NK cell function impairment in CLL patients is poorly understood. Previous reports have shown that the frequency and expression level of NKG2D and NCRs on NK cells were downregulated in B-CLL patients, which at least contributed partly to this impaired cytotoxicity of NK cells against tumor cells. As discussed in the previous chapter, in B-CLL patients the frequency of NK cells expressing adhesion molecules that mediate NK cell migration was significantly lower in B-CLL, in addition to up regulation of immune checkpoint molecules. It was worth to further investigate the functionality of NK cells from B-CLL patients and assess the impact of these phenotype changes in NK cell function.

Here, this chapter aimed to study the functionality of NK cells in B-CLL patients using a few more readouts other than cytotoxicity assay, which has been focused on the previous studies. At first, the ability of *in vitro* migration of NK cells from B-CLL patients was measured and compared to NK cells from healthy controls, which aims to demonstrate the impact of lower adhesion molecules on NK cells from B-CLL. In addition, a panel of cytokines production was measured after stimulation with K562, this was compared with NK cells from age-matched HCs. Last but not least, DNAM-1/CD96/TIGIT dependent killing capacity of NK cells was studied and compared to NK cells from HCs to explore the possible beneficial effect of

blocking checkpoint molecules CD96 and TIGIT as a potential therapeutic strategy in enhancing of NK killing in CLL patients.

4.2 Results

4.2.1 NK cells from B-CLL patients have impaired migration capacity

As demonstrated in the previous chapter, NK cells from B-CLL patients express significantly lower adhesion molecules, including alpha 1 (CD49a), alpha 4 (CD49d|), sialophorin (CD43) subunits and homing receptor CD162, which have been reported to be able to mediate NK migration (Aguado et al., 1999; Böning et al., 2019). The function of NK cells depends critically on their ability to migrate through extracellular matrix toward target cells or target tissue in case of solid tumors. Next, we investigated the effect of this reduction on the functionality of NK cells from B-CLL patients. The analysis aimed to assess the migration capacity of resting NK cells from B-CLL patients and age matched healthy controls toward tumor cell line using *in vitro* Trans-well migration assay. K562 cell line was used in this assay as a target/attractive tumor cell line. K562 cells are immortalised human myelogenous leukaemia cell line and have been a very useful tool to study NK cell function, due to the lack of MHC-I molecule expression (Lozzio & Lozzio, 1979).

The resting NK cells from B-CLL or healthy controls were placed on the upper chamber of trans-well plate and K562 cells were cultured on the bottom chamber, followed by incubation at 37c 5% Co2 for 12 – 16h. Migrated NK cells in response to K562 cell line were collected from lower chamber of trans-well plate after the incubation and the percentage of migrated NK was calculated (Number of migrated NK cells ÷ starting number of NK cells added to the upper chamber) × 100.

The mean percentages of NK cell that migrated toward K562 cell line was compared between B-CLL patients and age-matched healthy controls 20.3±2.2% vs 29.1±1% respectively (p=0.0051) (**Figure 4.1**). The result indicates that NK cells from B-CLL patients have less ability to migrate to the target cells which can be explained at least partially by the lower adhesion molecule expression phenotype.

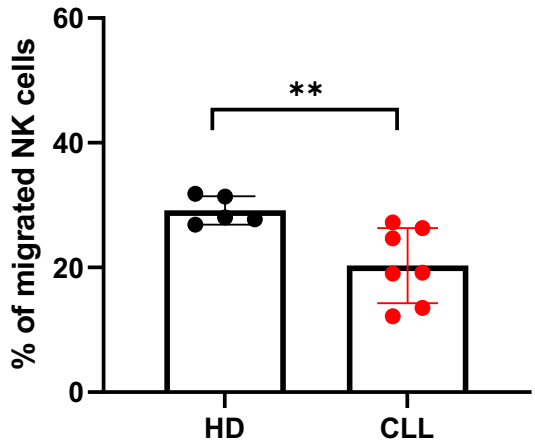

Figure 4.1 *In vitro* assessment of CLL derived NK cell migration towards K562 compared to healthy NK cells.

0.1 × 10^6 NK cells were seeded in the upper trans-well chamber and 0.5×10^6 K562 cells into lower chamber. After overnight incubation NK cells were recovered from the lower chamber, counted, and analysed by flow cytometry to determine the percentage of migrated NK cells. Data are presented as mean for 7 B-CLL patients and 5 healthy controls from 4 independent experiments. Groups were compared by Mann Whitney nonparametric test (**p<0.01).

4.2.2 Impaired cytokines production by NK cells from B-CLL patients

Upon activation, NK cells can produce a wide range of cytokines, predominantly proinflammatory cytokines such as IFN-γ, TNF−α, IL−2 and also anti-inflammatory cytokines like IL-5 and IL-10 (Fauriat et al., 2010; Roda et al., 2006). They can also produce GM-CSF and chemokines such as MIP-1α, MIP−1β and IL−8. IFN−γ, TNF−α are the most prominent cytokines produced by NK cells. IFN-γ has been shown to be one of the most potent cytokines produced by NK cells, as it modulates caspase, Fas-L expression and activate antiviral and antitumoral immunity (Schroder et al., 2004). Unlike chemokines (chemoattractant cytokines) that induce direction of immune cells, cytokines that control the growth and activity/inflammation response of the immune cells need stronger activating signals and longer period to be secreted by NK ells (Fauriat et al., 2010). Particularly, IFN-γ and TNF-α secretion occurs after 6 hours and reach to the peak during overnight incubation with target cells. Engagement of 2B4 receptor is sufficient to induce chemokines, whereas stronger signals triggered by 2B4 and NKG2D is required for Interferon-II and TNF-α. In addition, CD16 engagement could induce both IFN-γ but not TNF-α that require additional signals such as FLA-1or 2B4 (Fauriat et al., 2010).

This work aimed to investigate the cytokines profile of NK cells from B-CLL patients upon interaction with tumor cell lines K562 compared to NK cells from healthy controls. In addition, the differentiated cytokines production profile by different NK subsets was also analysed. To this end, flow cytometry was used to measure the expression of 6 different pro and anti-inflammatory cytokines produced by NK cells (IFN-γ, TNF-α, IL-2, IL-4, IL5 and IL10) and was compared to healthy NK cells and dissected according to four different NK subsets.

4.2.2.1 NK cells from B-CLL patients produce lower levels of IFN-γ after interaction with tumor target cells compared to healthy controls.

To further investigate NK cell function in B-CLL patients, the ability of cytokines production by NK cells was measured in comparison to NK cells from age-matched healthy controls. Cytokines production was determined by intracellular FACS staining after overnight stimulation with tumor target cells K562 and the amount of cytokines were expressed as a percentage to demonstrate the frequency of NK cells that produce cytokines. The findings showed that the cytokines production of NK cells in both B-CLL and healthy controls was similar without stimulation. The most prominent cytokines produced by NK cells after stimulation were TNF-α (Mean) 4.2% followed by IFN-γ 3.2% and with less extend of IL-2 2.1%, IL-4 1.7% and IL-5 1.6% respectively. The same pattern was observation for healthy controls. In addition, NK cells from B-CLL patients produced small amount of anti-inflammatory cytokine IL-10 1.9% and it was similar to that expressed by NK cells from healthy controls. However, NK cells from B-CLL patients produce significantly lower IFN-γ compared to NK cells from healthy controls with 3.2±0.3% vs 5.2±0.5% ($p=0.0054$) (**Figure 4.2**). There were no significant differences between other cytokines production that were investigated (**Figure 4.2**).

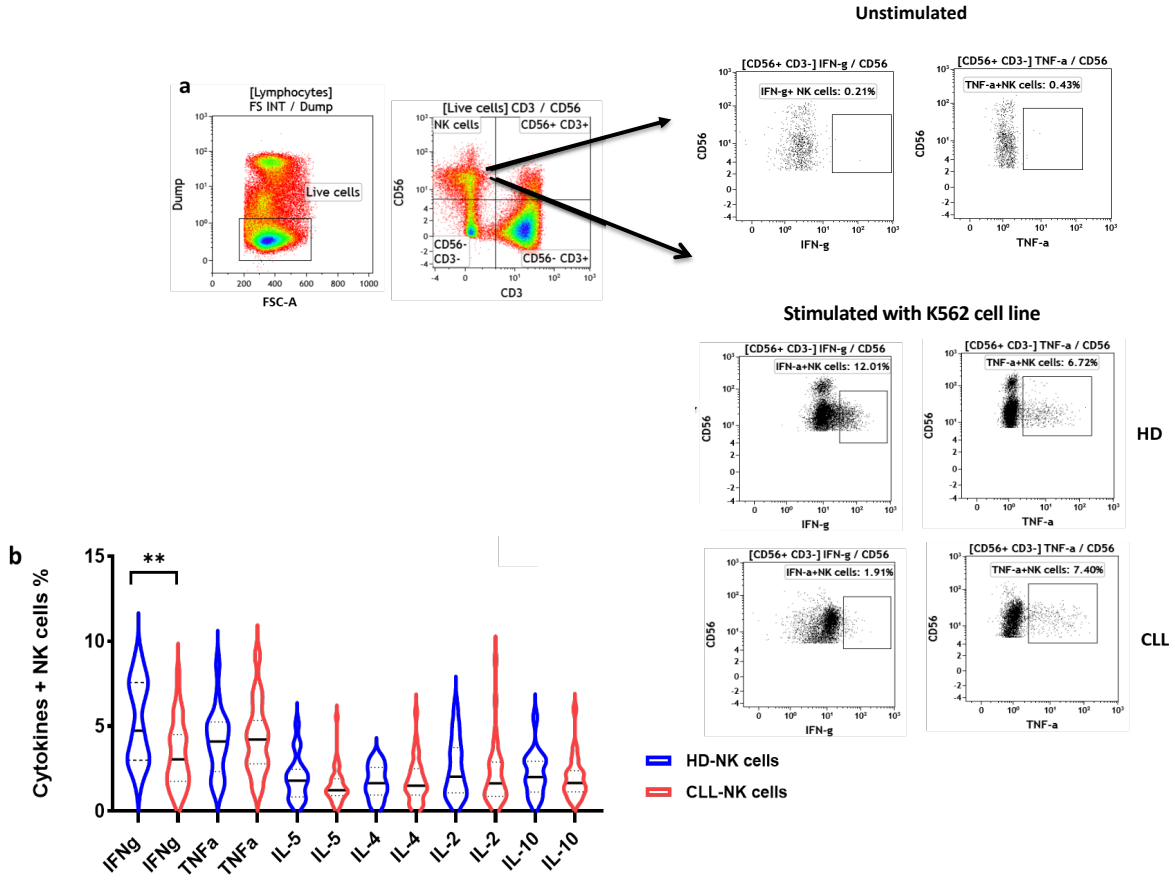

Figure 4.2 Gating strategy and cytokines production profile following K652 stimulation.

Representative flow cytometric analysis of IFN-γ and TNF-α production by NK cells from B-CLL patients and healthy NK cells following K562 stimulation (overnight) at E/T ratio 1:1. NK cells without stimulation are also shown as a control (**a**). The expression of various pro and anti-inflammatory cytokines is shown in violin plots for B-CLL (n=29) (red violin) and healthy NK cells (n=22) (blue violin) (**b**). Data analysed by Mann Whitney nonparametric test (**p<0.01).

4.2.2.2 $CD56^{dim}$ $CD16^{neg}$ NK subsets are the major producer of cytokines upon target cell stimulation

As NK cells from B-CLL patients produce lower IFN-γ, it was important to evaluate which NK subset responsible for cytokines production in response to target cell stimulation. NK population was divided into four subsets based on surface expression of CD16 and CD56 as shown in the previous chapter, $CD56^{bright}$ $CD16^{neg}$, $CD56^{bright}$ $CD16^{pos}$, $CD56^{dim}$ $CD16^{neg}$ and $CD56^{dim}$ $CD16^{pos}$. Previous reports have demonstrated that $CD56^{bright}$ NK subsets are the major producer of cytokines upon stimulation with cytokines such as IL-12, IL-15, and IL-18 (G. M. Konjević et al., 2019). Here we sought to determine the main subset of NK cells in B-CLL patients that produce cytokines when stimulated overnight with K562 cell line at E/T ratio 1:1. Using flow cytometry, result showed that $CD56^{dim}$ $CD16^{dim}$ was the major NK subset that produce cytokines compared to the other three NK subsets (**Figure 4.3**). The mean frequency of IFN-γ and TNF-α production for these four NK subsets from B-CLL patients ($CD56^{bright}$ $CD16^{neg}$, $CD56^{bright}$ $CD16^{pos}$, $CD56^{dim}$ $CD16^{neg}$ and $CD56^{dim}$ $CD16^{pos}$) were 2.2±0.5% and 2.5±0.6, 2.4±0.7% and 1.9±0.7%, 6.8±0.5% and 7.5±0.9%, 2.9±0.4% and 2.6±0.5% respectively.

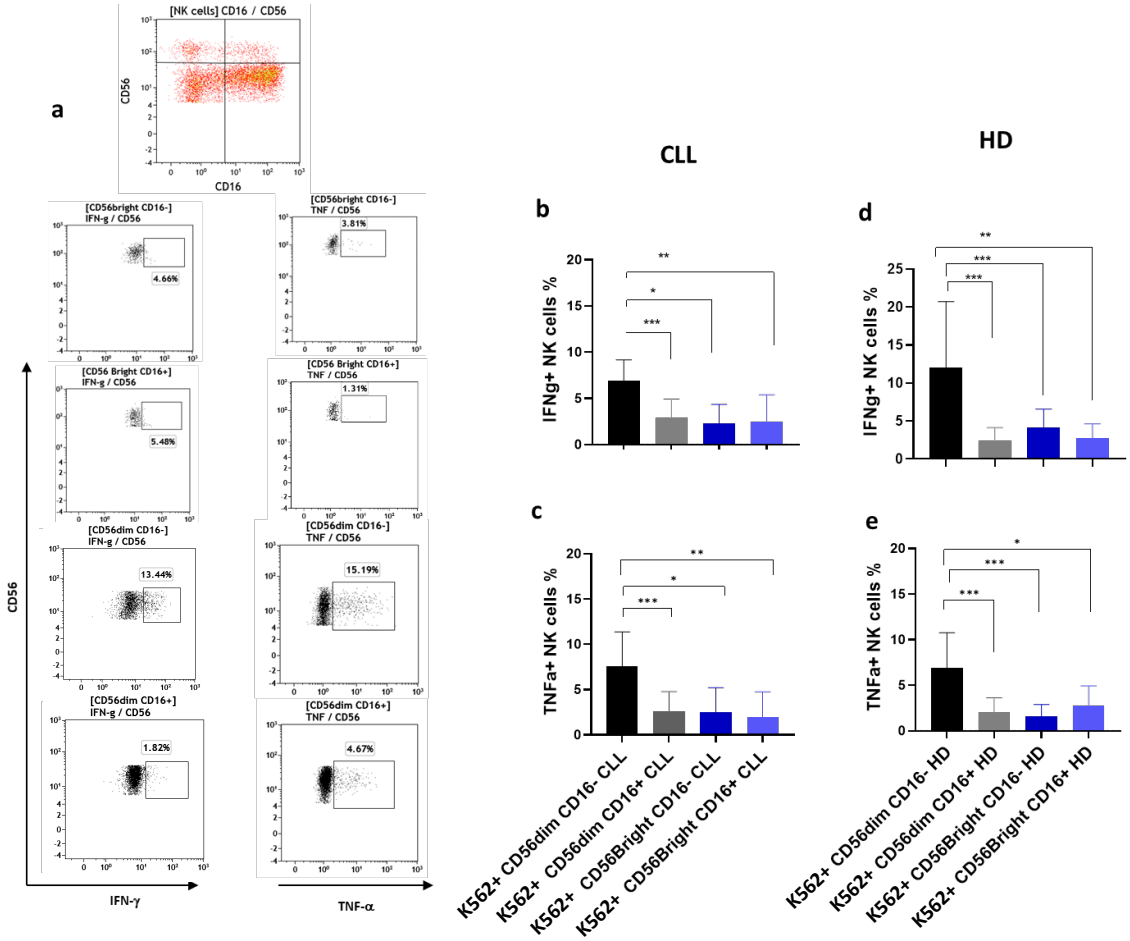

Figure 4.3 CD56^{dim} CD16^{neg} subset is the major cytokine producer after stimulation with K562 in both B-CLL patients and HCs.

The ability of NK cell subsets to produced IFN-γ and TNF-α in response to K562 cell line (overnight at E/T ration 1:1) was determined by flow cytometry. Flow dot blots represent an example of NK subsets gating defined by density of CD56 and CD16 expression and the cytokines production in each NK subset (**a**). Summary of IFN-γ and TNF-α production by different NK cell subsets CD56^{dim} CD16^{neg} (solid black bars), CD56^{dim} CD16^{pos} (solid grey bars), CD56^{bright} CD16^{neg} (felled blue bars) and CD56^{bright} CD16^{pos} (felled light blue bars) in both B-CLL patients (n=29) (**b**, **c**), and in healthy controls (n=22) (**d**, **e**). The expression of cytokines was determined as a percentage of cytokines positive population within NK subset and presented as Mean±SEM. One Way ANOVA with Dunn's multiple comparison test was used for statistical analysis.

4.2.2.3 Impaired IFN-γ Production by both CD56^{dim} CD16^{neg} and CD56^{bright} CD16^{neg} NK subsets in CLL

We have previously demonstrated that CD56^{dim} CD16^{neg} is the major cytokines producer among the four NK subsets upon K562 tumor cell line stimulation (**Figure 4.3**). Whilst CD56^{bright} CD16^{neg} NK subset has been shown to be the main cytokines producer upon stimulation with cytokines (G. M. Konjević et al., 2019). Next, in order to assess the different capacity of cytokines production from these NK subsets between B-CLL and HCs, further analysed was performed to compare IFN-γ and TNF-α production between B-CLL and HCs based on different NK subsets. Interestingly, our analysis showed that both NK subsets CD56^{dim} CD16^{neg} and CD56^{bright} CD16^{neg} produce significantly lower IFN-γ compared to their matched healthy NK subsets, the frequency of cytokines production was 6.8±0.5% vs 11.9±2.3% (p=0.0460) and 2.2±0.5% vs 4.1±0.6% (p=0.0299) respectively. Whilst TNF-α production was similar from all NK cell subsets in B-CLL patients compared to healthy controls (**Figure 4.4**). This data Indicates that lower IFN-γ production from NK cells in B-CLL patients can be partly explained by the observation of lower frequency of CD56^{dim} CD16^{neg} and CD56^{bright} CD16^{neg} NK subsets (**Figure 3.2.2**), which are the major cytokines producing NK cell subsets.

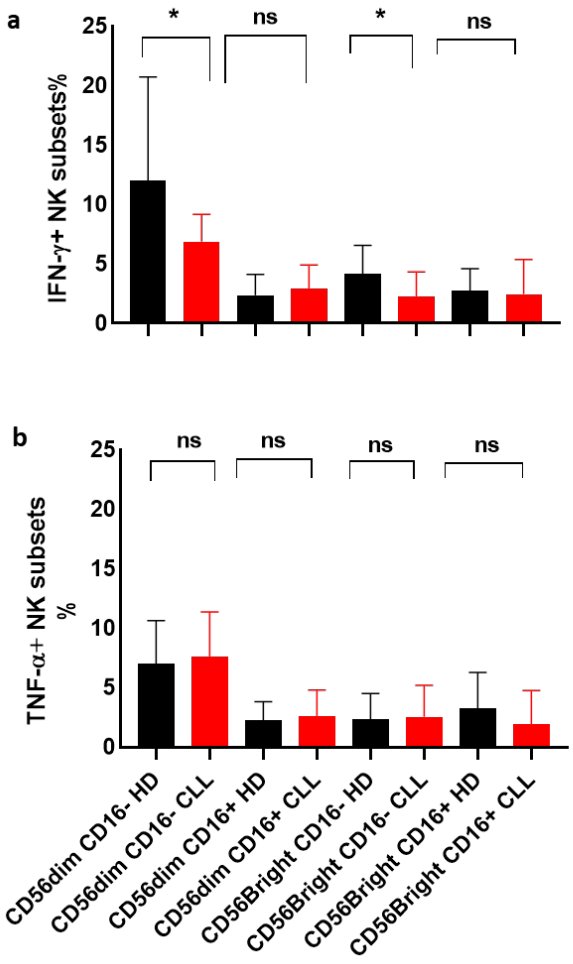

Figure 4.4 Impaired IFN-γ and TNF-α production by different NK cell subsets in B-CLL patients and healthy controls after stimulation with K562 cell line.

The ability of NK cell subsets in both B-CLL patients (solid red bars) and healthy controls (solid black bars) to produce cytokines was determined after co-culturing with K562 for overnight at E/T 1:1. Data was shown as Mean±SEM of the percentage of IFN-γ (**a**) and TNF-α (**b**) producing population from each NK subsets. The statistical significance was analysed by One-way ANOVA, Kruskal-Wallis with Dunn's multiple compassion test. (*$p<0.05$).

4.2.2.4 Low IFN-γ correlated with low CD56^{dim} CD16^{neg} NK subsets before stimulation

The previous data has shown that NK cells from B-CLL patients produce less IFN-γ, which is mainly produced by CD56^{dim} CD16^{neg} NK subset. We hypothesized that the reduced CD56^{dim} CD16^{neg} NK subset contributed to the low IFN-γ production. Notably, the proportion of CD56^{dim} CD16^{neg} NK subsets significantly increased after stimulation with K562 but still significantly lower than in HCs (**Table 4.1**). To investigate whether this less IFN-γ production is actually related with CD56^{dim} CD16^{neg} NK subset before stimulation, we further correlate the percentage of CD56^{dim} CD16^{neg} before and after stimulation, with levels of IFN-γ production.

As expected, percentage of CD56^{dim} CD16^{neg} straight from B-CLL patients before stimulation was significantly correlated with IFN-γ production ($p=<0.0001$, $r=0.77$). In addition, this correlation was moderate and not significant between the percentage of CD56^{dim} CD16^{neg} after stimulation and IFN-γ production ($p=0.1526$, $r=0.32$) (**Figure 4.5**). Looking at the quantity of IFN-γ per CD56^{dim} CD16^{neg} subset, MFI of IFN-γ was not significantly correlated with the percentage of CD56^{dim} CD16^{neg} either before or after stimulation (**Figure 4.5**). No difference was observed between B-CLL and HCs for TNF-α production (**Table 4.1**). Collectively, this data consolidates the hypothesis that lower IFN-g production in B-CLL patients is at least due to low CD56^{dim} CD16^{neg} subsets.

Also, the proportion of four different NK subsets were compared after K562 stimulation. The analysis showed that the percentage of CD56^{dim} CD16^{neg} NK subset was lower in B-CLL patients compared to HCs with 31.1±2.3% vs 40.3±2.7% ($p=0.0268$) (**Figure 4.6**). In contrast,

the percentage of $CD56^{dim}$ $CD16^{pos}$ NK subset remained markedly higher in B-CLL patients (p=0.0052), which is the same pattern observed before stimulation (**Figure 4.6**).

Group	n	mean of % $CD56^{dim}$ $CD16^{neg}$ and correspond cytokines production		
		$CD56^{dim}$ $CD16^{neg}$	**TNF-α %**	**IFN-γ %**
Healthy (1)	12	10.6 (3.9 – 19.0)	4.3 (1.5 – 8.6)	6.4 (1.1 – 18)
CLL (1)	19	4.9 (1.0 – 11.0)*	4.0 (1.3 – 7.4)	3.0 (0.9 – 6.9)**
Healthy (2)	12	40.3 (32.7 – 48.6)	4.3 (1.5 – 8.6)	6.4 (1.1 – 18)
CLL (2)	21	31.1 (19.2 – 42.9)*	4.0 (1.3 – 7.4)	2.9 (0.9 – 6.5)**

Table 4.1 The percentage of $CD56^{dim}$ $CD16^{neg}$ before (1) and after (2) in vitro stimulation and their correspond cytokines production, (p<0.01).**

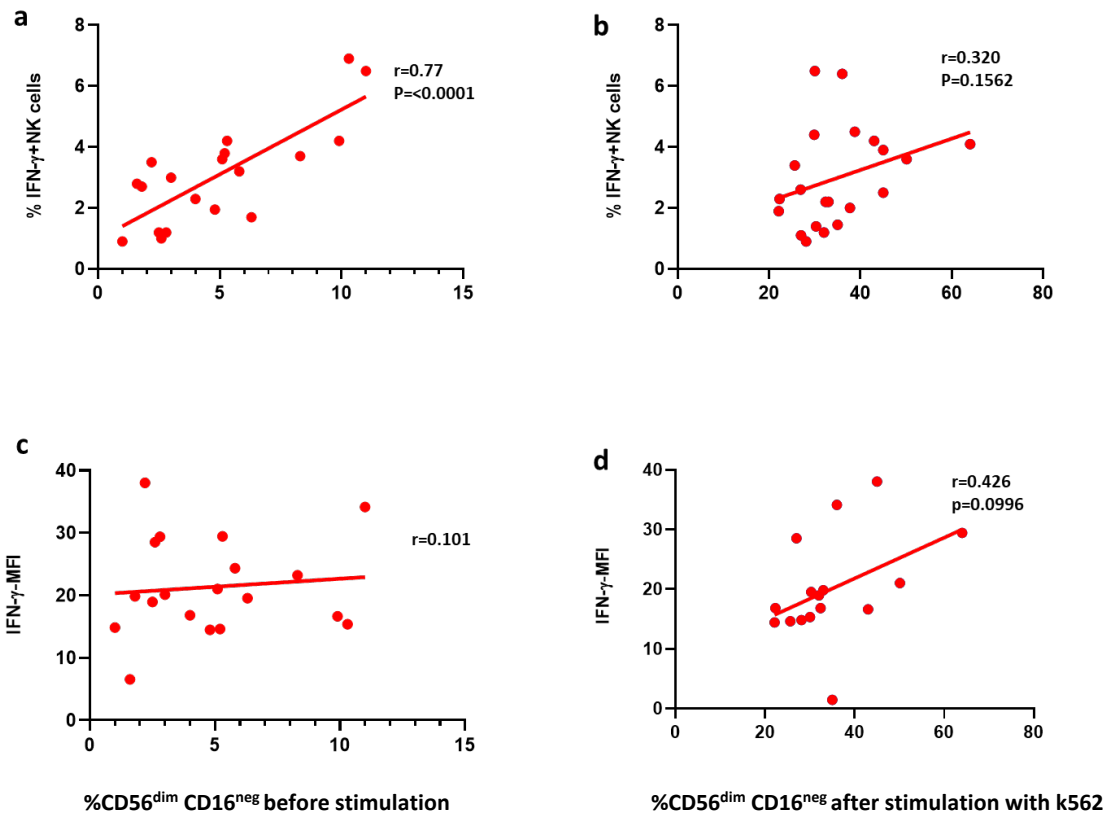

Figure 4.5 Correlation analysis between percentage of CD56^{dim} CD16^{neg} subset before and after stimulation and IFN-γ production from whole NK population in B-CLL patients.

NK cells from B-CLL patients were stimulated overnight with K562. Then the percentages and MFI of IFN-γ positive NK cells were measured and correlated with the percentage of CD56^{dim} CD16^{neg} NK subset (before stimulation) (**a, c**) and after stimulation (**b, d**) for (n=19). Significance was determined by spearman correlation test.

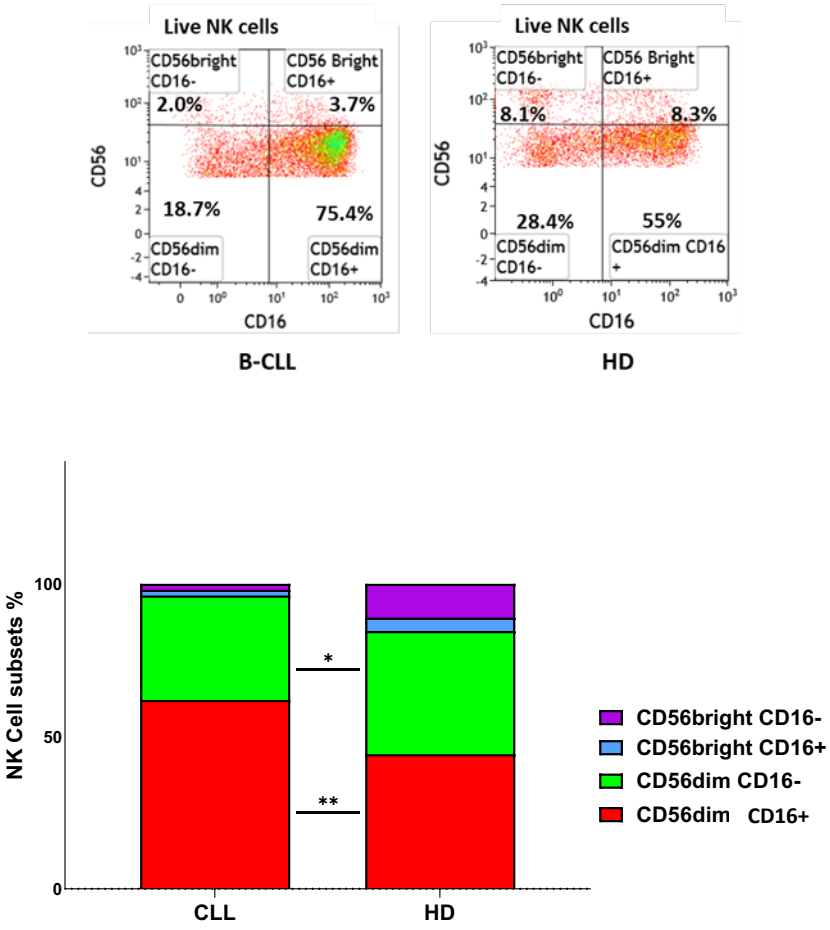

Figure 4.6 Comparison of NK cell subsets expansion upon stimulation with K562

Representative flow dot plots to show the gating strategy for identification of four NK subsets after overnight stimulation with K562 (top panel). Summary of distribution of NK cell subsets from (n=29) B-CLL patients and (n=22) healthy controls after stimulation. Data were analysed by Mann Whitney nonparametric test (*p<0.05,**p<0.01).

4.2.3 DNAM-1 dependent NK cytotoxicity is reduced in B-CLL patients

NK cells mediate cytotoxicity through a ray of activating receptors including NKG2D which represents the dominant signalling pathway, in addition to DNAM-1 and natural cytotoxicity receptors (NCRs). Previous studies have reported that NK cytotoxicity has been reduced in CLL patients. More specifically, NKG2D dependent cytotoxicity has been shown to be markedly reduced compared to healthy controls and this reduction attributed to the low surface expression of NKG2D on NK cells from B-CLL patients (Parry, Stevens, et al., 2016). In the same study, DNAM-1 expression on NK cells has also been shown to be downregulated in B-CLL patients compared to HCs. However, DNAM-1 mediated NK cytotoxicity has not been investigated in B-CLL patients. As such, we next went on to determine the capacity of DNAM1 dependent NK cytotoxicity in B-CLL patients compared to healthy controls.

To this end, a CHO cell line was stably transduced with lentiviral vector expressing CD155, a main ligand for DNAM-1 and used as target cells. In this assay, wild type CHO cells (wt-CHO) served as an internal negative control panel a **Figure 4.7**, which confirmed the expression of CD155. In short, Enriched primary NK cells (negative selection) from B-CLL patents and healthy controls (Panel b of Figure 4.2.7a demonstrated the purity after the enrichment) were activated overnight by IFN-α and co-cultured with mixture of labelled CHO-155 and wt-CHO cells at various E/T ratios (0.25:1, 1:1 and 4:1) for another 18hrs. All the experiments were carried out in triplicates. The percentage of cytotoxicity was calculated according to changes of the ratio of wt-CHO (CFSE negative) and CD155-CHO cells (CFSE positive), detailed method and calculations can be found in the material and methods. Panel c of **Figure 4.7** are examples of one experiment with and without NK cells from B-CLL patients and from HCs.

NK cytotoxicity was measured by flow cytometry and calculated as a percentage and data presented as (Mean±SEM). Importantly, this cytotoxicity was confirmed to be dependent on DNAM-1 by using anti DNAM-1 blocking antibody (**panel a of Figure 4.8**).

Our findings showed that NK cytotoxicity in both B-CLL patients and healthy controls increased in line with increase E/T ratios. Interestingly, DNAM-1 mediated NK killing was significantly reduced in B-CLL patients (>30%) in comparison to healthy controls at all E/T ratios. The percentage of cytotoxicity were (1.6±0.9% vs 7.1±1.3% (p=0.0057) at 0.25:1, (3.2±0.9% vs 11.3±0.8% (p=<0.0001) at 1:1 and (5.3±0.9% vs 13.8±2% (p=0.0005) at 4:1 (**Figure 4.8 panel b**). This data suggests that the DNAM-1 dependent cytotoxicity is defective in NK cells from B-CLL patients and is one of mechanisms underlying NK cytotoxicity impairment in B-CLL patients.

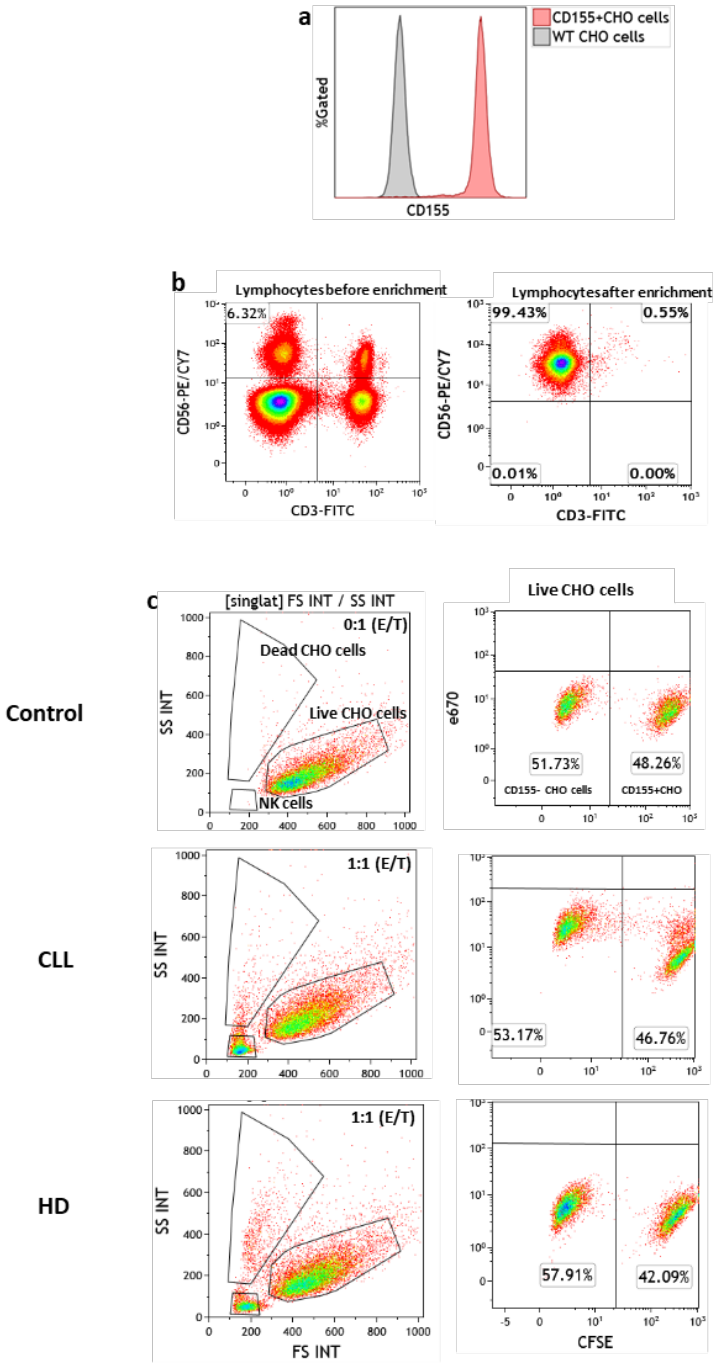

Figure 4.7 Gating strategy of optimisation of DNAM-1 dependent NK cytotoxicity assay.

Representative example of CD155 expression on CHO target cells (pink histogram) and wt CHO cells (used as internal control) (grey histogram) using flow cytometry (**a**). NK cell enrichment from B-CLL patients using negative selection magnetic bead-based kit, NK enrichment purity was >99% (**b**). Flow cytometry gating strategy of the DNAM-1 dependent cytotoxicity assay. Viable $CFSE^{pos}$ 670^{neg} CD155-CHO target cells and viable $CFSE^{neg}$ 670^{pos} wt-CHO target cells were identified from the live cells, in the absence (control) and presence of NK cells from B-CLL or HCs. Killing percentage was calculated as described in chapter 2.

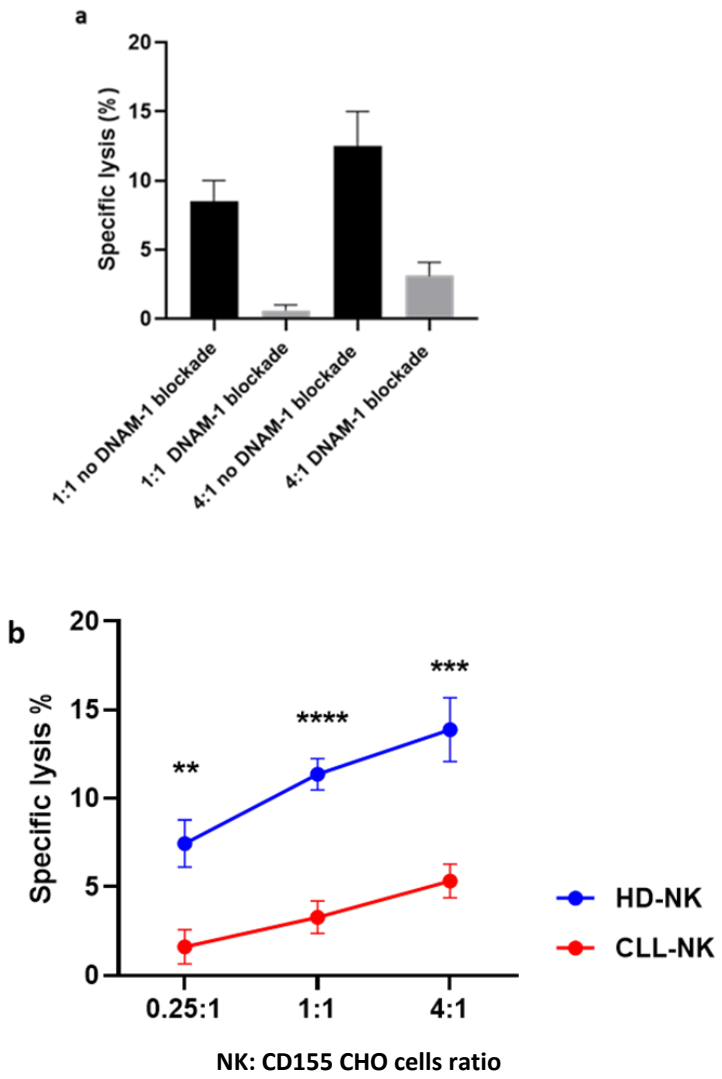

Figure 4.8 DNAM-1 dependent NK cytotoxicity is reduced in B-CLL patients

(**a**)The validation of DNAM-1 mediated killing from 3 different healthy controls. The assay was set up with or without DNAM-1 blocking antibody at two E/T ratio of 1:1 and 4:1. (**b**) Activated NK cells from B-CLL patients and healthy controls were co-cultured with mixture of 1:1 of CD155 CHO target cells and wt CHO cells at different E/T ratios (0.25:1, 1:1 and 4:1) for 18hrs. Following incubation, DNAM-1 dependent NK cytotoxicity against CD155 CHO target cells was calculated. Results presented are Mean±SEM for 15 B-CLL patients (red line) and 11 healthy controls (blue line). The experiments were all carried out in triplicate. Mann Whitney nonparametric test was used to analyse the data (**p<0.01, ***p<0.001, (****p<0.0001).

4.2.4 DNAM-1 expression is correlated with TIGIT expression

Our data indicate that DNAM-1 dependent NK cytotoxicity of B-CLL patients is substantially impaired. Recently, this family of paired receptors that interact with same ligands (CD155 and CD112) and mediate an activation/inhibitory function has gained great interest. These are activating receptor DNAM-1, and inhibitory receptors TIGIT and CD96 (Chan et al., 2014). Next, we measured the surface expression (% and MFI) of DNAM-1 and TIGIT on NK cells from B-CLL patients to determine whether these receptors are correlated with each other and tested the impact of their expression on NK cytotoxicity.

Flow cytometry analysis was performed on NK cells from B-CLL patients, to determine the correlation of expression levels of DNAM-1 and TIGIT. The correlation of CD96 expression with DNAM-1 was not carried out due to the fact that CD96 expression was minor on NK cells. Our data show that the percentage of DNAM-1 and TIGIT expression on NK cells B-CLL patients was strongly correlated ($r=0.48$, $p=0.0006$). This is also true for the density of these two receptors (MFI) on NK cells ($r=0.52$, $p=0.0002$) (**Figure 4.9**). This data implies that there are shared pathways to regulate these two receptors, DNAM-1 and TIGIT, which is important to modulate NK cell function.

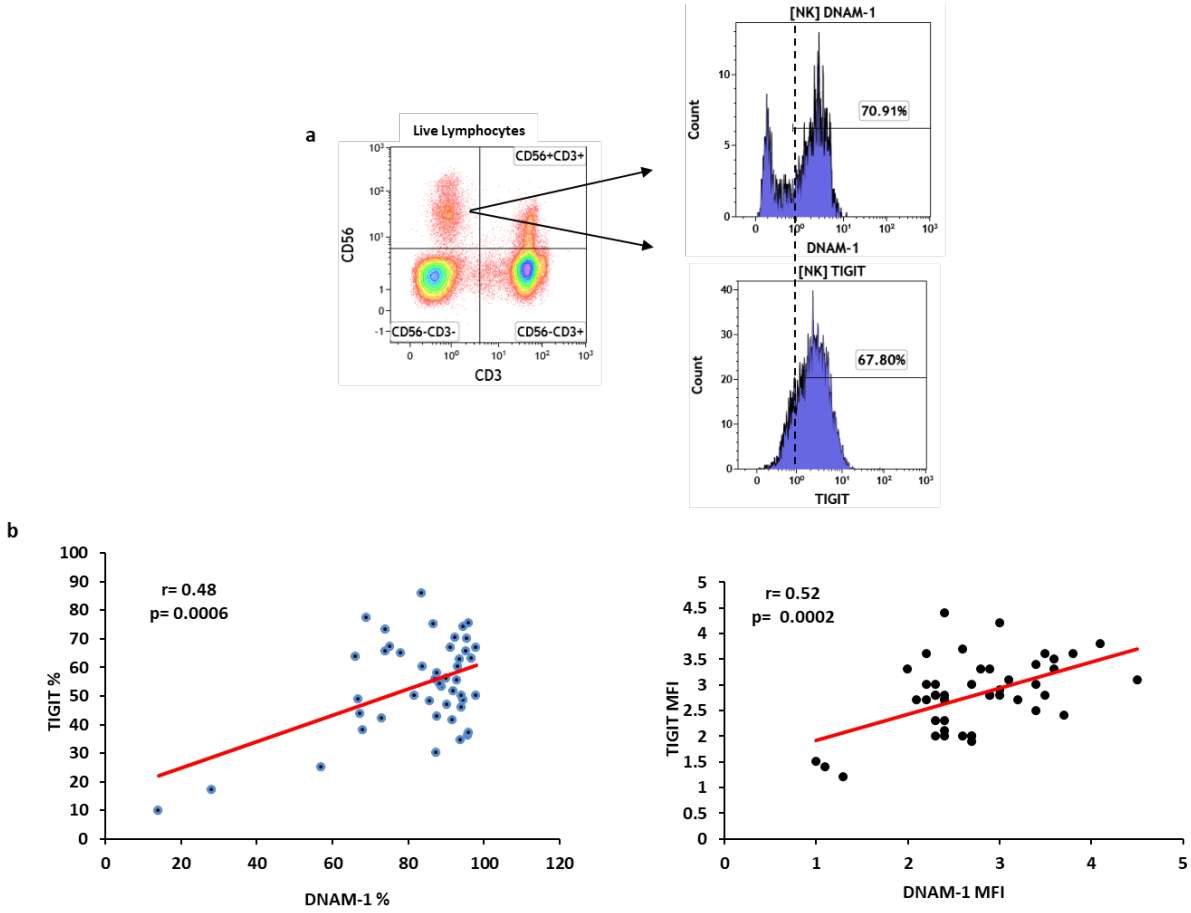

Figure 4.9 Correlation analysis between DNAM-1 and TIGIT expression.

NK cells were identified as $CD3^{-}$ $CD56^{+}$ and analysed for their expression of DNAM-1 and TIGIT, representative flow dot blot and histogram are shown (**a**). The correlation analysis between DNAM-1 and TIGIT expression for (n=42) on NK cells from B-CLL patients. Each dot represents one patient (**b**). Analysis was done by spearman correlation test.

4.2.5 DNAM-1 dependent NK cytotoxicity can be restored by TIGIT and CD96 blockade

As we have shown previously that DNAM-1 mediated NK cytotoxicity is significantly reduced in B-CLL patients, and CD96 and TIGIT expression were both upregulated on NK cells from B-CLL patients. Next, we sought to study whether this reduction in DNAM-1 dependent cytotoxicity can be restored by TIGIT or/and CD96 blockade. The experiment was carried out as in (**4.2.3**) in four conditions, without any blocking, with anti TIGIT only, with anti CD96 antibodies, and combined blockade with both anti TIGIT and anti CD96 antibodies. This experiments were carried out in triplicate and in different days.

First, in the B-CLL patients group, our data show that TIGIT blockade resulted in significant increase in DNAM-1 dependent cytotoxicity, particularly at 1:1 and 4:1 ratio, which increased from 4.0±1.8% and 6.8±1.4% to 12.3±3% and 16.6±2.6% ($p=0.0424$ and $p=0.0080$) respectively (**panel a Figure 4.10**). Notably, single CD96 blockade also showed increase in DNAM-1 dependent NK cytotoxicity in B-CLL patients, and this was effective at highest E:T ration (4:1) from 6.8±1.4% to 15.2±3.7% but statistically still not significant ($p=0.0698$). At 0.25:1 and 1:1 ratios, the percentage of cytotoxicity was increased from 1.6±0.9% and 4.6±2.0% to 4.0±1.4% and 10.7±4.9% respectively (**Panel a Figure 4.10**). The combination of anti-TIGIT and anti-CD96 did not increase the cytotoxicity further compared with the single blockade. At 0.25:1, 1:1 and 4:1 ratios, the cytotoxicity percentage was increased from 1.6±0.9%, 4.6±2.0% and 6.8±1.4% to 3.4±0.8%, 9.6±2.7% and 17.4±4.3% respectively.

For the healthy control group, it was a slightly different story. The response was much stronger in NK cells from HCs, as NK cells from HCs considered more functional than NK cells from B-CLL patients (**panel b Figure 4.10**). First, there was a dramatic increase in DNAM-1

dependent NK cytotoxicity after TIGIT/CD96 blockade in all the three E:T ratios. For TIGIT blocking, the cytotoxicity increased from 6.8±1.5%, 12.6±1.1% and 15.2±3.1% to 45.5±3.3%, 37.1±4.3% and 26.5±6.6% at 0.25:1, 1:1 and 4:1 ratios, respectively. For CD96 blocking, the cytotoxicity was increased from 6.8±1.5%, 12.6±1.1% and 15.2±3.1% to 40.2±4.6%, 39.8±4.7% and 26.4±3.4% at 0.25:1, 1:1 and 4:1 E/T ratio, respectively. At last, the dual TIGIT and CD96 blocking, the cytotoxicity increased from 6.8±1.5%, 12.6±1.1% and 15.2±3.1% to 45.0±2.6%, 42.0±4.0% and 36.6±8.8% at 0.25:1, 1:1 and 4:1 E/T ratio, respectively. One interesting observation is the big increase of DNAM-1 dependent cytotoxicity after blocking was at low E:T ratio. This could be due to that at low E:T ratio, NK cells have more space in 96 well plate to move around and perform multiple killing. Comparing DNAM-1 dependent NK cytotoxicity at 4:1 E:T ratio in B-CLL patients and HCs, the cytotoxicity was 16.6±2.6% and 15.2±3.7% in B-CLL patients, instead NK cytotoxicity was 26.5±6.6% and 26.4±3.4% in HCs respectively after TIGIT and CD96 blocking, which demonstrates no significant differences at 4:1 ratio between B-CLL and HCs.

Overall, these data show for the first time that checkpoint molecules TIGIT/DNAM-1/CD96 in B-CLL patients play an important role in NK cells cytotoxicity against CD155 expressing CHO cell line. TIGIT blockade restored DNAM-1 dependent NK function impairment which provides rational for using TIGIT intervention alone or in combination with anti CD96 in NK cell-based immunotherapy in B-CLL patients.

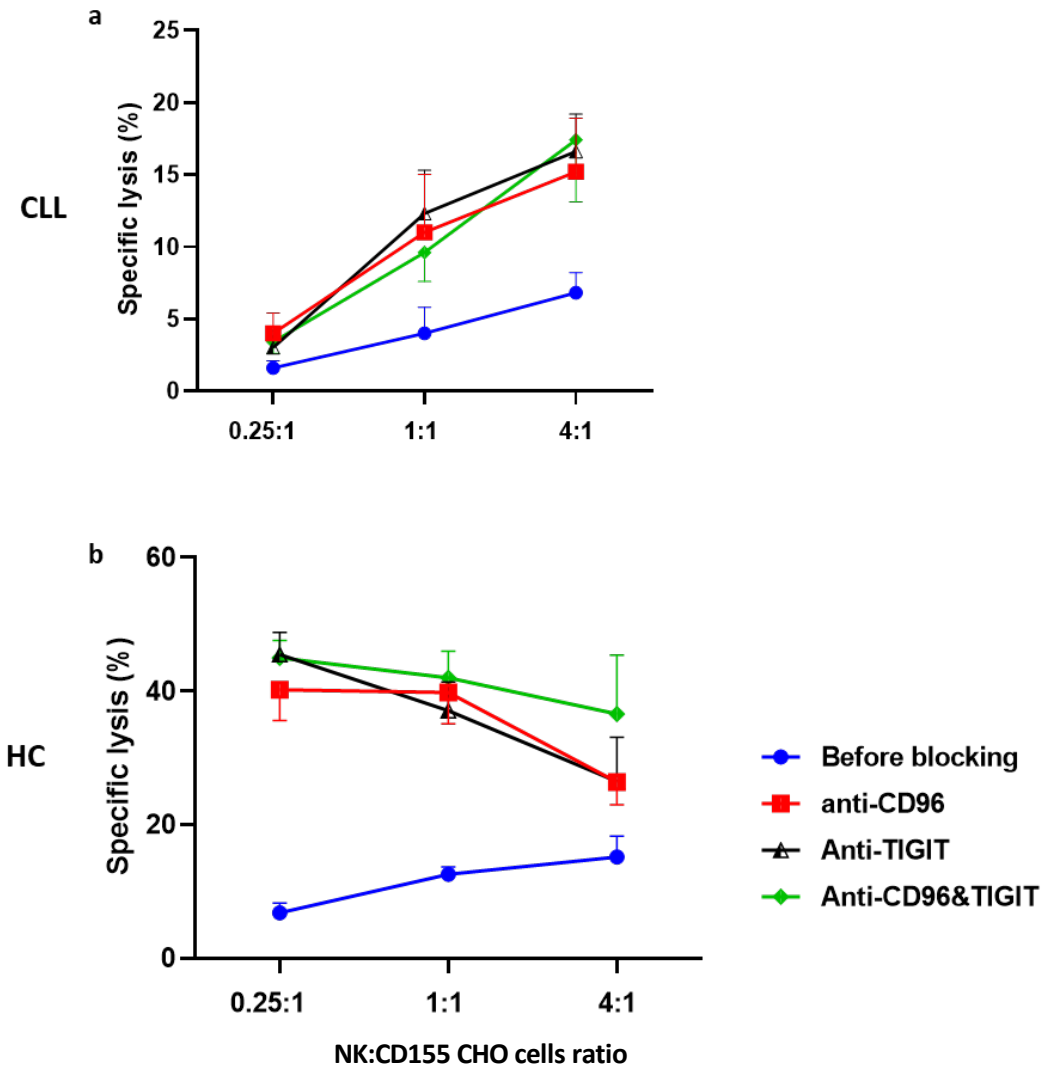

Figure 4.10 TIGIT and/or CD96 blockades restored DNAM-1 dependent NK cytotoxicity function

Experiments were set up as described above, TIGIT and/or CD96 blocking antibodies were added to the corresponding cultures and incubated for overnight to determine the effect of blocking on DNAM-1 dependent NK cytotoxicity function against CD155-CHO cells. Each experiment was performed in triplicate wells. The average percentage of specific DNAM-1 killing calculated and displayed as mean of 8 B-CLL patients (**a**) and 6 healthy controls (**b**) before (blue lines) and after blocking (red, black, and green lines). Statistical analysis was performed by One-way ANOVA test.

4.2.6 High TIGIT expressing NK cells are hyperresponsive after TIGIT blockade

Overexpression of TIGIT inhibits the function of NK and T cells in many tumor types, resulting in tumor immune escape. To further investigate whether TIGIT may serve as a potential NK-based therapeutic target, data was reanalysed by dividing B-CLL patients into two groups, high/low TIGIT expression based on cut off (55% TIGIT+ NK cells). Also, this applied for the CD96 as well as data was reanalysed based on high/low CD96 expression on NK cells from B-CLL patients (cut off 2% CD96+ NK cells). The cut off was determined from the mean of TIGIT/CD96 expression on NK cells from healthy controls.

At first, in B-CLL patients, DNAM-1 dependent NK cytotoxicity was compared before the blocking between high vs low TIGIT and high vs low CD96 expression. The data show no significant differences in DNAM-1 dependent cytotoxicity between high and low TIGIT expression with 0.2±0.1%, 1.3±0.9% and 5±0.5% compared to 0.4±0.05%, 0.3±0.2% and 5±0.1% ($p>0.05$) for low TIGIT expression at 0.25:1, 1:1 and 4:1 ratios, respectively. Similarly, DNAM-1 dependent NK cytotoxicity did not change much between high vs low CD96 expression with 0.3±0.08%, 1.3±0.9% and 5±0.5% compared to 0.2±0.08%, 1.1±0.9% and 4.8±0.4% ($p>0.05$), respectively. Interestingly, B-CLL patients with higher TIGIT expressing NK cells (> 55% TIGIT+ NK cells) have stronger DNAM-1 cytotoxicity compared to those patients who have TIGIT expressing NK cells less than 55% after TIGIT blocking. Although this was not statistically significant, the biggest difference was observed at E:T ratio of 4:1. The mean DNAM-1 dependent cytotoxicity was 11.9±5.6% for high TIGIT group and 9.3±3.8% for low TIGIT group. At the same time, after CD96 blocking, the highest DNAM-1 dependent cytotoxicity was seen at E:T ratio of 4:1 with 10.6±5.0% for the high CD96 group, and 8.5±3.4% for low CD96 B-CLL group (**Figure 4.11 panel a**).

Next, we went to test whether the TIGIT blockade has restored the DNAM-1 dependent NK cytotoxicity to the level of HCs. The DNAM-1 dependent cytotoxicity of NK cells from B-CLL patients after TIGIT blocking was compared with that from HCs without blocking. At 1:1 and 4:1 ratios, the cytotoxicity after TIGIT blocking was 17.3±1.7% and 18.3±3.4% for B-CLL and 11.3±0.8% and 13.8±1.8% for HCs before blocking (p=>0.05 for both ratios).

Altogether, these data indicate that TIGIT blockade by itself can restore DNAM-1 mediated cytotoxicity to the level as in healthy control (**Figure 4.11 panel b**). Notably, stronger restoration of DNAM-1 after TIGIT blockade was seen in high TIGIT expressing NK cells.

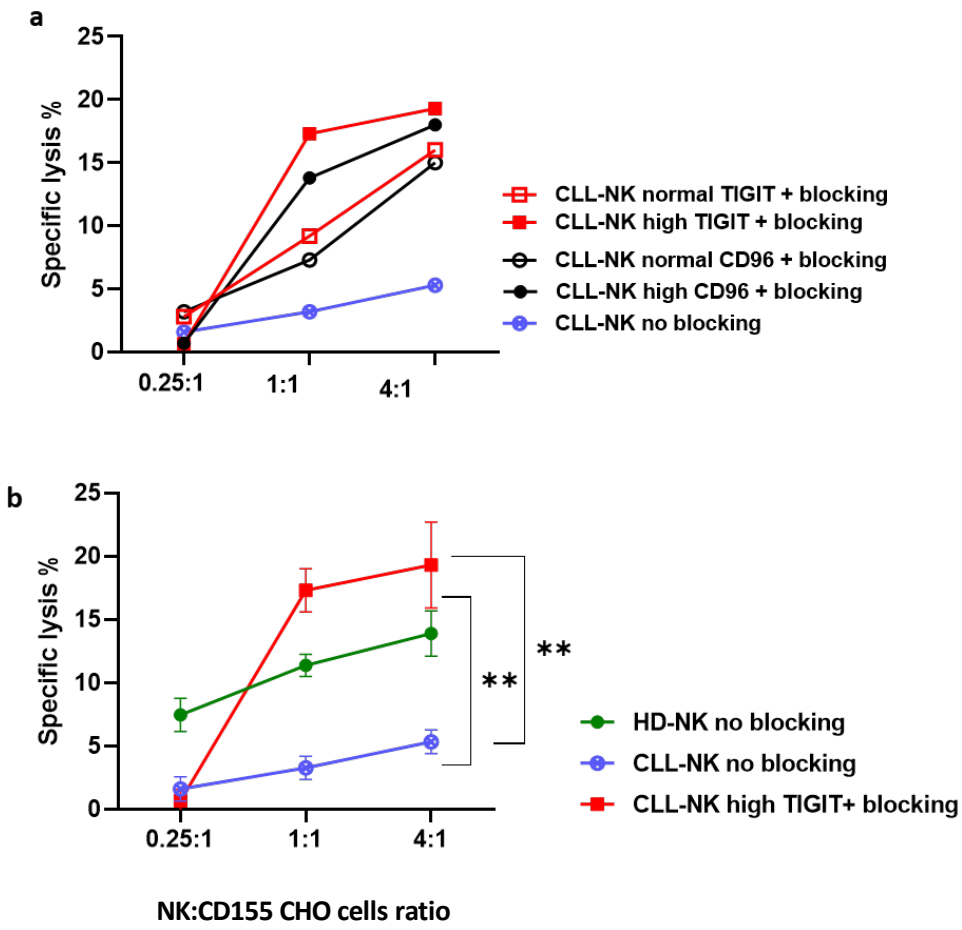

Figure 4.11 The effect of blockings on high vs low TIGIT and CD96 expression on DNAM-1 dependent cytotoxicity.

The previous data of DNAM-1 cytotoxicity of 8 B-CLL patients were divided into two groups based on the level of TIGIT and CD96 expression. Data reanalysed to investigate the response pattern of high vs low TIGIT and CD96 expression after TIGIT/CD96 blockades (**a**). The DNAM-1 dependent cytotoxicity of NK cells with high TIGIT from B-CLL patients and after TIGIT blocking was compared with that from HCs before blocking (**b**). One-way ANOVA test was used to analyse data (*$p<0.05$, **$p<0.01$).

4.3 Discussion

As we have shown in the last chapter that phenotype and frequency of NK cells in B-CLL patients were altered, the main object of this chapter was to investigate the functional capacity of NK cells from those patients and the possibility of restoring antitumor activity of NK cells by blocking immune check points. At first, a trans-well based assay was used to investigate the ability of *in vitro* migration of NK cells from B-CLL patients. The data demonstrated that NK cell migration towards K562 cells was higher than the migration towards the media alone (data not shown) indicating that NK cell migration was triggered/attracted specifically by K562 cells. Also, the motility of NK cells from B-CLL patients was significantly lower compared to NK cells from HCs, which is related at least partially to the lower expression of adhesion molecules on NK cells from B-CLL patients. Next, a panel of cytokines production was measured after stimulation with tumor cell line K562 and compared to NK cells from healthy controls. NK cells from B-CLL patients showed a significant impairment of IFN-γ production compared to NK cells from HCs. At last, DNAM-1/TIGIT/CD96 pathway was explored to study the DNAM-1 dependent killing capacity of NK cells in B-CLL patients. The DNAM-1 dependent NK cytotoxicity was substantially reduced in B-CLL patients compared to HCs. However, this reduction can be at least partially restored by TIGIT/CD96 blockade. This data implies the therapeutic potential of TIGIT/CD96 blocking to enhance the cytotoxicity capacity of NK cells from B-CLL patients.

4.3.1 NK cells from B-CLL patients produce lower IFN-γ upon tumor cell stimulation

Activated NK cells produce number of immune modulatory cytokines such as IFN-g, TNF-a, GM-CSF, IL-10, IL-5 and IL-18. Among these, IFN-γ is one of the most potent effector cytokines produced by NK cells. It has a crucial role in both antiviral and antitumor activities,

where, it has been shown to modulate expression of Fas ligand, caspase and TRAIL receptor (Roda et al., 2006). Deficient IFN-γ signalling in mice and human render them susceptible to cancer and infection (Bustamante et al., 2014). However, IFN-γ production is regulated by many factors as signalling through NKG2D receptor (which is reported to be low on NK cells from B-CLL patients) has been shown to promote IFN-γ expression (Paul & Lal, 2017), and low expression of IFN-γ receptor on NK cells negatively regulate its production (Lee et al., 2019). Although IFN-γ and TNF-α are normally produced at the same time, TNF-α production requires co-engagement of 2B4 and NKG2D. IFN-γ production however is particularly dependent on LFA-1, 2B4 and NKG2D co-engagement, which is not fully required for TNF-α secretion (Perez et al., 2003). This might explain at least partly the reduction of IFN-γ production by NK cells from B-CLL patients, as LFA-1 signalling on NK cells is needed to be investigated in those patients. Our study with NK cells from PDAC patients has shown that NK cells from that patients group also produce less IFN-g, but also less IL-2 and instead produce substantially higher IL-10 compared (Marcon et al., 2020). The difference observed from those two patients groups (B-CLL and PDAC) indicates that different tumor microenvironment will regulate NK cells towards different impaired phenotype.

NK cells from B-CLL patients produced significantly lower IFN-γ upon stimulation with K562, and this reduction was pronounced in two subsets of NK cells $CD56^{dim}$ $CD16^{neg}$, which is the main cytokines producer when stimulated with tumor cell lines, and $CD56^{bright}$ $CD16^{neg}$. The reduction in IFN-γ was correlated with the percentage of $CD56^{dim}$ $CD16^{neg}$ in the blood stream of B-CLL patients, which suggests that low frequency of $CD56^{din}$ $CD16^{neg}$ contributes in low IFN-γ secretion by NK cells in B-CLL patients. Many previous studies have focused on the cytokines production from $CD56^{bright}$ NK subsets (Cooper et al., 2001). Study from our

group has found that higher peripheral $CD56^{dim}$ $CD16^{neg}$ NK population is related with less disease recurrence in PDAC patients (Marcon et al., 2020). Further investigation is needed to explore the potential mechanism of reduction of $CD56^{dim}$ $CD16^{neg}$ population, which might indicate therapeutic approaches.

However, in addition to activating receptor signalling, regulation of IFN-γ production in NK cells is regulated by multiple levels including epigenetic, transcription and post-transcription levels (Mah & Cooper, 2016) which need to be investigated in future studies.

4.3.2 DNAM-1 dependent NK cytotoxicity is reduced in B-CLL patients

DNAM-1 is an important activating receptor involved in mediating NK cell cytotoxicity against tumor cells and is required for optimal NK killing of tumor target cells (de Andrade et al., 2014). As demonstrated previously by other studies that the cytotoxicity of NK cells in B-CLL patients is reduced and more specifically impairment in NKG2D dependent NK cytotoxicity (Parry, Stevens, et al., 2016). Herein, to further uncover the underlying mechanisms of NK cell function impairment, killing capacity of DNAM-1 on NK cells was *in vitro* assessed using CD155 expressing CHO cells. Interestingly, DNAM-1 mediated NK cytotoxicity was impaired and significantly lower in B-CLL patients compared to healthy controls indicating this is another mechanism of which tumor B cells utilise to escape and reduce activation of NK cells. The NK cells from B-CLL patients have impaired cytotoxicity function, which can be explained by the downregulation of NKG2D/DNAM-1, and this in turn reduced both NKG2D dependent and DNAM-1 dependent NK cytotoxicity.

DNAM-1 belongs to the poliovirus receptor nectin family that includes TIGIT and CD96 that compete DNAM-1 for binding to its ligands CD155/CD112 and have opposite effects on NK cell function (i.e. inhibitory signals) (Du et al., 2018). TIGIT was found to be highly expressed on most of NK subsets of the peripheral blood, and has a negative role in regulating /controlling NK cell function (Stanietsky et al., 2009). TIGIT expression can be upregulated after activation and can bind to CD155 and CD112 with higher affinity than DNAM-1 to perform its function by inhibiting both NK cell cytotoxicity and IFN-γ secretion as shown in human and mouse models (Stanietsky et al., 2013). In addition, triggering TIGIT led to inhibition of anti-tumor activity of NK cells including IFN-γ, TNF-α production and degranulation, whilst blocking TIGIT reversed the anti-tumor effects of NK cells (Meng et al., 2020). CD96 (TACTILE) has also been shown to be able to compete with DNAM-1 for CD155 ligand and limits NK cell function by direct inhibition of cytokines production particularly IFN-γ (Chan et al., 2014). The binding affinity of CD96 to its main CD155 ligand has been found to be in the middle of DNAM-1 and TIGIT. CD96 and TIGIT serve as co-inhibitory receptors with co-stimulatory DNAM-1, similar to CD28/CTLA-4 pathway in T cells, implying that CD96 and TIGIT could be targeted for cancer immunotherapy (Dougall et al., 2017). Both TIGIT and CD96 overexpression on NK cells has been demonstrated in various cancer types and considered as a promising candidates for immunotherapy including glioma, Acute Myeloid leukaemia (AML) and Myelodysplastic syndrome (F. Liu et al., 2020; G. Liu et al., 2021; Meng et al., 2020).

In leukaemia disease setting, DNAM-1 expression has been shown to be reduced on NK cells from AML patients (Sanchez-Correa et al., 2012), and on bone marrow NK cells in myelodysplastic syndrome (Carlsten et al., 2010). Accordingly, TIGIT and CD96 expression on NK cells from B-CLL patients were measured by flow cytometry and our data showed that

CD96 expression was significantly upregulated on NK cells but not TIGIT compared to HCs. The underlying hypothesis of no difference in TIGIT expression could be that TIGIT expression is generally very high on NK cells from HCs and the difference of TIGIT could be in quality instead of quantity difference. Interestingly, TIGIT expression was significantly corelated with DNAM-1 expression.

Another important factor is the expression of the ligands, including CD155 and CD112. One study has shown the high expression of CD112/CD155 on leukemic blasts (Sanchez-Correa et al., 2012). To date there is no systemic study of the expression of CD112 and CD155 ligands been carried out with B-CLL tumor cells, which is worth to be investigated in future studies (Arruga et al., 2019).

Altogether, these data indicate that CD96 and TIGIT are involved in reducing the capacity of DNAM-1 dependent killing in B-CLL patients. As such, these might be successful therapeutic targets to restore DNAM-1 cytotoxicity in B-CLL patients.

4.3.3 TIGIT/CD96 blockade effectively restored DNAM-1 mediated NK cytotoxicity

In order to enhance DNAM-1 NK cytotoxicity in B-CLL patients, single blockade, and co-blockade of TIGIT and CD96 were performed *in vitro* using specific monoclonal antibodies. DNAM-1/TIGIT/CD96 axis has recently been discovered and has not been studied in B-CLL patients. But this pathway has been explored using other disease modules. Single TIGIT blockade has been demonstrated to increase IFN-γ production and degranulation of rhIL-15 activated NK cells against ovarian cancer cell line, which can be inhibited by DNAM-1

blocking (Maas et al., 2020). In contrast, single CD96 blockade or co-blockade CD96 with TIGIT have not been effective in enhancing NK activity against same target cells, while they attributed this to the CD96 antibody clone and factors related to *in vitro* model assay (Maas et al., 2020).

We developed an *in vitro* cell model using CD155 expressing CHO cell line. Using our model, NK cells from B-CLL patients show significantly enhanced DNAM-1 dependent NK cytotoxicity either after single TIGIT and CD96 blockade or co-blockade of both receptors. Similar pattern of blocking effective was observed in NK cells from HCs. One interesting observation was there is no significant improvement after dual blockade with anti-CD96 and anti-TIGIT compared to single blockade. This could be due to the fact that both of CD96 and TIGIT work through the competition of binding with the shared ligands of DNAM-1, so there is no add on effect for dual blockade. Another finding was there is stronger increase of DNAM-1 dependent cytotoxicity from HCs after blocking at lower E:T ratio. This could be due to that at low E:T ratio, NK cells have more space to move around and perform multiple killing (Choi & Mitchison, 2013). This makes the low E:T ratio a more sensitive set-up for the blockade experiment.

Prior to perform the experiments, B-CLL patients were chosen based on the level of TIGIT and CD96 expression, they were divided into two groups: high and normal expression. Notably, we observed that B-CLL patients group with high TIGIT expression on NK cells have higher DNAM-1 cytotoxicity after TIGIT blockade compared to B-CLL group with normal/low TIGIT expression. This attributed to the strong correlation of TIGIT with DNAM-1 expression (% and MFI) observed on NK cells from B-CLL patients, indicating that high TIGIT expression

on NK cells are more responsive and favourable feature for TIGIT blockade therapy in B-CLL patients.

4.4 Conclusion

In conclusion, the function capacity of NK cells from B-CLL patients is substantially impaired. *In vitro* migration assay shows that the migratory function of NK cells from B-CLL patients towards tumor target cells (K562 as the model) is reduced compared to NK cells from HCs. In addition, NK cells from B-CLL patients produce lower IFN-γ upon target cell stimulation whilst TNF-α production is conserved. Low IFN-γ is correlated with the lower frequency of the main cytokines producer NK subsets $CD56^{dim}$ $CD16^{neg}$ and $CD56^{bright}$ $CD16^{neg}$ after K562 stimulation. The balance of DNAM-1/TIGIT/CD96 expression on NK cells from B-CLL patients shift to be more inhibitory phenotype, which significantly reduce DNAM-1 activity against CD155 expressing CHO cells. However, this reduction can be robustly increased by TIGIT/CD96 blockade.

CHAPTER 5: PD-1^{pos} NK CELLS DEMONESTRATE AN EXHAUSTED PHENOTYPE AND FUNCTIONALITY

5.1 Introduction

As demonstrated in the last chapters, NK cells have cytolytic activity that involved in elimination of transformed cells. NK cells reactivity against target cells is regulated by the balance of signals from activating and inhibitory receptors expressed on its surface. Immune checkpoint receptors are important cancer immunotherapy targets in the recent years. PD1 is the most studied checkpoint receptor, which is a key negative regulatory receptor expressed on T and B cells and recently has been described on NK cells. PD1 expression on T cells has been studied in great details, as interaction of PD1 with its ligands PDL1/L2 inhibited T cell activity. However, PD-1 expression and its function on NK cells is poorly investigated and never investigated in B-CLL patients. Therefore, this study covers mainly this gap of knowledge. Preliminary studies on PD-1^{pos} NK cells from Multiple myeloma, lung cancer and Kaposi carcinoma have showed that PD-1^{pos} NK cells are functional impaired compared to PD-1^{neg} NK cells.

In chapter 3, we have demonstrated that there is upregulation of a few checkpoint receptors such as PD-1, CTLA-4, CD96 and LAG-3 on NK cells from B-CLL patients compared to HCs. In this chapter, a comprehensive comparative analysis of phenotype and functional capacity of PD-1^{pos} and PD-1^{neg} NK cells from untreated B-CLL patients were performed, using Flow cytometry and CyTOF platforms. This chapter aimed to identify the differential expression level of activating receptors on PD-1^{pos} vs PD-1^{neg} NK cells. In addition, the expression pattern of PD-1 on different NK cell subsets and co-expression pattern of other markers with PD-1

including immune checkpoints, adhesion molecules and chemokine receptors were investigated using CyTOF. Moreover, functional capacity for a variety of cytokines production (IFN-γ, TNF-α, IL-2, IL-4 and IL-5) and degranulation ability of PD-1^{pos} vs PD-1^{neg} NK cells were investigated after stimulation with two different target cells K562 and 721.221. At last, the impact of PD-1 and PDL1/2 interactions blockade on NK cells functionality was investigated.

5.2 Results

5.2.1 PD-1 is expressed mostly on CD56^{dim} NK subsets in B-CLL patients

There is a discrepancy regarding PD1 expression on NK cells from human and murine, as PD-1 expression has been described as a hallmark of early and later antigen specific T cell activation (Judge et al., 2019, 2020). Therefore, PD1 expression on NK cells from B-CLL patients was measured using different readouts including Flow cytometry, confirmed by CyTOF and scRNA-seq, also they were compared to healthy controls where appropriate.

As shown from (**Figure 3.6 panel a**) at chapter 3, flow cytometry analysis showed that PD-1 expression is significantly upregulated on NK cells from B-CLL patients compared to age-matched HC 1.8±0.4% vs 0.5±0.1% ($p<0.0001$). (**Figure 5.1**) Further analysis was done to determine the pattern of PD-1expression on NK cell subsets, which revealed that most PD-1 positive NK cells belong to CD56^{dim} but not CD56^{bright} NK subsets, with up to 23% of PD-1^{pos} CD56^{dim} NK cells and 0.8% of PD-1^{pos} CD56^{bright} NK cells. Particularly, most PD-1 expression was more pronounced on the cytotoxic NK cells CD56^{dim} CD16^{pos} and small fraction of CD56^{dim} CD16^{neg} (**Figure 5.1 panel b**). From the summary of 10 patients with high PD-1 NK cells, (**Right panel, Figure 5.2**), the proportion of PD-1positive NK cells was 11.2±3.1% (Mean±SEM)from the total NK cell population, and this expression was more pronounced on mature CD56^{dim} NK subsets particularly cytotoxic NK subsets compared to less mature CD56^{bright} NK subsets with 13.6±3.3%, 6.5±1.7% from CD56^{dim} CD16^{pos}, CD56^{dim} CD16^{neg}, and 0.9±0.4%, 0.07±0.05% from CD56^{bright} CD16^{pos} and CD56^{bright} CD16^{neg}, respectively.

The panel b from **Figure 5.1** is generated from CyTOF analysis, which will be discussed in more detail later in this chapter. The result from CyTOF has elegantly showed the exact same pattern of PD-1 expression on NK cells from B-CLL patients as in conventional flow cytometry. The PD-1^{pos} and PD-1^{neg} NK population were flow sorted and scRNA-seq was carried out with these two populations from two B-CLL patients. This data will be discussed in the next chapter. The scRNA-seq data has confirmed the transcription of PD-1 was exclusively be found in PD-1^{pos} NK cells but not PD-1^{neg} NK cells (**Figure 5.1 panel c**).

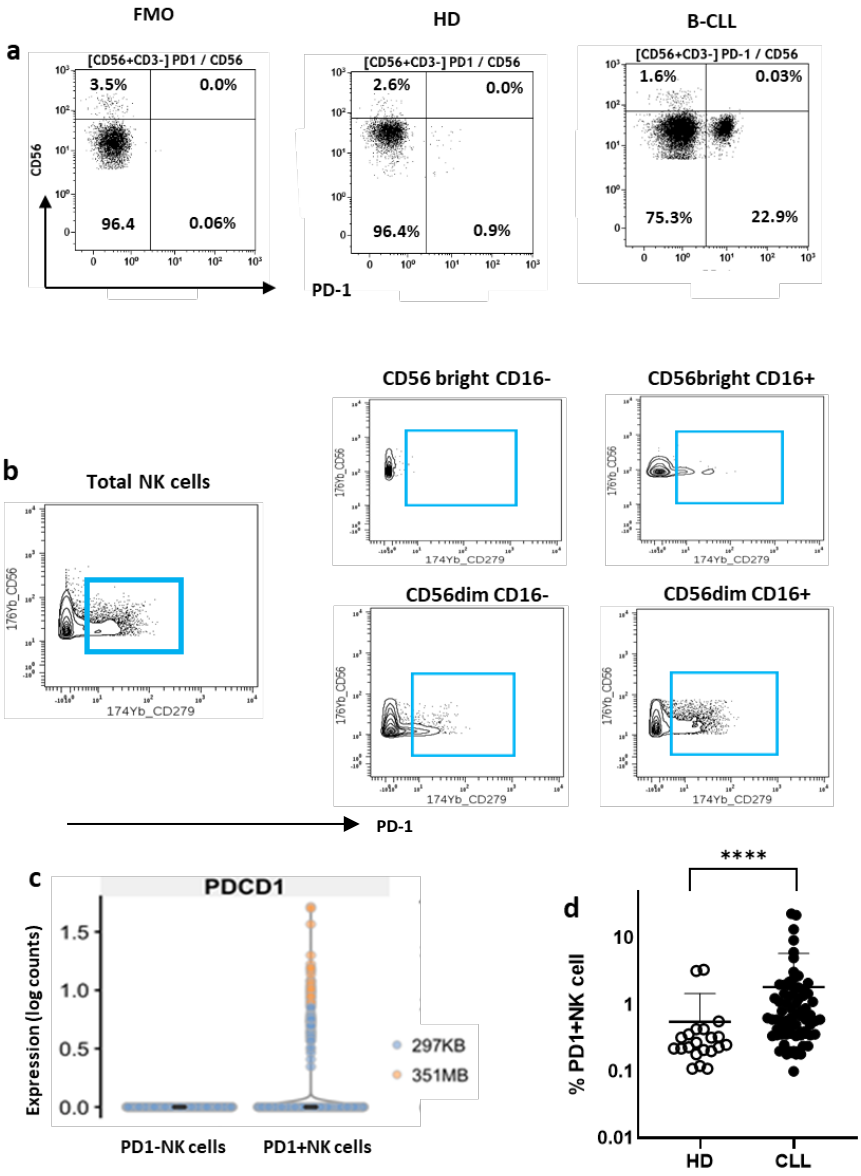

Figure 5.1 PD-1 expression on NK cells from B-CLL using different platforms.

(**a**) Representative flow dot plots to show PD-1 expression on NK cells from 1× 10^6 PBMC of B-CLL patient and HC, FMO on left graph, HC on middle graph and B-CLL on right graph.

(**b**) Contour-uncolored plots from CyTOF analysis of 3 concatenated B-CLL patients with high PD-1^{pos} NK cells to show PD-1 expression on global NK population and differential expression on NK cell subsets.

(**c**) Quantitative analysis of PD-1 mRNA counts between sorted PD-1^{pos} and PD-1^{neg} NK cells using 10x Genomic single cell RNA-seq (scRNA-seq) technology of two B-CLL patients with high PD-1^{pos} NK cells.

(**d**) Scatter dot plot from flow cytometry data to compare PD-1 expression on NK cells from B-CLL patients (filled black circles) and HC (empty circles) form flow cytometry analysis, each circle represent a single donor.

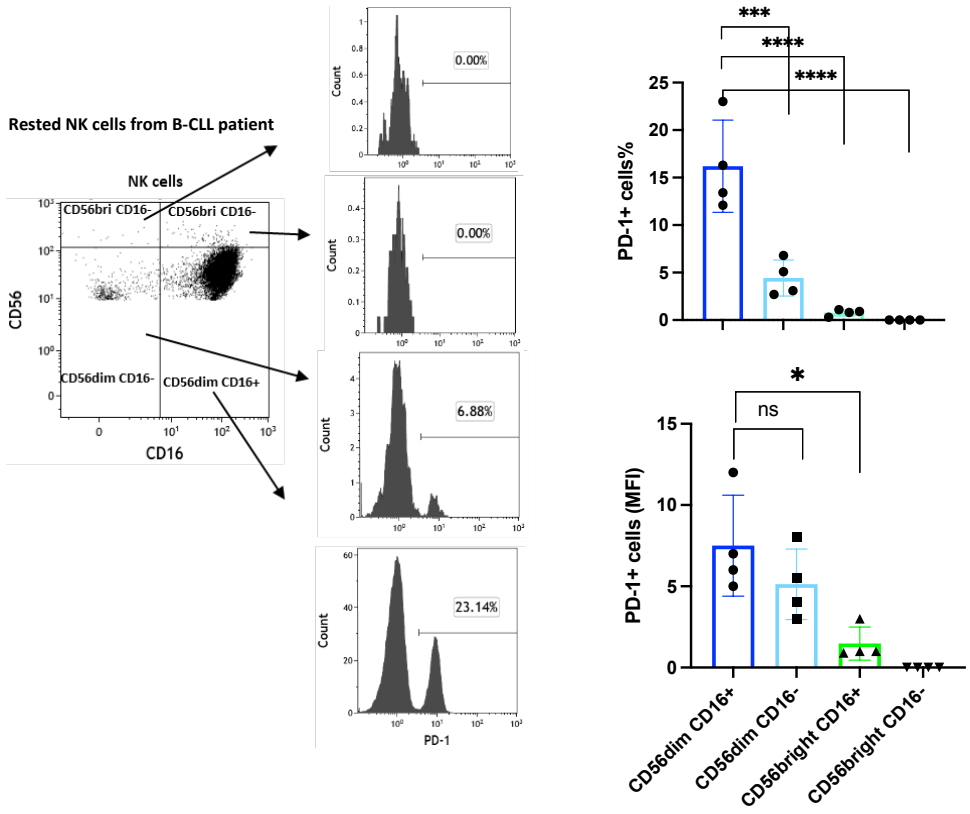

Figure 5.2 Pattern of PD-1 expression on NK cell subsets from B-CLL patients.

Left panel, example of dot plot from flow cytometry analysis of NK cells from B-CLL patients to show the gating strategy for the four different NK cell subsets. The middle histogram graphs show differential PD-1 expression on different NK subsets of the donor from the left panel. Right panel, bar charts with the mean values and standard errors to summarise the percentage and MFI of PD-1 expression on different NK subsets from 10 B-CLL patients with high PD-1 positive NK population, $CD56^{dim}$ $CD16^{+}$ (blue bar), $CD56^{dim}$ $CD16^{-}$ (light blue bars), $CD56^{bright}$ $CD16^{+}$ (light green bars), and $CD56^{bright}$ $CD16^{-}$. Statistics was performed by Repeated measurement one-way ANOVA test (*p<0.05, ***p<0.001,****p<0.0001

5.2.2 PD-1^{pos} NK cells are not exclusively CMV memory-like NK cells

Previous research has hypothesized that PD-1pos NK cells are related to CMV infection, as PD-1pos NK cells can only be found in CMV positive individuals (M. M. Cho et al., 2020). To determine whether PD-1 expression was also related to the tumor process or just CMV infection, B-CLL patients with high PD-1^{pos} NK cells were analysed based on CMV serostatus. Using in house CMV testing, our data showed that 63% (47 out of 75) of our B-CLL cohort were CMV seropositive and 37% (28 out of 75) were CMV seronegative (**Figure 5.3 panel a**). Looking at B-CLL patients with high PD-1^{pos} NK cells, we found that the vast majority of patients about 91% were CMV seropositive, whereas 9% was CMV seronegative (**Figure 5.3 panel b**). This data hints that CMV infection may play an important role in the induction of PD-1 expression on NK cells, however this assumption needs more investigation using lager cohort of B-CLL patients with high proportion of PD-1positive NK cells. In addition, there is a possibility that PD-1^{pos} NK cells can also be induced in the tumor microenvironment. Although other viruses infection such as HCV, EBV might induce PD-1 expression as reported by other studies (Beldi-Ferchiou et al., 2016), this is not pursued due to the data availability.

NKG2C^{+} NK cells represent memory like NK cells that are known to be expanded following CMV infection (Grutza et al., 2020). In the context of CMV infection, majority of NKG2C receptor is expressed on the cytotoxic NK subset CD56^{dim} CD16^{pos}, which is the same subset that exclusively express PD-1 in B-CLL patients. Therefore, the co-expression of NKG2C and PD1 was checked using CyTOF platform. Three B-CLL patients with high percentage of PD-1 NK cells (22%, 13%, 10.5%) and CMV seropositive were used for this experiment. The data from the three patients were combined and analysed using Cytobank software. First, there are 15.9% of NK cells that express NKG2C from the total combined NK population (**Panel a**

Figure 5.4). Next NKG2C expression was measured on PD-1^{pos} NK vs PD-1^{neg} NK cells. Interestingly, there were 18.6% of NKG2C^{+} NK cells in PD-1^{neg} NK population, instead there were only 1.5% of NKG2C^{+} NK cells in PD-1^{pos} NK population (**Figure 5.4 panel b**). At last, the co-expression pattern of PD-1 and NKG2C was analysed on the total NK population (**Figure 5.**4, right panel), on CD56^{dim} CD16^{pos} subsets, and CD56^{dim} CD16$^{pos/neg}$ (**Figure 5.4 panel c**). The data showed that PD-1 and NKG2C expression were exclusively to each other, and there was very small portion of NK cells that express both PD-1 and NKG2C at the same time.

Table 5.1 CMV serostatus of the whole cohort of B-CLL patients and B-CLL patients with high PD-1NK cells

	n	CMV serostatus	Percentages
B-CLL patients	47	+	63%
	28	-	37%
High PD-1 NK patients	10	+	91%
	1	-	9%

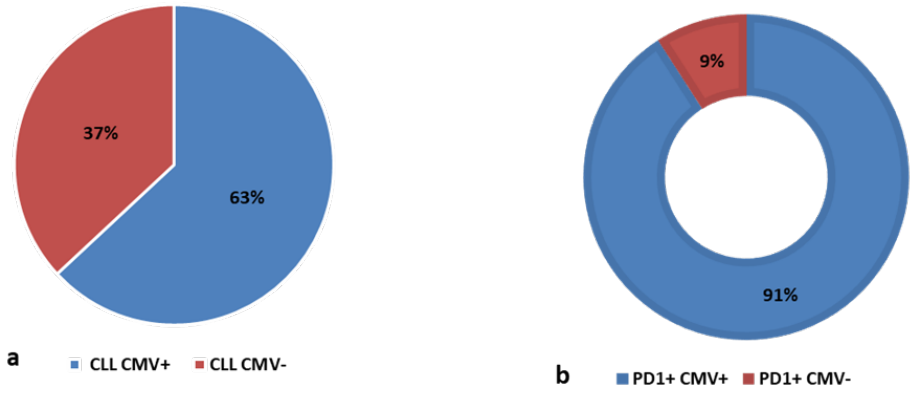

Figure 5.3 Percentage of CMV seropositive and seronegative in B-CLL patients and specifically in patients with high PD-1pos NK cells.

(**a**) 63% of B-CLL patients (n=75) were CMV seropositive (blue chart) and 37% were seronegative (red chart) in the whole B-CLL cohort. (**b**) majority of B-CLL patients (n=10) with high percentage of PD-1 NK cells (≥3% as a cut off) were CMV seropositive (blue chart) and only 9% were CMV seronegative. CMV test was performed using House CMV test at lab and the positivity was determined by ELISA and analysed by GraphPad prism 9.

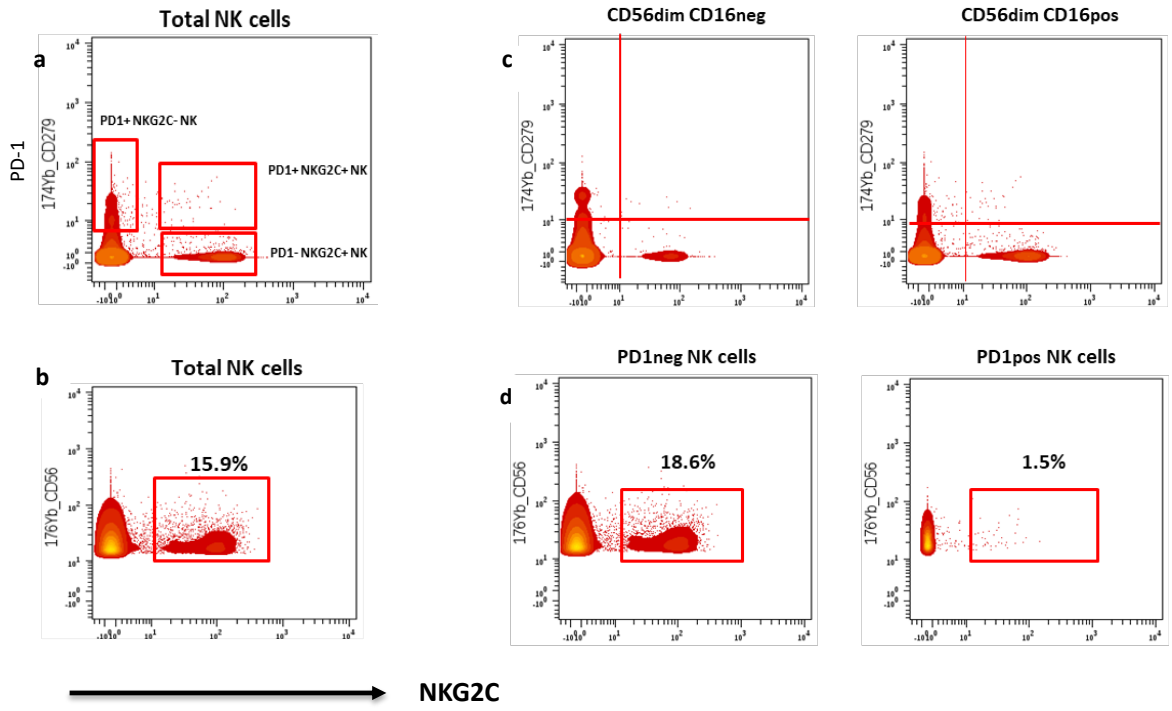

Figure 5.4 Co-expression pattern of NKG2C and PD-1 on NK cells from CyTOF analysis.

Three B-CLL patients with high percentage of PD-1 NK cells and CMV seropositive were stained with CyTOF panel. The data from three patients were combined and analysed using Cytobank software. (**b**) Top left panel: NKG2C expression was analysed on the total NK cells from 3 concatenated B-CLL patients with high PD-1^{pos} NK cells, with x axis represents NKG2C and y axis represents CD56. Co-expression pattern of NKG2C and PD-1 was analysed on total NK cells, x axis represents NKG2C and y axis PD-1. The NKG2C^{pos} PD-1^{pos}, NKG2C^{pos} PD-1^{neg} and NKG2C^{neg} PD-1^{pos} NK populations were labelled on the dot plot (**a**). NKG2C expression was compared between PD-1^{pos} NK cells and PD-1^{neg} NK cells, with x axis represents NKG2C and y axis represents CD56 (**d**). Co-expression pattern of NKG2C and PD-1 was analysed on CD56^{dim} CD16^{pos} and CD56^{dim} CD16^{neg} NK population, x axis represents NKG2C and y axis PD-1(**c**).

5.2.3 Characterisation of PD-1^{pos} NK cell phenotype

NK cells vary in their expression of several receptors, which often correspond to different stages of NK cell differentiation, maturation, and function. In B-CLL patients, PD-1 expression was confined on CD56^{dim} CD16^{pos} and with less extend on CD56^{dim} CD16^{neg}. Next, we went to investigate whether PD-1^{pos} NK cells have particular phenotype in comparison to PD-1^{neg} NK cells from the same patients. Using flow cytometry, the expression pattern of large panel of differentiation and activating receptors were measured and compared between PD-1^{pos} and PD-1^{neg} CD56^{dim} NK cells, including CD57, NKG2A, DNAM-1, NKp30, NKp46 and NKG2D.

5.2.3.1 PD-1^{pos} NK cells are highly differentiated NK cells

Several studies have described CD57 as a marker of replicative senescence and is associated with terminal differentiation of both NK and CD8^{+} T cells (Brenchley et al., 2003; Papagno et al., 2004). Thus, to determine the differentiation stage of PD-1^{pos} NK cells, CD57 expression was analysed alongside with immature NKG2A marker on PD-1^{pos} CD56^{dim} NK and PD-1^{neg} CD56^{dim} NK cells. PBMCs from B-CLL patients with high PD-1 NK cells were stained with CD57 and NKG2A and analysed by Flow cytometry. The analysis showed that PD-1^{pos} NK cells were at terminal maturation stage compared to PD-1^{neg} NK cells. PD-1^{pos} NK cells express significantly higher maturation marker CD57 and lesser immature marker of NKG2A with 82.6±3.5% and 22±9.4% vs PD-1^{neg} NK cells with 77.9±2.4% and 34.8±9.1% ($p= 0.0181$ and $p=0.0078$) respectively, acquiring phenotype of NKG2A^{low} CD57^{high} PD-1^{pos} NK cells (**Figure 5.5**).

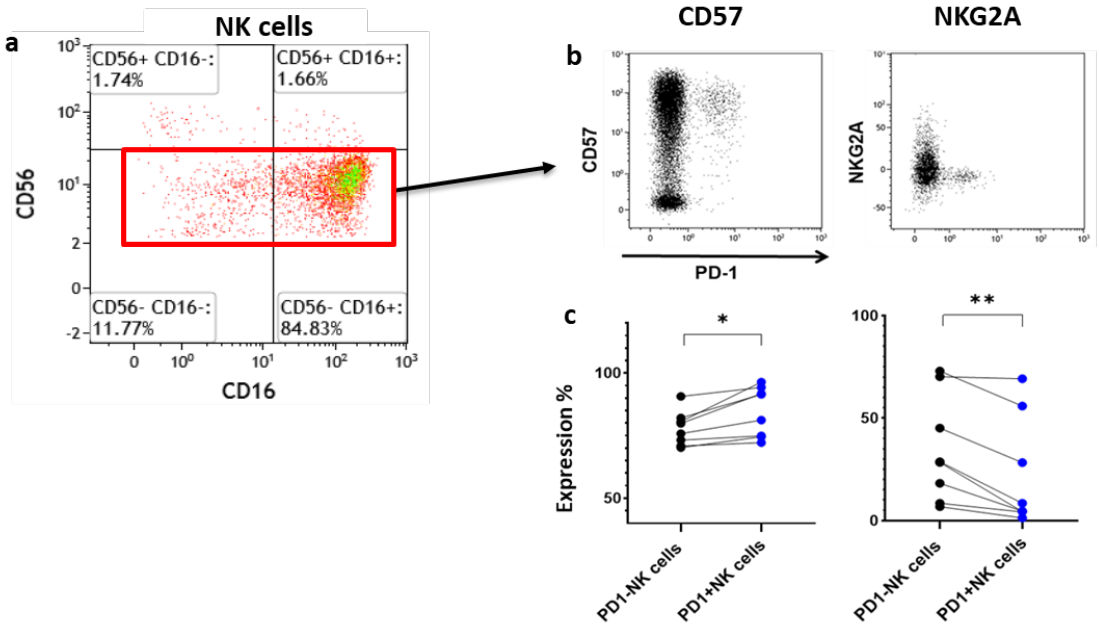

Figure 5.5 Expression of differentiation markers (CD57& NKG2A) on PD-1pos vs PD-1neg NK cells using flow cytometry.

The left graph (**a**) is a representative flow dot plot to show the gating strategy of $CD56^{dim}$ NK cells from total NK population. The gated $CD56^{dim}$ NK cells were further analysed for co-expression pattern of PD-1 with CD57 and NKG2A from B-CLL patients with high percentage of PD-1 NK cells (n=8). The top right panels (**b**) are representative dot plot examples to demonstrate the co-expression of PD-1 with CD57 and NKG2A. The dot plots compare the percentages of $CD57^{pos}$ (left) and $NKG2A^{pos}$ (right) NK cells between the $PD\text{-}1^{pos}$ NK cells (blue circles) vs $PD\text{-}1^{neg}$ NK cells (black circles), bottom right panel (**c**). Data were acquired by flow cytometry and analysed by Kalusa, and statistical differences were determined by Wilcoxon matched-paired non-parametric test, (*$p<0.05$, **$p<0.01$).

5.2.3.2 PD-1^{pos} NK cells express lower levels of activating receptors

The expression of activating receptors on NK cells, including NKG2D, DNAM-1 and NCRs, which regulate NK cell anti-tumor function, is often down regulated in malignancy (Koch et al., 2013). This often coincided with slight increase in expression of inhibitory receptors such as KIRs and NKG2A (G. Konjević et al., 2017). The alteration in the expression of activating receptors on NK cells is believed to be induced by tumor suppressive microenvironment such as cytokines, growth factors, in addition to chronic NK cell receptor engagement with tumour ligands (Delahaye et al., 2011). Therefore, we determined the phenotypic status of PD-1^{pos} CD56^{dim} NK cells by measuring their expression of activating receptors in comparison to PD-1^{neg} CD56^{dim} NK cells from the same B-CLL patient using flow cytometry. Interestingly, PD-1^{pos} NK cells exhibited significantly lower expression of activating receptors, including NCRs, DNAM-1 and NKG2D compared to PD-1^{neg} NK cells (**Figure 5.6**). The expression of NKp30 and NKp46 were 49.5±13.6% and 9.4±3.7% vs 71.9±8.2% and 27.9±6% (p=0.0420 and p=0.0020), MFI 2.3±0.3 and 0.7±0.08 vs 4.0±0.4 and 0.9±0.1 (p=0.0049 and p= 0.0039) for PD-1^{pos} vs PD-1^{neg} respectively. In addition, NKG2D was also down regulated on PD-1^{pos} NK cells with 81.3±4.8% vs 89.5±3.6% (p=0.0137), MFI 3.8±0.8 vs 5.0±0.8 (p=0.0005) for PD-1^{pos} vs PD-1^{neg} respectively. The percentage of DNAM-1 expression was lower on PD-1^{pos} vs PD-1^{neg} NK cells but statistically was not significant in our study, however MFI for DNAM-1 was significantly lower on PD-1^{pos} compared to PD-1^{neg} NK cells with 0.3±0.3% vs 4.3±2.5% (p=0.0020).

Therefore, lower activating receptors expression on PD-1^{pos} NK cells may indicate that these NK cells are less functional than PD-1^{neg} NK cells. Functional analysis will be carried out to investigate this in the next sections.

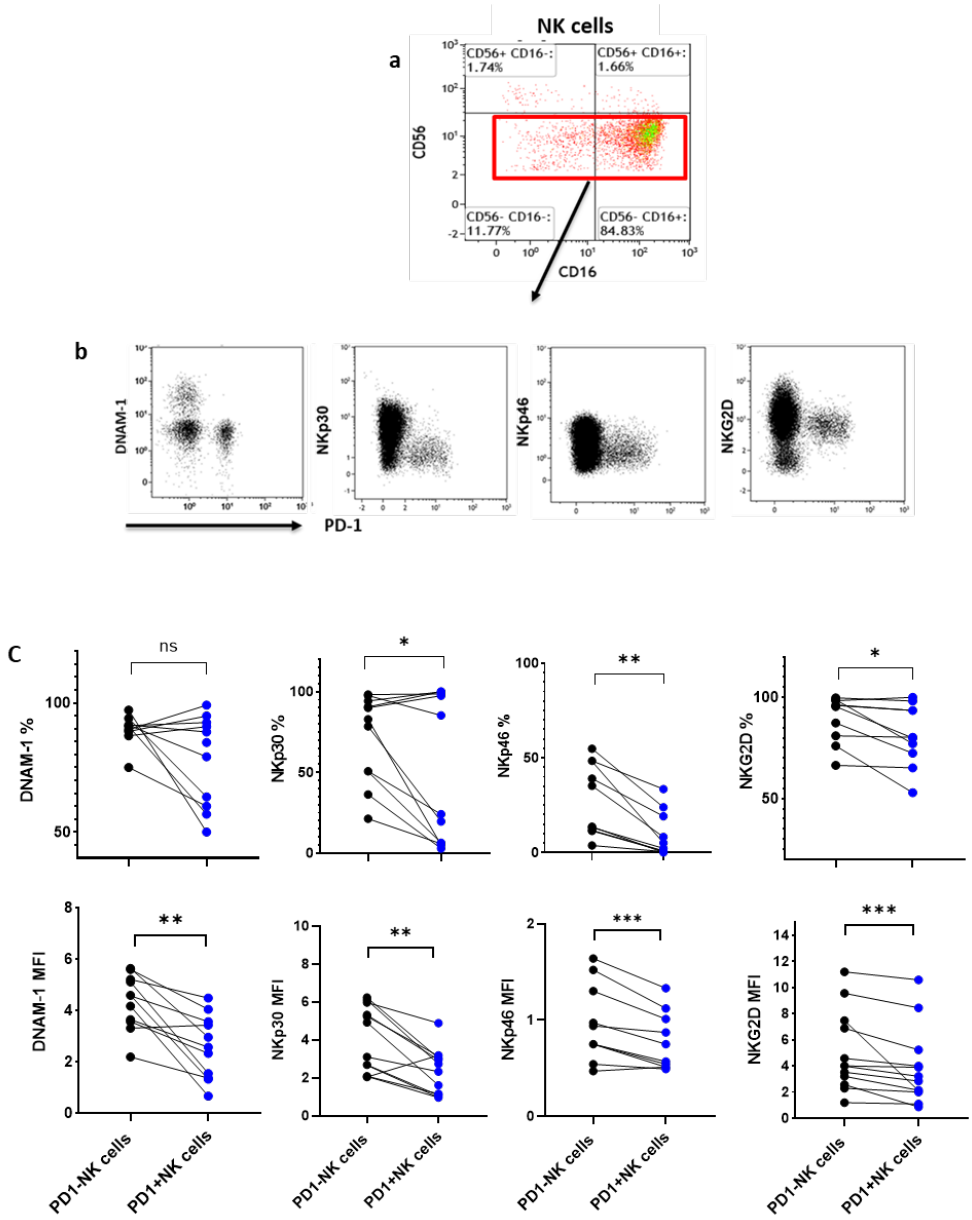

Figure 5.6 Expression of activating receptors on PD-1^{pos} vs PD-1^{neg} NK cells.

(**a**) Representative flow dot plot to show the gating strategy of CD56^{dim} NK cells from the total NK population. The expression pattern of DNAM-1, NKp30, NKp46 and NKG2D on gated CD56^{dim} PD-1^{pos} vs CD56^{dim} PD-1^{neg} NK cells were further analysed from B-CLL patients (n=11). (**b**) Representative flow dot plot examples to demonstrate the co-expression of PD-1 with indicated activating receptors. (**c**) Dot plots to compare the percentage and MFI of DNAM-1^{pos}, NKp30^{pos}, NKp46^{pos} and NKG2D^{pos} NK cells between the PD-1^{pos} (blue circles), and PD-1^{neg} (black circles). Statistical significances were determined by Wilcoxon matched-paired non-parametric test using GraphPad Prism, (*p<0.05, **p<0.01,***p<0.001).

5.2.4 High dimensional analysis to compare phenotype of PD-1^{pos} and PD-1^{neg} NK cells

We have demonstrated previously that PD-1^{pos} NK cells have a phonotype of CD57^{high} NKG2A^{low} PD-1^{pos} NK cells and they express lower activating receptors compared to PD-1^{neg} NK cells, including NKG2D, NCRs and DNAM-1. We decided to further characterise the phenotype of PD-1^{pos} NK cells by investigating the co-expression of PD-1 with other markers including checkpoint receptors, adhesion molecules and chemokine receptors to reveal the clustering pattern of PD-1^{pos} vs PD-1^{neg} NK cells. PBMCs from 3 B-CLL patients with high percentage of PD-1 NK cells were investigated in this experiment using Mass cytometry.

5.2.4.1 High dimensional analysis workflow of NK cells

Total number of NK cell events collected in the CyTOF analysis was 4000 in average per patient (n=3). They were merged by Flowjo v10.7.1 and analysed using Cytobank software. Downstream analysis to get rid of beads, dead and duplicate cells was carried out to identify single live CD45^{pos} cells (**Chapter 2 Figure 2.5**). Initially, NK cells (CD45^{pos} CD14^{neg} CD19^{neg} CD3^{neg} CD56^{pos}), followed by different NK cell subsets CD56^{bright} CD16^{neg}, CD56^{bright} CD16^{pos}, CD56^{dim} CD16^{pos}, CD56^{dim} CD16^{neg} and PD-1^{pos}, PD-1^{neg} NK cells were identified and gated manually (**Figure 5.7**). In addition, expression of other markers on NK cells including adhesion molecules and chemokine receptors were also checked using histogram and dot blots. To visualise cells including NK and NK subsets, high dimensional data was initially analysed using t- distributed Stochastic Neighbor Embedding (tSNE) tool, which projects high dimensional data into two-dimensional space (tSNE1 and tSNE2) based on cellular marker expression resulting in four clusters of closely related cells CD56^{pos} NK cells, CD19^{pos} B cells, CD3^{pos} T cells and CD14^{pos} monocytes (**Figure 5.8 panel a**). As our main interest is NK cells particularly PD-1^{pos} and PD-1^{neg} NK cells, the focus was to identify markers associated with

NK cells. To this end, NK cell population was zoomed in, and NK subsets clusters were nicely identified by CD56 and CD16 expression. In addition, PD-1^{pos} and PD-1^{neg} NK cells were distinguished by PD-1 expression on NK cells (**Figure 5.8 panel c**). The clustering analysis based on expression of at least 30 markers (**Chapter 2 CyTOF panel 2.20**) on NK cells generated distinct clusters, and expression pattern of these single markers including checkpoint receptors (PD-1, TIGIT, CD96, CD39 and NKG2A), adhesion molecules (CD11c, CD11b), chemokines receptors (CD184, CD197) and activating receptors (DNAM-1 and NKG2C) were demonstrated on the tSNE plots (**Figure 5.9**).

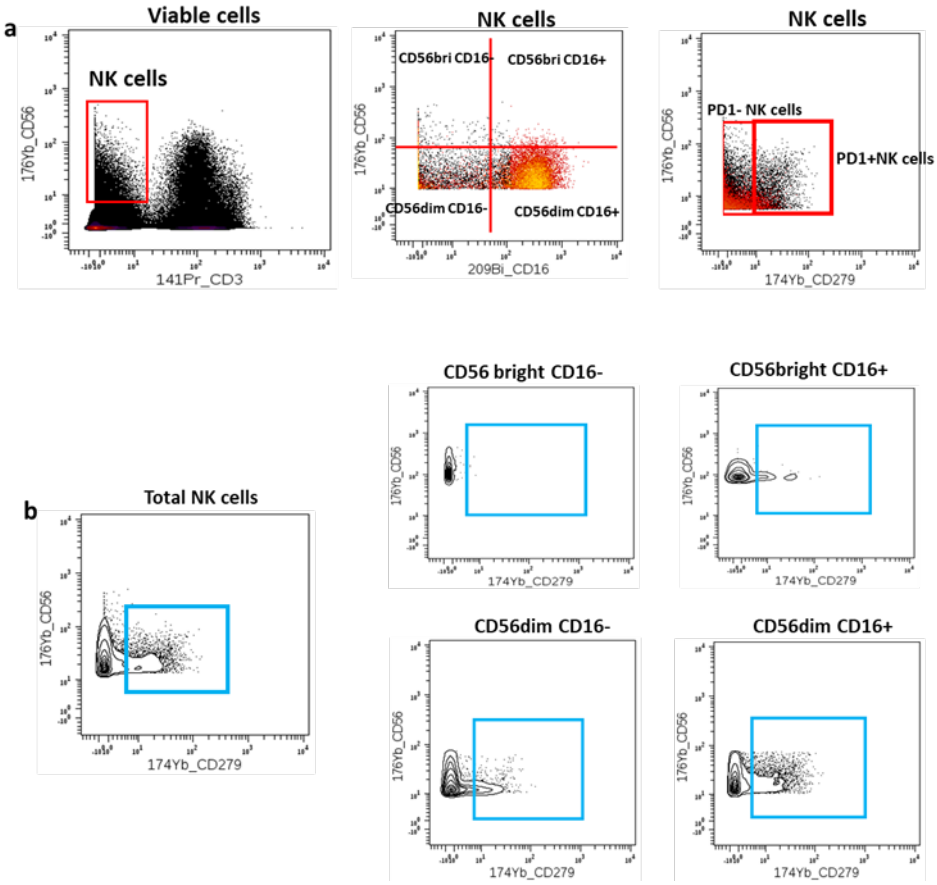

Figure 5.7 NK and NK subsets identification and differential expression of PD-1 on NK cell subsets

(**a**) Representative dot colour plots to identify live NK, NK subsets and PD-1^{pos} NK cells, which generated from CyTOF analysis of 3 concatenated B-CLL patients with high PD-1^{pos} NK cells. After equalising NK cell count between patients, the total events of live NK cells were around 10500 and about 1400 of PD-1^{pos} NK events were identified in this analysis. (**b**) PD-1 expression was analysed on global NK cells and different NK subsets. The analysis was performed using Premium Cytobank platform.

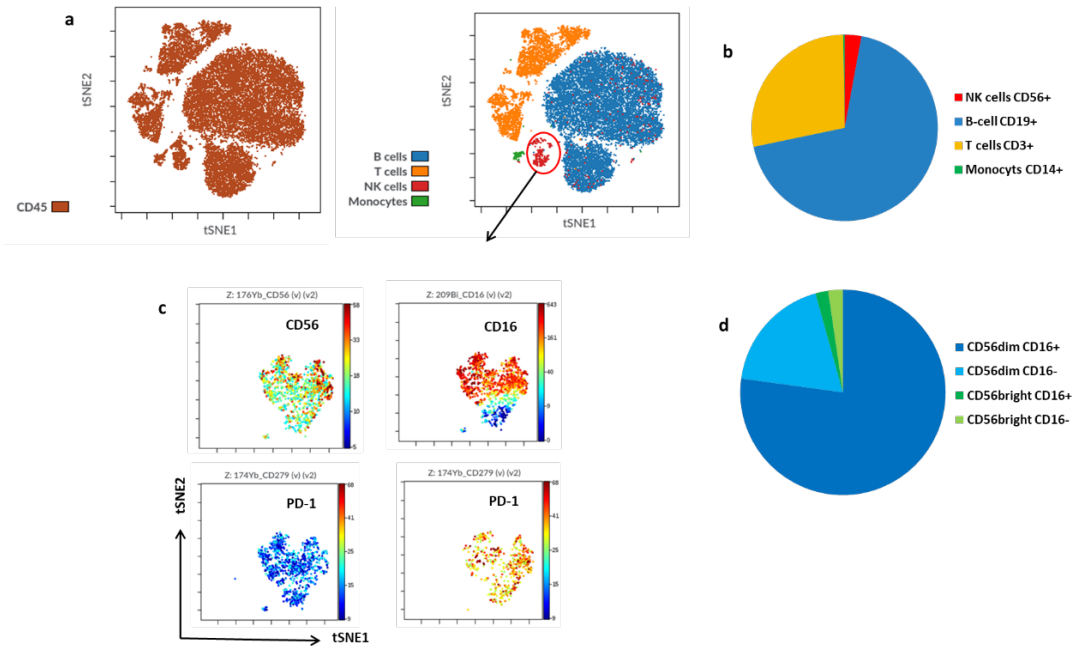

Figure 5.8 viSNE analysis plots based on 5 different lineage markers of cells from PBMCs.

(**a**) ViSNE analysis of $CD45^{+}$ cells from 3 concatenated PBMCs with high $PD\text{-}1^{pos}$ NK cells of B-CLL patients, viSNE was run with perplexity =30, 1000 iterations and seed =5. This was followed by two dimentinal analysis of manually gated PBMCs (dots) which plotted according to their expression of lineag markers CD3 (T cells), CD19 (B cells), CD56 (NK cells) and CD14 (monocytes). (**b**) proportions of different immiune cells partecepated in the analysis represented in bi chart. (**c**) Further clustering analysis on NK cells based on CD56, CD16 and PD-1 expressions to idintify $PD\text{-}1^{pos}$ and $PD\text{-}1^{neg}$ NK cells and clustering behavoiurs of these cells**.** (**d**) bi chart to represent NK cell subsets proportions used in the analysis.

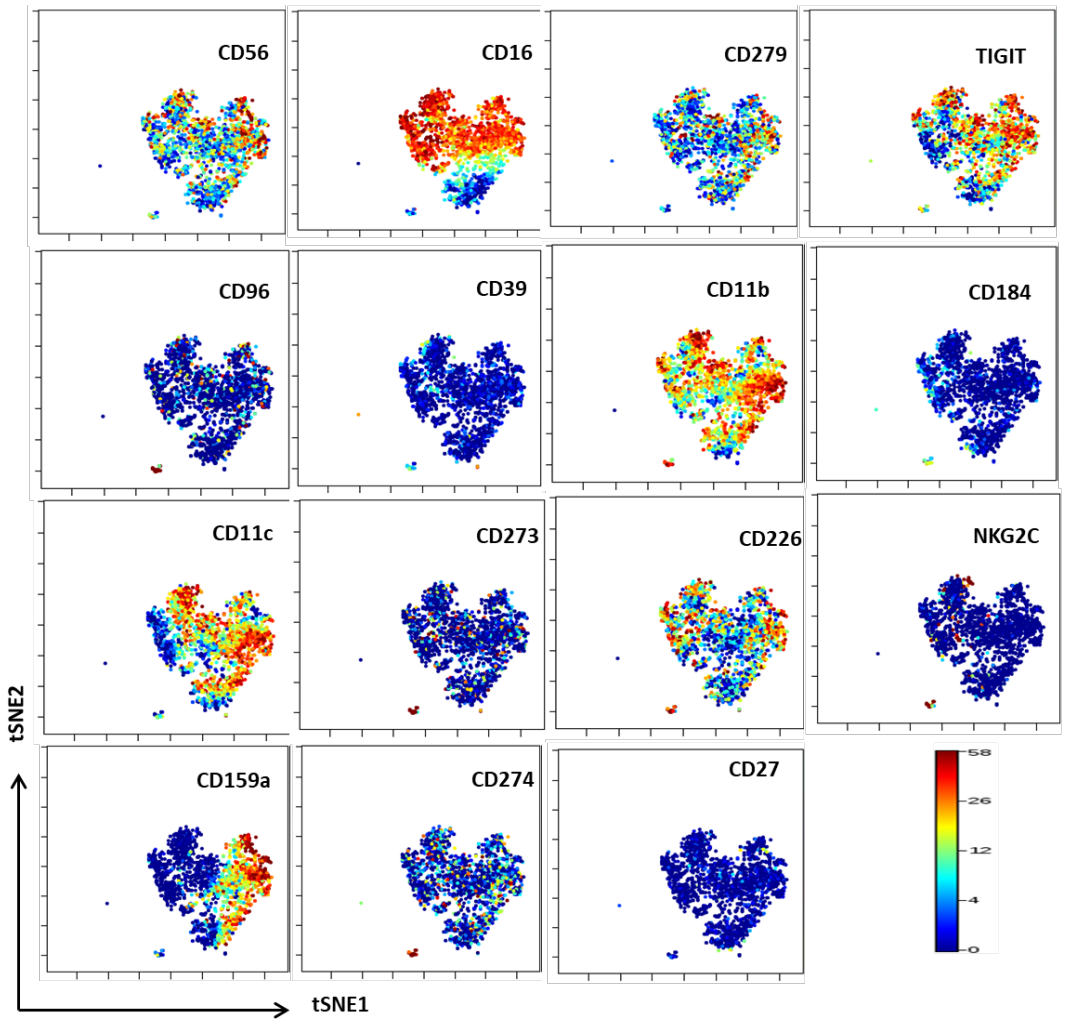

Figure 5.9 viSNE analysis of marker expression on total NK cells.

Expression profile of activating receptors, immune checkpoints, chemokine receptors and adhesion molecules on NK cells projected on viSNE analysis. Results are presented as interquartile ranges minimum to high of median expression.

5.2.4.2 Co-expression pattern of PD-1 with other immune checkpoints

We have shown previously (chapter 3) using Flow cytometry that multiple immune checkpoint receptors including PD-1, CTLA-4, LAG-3 and CD96 were up-regulated on NK cells from B-CLL patients compared to HCs. Given the critical role of immune checkpoint receptors and their ligands in modulating NK cell function, we decided to further interrogate this by investigating the co-expression of PD-1 with other checkpoint receptors particularly on PD-1^{pos} NK cells. CyTOF panel (**Table 2.20**) was expanded to include CD39 checkpoint receptor along with PD-1, TIGIT and CD96. tSNE analysis was used to explore the expression level of checkpoint receptors on PD-1^{pos} NK cells compared to PD-1^{neg} NK cells from 3 concatenated B-CLL PBMCs. The tSNE analysis revealed immune checkpoint receptors particularly TIGIT which is major checkpoint receptor on NK cells was expressed on both PD-1^{pos} and PD-1^{neg} NK cells, but interestingly TIGIT expression was upregulated on PD-1^{pos} NK cells. In addition, CD39 which has been demonstrated to suppress NK and $CD8^{+}$ T cells antitumour function (H. Zhang et al., 2019), was also upregulated on PD-1^{pos} NK cells compared to PD-1^{neg} NK cells (**Figure 5.10**).

Then the manual gating was used to confirm the upregulation of TIGIT and CD39 on PD-1^{pos} NK cells compared to PD-1^{neg} NK cells. The percentage of TIGIT positive NK cells from the whole NK population was 64% (MFI=15.6), whilst there was 77.3% (MFI=20.8) TIGIT positive NK cells from PD-1^{pos} NK population. Instead, only 52.7% (MFI=13.4) (**Figure 5.11**). From the whole NK population, the majority of TIGIT single positive cells was 52.7%, followed by the TIGIT/PD-1 double negative cells 32.5% and TIGIT/PD-1 double positive cells 11.3%, with PD-1 single positive cells represent about 3.4% of the whole NK population (**Figure 5.11 panel c left chart**).

CD39 expression was detected on total NK cells with 11.2% (MFI=10.5). There was 14.2% (MFI=36.7) CD39 positive NK cells from PD-1^{pos} NK population compared to 5.5% (MFI=15.8) on PD-1^{neg} NK cells (**Figure 5.11, panel c right charts**), demonstrating that CD39 expression is up-regulated on PD-1^{pos} NK cells. From the whole NK population, the majority are CD39/PD-1 double negative cells 76.5%, followed by PD-1single positive cells 12.1% and CD39 single positive NK cells 9%, with the CD39/PD-1 double positive NK cells represent about 2.2% of the whole NK population.

CD96 checkpoint receptor was expressed at minimal levels on NK cells with only 1.9% CD96 positive NK cells. There is also up-regulation of CD96 was observed on PD-1^{pos} NK cells with 3%, instead only 1.6% CD96 expression on PD-1^{neg} NK cells. Although there was up-regulation of TIGIT, CD39 and CD96 on PD-1^{pos} NK cells compared to PD-1^{neg} NK cells, these data were not statistically significant due to sample size limitation (n=3).

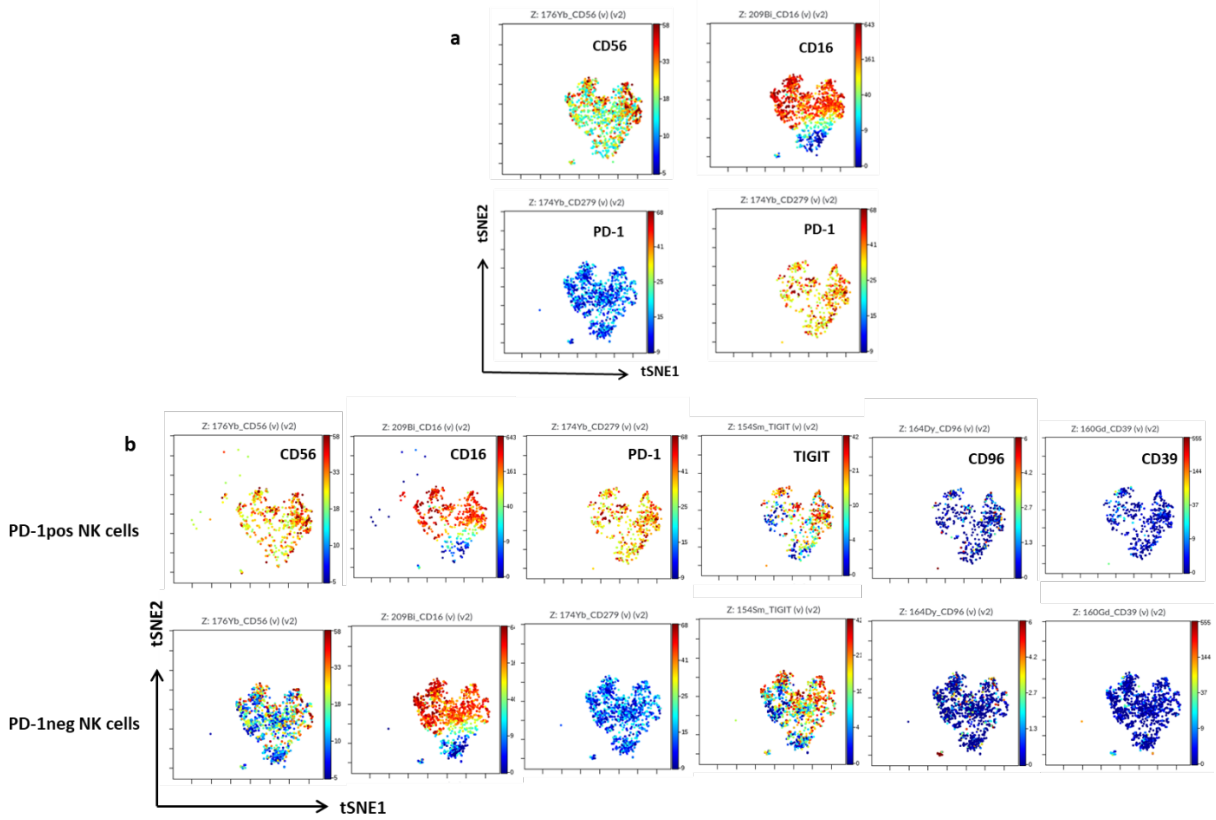

Figure 5.10 Immune checkpoint expression on the clusters of PD-1^{pos} vs PD-1^{neg} NK cells

(**a**) Top panel: tSNE plots to demonstrate the clustering of total NK population with the expression pattern of CD56 and CD16. Middle panels: PD-1^{pos} NK cells and PD-1^{neg} NK cells were manually gated and tSNE analysis was run to confirm the PD-1 expression. (**b**) CD56, CD16, PD-1, TIGIT, CD39 and CD96 expression was projected on the tSNE plots to enable of comparison between two clusters of PD-1^{pos} vs PD-1^{neg} NK cells. Results are presented as interquartile ranges minimum to high of median expression.

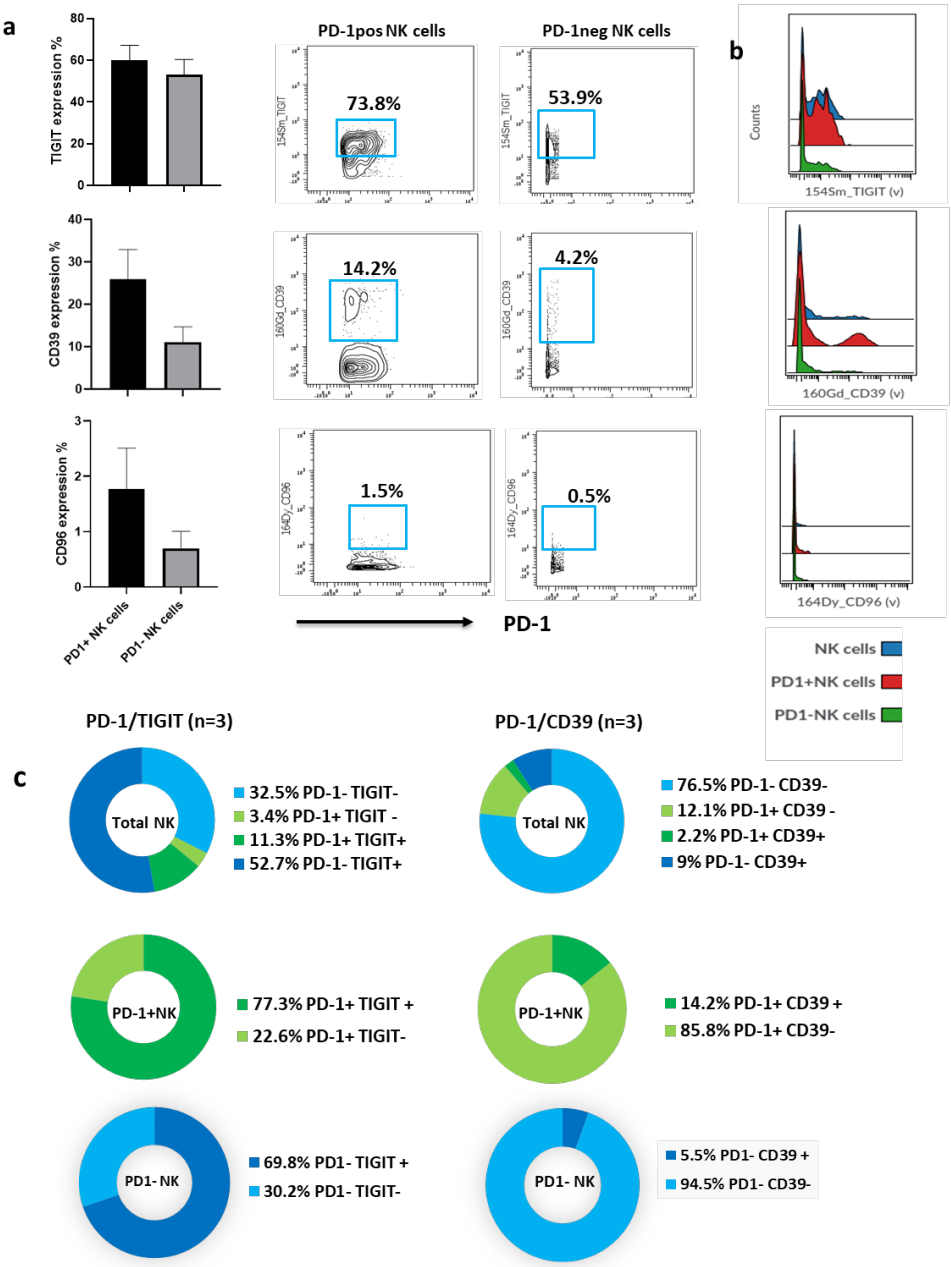

Figure 5.11 Co-expression of TIGIT, CD39 and CD96 with PD-1 on NK cells

(**a**) Left panel: bar charts to show the mean with error bar of TIGIT, CD39 and CD96 positive NK cells based on PD-1^{pos} (black bars) and PD-1^{neg} (grey bars) NK population from 3 B-CLL PBMCs. The right panel: Black contour blots from 3 concatenated PBMCs of B-CLL patients with high PD-1 NK cells to demonstrate the expression of TIGIT, CD39 and CD96 on PD-1^{pos} vs PD-1^{neg} NK cells, with percentages labelled on the graphs. (**b**) Histograms to demonstrate the TIGIT, CD39 and CD96 expression on the global NK cells (blue), PD-1^{pos} (red) and PD-1^{neg} (green) NK cells. (**c**) Pie chart to show the co-expression pattern of TIGIT (left charts) and CD39 (right charts) with PD-1 on NK, PD-1^{pos}, PD-1^{neg} NK cells. Data were analysed using Cytobank, GraphPad Prism and Excel.

5.2.4.3 Co-expression of PD-1 with adhesion and chemokine receptors

Having shown using flow cytometry that some adhesion molecules were down-regulated such as CD49a, CD49d, CD43 and others were up-regulated including CD18 and CD11c on NK cells from B-CLL patients, we went to extend CyTOF analysis of 3 concatenated B-CLL patients to determine the expression pattern of some adhesion molecules and chemokines on PD-1^{pos} NK cells compared to PD-1^{neg} NK cells. Similarly, tSNE analysis was used as initial tool to visualise NK cells and marker expression. Interestingly, CD11c integrin and CD197 chemokine receptor (CCR7) that regulate NK cell migration and trafficking were evidently upregulated on PD-1^{pos} NK cells compared to PD-1^{neg} NK cells (**Figure 5.12**). Manual gating shown in contour plots and histogram of marker expression confirmed the up-regulation of CD11c and CD197 expression on PD-1^{pos} NK cells compared to PD-1^{neg} NK cells with 89.8% vs 45.3% and 16.8% vs 3.4% respectively, due to low sample size we could not get statistic p value for this analysis (**Figure 5.13**).

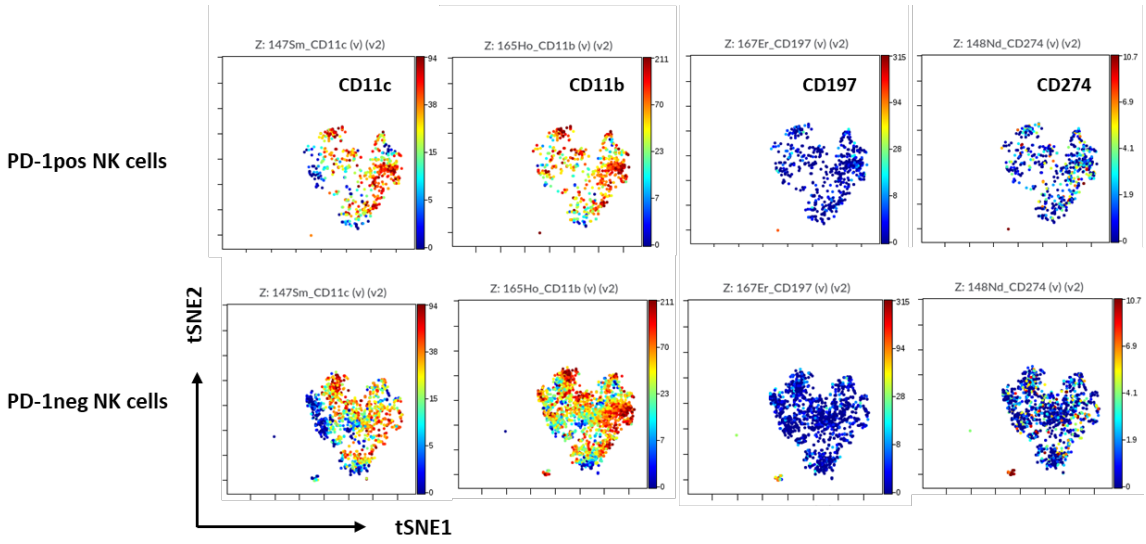

Figure 5.12 Expression of adhesion molecules, CD197 on the clusters of PD-1^{pos} vs PD-1^{neg} NK cells

Expression of CD11c, CD11b, CD197 and PDL1 on clusters of PD-1^{pos} NK cells (top row) and PD-1^{neg} NK cells (bottom row), cells were manually gated to enable quantification of differences between two clusters of NK cells. Results are presented as interquartile ranges minimum to high of median expression.

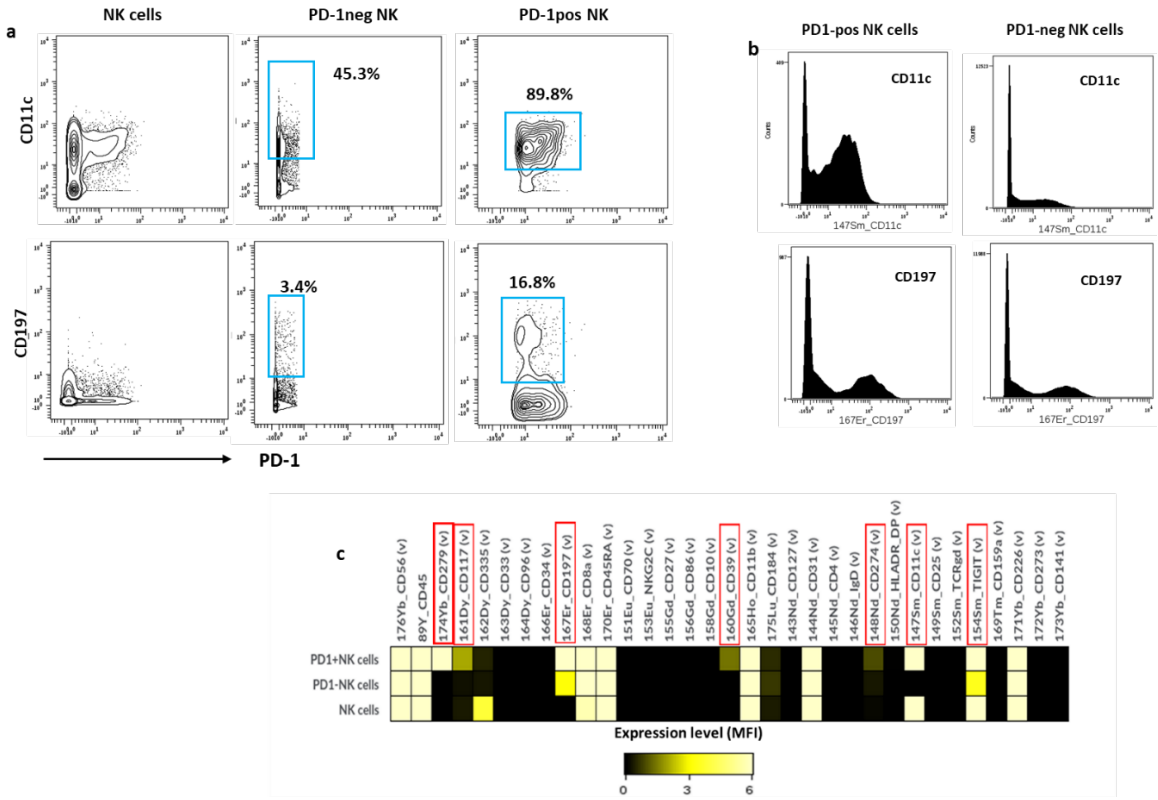

Figure 5.13 Expression pattern CD11c and CD197 on PD-1^{pos} vs PD-1^{neg} NK cells

(**a-b**) Contour uncolored blots and histograms of 3 concatenated PBMCs of B-CLL patients to show the expression pattern of CD11c and CD197 on the whole NK cells, PD-1^{pos} and PD-1^{neg} NK cells. (**c**) Heatmap to summarize the phenotype characteristic of PD-1^{pos} vs PD-1^{neg} NK cells identified by viSNE analysis.

5.2.4.4 PDL1/PDL2 expression on tumour B cells and other immune cells

NK cell impairment in the microenvironment has been linked to the increased expression of inhibitory receptors, which do not bind to the classical MHC-I molecules, instead they have unique ligand expressed on tumor cells. This promotes a key mechanism of NK suppression and tumor evasion from NK cell recognition (Mariotti et al., 2020). Among these inhibitory receptors is PD1 and its cognate ligands, therefore the goal of this experiment was to check the expression of PD-1 ligands on different immune cells including tumor B cells from 3 concatenated B-CLL patients with high PD-1^{pos} NK cells. Interestingly, the main ligand for PD-1 receptor CD274 (PDL1) was expressed on 2.1% of whole NK population and was slightly higher in expression on PD-1^{pos} NK cells compared to PD-1^{neg} NK cells with 5.1% vs 1.8% (**Figure 5.14 panel a**). However, tumor B cells and T cells express very low of CD274 with 0.9% and 1% respectively. Notably, monocytes express the highest level of CD274, as 13% of monocytes were CD274 positive cells, which may contribute to the suppressive mechanism of PD-1 expressing NK cells upon PD-1/PDL1 interaction. However, CD273 (PDL2) was expressed as very low levels on all cell types including tumor B cells as shown in heatmap (**Figure 5.14 panel b**).

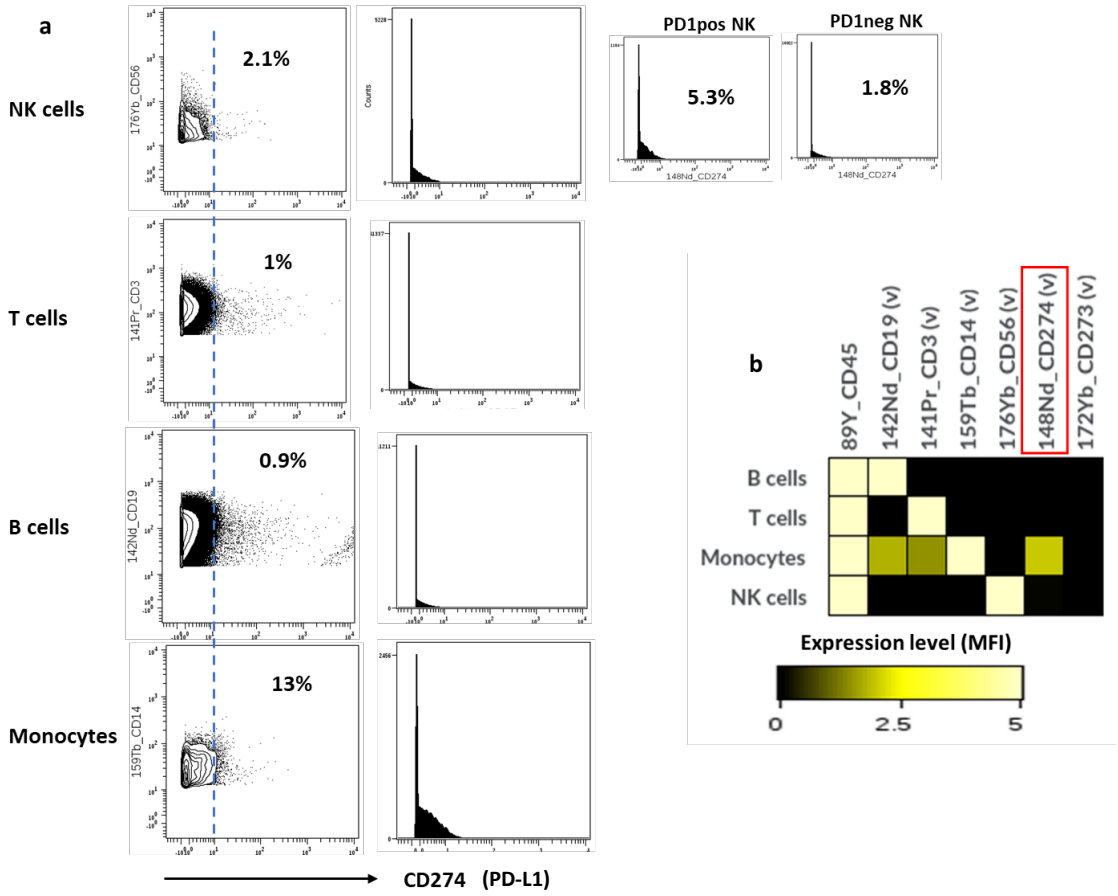

Figure 5.14 PDL-1 and PDL-2 expression on immune cells

(**a**) Using Cytobank analysis, contour uncolored blots and histograms of 3 concatenated PBMCs of B-CLL patients to show the percentage of PDL1 (CD274) and PDL2 (CD273) expression on T cells, B cells, total NK, PD-1^{pos} and PD-1^{neg} NK cells, and monocytes. (**b**) Heatmap to summarize the expression of PDL1 and PDL2 on tumor B cells, T cells, monocytes and NK cells including PD-1^{pos} and PD-1^{neg} NK cells that identified by viSNE analysis.

5.2.5 Functionality of PD-1^{pos} NK cells compared to PD-1^{neg} counterparts

Sustained expression of PD-1 on T cells induced dysfunctional or exhaustion state of $CD8^+$ T cells within the tumor microenvironment, rendering them less responsive, non-proliferative and apoptotic (Simula et al., 2020). In order to explore the potential mechanisms of NK cell dysfunction in B-CLL patients (demonstrated in chapter 4), we went to assess the functional significance of PD-1 expression on NK cells. *Ex vivo* functional capacity of PD-1^{pos} NK cells from B-CLL patients was studied and compared to PD-1^{neg} counterparts. This includes cytokines production and degranulation capacity using two tumor cell lines K562 and PDL1/L2 expressing 721.221 cells. These cells are classical NK cell target lacking expression of HLA-class I and express variety of activating ligands for NK activating receptors. Particularly 721.221 is another classic B-lymphoblastoid cell line that is normally used for NK stimulation due to the lack of MHC-I expression (Shimizu & DeMars, 1989). Using both K562 and 721.221 cell lines is to make sure that this result is not biased due to cell line background. Moreover, the effect of PD-1/PD-1 ligands interactions blockade on NK cells function was investigated in B-CLL patients. The limitation of this experiment was the inability to assess the killing capacity of PD-1^{pos} NK cells, as we could not collect enough cells during cell sorting and theses cells tend undergo apoptosis and do not survive long for cytotoxicity assay. However, complementary *in vitro* study was performed using PD-1 transduced NK-92 and PD-1 transduced NKL cell lines to investigate the killing capacity, cytokines production and degranulation of PD-1^{pos} NK cell lines compared to PD-1^{neg} NK cell lines before and after PD-1 ligands blockade.

5.2.5.1 PD-1 expression on NK cells is associated with lower cytokines production

Engagement of PD-1 with its ligand PDL1 reduces the proliferation, cytotoxicity and cytokines production of T cells and induces apoptosis of tumor specific T cells (Zitvogel & Kroemer, 2012). Differently from T cells which upregulates PD-1 upon activation, PD-1 expression on NK cells from primary and metastatic tumor is thought to be induced by tumor microenvironment including high levels of cytokines, including IL-2, IL-12 and IL-15 and other components of tumor microenvironment such as glucocorticoids (Sivori et al., 2020). PD-1^{pos} NK cells has been shown to be functionally impaired compared to PD-1^{neg} NK cells from lung cancer patients (Niu et al., 2020), and gastrointestinal tract cancer (Y. Liu et al., 2017), as they produce low IFN-γ and have low CD107a expression.

To this end, the PBMCs from B-CLL patients and age-matched HCs were stimulated with target cells overnight (16 hrs) at 1:1 ratio with either HLA-class I negative K562 or 721.221, before the cytokines production was measured using intra-cellular flow cytometry staining, K562 cell line was negative for PD-1 ligands expression, instead 721.221 cells expressed both PD-1 ligands, PDL-1 and PDL-2 on their surface. As shown in panel a, **Figure 5.16 ,** PDL1 and PDL2 expression was detected on 721.221 cells using flow cytometry with 64.8±2.3% and 13.4±0.9% respectively. This data generated from three independent experiments. For the cytokines production, negative control was set up with PBMCs and without target cells stimulation (**Figure 5.15**). A panel of cytokines including IFN-γ, TNF-α, IL-2, IL-4 and IL-5 (**Table 2.13**) were measured using flow cytometry based intra-cellular staining. Since PD-1 expression was confined to $CD56^{dim}$ NK subsets, comparison of cytokines production of PD-1^{pos} vs PD-1^{neg} NK cells was restricted to the $CD56^{dim}$ NK population, this is to rule out the functional variations of $CD56^{Bright}$ and $CD56^{dim}$ NK subsets.

Interestingly, PD-1^{pos} NK cells produced significantly lower cytokines compared to PD-1^{neg} counterpart after stimulation with K562 cell line. In particular, the percentage of cytokines producing NK cells from PD-1^{pos} and PD-1^{neg} cells were 0.27±0.06% vs 2.72±0.5% (p=0.0010) for TNF-α, 0.32±0.06% vs 2.72±0.5% (p=0.0026) for IFN-γ, 0.22±0.1% vs 1.68±0.4% (p=0.0075) for IL-2, 0.21±0.09% vs 1.59±0.6% (p=0.0250) for IL-4 and 0.28±0.1% vs 1.67±0.5 (p=0.0109) for IL-5. On the other hand, stimulation with PDL1/L2 expressing 721.221 tumor cells induced almost same level of cytokines production by PD-1^{neg} NK cells as by K562 cells, however cytokines produced by PD-1^{pos} NK cells was further reduced after stimulation with 721.221. In particular, the percentage of percentage of cytokines producing NK cells from PD-1^{pos} and PD-1^{neg} cells were 0.23±0.06% vs 2.40±0.43% (p=0.0036) for TNF-α, 0.21±0.07% vs 2.62±0.42% (p=0.0009) for IFN-γ, 0.20±0.0.05% vs 1.13±0.23% (p=0.0069) for IL-2, 1.0±0.3% vs 0.1±0.9% (p=0.0156) for IL-4 and 0.15±0.07% vs 1.37±0.34 (p=0.0147) for IL-5 (**Figure 5.16**).

Collectively, lower cytokines production produced by PD-1^{pos} NK cells particularly IFN-γ and TNF-α indicate the impairment antitumor function of PD-1^{pos} NK cells which implies the suppression role of PD-1 expression on NK cells.

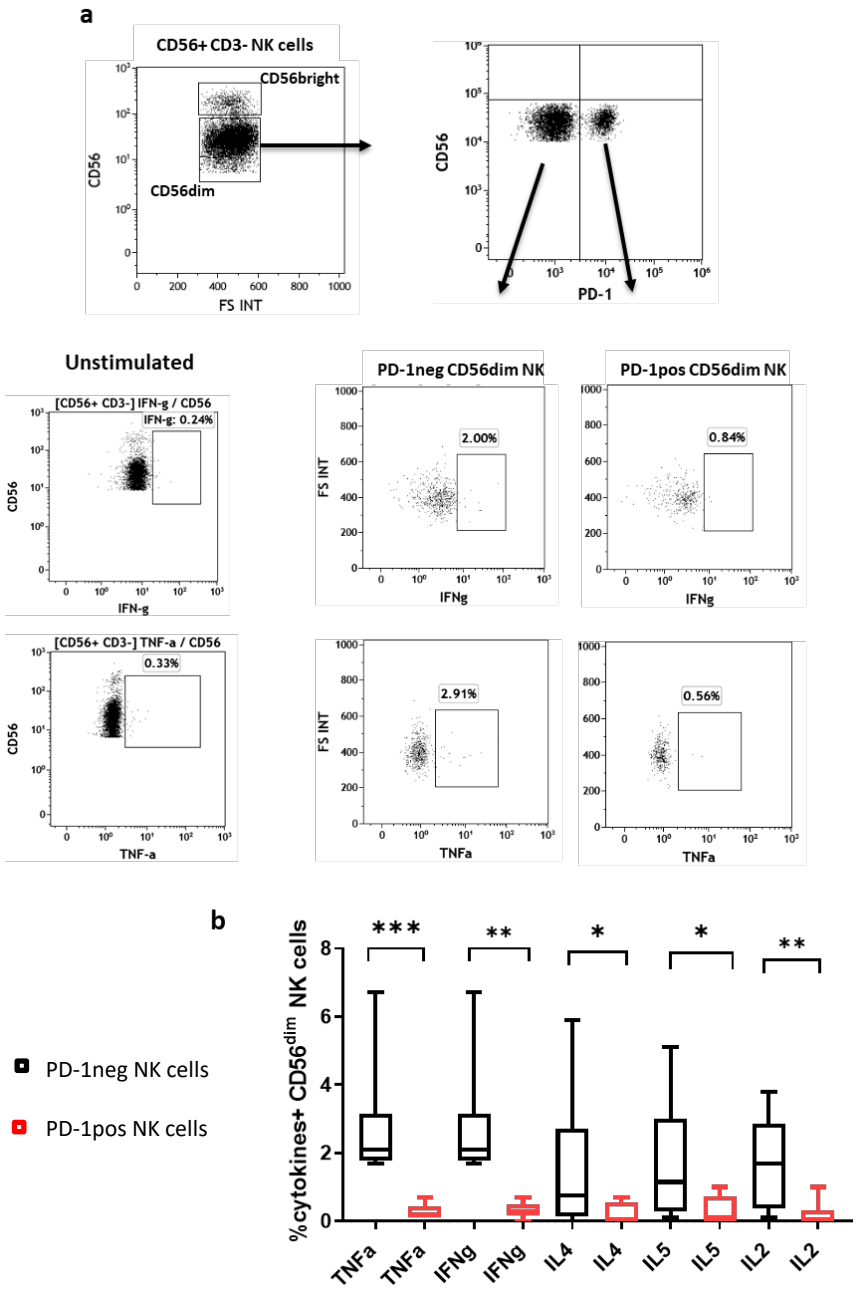

Figure 5.15 Cytokines production by PD-1^{pos} vs PD-1^{neg} NK cells after stimulation with K562 target cells

PBMCs with high percentage of PD-1 NK cells were co-cultured with K562 target cells (E:T ratio 1:1) overnight and cytokines were measured by flow cytomerty. (**a**) Flow dot plots to represent examples of gating strategy for PD1^{pos} NK cells, IFN-γ and TNF-α production after stimulation (right panals), and befor stimulation (non-stimulated). (**b**) Bar charts to summarise cytokines production by CD56^{dim} PD-1^{pos} (red bars) vs CD56^{dim} PD-1^{neg} (black bars) NK cells from 10 B-CLL patients. Data presentd with mean and error bars and statistical significance were determined by Mann whitney test by GraphPad Prism (*p<0.05, **p<0.01,***p<0.001).

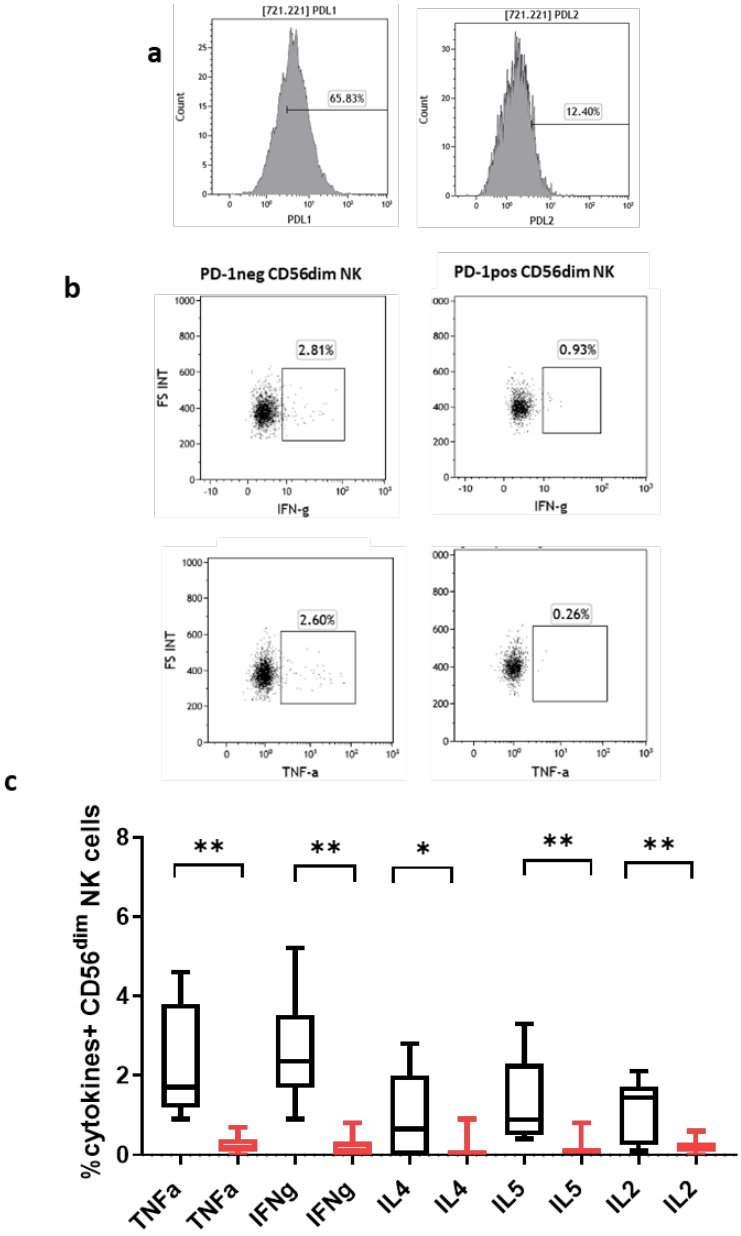

Figure 5.16 Cytokines production by PD-1^{pos} vs PD-1^{neg} after stimulation with 721.221 target cells which express PDL1 and PDL2

(a) Flow cytometry analysis of PDL1 and PDL2 expression on the target cells 721.221. (**b**) Representative flow dot plots of IFN-γ and TNF-α production by PD-1^{pos} vs PD-1^{neg} NK cells after stimulation overnight with 721.221 target cells (1:1). (**c**) Bar charts to summarise the cytokines production by CD56^{dim} PD-1^{pos} (red bars) vs CD56^{dim} PD-1^{neg} (black bars) NK cells from 10 B-CLL patients after stimulation with 721.221. Data presentd with mean and error bars and statistical significance were determined by GraphPad Prism (*p<0.05, **p<0.01).

5.2.5.2 PD-1 expression inhibits NK cell degranulation

A study (Pesce et al., 2017) has shown that PD-1 is expressed on NK cells from peripheral blood and peritoneal fluid of cohort of patients with ovarian carcinoma. These PD-1^{bright} NK cells displayed impaired degranulation and cytokines production compared to PD-1^{neg} NK cells after *in vitro* stimulation with ovarian cell line. Degranulation is a marker of NK cell activation, which represents the process of releasing lytic granules. CD107a is part of lytic granule molecules that exposed on the surface of NK cells after degranulation and normally serve as marker for activation and degranulation. To further quantify the antitumor function of PD-1^{pos} NK cells compared to PD-1^{neg} NK cells from B-CLL patients, NK cell degranulation was evaluated based on the surface expression of CD107a after co-culture with different target cell lines either K562 or 721.221 for 5 hours at 37c, 5% Co2 and E/T ratio 1:5. PD-1^{pos} and PD-1^{neg} NK cells were comparatively analysed for their ability to undergo degranulation using flow cytometry.

Interestingly, in line with lower cytokines production, PD-1^{pos} NK cells expressed significantly lower CD107a compared to PD-1^{neg} NK cells after stimulation with K562 10.8±1.7% vs 19.2±3.6% (p=0.0156) respectively (**Figure 5.17 panel b**). K562 does not express PD-1 ligands, thus the difference in degranulation does not reflect the interaction of PD-1 and its ligands, but rather lower expression of main activating receptors including NKG2D, DNAM-1, NKp46 and NKp30 on PD-1^{pos} NK cells as demonstrated earlier in this chapter.

In addition, after NK cells were stimulated with 721.221 which express PDL1 and PDL2 ligands, PD-1^{pos} NK cells also express significantly lower CD107a on their surface compared to PD-1^{neg} NK cells 9.0±1.0% vs 13.4±1.9% (p=0.0010) respectively (**Figure 5.18 panel b**).

The degranulation of PD-1^{pos} NK cells was slightly further lower after stimulation with 721.221 than in K562 9.0±1.0% vs 10.8±1.7% (**Figure 5.18 panel c**), which can be attributed to the interaction of PD-1 with its ligands expressed on 721.221 target cells. The killing capacity of primary PD-1^{pos} NK cells from B-CLL patients was not investigated as getting enough number of these distinct NK cells populations using sorter was challenging. However, since the level of NK cell degranulation represents their killing capacity, it is reasonable to anticipating that PD-1^{pos} NK cells have lower killing capacity than PD-1^{neg} NK cells.

All in all, these experiments indicate that PD-1^{pos} NK cells from B-CLL patients have impaired degranulation and cytokines production compared to PD-1^{neg} counterparts. This impairment was more pronounced after stimulation with 721.221, indicating that the hyporesponsive of NK cells from B-CLL patients is related at least partly to PD-1 expression. This data implies the possibility to reverse the NK cell functional impairment in B-CLL patients by blocking PD-1-PDL1/2 interaction on NK cells.

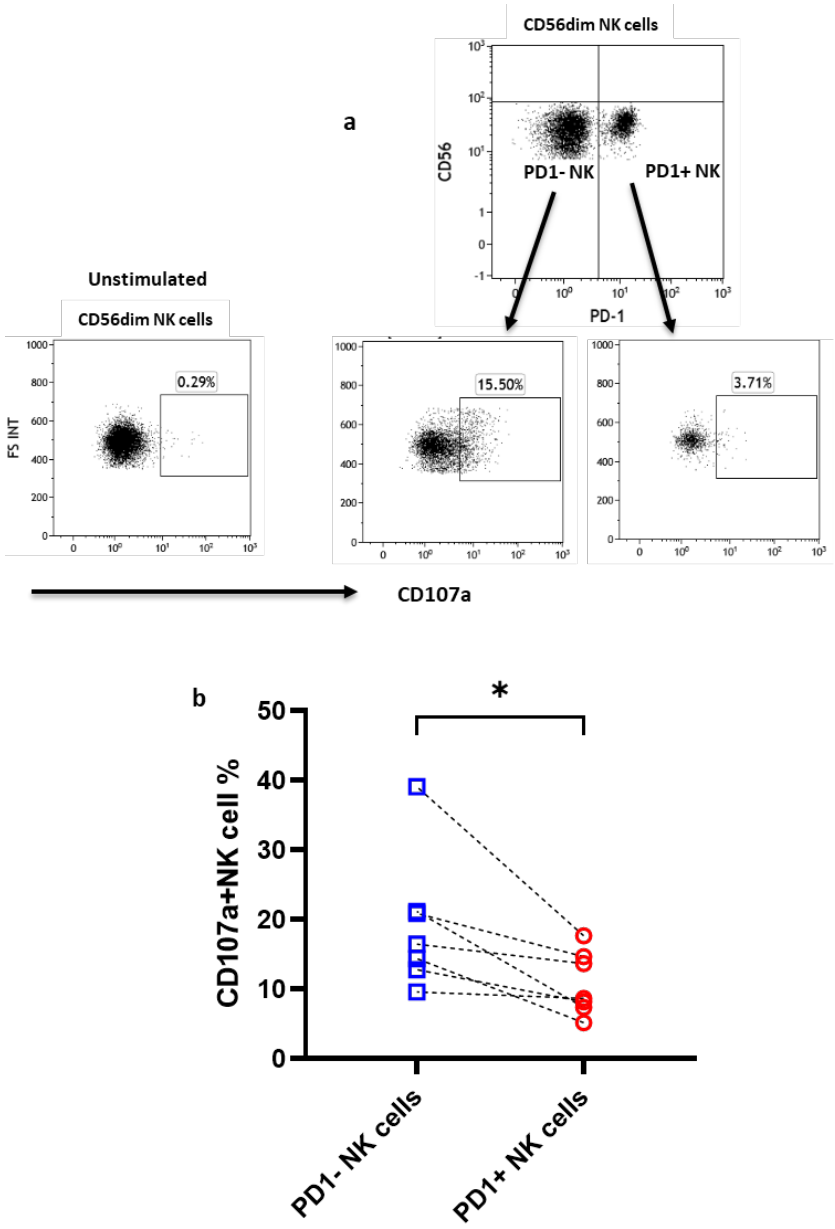

Figure 5.17 CD107a expression of PD-1^{pos} vs PD-1^{neg} NK cells after stimulation with K562 target cells.

(**a**) Top panel is the example of flow dot plot to show the gating strategy for CD56^{dim} PD-1^{neg} and CD56^{dim} PD-1^{pos} NK cells. The bottom panels are examples of flow dot plots to show the CD107a staining for unstimulated NK cells, K562 stimulated PD-1^{pos} and PD-1^{neg} NK cells. NK cells were stimulated 5h at 1:5 E/T ratio, cells were run by flow and analysed by Kalusa. (**b**) Summary of CD107a expression on CD56^{dim} PD-1^{pos} NK cells (red circles) vs CD56^{dim} PD-1^{neg} NK cells (blue squares) after K562 stimulation. Data was shown as the percentage of CD107a expressing NK subsets. Data were analysed by GraphPad Prism using Wilcoxon matched-paired non-parametric test, (*p<0.05).

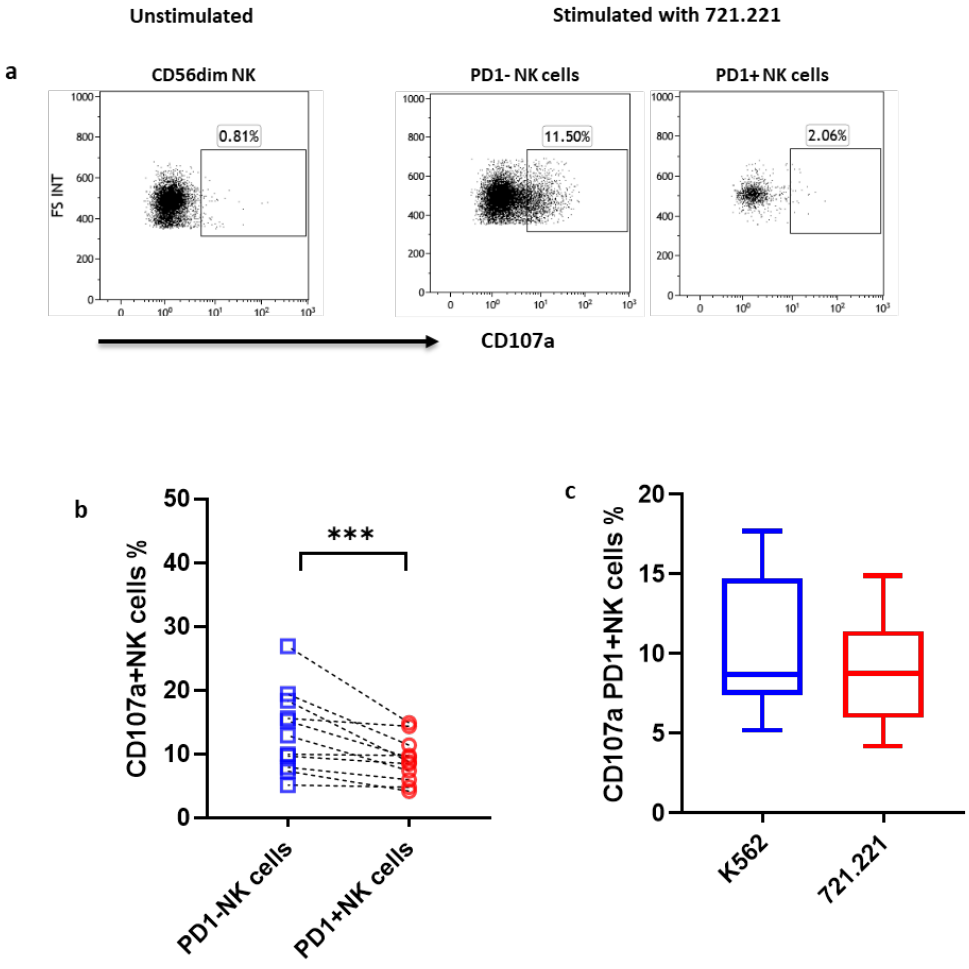

Figure 5.18 CD107a expression of PD-1^{pos} vs PD-1^{neg} NK cells after stimulation with 721.221 target cells.

(**a**) Representative flow dot plots to show CD107a staining for unstimulated NK cells, 721.221 stimulated PD-1^{pos} and PD-1^{neg} NK cells. Enriched NK cells were co-cultured with 721.221 for 5h at 1:5 E/T ratio, cells were run by flow and analysed by Kalusa. (**b**) Summary of CD107a expression on CD56^{dim} PD-1^{pos} NK cells (red circles) vs CD56^{dim} PD-1^{neg} NK cells (blue squares) after 721.221 stimulation. Data was shown as percentage of CD107a expressing NK cell subsets. (**c**) Comparison of the percentage of CD107a expression on PD-1^{pos} NK cell induced by K562 or 721.221. Data were analysed by GraphPad Prism using Wilcoxon matched-paired non-parametric test, (*$p<0.05$).

5.2.5.3 PD-1/PD-1Ls blockade can partially reverse anti-tumor activity of NK cells in B-CLL patients

As we have demonstrated that PD-1^{pos} NK cells from B-CLL patients are functionally impaired and become more dysfunctional upon PD-1/PD1Ls interaction. Although data on NK for PD-1 expression and function have been highly variable compared to PD-1 on T cells, some studies have shown that blocking signal transmission between PD-1 and PD-1 ligands on NK elicits anti-tumor function of NK cells in many tumours including multiple myeloma (Benson et al., 2010) and advanced melanoma (Quatrini et al., 2020). However, the impact of PD-1/PD-1Ls blockade on NK cells of B-CLL has not been evaluated. Therefore, we investigated whether the dysfunctional state of PD-1^{pos} NK cells can be restored by blocking PD-1/PD-1Ls axis, which aims to improve B-CLL immunotherapy.

Same steps were carried out for evaluation of cytokines secreted by PD-1^{pos} vs PD-1^{neg} NK cells using 721.221 cell line which expresses PDL1 and PDL2 ligands (briefly described in 5.2.5.1). In addition, anti PDL1 and anti PDL2 antibodies were added to the culture where appropriate to block the interaction between PD-1 and PDL1 and PDL2 expressed on 721.221 cell line. Main cytokines including IFN-γ and TNF-α produced by PD-1^{pos} NK cells before and after PDL1 and PDL2 blockade were measured and compared. Also, the effect of PDL1/L2 blockade on PD-1neg NK cells was evaluated. Our findings showed that blocking PD-1/PDL1,L2 interactions can significantly induced IFN-γ production particularly by PD-1^{pos} NK cells. There were 3.1±0.4% PD-1^{pos} NK cells that produce IFN-γ after blocking, instead there were only 1.5±0.4% PD-1^{pos} NK cells producing IFN-γ before blocking (p=0.0313) (**Figure 5.19**). Interestingly, the increase in cytokines production does not only induced on PD-1^{pos} NK cells after blocking PDL1/L2, but there was also an increase of IFN-γ observed with PD-1^{neg}

NK cells from 4.4±0.7% before blocking to 7.7±1.3% after PDL1 and PDL2 blockade (p=0.0311). No changes in TNF-α production were observed before and after PDL1 and PDL2 blockade by either PD-1^{pos} NK cells with 1.1±0.4% vs 0.9±0.3% nor PD-1^{neg} NK cells 5.0±1.9% vs 5.0±2.0%.

Moreover, Degranulation level of PD-1^{pos} NK cells was evaluated after blocking of PD-1 ligands PDL1 and PDL2, to investigate whether the disruption of PD1/PDL1,L2 axis would reverse the impaired degranulation of PD-1^{pos} NK cells from B-CLL patients. Adding anti-PD-1 antibody to expansion NK cell culture has been shown to improve degranulation of expanded NK cells against multiple myeloma target cell line (RPMI8226) which express PDL1 and PDL2 ligands. In addition, PD-1 blockade induced more pronounced killing of RPMI8226 target cells mediated by expanded NK cells than without blocking (Guo et al., 2016). Here, 721.221 target cells were first preincubated with anti-PDL1 and anti-PDL2 antibodies for at least 30 minutes before NK cells being added to them for 5h at 37c, 5% Co2. Importantly, PDL1 and PDL2 blockade resulted in significant increase of degranulation (CD107a expression) of PD-1^{pos} NK cells, with 11.6±2.1% positive for CD107a compared to PD-1^{pos} NK cells without PDL1 and PDL2 antibodies 9.9±1.5% (p=0.0269) (**Figure 5.20**).

These data showed that blocking PD-1/PDL1 and PDL2 interactions can partially reverse the anti-tumor function of PD-1^{pos} NK cells from B-CLL patients by significantly increase IFN-γ and degranulation level. Also, blocking PD-1/PD-1 ligands pathway can augment IFN-γ production by PD-1^{neg} NK cells as well. This indicates that blocking PD-1/PDL1 and PDL2 signals could be one of the effective therapeutic approaches to improve NK cell based immunotherapy in B-CLL patients, particularly PBMCs from B-CLL patients express

considerable levels of PDL-1 including monocytes and PD-1^{pos} NK cells themselves as shown in **Figure 5.14.**

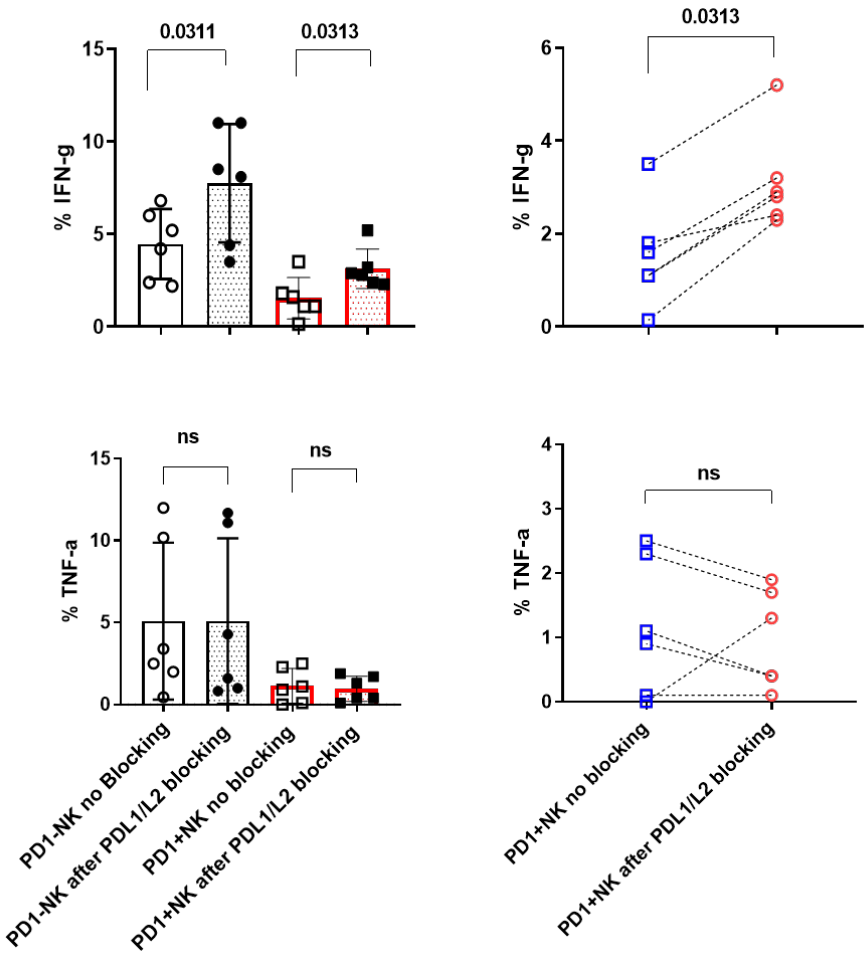

Figure 5.19 The production of IFN-γ and TNF-α by PD-1^{neg} and PD-1^{pos} NK cells after stimulation with 721.221, before and after blocking PD-1/PD-1ligands interactions.

PBMCs with high PD-1NK cells were co-cultured with 721.221 (1:1) with or without anti-PDL1 and antiPDL2 antibodies for overnight. Cells were washed, stained, and analysed by flow cytometry. Left panel: Bar charts to summarise the IFN-γ and TNF-α production by PD-1^{pos} NK cells (red bars) and PD-1^{neg} NK cells (black bars) before and after blocking. Right panel: dot plots to compare IFN-γ and TNF-α production by PD-1^{pos} NK cells before (blue squares) and after blocking (red circles). Each dot represents a single donor. Data were analysed by GraphPad Prism using Wilcoxon matched-paired non-parametric test, (*p<0.05).

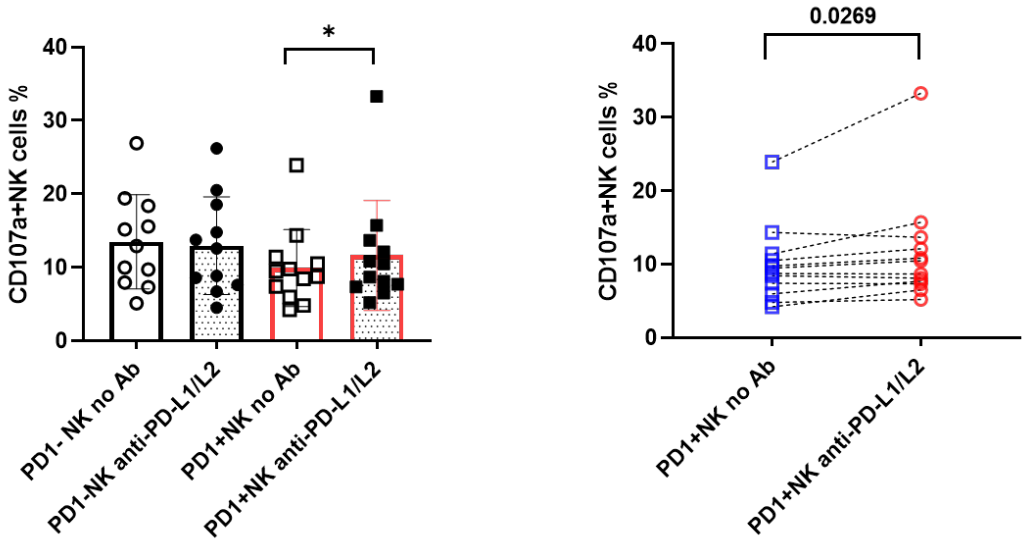

Figure 5.20 CD107a expression by PD-1^{neg} and PD-1^{pos} NK cells after stimulation with 721.221, before and after blocking PD-1/PD1ligands interactions.

Enriched NK cells from PBMCs with high PD-1NK cells were co-cultured with 721.221 (1:5) with or without anti-PDL1 and antiPDL2 antibodies for 5h. Cells were analysed by flow cytometry. Left panel: Summary of CD107a expression after stimulation with 721.221 by PD-1^{pos} NK cells (red bars) and PD-1^{neg} NK cells (black bars) before and after blocking. Right panel: Dot plot to compare the CD107a expression by PD-1^{pos} NK cells before (blue squares) and after blocking (red circles). Each dot represents a single donor. Data were analysed by GraphPad Prism using Wilcoxon matched-paired non-parametric test, (*p<0.05).

5.2.6 Validation of PD-1 function on NK cells using PD-1^{positive} NK cell lines

5.2.6.1 Phenotype of PD-1^{pos} NK-92 and PD-1^{neg} NKL cell lines

To complement the phenotype and functionality study of primary PD-1positive NK cells from B-CLL patients, and to better understand the role of PD-1 expression on NK cells, we transduced two NK cell lines NK-92 and NKL with PD-1 lentiviral construct containing PD-1 gene. The control lentivirus transduced NK-92 and NKL serve as wild type cell lines. Stable PD-1 expression > 98% was observed on both types of NK cell lines (**Figure 5.21**). NK-92 is NK cell line derived from NK cells from 50 years old patients with non-Hodgkin's lymphoma and is IL-2 dependent. Like primary NK cells, NNK-92 cells demonstrated strong cytotoxicity against cancer cells and viral infected cells, as they lack the major inhibitory receptors expressed on human primary NK cells whilst retain the majority of activating receptors (Gong et al., 1994). NKL is another NK cell line established from patient with large granular lymphocyte leukaemia (LGL) and like NK-92, NKL cells require IL-2 for survival. Similar to human primary NK cells, NKL cells can mediate natural killing and ADCC, and their phenotype resembles that in normal human NK cells (Robertson et al., 1996).

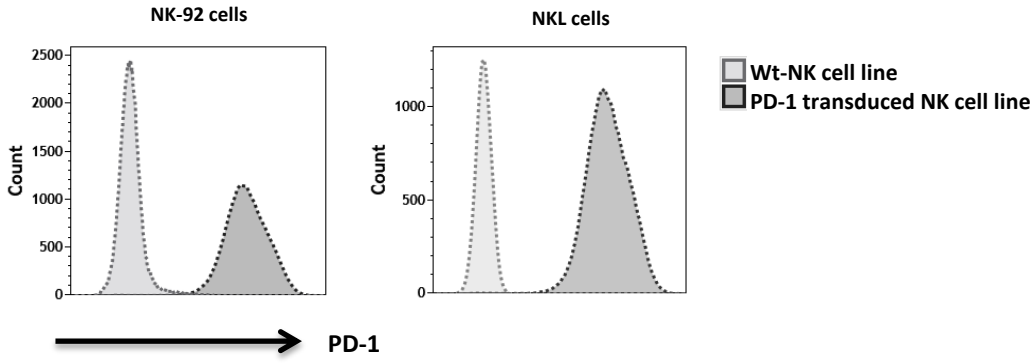

Figure 5.21 Histogram plots from flow cytometry illustrate PD-1 expression on PD-1 transduced NK cell lines (Dark grey) compared to wild type control NK cell lines (light grey).

At first, the phenotype including maturation markers, activating receptors and activation markers were studied in wild type NK cell line (wt-NK cells) as a control and compared to PD-1 transduced NK cell lines (PD-NK cells), particularly before and after overnight activation by co-culturing them with 721.221. Both wt-NK92 and PD-1-NK92 cell lines express high levels of CD56, NKG2D and CD28, but they express detectable levels of CD16, DNAM-1, NKp46 and maturation marker CD57. Interestingly, PD-1 expression on transduced NK-92 cells (PD-1^{pos} NK-92) significantly reduced the expression of NKG2D activating receptor compared to wt-NK-92 with 9.5±1.3% and 31.4±1.4% (p=0.0286) respectively. On the other hand, expression of activating molecule CD28 was significantly higher in PD-1NK92 cells than wt-NK92 98.3±0.4% and 24.2±0.7% (p=0.0286) (**Panel a Figure 5.22**). After stimulation NKG2D was substantially increased on wt-NK-92 with 85.4±3.0% vs 31.4±1.4% post and before stimulation respectively (p=0.0286). Whilst on PD-1NK-92, even NKG2D did not significantly increase after stimulation 29.8±1.7% compared to 9.5±1.3% before stimulation (p>0.05). NKG2D expression level is still very low compared with wt-NK-92.

Similarly, wt-NKL and PD-1 transduced NKL cells (PD-1^{pos} NKL) were screened using flow cytometry for expression of activating receptors, maturation, and activation markers before and after stimulation with 721.221 tumor cells. From the flow cytometric analysis, the data showed in **Figure 5.22 panel b**, that both wt-NKL and PD-1NKL cells are positive for CD56, CD57 and express a broad range of activating receptors including CD16, DNAM-1 and NKG2D. In case of NKL cells, PD-1 expression did not significantly alter the expression of activating receptors, including CD16, DNAM-1 and NKG2D in comparison to wt-NKL cells with 5.6±0.5%, 66.6±0.3% and 84.0±8.8% vs 7.1±0.8%, 42.8±2.1% and 78.2±0.1% ($p>0.05$) respectively. In addition, after 721.221 stimulation both types of NKL cells had the similar increase in the activating receptors CD16, DNAM-1, NKG2D, and CD69, implying that PD-1 expression on NKL cells did not influence the expression of activating receptors on the surface of NKL cells. However, it might influence the intracellular signalling of NKL cells rather than their phenotype. Overall, NKL cells appeared to be more mature (CD57bright) phenotype and express higher activating receptors compared to NK-92. These data were collected from 5 independent experiments and were in agreement with previous studies (Bouteiller et al., 2002; Drexler & Matsuo, 2000).

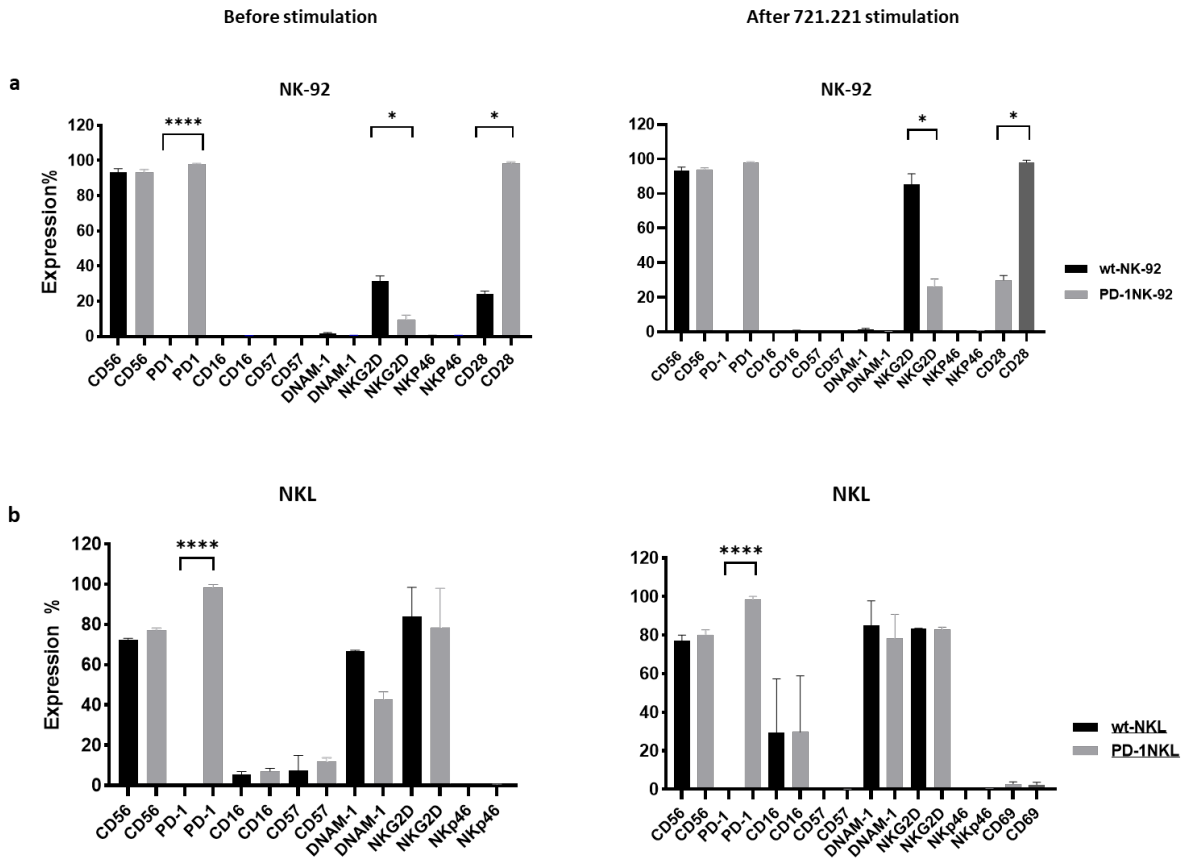

Figure 5.22 Differential expression of activating receptors on PD-1^{pos} NK cell line vs wt-NK cell line before and after stimulation.

About 1×10^6 of PD-1transduced NK cell line (grey columns) and wt-NK cells line (black columns) from two types of NK cells, NK-92 (**a**) and NKL (**b**) were collected from culture washed and stained for expression of PD-1, activating receptors and maturation marker CD57, then analysed by flow cytometry. The top graphs (**a**) are comparison of activating receptors expression level between PD-1^{pos} NK-92 vs wt-NK-92 cell line before (left top panel) and after 721.221 stimulation (right top panel). The bottom graphs (**b**) are comparison of activating receptors expression level on PD-1^{pos} NKL vs wt-NKL cells before (bottom left panel) and after 721.221 stimulation (bottom right panel). These data are from 5 independent experiments. Data were acquired by flow cytometry and analysed by Kalusa, and statistical differences were determined by Mann Whitney non-parametric test, (*$p<0.05$).

5.2.6.2 Functionality of PD-1positive NK cell line

NK-92 cells can kill target cells using lytic granules and through lytic granules independent pathway by expression of FasL, TNF-α and TRIAL. NK-92 cells have a high potential cytotoxic capacity against K562 and 721.221 target cells (Chen et al., 2007). Likewise, the lytic function of NKL cells can be mediated through different pathways, particularly NKL cells have the ability of killing antibody-coated target cells through ADCC. However, NKL cells' lytic capacity can vary, with high and low selective lysis of susceptible K562 and 721.221 target cells (Bouteiller et al., 2002). Here, to further investigate the functionality of PD-1 expression on NK cells, we investigated the cytokines, degranulation and killing capacity of PD-1^{pos} NK cell line compared to wt-NK cell line against the same target cells (K562 and 721.221) used in the study of primary PD-1^{pos} NK cells. In addition, the functionality has also been explored before and after blocking of PD-1/PD1Ls interaction using these two models of NK cell lines NK-92 and NKL cells.

5.2.6.2.1 Cytokines production

To compare the cytokines production between wt-NK cell line and PD-1^{pos} NK cell lines, wt-NK-92, PD-1NK-92, wt-NKL and PD-1NKL cells were separately stimulated overnight at 37c, 5% CO2 using K562 or 721.221 tumor cells at E:T ratio 1:1. Then the cytokines production was measured by intra-cellular staining and flow cytometry before and after blocking PD-1/PDL1-2 interactions. The main cytokines including IFN-γ, TNF-α and IL-10 were measured from 5 independent experiments. Notably, both types of NK cell lines (NK-92 and NKL) did not produce considerable amount of IFN-γ, TNF-α and IL-10, 1.0% of cytokines positive NK cells was the highest percentage of cytokines production. Moreover, PD-1/PDL1-2 blockade did not enhance the cytokines production from PD-1NK-92 and PD-1NKL (**Figures 5.23 and**

5.24) This indicates that the cytokine production is not the dominant function of NK cell lines and PD-1 expression does not alter this function either.

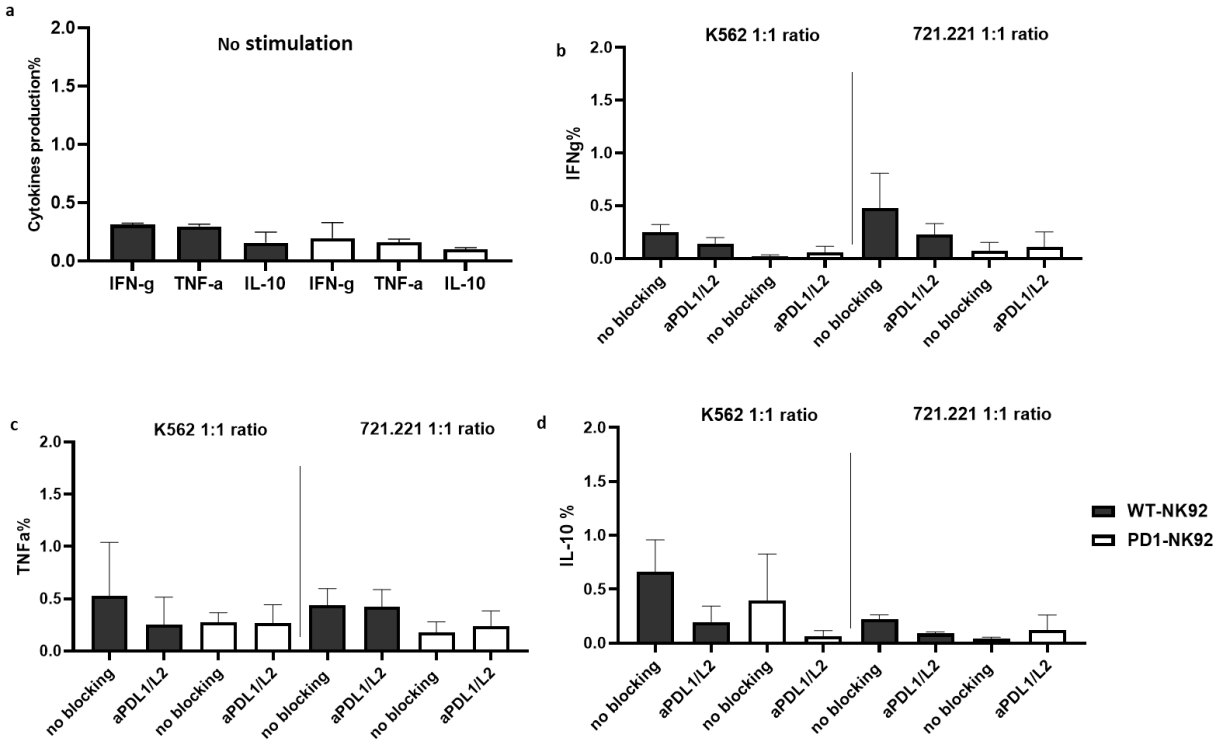

Figure 5.23 Cytokines secretion by PD-1^{pos} NK-92 vs wt-NK-92 cell lines after stimulation before and after PDL1,2 blockade

2×10^6 PD-1^{pos} NK-92 and wt-NK-92 cells were co-cultured with either K562 or 721.221 target cells (E:T ratio 1:1) overnight and cytokines were measured by flow cytometry. (**a**) Baseline of cytokines production of PD-1^{pos} (white columns) and wt-NK-92 (black columns) cells. (**b**, **c ,d**) are IFN-γ, TNF-α and IL-10 production respectively, after stimulation with either K562 (left parts of the graphs) or 721.221 (right parts of the graphs) and before and after PDL1, PDL2 blockade. These data were summary of 5 independent experiments which presented with mean and standard error bars, statistics were determined by Mann Whitney test by GraphPad.

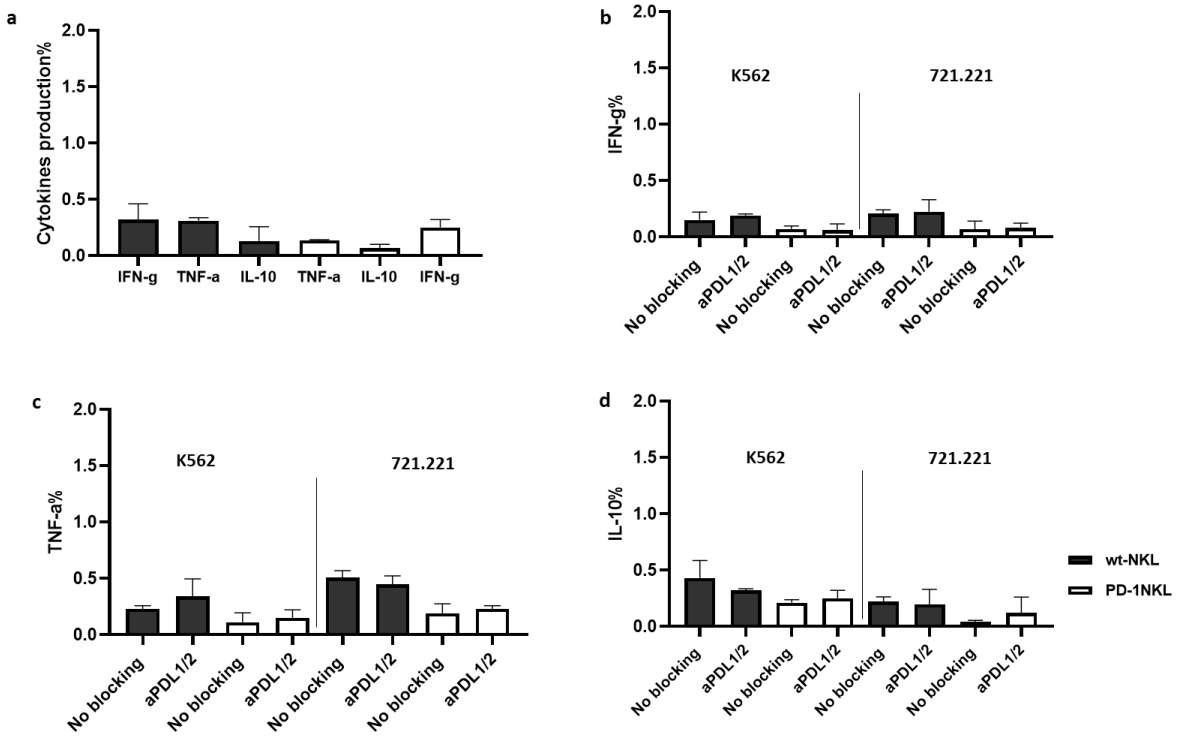

Figure 5.24 Cytokines secretion by PD-1^{pos} NKL vs wt-NKL cells after stimulation, before and after PDL1,2 blockade.

Similar to what we have done with NK-92 cells, cytokines production was measured by flow cytometry after 2×10^6 PD-1^{pos} NKL and wt-NKL cells were co-cultured overnight with either K562 or 721.221 target cells (E:T ratio 1:1). (**a**) Cytokines production of PD-1^{bright} (white columns) and wt-NKL (black columns) cells before stimulation. (**b**, **c, d**) are IFN-γ, TNF-α and IL-10 production respectively, after stimulation with either K562 (left bars of the graphs) or 721.221 (right bars of the graphs) and before and after PDL1, PDL2 blockade. These data were summary of 3 independent experiments which presented with mean and error bars, statistics were determined by Mann Whitney test by GraphPad

5.2.6.2.2 Degranulation capacity of PD-1^{bright} NK cell line

As we showed earlier in this chapter that PD-1 expression inhibited the degranulation of primary NK cells from B-CLL patients, and this impairment can be partially restored by blocking PD-1/PD-1Ls interactions. To validate this, tow PD-1 transduced NK cell lines, PD-1^{pos} NK-92 and PD-1^{pos} NKL were used and compared to wt-NK-92 and wt-NKL respectively. Like we did with primary NK cells, NK cell line degranulation was evaluated based on the expression of CD107a after co-culture with different target cell lines either K562 or 721.221 for 5 hours at 37c, 5% Co2 and E/T ratio 1:5. PD-1^{pos} and wt-NK cells lines were comparatively analysed for their ability to undergo degranulation using flow cytometry. These experiments were performed in 5 independent days.

Interestingly, in line with observations seen in primary PD-1^{pos} NK cells, PD-1^{pos} NK-92 expressed significantly lower CD107a compared to wt-NK-92 cells after stimulation with K562 5.5±0.3% vs 10.2±2.2% (p=0.0317) respectively (**Figure 5.25, panel a**). As there is no PD-1 ligands expressed on K562 cells, the difference in degranulation does not reflect the interaction of PD-1 and its ligands but is rather due to the lower expression of main activating receptors particularly NKG2D on PD-1^{pos} NK-92 cells as shown in **Figure 5.22 panel a**. Moreover, after stimulation with 721.221 which express PDL1 and PDL2 ligands, PD-1^{pos} NK-92 cells also express significantly lower CD107a compared to wt-NK-92 cells with 1.6±0.2% vs 8.7±1.5% (p=0.0079) respectively (**Figure 5.25 panel b**). The degranulation of PD-1^{bright} NK-92 cells was significantly further lower after stimulation with 721.221 than in K562 1.6±0.2% vs 5.5±0.3% (p=0.0079) (**Figure 5.25 panel c**), which can be attributed mainly to the interaction of PD-1 with its ligands expressed on 721.221 target cells.

Similarly, using the second model of PD-1^{pos} NK cell line (PD-1^{pos} NKL), the data showed that the degranulation level of PD-1^{pos} NKL cells was significantly lower than wt-NKL cells after stimulation with K562 with 8.0±1.7% vs 12.0±1.0% (p=0.0476) (**Figure 5.26 panel a**). However, using 721.221 as a stimulator, PD-1^{pos} NKL cells also express lower CD107a compared to wt-NKL cells but not statistically significant 8.7±1.7% vs 14.1±2.4% (p=0.0873). The possible explanation of this is that the difference of activating receptors, including NKG2D and DNAM-1 is minimal between PD-1^{pos} NKL and wt-NKL cells (**Figure 5.22 panel b)**.

Blocking PD-1/PDL1/L2 interactions using anti-PDL-1 and PDL-2 antibodies can partially increase the degranulation level of PD-1^{pos} NK-92 when using PDL1/2 expressing 721.221 cells but not K562 cells. The degranulation level after PD-1/PD-1Ls blockade in PD-1^{pos} NK-92 was 3.3±0.3% vs 1.6±0.2% before blockade (p=0.0650) (**Figure 5.25 panel b**). Similar observation was seen with PD-1^{pos} NKL cells, blocking PD-1/PD-1Ls interactions did slightly increase the degranulation of PD-1^{bright} NKL cells to 12.1±2.7% compared to 8.7±1.7% before blocking. Interestingly, this observation was only seen when using 721.221 but not K562 cells (**Figure 5.26 right graph**). This indicates that PDL1 and/or PDL2 expression on the target cells is essential in order to be beneficial from PD-1 blockade and reversing the functionality of PD-1^{pos} NK cells.

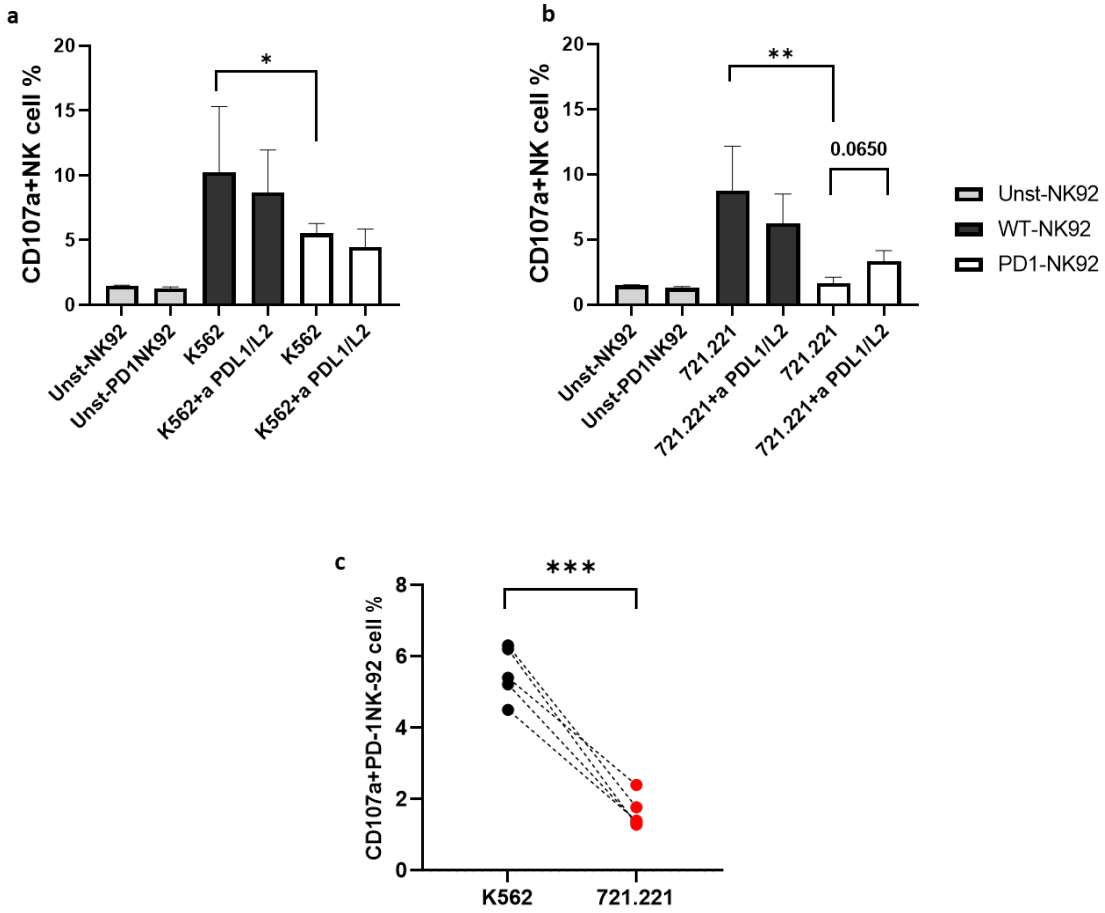

Figure 5.25 Degranulation capacity of PD-1^{pos} NK-92 vs wt-NK-92 after stimulation and before, after PDL1 and PDL2 blockade.

PD-1^{pos} NK-92 and wt-NK-92 cells were co-cultured with either K562 or 721.221 target cells at E:T ratio (1:5) with or without anti-PDL1 and antiPDL2 antibodies for 5h. Degranulation was measured by CD107a expression using flow cytometry. Summary of CD107a expression of PD-1^{pos} (white bars) and wt-NK-92 (black bars), after stimulation with K562 (**a**) and 721.221 (**b**), before and after PDL1, PDL2 blockade. (**c**) Dot plot to compare the CD107a expression in PD-1^{pos} NK-92 after stimulation with K562 (black dots) and 721.221 (red dots) target cells. 721.221 cells that express PDL1 and PDL2 markedly inhibited the degranulation of PD-1^{pos} NK cells through PD-1/PD1 ligands interactions. Each dot represents a single independent experiment (n=5). Data were analysed using Mann Whitney, and Wilcoxon matched-paired non-parametric test, (*p<0.05, **p<0.01, ***p<0.001)

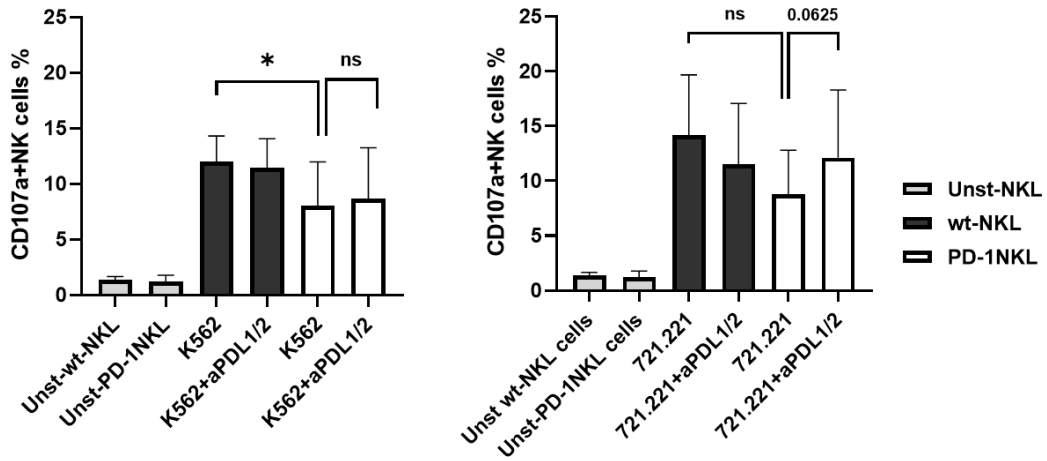

Figure 5.26 Degranulation capacity of PD-1^{pos} NKL vs wt-NKL after stimulation and the effect of PDL1 and PDL2 blockade.

PD-1^{pos} NKL and wt-NKL cells were co-cultured with either K562 or 721.221 target cells at E:T ratio (1:5) with or without anti-PDL1 and antiPDL2 antibodies for 5h. Summary of 5 independent experiments showing CD107a expression of PD-1^{pos} NKL (white bars) and wt-NKL (black bars), after stimulation with K562 (left graph) and 721.221 (right graph), before and after PDL1, PDL2 blockade. Data were analysed using Mann Whitney, and Wilcoxon matched-paired non-parametric test, (*$p<0.05$).

5.2.6.2.3 Killing capacity of PD-1^{pos} NK cell line

NK cells can recognise and eradicate tumor cells using different strategies of killing. The better understanding of molecular mechanisms implicated in tumor recognition and elimination has led to identification of checkpoint signalling pathways involved in limiting the antitumor immune response. PD-1 is one of the most critical checkpoints that suppress antitumor immune response particularly on T cells (Keir et al., 2008). PD-1 function on NK cells is less investigated and has not been studied in B-CLL patients. We showed using primary PD-1^{pos} NK cells from B-CLL that PD-1 inhibits the cytokines production and degranulation of NK cells after stimulation; however, we could not perform the cellular cytotoxicity of PD-1^{pos} NK cells from B-CLL patients due to technical limitations including getting low number of PD-1^{pos} NK cells from sorter and low viability of these cells. To this end, we used NK cell lines described earlier to assess the killing capacity of PD-1^{pos} NK cells vs wt-NK cells and to investigate the potential beneficial of PD-1/PD-1Ls blockade

PD-1^{pos}, wt-NK-92 and PD-1^{pos}, wt-NKL cells were co-cultured with the same target cells used for assessing degranulation and cytokines production, K562 or 721.221 for overnight 37c, 5% Co2 at different E:T 2.5:1, 5:1 and 10:1 with and without PD-1/PD-1Ls blocking. The target cells were labelled with fluorescence dye to allow absolute counting of viable cells by flow cytometry after co-culture. At first, the cytotoxicity of NK cell lines increases in line with the increase E:T ratios. Interestingly, PD-1^{pos} NK-92 cells displayed a significant reduction of killing capacity against both K562 and PDL1/2 expressing 721.221 cells compared to wt-NK-92 cells at all three E:T ratios (**Figure 5.27**). However, in case of 721.221 target cells, the most pronounced difference between PD-1^{pos} NK-92 and wtNK-92 cells was observed at 5:1 E:T ratio with 9.3±2.2% vs 33.3±4.8% for wt-NK-92 (p=0.0079) (**Figure 5.27 panel b**).

In addition, same experiment was performed using PD-1^{pos} NKL cells as another model of PD-1^{pos} NK cell line. Data showed a reduction in cytotoxicity by PD-1^{pos} NKL against K562 and 721.221 compared to wt-NKL cells, but unlike PD-1^{pos} NK-92 this reduction was not statistically significant (**Figure 5.28 panel a and b**), which is possibly due to the retainment of activating receptors expression on PD-1^{pos} NKL cells (**Figure 5.22 panel b**).

Blocking PD-1/PD-1Ls interactions using anti PDL1 and PDL2 antibodies partially improved the cytotoxicity of PD-1^{pos} NK-92 cells 721.221 target cells but not K562 cells. The cytotoxicity of PD-1^{pos} NK-92 increased from 9.3±2.2% before blocking to 17.7±3.1% after blocking at E:T ratio 5:1 ($p=0.0625$) (**Figure 5.27 panel b**). In contrast, no significant changes in cytotoxicity were observed between PD-1^{pos} NKL before blocking and after blocking with 721.221 target cells (**Figure 5.28 panel b**).

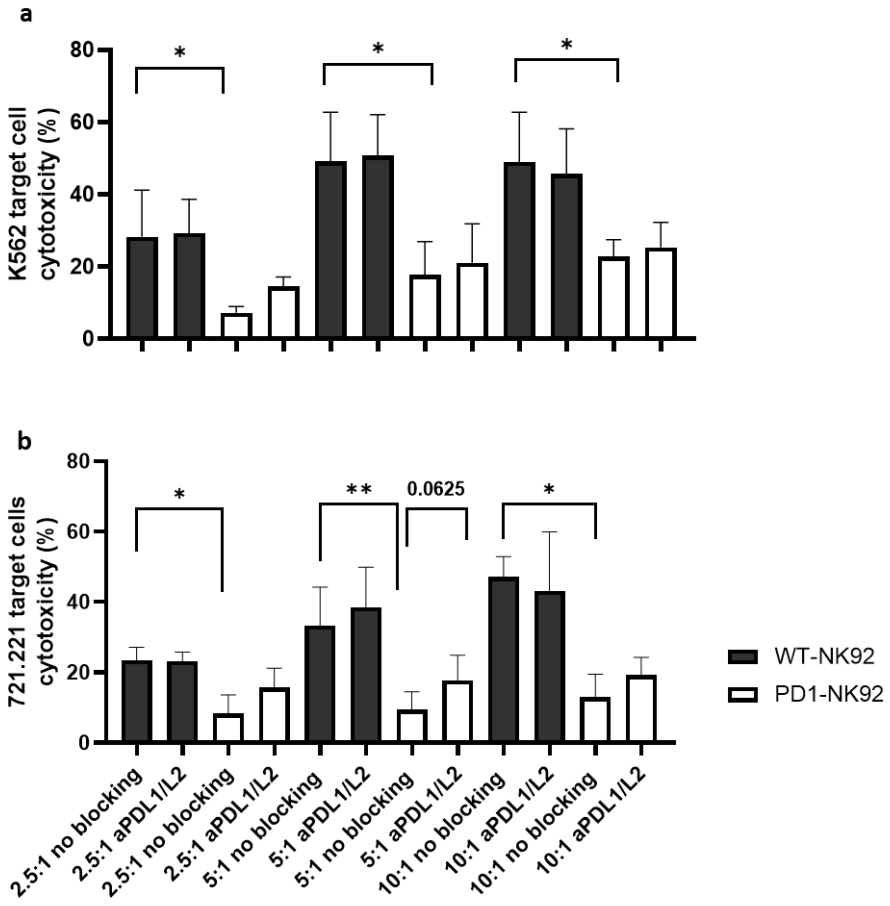

Figure 5.27 The comparisons of cytotoxicity capacity of PD-1^{pos} NK-92 vs wt-NK-92 and the effect of PDL1 and PDL2 blockade on both PD-1pos and wt-NK92.

Flow cytometry based cytotoxicity assays were done by co-incubation of PD-1^{pos} NK-92 and wt-NK-92 with either K562 (**a**) or 721.221 (**b**) target cells in an overnight at three different E:T (NK:K562 or 721.221) ratios 2.5:1, 5:1 and 10:1. The bar graphs summarise 5 independent killing assays of PD-1^{pos} NK-92 (white bars) and wt-NK-92 (black bars) against K562 target cells (**a**) and 721.221 target cells (**b**) with and without PDL1 and PDL2 blockade. Data were analysed using repeated measures ANOVA test (*$p<0.05$, **$p<0.01$).

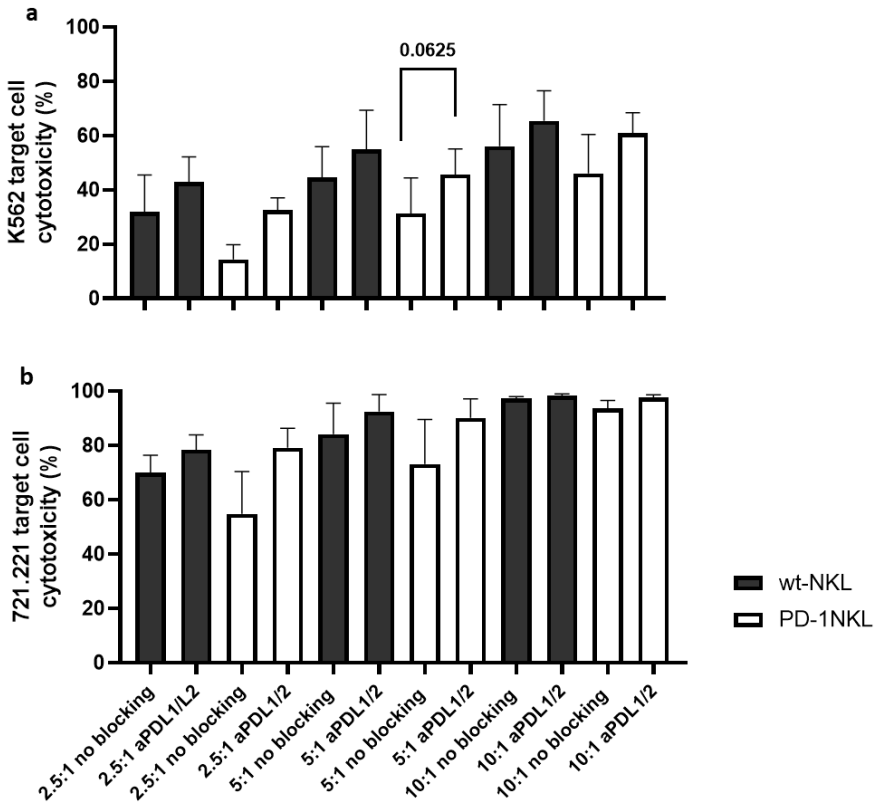

Figure 5.28 Cytotoxicity capacity of PD-1^{pos} NKL vs wt-NKL and the effect of PDL1 and PDL2 blockade.

The cytotoxicity capacity of PD-1^{pos} NK cells using another model of PD-1^{pos} NKL cell line. PD-1^{pos} NKL and wt-NKL cells were co-incubation with either K562 (**a**) or 721.221 (**b**) target cells in an overnight at three different E:T (NK:K562 or 721.221) ratios 2.5:1, 5:1 and 10:1. The bar graphs summarise 5 independent killing assays of PD-1^{pos} NKL (white bars) and wt-NKL (black bars) against K562 target cells (**a**) and 721.221 target cells (**b**) with and without PDL1 and PDL2 blockade. Data were analysed using repeated measures ANOVA test (*$p<0.05$).

5.2.6.2.4 Blocking PD-1/PD1Ls interactions did not increase NKG2D activating receptor on PD-1^{pos} NK-92

As NKG2D expression was significantly reduced on PD-1^{pos} NK-92 compared to wt-NK-92 cells with 9.5±1.3% vs 31.4±1.4% (p=0.0286) respectively. Furthermore. we demonstrated earlier that NKG2D expression on wt-NK-92 after overnight stimulation with 721.221 significantly increased compared to its expression before stimulation 85.4±3.0% vs 31.4±1.4% respectively. However, the expression of NKG2D on PD-1^{pos}NK-92 after overnight stimulation with 721.221 did not significantly increase 29.8±1.7% compared to 9.5±1.3% after and before stimulation (p>0.05) (**Figure 5.22**). Thus, we want to check whether blocking PD-1/PDL1-2 interactions will restore the reduction of this main activating receptor on NK cells. Our data showed that blocking PD-1/PDL1-2 interactions using anti PDL1 and PDL2 antibodies induced a minimal increase of NKG2D expression on PD-1^{pos} NK-92 cells with 26.3±2.2% vs 29.8±1.7% before stimulation. Wt-NKL and PD-1^{pos} NKL cells express higher levels of DNAM-1, NKG2D and CD16 receptors compared to NK-92 cell types, and these expressions became higher after stimulation (**Figure 5.29**). Meanwhile, blocking of PD-1/PDL1-2 interactions did not influence the expression of activating receptors either on PD-1^{pos} NKL or wt-NKL cells.

These data indicate that blocking PD-1 signalling on PD-1NK-92 and PD-1-NKL cells did not improve the expression of activating receptors.

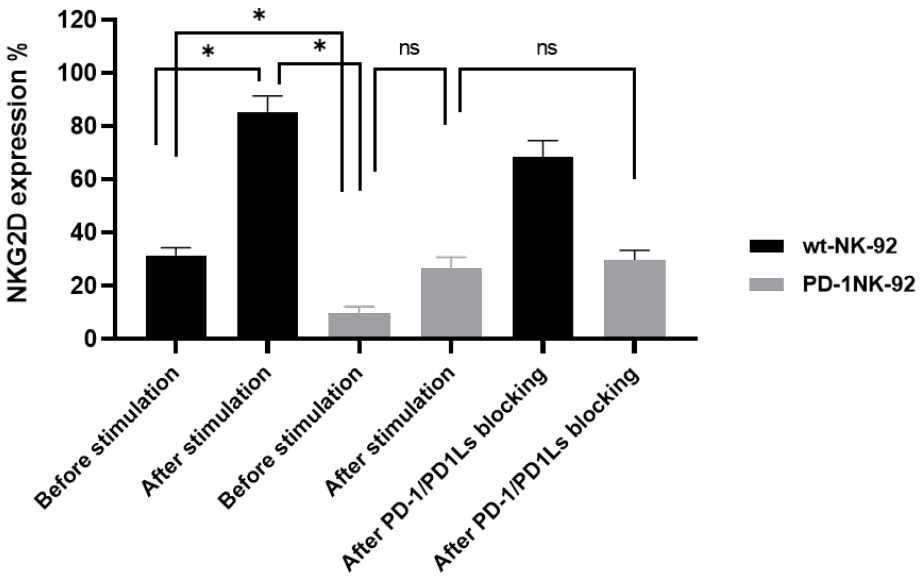

Figure 5.29 NKG2D expression pattern on PD-1^{pos} NK-92 before, after stimulation and with or without PD-1 blockade.

The expression level of activating receptor NKG2D on PD-1^{pos} NK-92 (grey bars), and wt-NK-92 cells (black bars) was measured before and after overnight stimulation (16 h) with 721.221 target cells. The effect of blocking PD-1 signalling on expression of NKG2D on both NK cells were investigated at the same time. These data collected from 5 independent assays and presented as Mean±SEM. Data were analysed using Mann Whitney, and Wilcoxon matched-paired non-parametric test, (*$p<0.05$).

Collectively, similar data was observed on both primary NK cells and NK cell lines in terms of PD-1^{pos} NK cells, which demonstrated that PD-1^{pos} NK cells have significantly strongly reduced capacity of cytokines production, degranulation, and cytotoxicity against tumor cell line compared to PD-1^{neg}/wt-NK cells. The functional impairment of PD-1^{pos} NK cells was more pronounced against PDL1 and PDL2 expressing tumor cell line 721.221, due to the expression of inhibitory checkpoint PD-1 on their surface and lower levels of activating receptors. Blocking pd-1 signalling did not significantly improve the activating receptors expression on PD-1^{pos} NK cells. But blocking PD-1/PD1Ls interactions can partially restore the anti-tumor activity of PD-1^{pos} NK cells including degranulation and killing capacity against 721.221.

5.3 Discussion

We have shown earlier (in chapter 3) that the expression of a number of immune checkpoints including PD-1 were upregulated on NK cells from B-CLL patients. This chapter deeply investigated the phenotype and functional capacity of PD-1^{pos} NK cells compared to PD-1^{neg} counterparts, particularly cytokines production and degranulation level. In addition, the effect of blocking of PD-1/PDL1 and PDL2 interaction on PD-1^{pos} NK cells of B-CLL patients was also studied. First, phenotypic comparison was carried out using flow cytometry between PD-1^{pos} and PD-1^{neg} NK cells, which focused on the expression of activating receptors including NKG2D, DNAM-1, NKp30 and NKp46, and differentiation markers NKG2A and CD57. The analysis showed that PD-1 expression can be mostly found on $CD56^{dim}$ NK cells, and these $CD56^{dim}$ PD-1^{pos} NK cells express higher level of maturation marker CD57 compared to $CD56^{dim}$ PD-1^{neg} NK cells. However, $CD56^{dim}$ PD-1^{pos} NK cells express significantly lower activating receptors, which could be one of the mechanisms that PD-1 utilizes to inhibit NK cell function. Moreover, co-expression of PD-1 with other immune checkpoints and the clustering behaviour of PD-1^{pos} NK cells compared to PD-1^{neg} NK cells were investigated using CyTOF technique. The data demonstrated that the expression of checkpoint receptors, including CD39 and TIGIT, and adhesion molecule CD11c were up-regulated on PD-1^{pos} NK compared with PD-1^{neg} NK cells.

The anti-tumor functional capacity of PD-1^{pos} NK cells was assessed after stimulation with two different cell lines K562 and 721.221. PD-1^{pos} NK cells produced significantly lower levels of cytokines, particularly IFN-γ and TNF-α and they have substantially impaired degranulation capacity compared to PD-1^{neg} counterparts. This impairment was slightly more pronounced after stimulation with 721.221 cells compared with K562, due to the effect of PD-1/PD-1Ls

interactions, which indicates that the dysfunctional of NK cells is correlated with PD-1 expression. Blocking PD-1/ PD-1Ls interaction by PDL1 and PDL2 antibodies led to the partial reversion of anti-tumour activity by PD-1^{pos} NK cells, implying that there might be more checkpoint molecules still involved in the functional suppression of PD-1^{pos} NK cells such as CD39 and TIGIT, which might be worth to be blocked as well in order to unleash PD-1^{pos} NK cells.

5.3.1 PD-1^{pos} NK cells are highly differentiated NK cells and express reduced levels activating receptors

NK cell subsets differ in their expression of surface receptors, which generally correspond to their distinct stages of maturation, differentiation and function (Freud et al., 2006). Despite there were some controversial of PD-1 expression on NK cell subsets, PD-1 expression on NK cells from either a group of healthy controls or cancer patients such as Kaposi carcinoma, advanced melanoma and multiple myeloma were always found to be restricted to a fraction of mature NK subsets CD56^{dim} NK cells (Beldi-Ferchiou et al., 2016; Coaña et al., 2020). PD-1^{pos} NK cells acquired a homogenous phenotype of CD56^{dim}KIR^{+}NKG2A^{neg}CD57^{+}NCR^{dim} when compared to PD-1^{neg} NK cells from the same donor. Similarly, our findings showed that PD-1 is expressed and upregulated on NK cells from B-CLL patients compared with HCs, which was confirmed using few platforms including conventional flow cytometry, CyTOF and scRNA-seq. There is a group of B-CLL patients who has reasonably high PD-1^{pos} NK population (higher than 5%), which are useful cohort for deep phenotyping and functional study. In addition, PD-1 expression was confined on CD56^{dim} NK cells, more pronounced on CD56^{dim} CD16^{+} cytotoxic NK subsets and was not observed on CD56^{bright} NK cells. Therefore, to avoid data misleading and misinterpretation, all downstream analysis of PD-1^{pos} vs PD-1^{ned}

NK cells were gated on $CD56^{dim}$ NK subsets. The phenotypic data from our study has also showed that PD-1^{pos} NK cells bear a highly differentiated status, with stronger expression of CD57 and lower expression of NKG2A compared with PD-1^{neg} counterparts (Figure 5.5).

The balance between the expression of activating and inhibitory receptors on NK cells is crucial for initiating NK cell activation and in regulating NK cytotoxicity (Vivier et al., 2011). Activating receptors include NKG2D, DNAM-1 and NCRs such as NKp30, NKp46 and NKp44, which have important role in mediating NK cell killing. Activating receptors trigger granule-depending NK killing through releasing perforin and granzymes after forming an immune synapse with target cells (Giuliani et al., 2017). Interestingly, the expression of activating receptors on the global NK cells from B-CLL patients has been reported to be significantly lower compared to HC, including NKG2D, DNAM-1 and NCRs (Parry., et al 2016). Importantly, the downregulation of most of these receptors IS not associated with HCMV infection, indicating a direct effect of B-CLL tumor cells on the expression of activating receptors (Hofland et al., 2019). One of the mechanisms utilized by malignant B-CLL cells to reduce or block activating receptors on NK cells is secreting high amounts of soluble NK activating ligands, which lead to the impairment of NK killing capacity (Reiners et al., 2013). However, although the expression of activating receptors on NK cells are low, PD-1^{pos} NK cells showed substantial further downregulation of activating receptors compared to PD-1^{neg} counterparts including NKG2D, DNAM-1, NKp46 and NKp30 (Parry., et al 2016). 10% of B-CLL patients with high PD-1 NK cells participated in this analysis were CMV seronegative, so the PD-1 upregulation on NK cells from B-CLL patients is not restricted to CMV infection and could be influenced by the tumor microenvironment. Based on all the data, we could reasonably hypothesize that PD-1 expression on NK cells contributes to the downregulation of activating receptors on NK cells as an inhibitory mechanism of NK cell

activity in B-CLL patients. This is potentially due to the tumor microenvironment created by the B-CLL tumor cells.

5.3.2 High dimensional analysis of PD-1^{pos} NK cells

Next, we went to deep phenotype and identify the markers that are co-expressed with PD-1 using high-dimensional flow cytometry technique CyTOF (also called Cytometry by time of flight). CyTOF is a technology that can be used to quantify up to 50 parameters for each cell. It uses different ions to label the cells to avoid spectral overlap issue, which is the limiting factor in conventional flow cytometry. The advantage of CyTOF is the ability to allow the understanding of heterogenicity of cells. The CyTOF has been used to study NK population in disease and healthy settings (Chretien., et al 2021; Mahapatra., et al 2017). In this study, CyTOF has been used to try to understand the clustering characterisation of PD-1^{pos} NK cells. Due to the cost and limitation of the time, we managed to run samples through CyTOF from three B-CLL patients. In all of these three B-CLL PBMCs samples, there are more than 10% NK population with high PD-1 expression. The will allow us to collect decent PD-1^{pos} and PD-1neg NK cells for downstream analysis. The high dimensional data was initially analysed using t-distributed Stochastic Neighbor Embedding (tSNE) tool and resulted in four clusters of closely related cells CD56^{pos} NK cells, CD19^{pos} B cells, CD3^{pos} T cells and CD14^{pos} monocytes. The identified NK population was further clustered according to CD56, CD16 and PD-1 expressions. The clustering result showed that CD16 is the best marker for identification of NK populations. NK populations can be separated nicely to CD16^{neg} and CD16^{pos} NK population, instead CD56 and PD-1 positive NK cells are dotting around on the map without clear clusters. This data suggest that PD-1 cannot be used as a lineage marker for NK cell differentiation, and PD-1^{pos} NK cells are not a separate NK population. But the CyTOF data does allow to study

the co-expression pattern of PD-1with quite few other markers that we have not been able to study using conventional flow cytometry.

Our date showed that in comparison with PD-1^{neg} NK cells, PD-1^{pos} NK cells up-regulated some markers of activated NK cells including CD11c, chemokine receptors CD117 and CD197, which play an important role in NK cytolytic function. Moreover, we analysed the expression level of NKG2C, a marker of CMV infection ' CMV-memory like NK cells' compared to PD-1^{neg} NK cells. In human with CMV seropositive, a fraction of NK cells (both CD56^{dim} and CD56^{bright}) express NKG2C activating receptor and these NKG2C^{+}NK cells described as HCMV specific cells, which recognize ligands (HLA-E) expressed on CMV infected cells (Ma et al., 2017). Although PD-1 is expressed on the cytotoxic CD56^{dim} CD16^{+} NK cells and all patients (3) participated in CyTOF analysis were CMV seropositive, PD-1^{pos} NK cells express minimal level NKG2C on their surface instead NKG2C was expressed on PD-1^{neg} NK cells. These results indicate that PD-1^{pos} NK cells are not CMV specific cells whilst their phenotype are potentially driven by tumor cells or tumor microenvironment.

In addition, PD-1 expression on a subset of infiltrating NK cells has been reported in small lung carcinoma. These intratumoral PD-1^{pos} NK cells co-expressed more inhibitory receptors on their surfaces compared to PD-1^{neg} NK cells. In addition, these infiltrating NK cells were less functional compared to the peripheral NK cells and the dysfunctional correlated with PD-1 expression (Trefny et al., 2020). In line with this, we found that PD-1^{pos} NK cells from B-CLL patients co-expressed other immune checkpoints such as CD39 and TIGIT compared to PD-1^{neg} NK cells. This might contribute to the further impairment of PD-1^{pos} NK cells and

indicates that these receptors might need to be blocked as well in order to fully reverse the anti-tumor function of PD-1^{pos} NK cells.

5.3.3 Functionality of PD-1^{pos} NK cells

PD-1 is a key inhibitory checkpoint receptors that its function was first characterised on T cells. High levels of PD-1 due to sustained TCR stimulation lead to T cell exhaustion and tumor evasion. Evidence of PD-1 involvement in T cells dysfunction and tumor evasion has first been reported from a study that found PDL-1 transduced tumor cell line rendered them less sensitive to specific TCR cytolytic T cells, leading to increased their survival and T cell dysfunction (Iwai et al., 2002). In the recent years, PD-1 blockade on T cells has developed to a very successful cancers treatment through reviving T cells and preventing tumor escape from T cell response (Robert, 2020; Okazaki & Honjo, 2006). NK cell modifications by the tumor microenvironment (TME) in solid and haematological tumours have been linked to poor clinical outcomes. In addition, NK cell function impairment is associated with marked phenotypic alterations of NK cells, such as decreased expression of activating receptors and increased expression of inhibitory/checkpoint receptors (Mamessier et al., 2011). Among these checkpoint receptors PD-1, which does not recognise and bind to the classical HLA-class I, whilst it binds to ligands (PDL1 and PDL2) expressed on tumor cells and other adjacent immune cells, is believed to be one mechanism of NK cell dysfunctional and tumor evasion from NK cells recognition (Quatrini et al., 2020).

The critical role of PD-1 as a checkpoint for NK cell activation was observed in MHC-deficient tumors. PD-1 found to be expressed on a subsets of infiltrated NK cells at early timepoint in mice following tumor injection (Hsu et al., 2018). The functionality of PD-1^{pos} NK cells were

investigated in many cancer settings including Kaposi carcinoma, Multiple myeloma (MM), and lung cancer (Beldi-Ferchiou et al., 2016; Bi & Tian, 2017). In Kaposi carcinoma patients, PD-1^{pos} NK cells showed significantly impaired degranulation after NK cells activation through three different activation pathways using plate-bound for CD16 or NKp30 or NKp46 antibodies. The degranulation of PD-1^{pos} NK cells was significantly less potent than PD-1^{neg} NK cells in the presence of either PDL-1^{+} tumor cell line or PDL-1^{-} tumor cell line (Beldi-Ferchiou et al., 2016). However, PDL-1expresstion on target cells did not further suppress PD-1^{pos} NK cells. This was hypothesized to the possible expression of PDL-1 on NK themselves or on other PBMCs which compensate the absence of PDL-1 on PDL-1^{-} target cell condition (Beldi-Ferchiou et al., 2016). In multiple myeloma, a study has confirmed the PD-1 expression on NK cells (Benson et al., 2010), and engagement of PDL-1 expressing MM cells and bone marrow stromal cells with PD-1^{pos} NK cells inhibit their anti-tumor function and is related to the disease progression of MM (Benson et al., 2010; Kawano et al., 2015). This observation has also been confirmed in lung cancer setting. PD-1^{pos} NK cells from peripheral blood of lung cancer patients demonstrated impaired effector functions, including lower degranulation, perforin and granzymes and IFN-γ secretion after K562 cells stimulation compared to PD-1^{neg} NK cells. (Niu et al., 2020).

From our study, PD-1^{pos} NK cells in B-CLL patients showed similar results after stimulation with two different tumor cell lines K562 and 721.221, where the degranulation of PD-1^{pos} NK cells were substantially lower and PD-1^{pos} NK cells produce significantly lower cytokines such as IFN-γ, TNF-α, IL-2, IL-4 and IL-5 compared to PD-1^{neg} counterparts. One interesting observation is that PD-1^{pos} NK cells showed impaired functionality when they are stimulated with either K562 cells or 721.221 cells. K562 cells has been reported to be absent of PD-1 ligand, whilst from our data 721.221 cells do express both PDL1 and PDL2. So, the reduced

functionality of PD-1^{pos} NK cells come from two mechanisms. First, the PD-1^{pos} NK cells represent the exhausted NK population with reduced expression of activating receptors. Thus, they demonstrate impaired functionality after stimulation compared with PD-1^{neg} NK cells with or without PD-1/PD-1Ls interaction. Importantly, 721.221 target cells induced even further inhibition of PD-1^{pos} NK cells compared to K562 cells that do not express PD-1 ligands. This indicates that PD-1/PD-1Ls interactions with these PD-1pos NK cells will activate tyrosine phosphatase containing Src Homology-2 (SHP-2) which in turn interferes with PI3K, ERK and AKT activation pathways effecting NK cell activation, proliferation, and survival (Xia et al., 2016). Another explanation of the functional impairment without PD-1 ligation of PD-1^{pos} NK cells is the expression of PDL-1 on NK cells particularly on PD-1^{pos} NK cells themselves, as shown in **Figure 5.14**, which will interact with PD-1 receptor on PD-1^{pos} NK cells and suppress the activation. Altogether, these data demonstrate that the functionality of PD-1^{pos} NK cells are suppressed compared with PD-1^{neg} NK cells after stimulation, which potentially contributes to the overall function impairment observed in the whole NK population in B-CLL patients.

5.3.4 Blocking PD-1/PDL1,L2 interactions partially reversed PD-1^{pos} NK cells.

Checkpoint blockade immunotherapy, including PD-1/PD-1Ls blockade is a very successful cancer immunotherapy. It targets one key regulator of the immune system to revive the anti-tumor immune response. PD-1 and PDL-1 blockade is a very successful treatment for several solid cancers, particularly cancers with high mutational load due to emerging neo-antigens. PD-1 blockade (nivolumab) has been shown to be very efficient in patients with refractory metastatic melanoma, non-small cell lung cancer (NSLCL), colorectal cancer and renal cell carcinoma (Jimbu et al., 2021). Recently, same strategy was applied on haematological malignancies including AML, B-CLL but with less efficacy compared to the solid cancers,

which demonstrates a limited single agent efficacy of PD-1 inhibitors in those patients. The less success attributed possibly to the high tumor burden and to the different immune pathways mediating immune tolerance effect the response of PD-1 inhibitor (Boddu et al., 2018). However, study has shown that there is expression of multiple molecules that interact with the immune checkpoints expressed on T cells such as CTLA-4, PD-1, and Tim-3 on the acute Myeloid Leukaemia (AML) cells, which indicates the potential beneficial effect of these checkpoint blockade treatment. Extensive clinical trials are ongoing (Austin et al., 2016). Also, recent study (Nagasaki et al., 2020) showed that PD-1 blockade can improve the anti-tumor function specifically for $CD4^+$ T cells against MHC-II expressing tumor cells in Classical Hodgkin lymphoma (cHL), and this efficacy has been further improved after combination with anti-LAG-3 antibody. In addition, in B-CLL patients blocking PD-1/PDL1 interactions by anti-PDL1 can enhance the efficacy of Ibrutinib (TKI agent) against malignant B-CLL cells and the expansion and effector function of $CD8^+$ T cells. This was accompanied by increased expression of activation markers on $CD8^+$ T cells and delay in CLL disease progression (Hanna et al., 2021).

In regard to NK cells, less is known about the role PD-1 plays to regulate NK cell function and what does the blocking of PD-1/PDL1 and PDL2 axis will affect the NK function. No such study has been carried out to study PD-1 on NK cells in B-CLL disease. However, using several types of mouse cancer models (haematological and solid tumors) in condition which T cells do not take part in anti-tumor response against tumor cells, PD-1 or PDL1 blockade has activated NK cells and augmented anti-tumor activity of NK cells against tumor cells resulted in decreased tumor growth (Hsu et al., 2018). In this study, we used the $PD\text{-}1^{pos}$ NK cells from B-CLL patients as ex-vivo model to study the effect of blocking PD-1/PD-1Ls interaction on NK cells function. The results showed that blocking PD-1signalling with PDL1 and PDL2

antibodies indeed can enhance the anti-tumor activity of PD-1^{pos} NK cells in terms of IFN-γ production and degranulation. But the reverse of the function is only partially and there is still a suppression for PD-1^{pos} NK cells compared with PD-1^{neg} NK cells after blocking. As we know there are multiple checkpoint molecules expressed on those PD-1^{pos} NK cells, such as CD39 and TIGIT. Also like we discussed earlier, PD-1 expression is only an indicator of exhausted NK cells, there are underlying transcriptional or epigenetic modifications, which has contributed the functional impairment. This will be addressed in the next chapter. Another interesting observation is the cytokines production by PD-1^{neg} NK cells can also be improved by PDL1 and PDL2 blocking. The possible explanation of this phenomena is there might be very low PD-1 expression on such called PD-1^{neg} NK cells. Altogether, the data has demonstrated a significant increase in anti-tumor function of PD-1^{pos} NK cells from B-CLL patients after blocking of PD-1/PDL1 and PDL2 interactions, which implies that PD-1 blockade can potentially revive NK cells in B-CLL patients. As this reversion was partially, therefor a combination blockade might be required such as anti-PD-1 with LAG-3 or CD39 or TIGIT. Further studies will be needed to investigation these sitting in future.

5.4 Conclusion

PD-1 was expressed on a fraction of $CD56^{dim}$ NK cells and was more pronounced on cytotoxic NK cells ($CD56^{dim}$ $CD16^{+}$), which bear a highly differentiated phenotype of PD-1^{pos} $CD56^{dim}$ $CD16^{pos/neg}$ $CD57^{pos}$NKG2A^{neg}. There is lower expression of activating receptors on PD-1^{pos} NK cells compared to PD-1^{neg} counterparts, suggesting this is one of the mechanisms for function impairment with PD-1^{pos} NK cells. In addition, on NK cells, PD-1 was co-expressed with other immune checkpoints, adhesion molecules and chemokine receptors acquiring an activated phenotype of PD-$1^{pos}$$CD56^{dim}$$CD16^{pos/neg}$$CD57^{pos}$NKG2A^{neg}TIGIT^{pos}$CD39^{pos}$ $CD11c^{pos}$$CD197^{pos}$NKG2C^{neg} (**Figures 5.5 and 5.13**). Functionally, cytokines production and degranulation of PD-1^{pos} NK cells were substantially lower than PD-1^{neg} NK cells after stimulation with target cell lines using both primary PD-1^{pos} NK cells and PD-1^{pos} NK-92 cell lines. The functional impairment of PD-1^{pos} NK cells can be partially reversed after PD-1/PD-1Ls axis blockade by PD-L1 and PDL-2 antibodies, which implies that PD-1 blockade in B-CLL patients can potentially activate NK cells to target the B-CLL tumor cells.

CHAPTER 6: PILOT STUDY OF TRANSCRIPTION PROFILE OF PD-1^{pos} and PD-1^{neg} NK CELLS

6.1 Introduction

In the previous chapter using conventional flow cytometry and CyTOF, we have demonstrated that PD-1^{pos} NK cells from B-CLL patients have distinct phenotype compared to PD-1^{neg} NK cells. The expression of activating receptors was significantly lower whilst expression of checkpoint molecules including CD39 and TIGIT, and some adhesion molecules CD18 and CD11c was higher on PD-1^{pos} NK cells compared to PD-1^{neg} counter parts. In addition, the functional capacity of PD-1^{pos} NK cells such as cytokines production (particularly IFN-γ and TNF-α), degranulation and cytotoxicity level were substantially lower after stimulation with K562 and 721.221 cell lines. To further investigate the potential underlying mechanisms of this phenotype and function changes for PD-1^{pos} NK cells, we used the recent breakthrough of single cell RNA-sequencing (scRNA-seq) technology to study the heterogeneity of transcription profile of PD-1^{pos} vs PD-1^{neg} NK cells. Furthermore, the dynamic of transcription regulatory machinery was investigated by measuring the differentially accessible chromatin (DAC) by comparing PD-1^{pos} vs PD-1^{neg} NK cells and whole NK cells from B-CLL vs HDs using ATAC-seq.

6.2 Results

6.2.1 Single cell RNA-seq analysis of PD-1^{pos} and PD-1^{neg} NK cells

Unlike bulk RNA-seq which only offers the average of transcription signal for millions of cells, scRNA-seq provides simultaneous analysis of thousands transcriptions for every single cell. Therefore, scRNA-seq reveals changes in each individual cell and illustrate the heterogeneity of gene expression pattern (Reyfman et al., 2019). To study the heterogeneity based on transcriptome of PD-1^{pos} and PD-1^{neg} NK cells. fresh PBMCs of two B-CLL patients (patient's code 297KB and 351MB) with high PD-1^{pos} NK cells (22% and 13% of PD-1^{pos} NK cells respectively) were used. NK cell populations were enriched using negative selection from PBMCs before they were stained with anti-CD3, CD56, PD-1 antibodies and live/dead dye, then CD56 and PD-1 then PD-1^{pos} and PD-1^{neg} NK cells were sorted using cell sorter (**Figure 6.2**). The average numbers of each cell type were about 19,000 and the viability was 98% for 297KB and 60,000 NK cell types with 58% viability for 351MB. Next, cells were handed in to the Genomic Centre-University of Birmingham for droplet based single cell RNA sequencing using 10X platform.

Initially, the workflow analysis was started by removing ambient RNA that released in the cell suspension from cells that are stressed or undergone apoptosis, using 10X Genomics v2.1.1 to prevent contamination of transcripts between NK cell populations and reduce batch effect. Cells fall into assigned thresholds and duplicates (more than one cell captured in droplet) were also removed using Seurat, followed by data integration and clustering. The Quality control analysis revealed good library assembly and sequencing. The median number of sequenced NK cells unique molecular identifiers (UMIs) is 3,500, and 1,500 detectable genes per cell that are associated with the cell barcode for 297KB and 351MB patients respectively. In addition,

the cells with high mitochondrial related gene expression (>15%) were excluded from the analysis rendering the viability of the cells is robust (**Figure 6.1**). After the QC filtering and data integration of both patients (297KB and 351MB), we had a total NK cell count of 6427 (4726 and 1701 respectively), which can be divided into 3017 (47%) of PD-1^{pos} NK cell and 3410 (53%) of PD-1^{neg} NK cells.

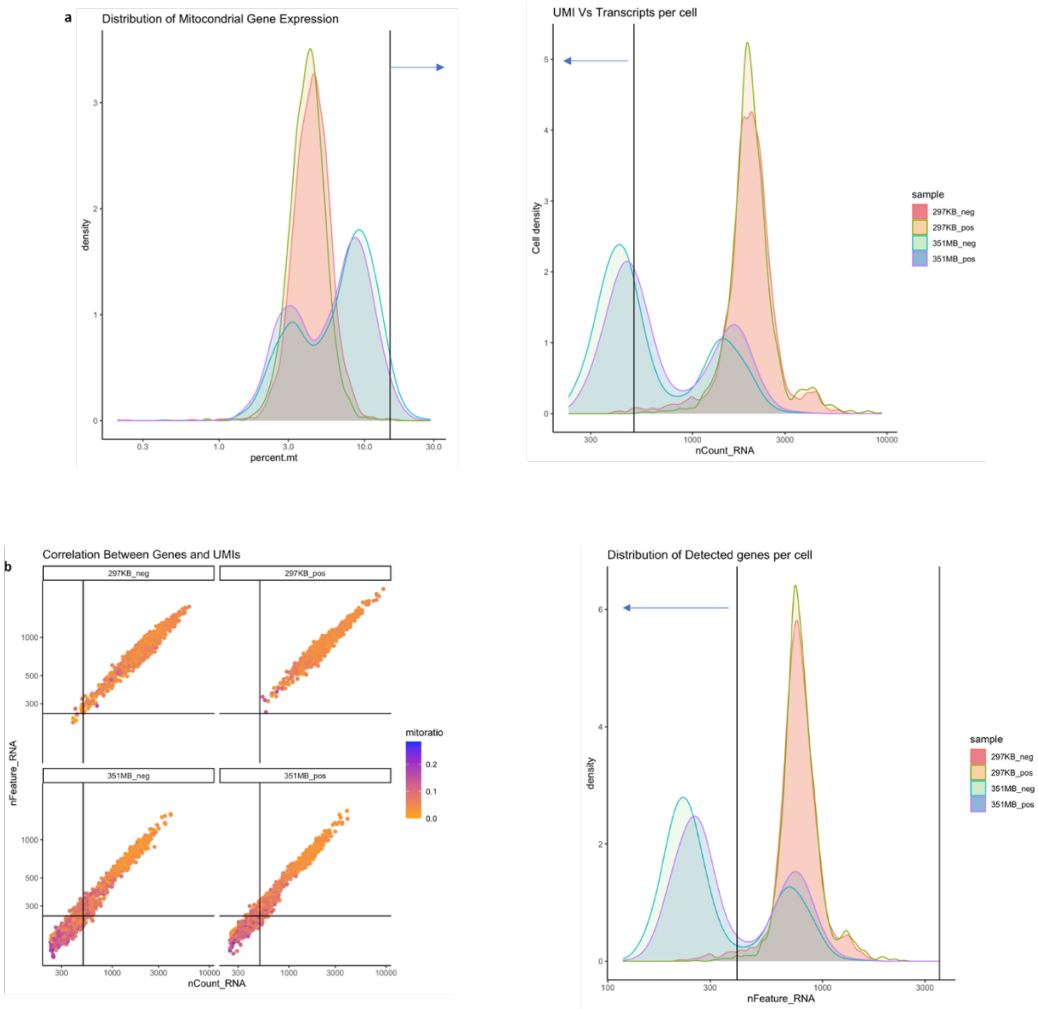

Figure 6.1 Quality control plots for raw read data to filter out contaminated cells.

Raw read data was processed with CellRanger (10X Genomic). (**a**) Raw read bcl files were converted to fastq (bcl2fastq) and aligned to the human reference genome GRCh38 resulting in a matrix representing the UMI's per cell barcode per gene (cellranger count). Cells were filtered to keep only cells above 500 of UMI reads. Around 15% cells with high detected mitochondrial genes are deemed to be poor quality samples, so they were removed . (**b**) In the right graph, nFeatures metrics shows the distribution number of genes detected in each cell. The cells with number of detectable genes below 500 and above 3500 were removed as these cells might be stressed or undergone apoptosis. Left graph, dot plots to demonstrate the correlation of number of genes verses UMIs, which are coloured by the fraction of mitochondrial reads. Cells that are poor quality are likely to have low number of genes and low UMIs and high mitochondrial reads per cell. The left lower quadrant suggests low complexity cell types such as Red Blood Cells.

6.2.1.1 Clustering and identification of NK cell populations

Highly variable genes were used for 2-dimensional reduction analysis using Uniform Manifold Approximation (UMAP) for data clustering and visualisation. A total of 7 clusters were recognised after UMAP analysis (**Figure 6.2**). PHATE (Potential of Heat-diffusion for Affinity-based Trajectory Embedding) was also applied to confirm the 7differnt NK clusters. In order to confirm the identity of NK cells and to identify each cluster, analysis was performed on differential gene expression on each cluster based on the mean of gene expression. Due to the relatively poor signal of CD56 transcription that might be degraded during processing, *NCAM1*/CD56 transcripts were not well presented in this data. So, the NK cells cannot be clustered into $CD56^{dim}$ and $CD56^{bright}$ population. Unfortunately, the PD-1^{pos} and PD-1^{neg} NK cells cannot be separated into two clusters. This means PD-1 is not a lineage marker of NK cells. Also, it can be noticed that NK cells from these two patients are not all merged to on population.

Instead, the differentiation markers (CD56, CD16,NKG2A and NKG2C), activation receptors (NCRs, NKG2D and DNAM-1), exhaustion markers (PD-1, CD39, Tim-3, Lag-3, and CTLA-4), transcription factors (TBX, EOMES and Hobit) and other important markers (Ki67, CD69,GZMB and PRF1) were used to identify and name these 7 NK clusters. The expression pattern of some markers between 7 NK clusters was demonstrated in (**Figure 6.3**). In addition, some other markers related to NK cells were used to confirm the identity of NK cells (**Figure 6.4**).

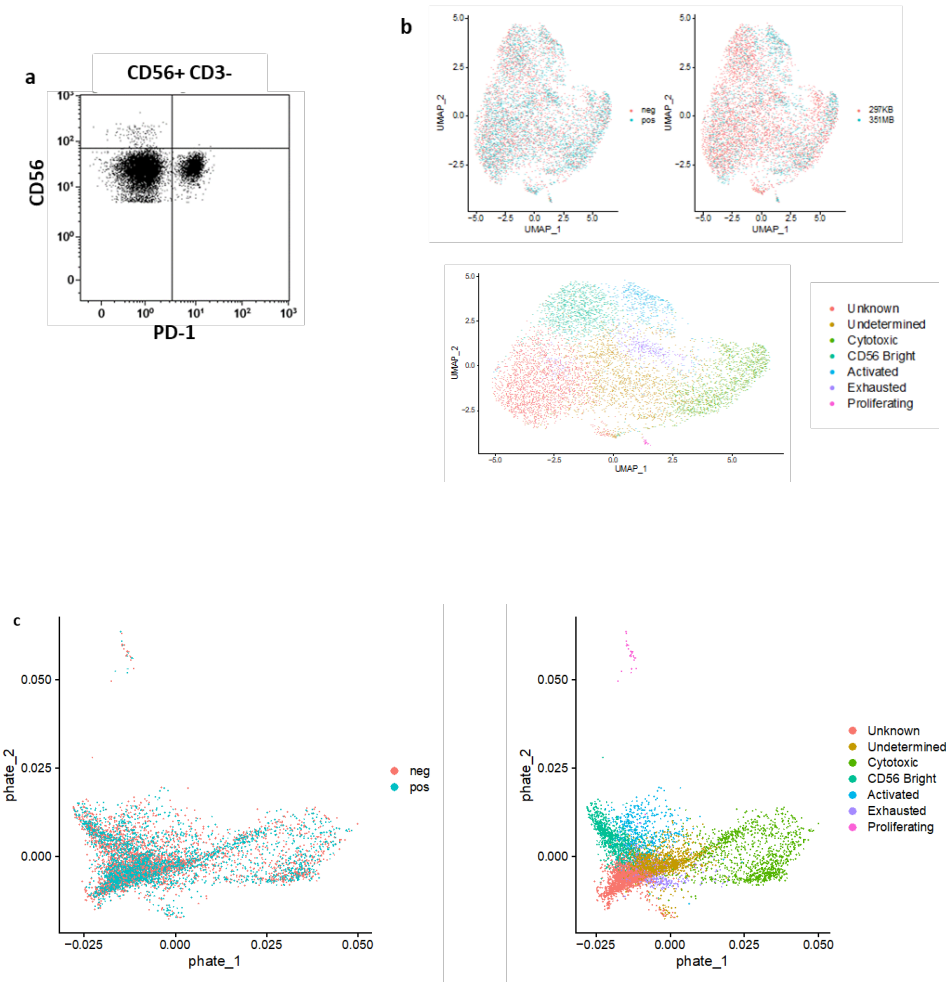

Figure 6.2 UMAP and PHATE dimentional reduction analysis of NK subsets

(**a**) Flow plot shows gating stratigy of PD-1^{pos} and PD-1^{neg} NK cells for cell sorting. (**b**) Unbiased 2-dimention UMAP clustering analysis to represent all sequenced cells, which has separated the whole NK population to 7 clusters. Top right graph, the whole NK population was separated according to the patient's ID, red dots represent the NK cells from 297KB and blue dots represent NK cells from 351MB patient. The top left graph demonstrates the whole NK cells clustered based on PD-1 expression. Red dots represent the PD-1^{neg} NK cells and blue dots represents PD-1^{pos} NK cells. (c) The bottom graphs show 7 clusters of NK cell subsets that were labelled with different colors. The bottom right graph is PHATE analysis to demonstrate the different 7 NK clusters. PHATE (Potiental of Heat-diffusion Affinety-based Trajectory Embedding) is a new stable dimensionality reduction method that generates a non-linear embedding of high dimensional data that simultaneously denoises the data. The left graph demonstrates whole NK clusters according to PD-1 expression, red dots represent the PD-1^{neg} NK cells and blue dots represent the PD-1^{pos} NK cells.

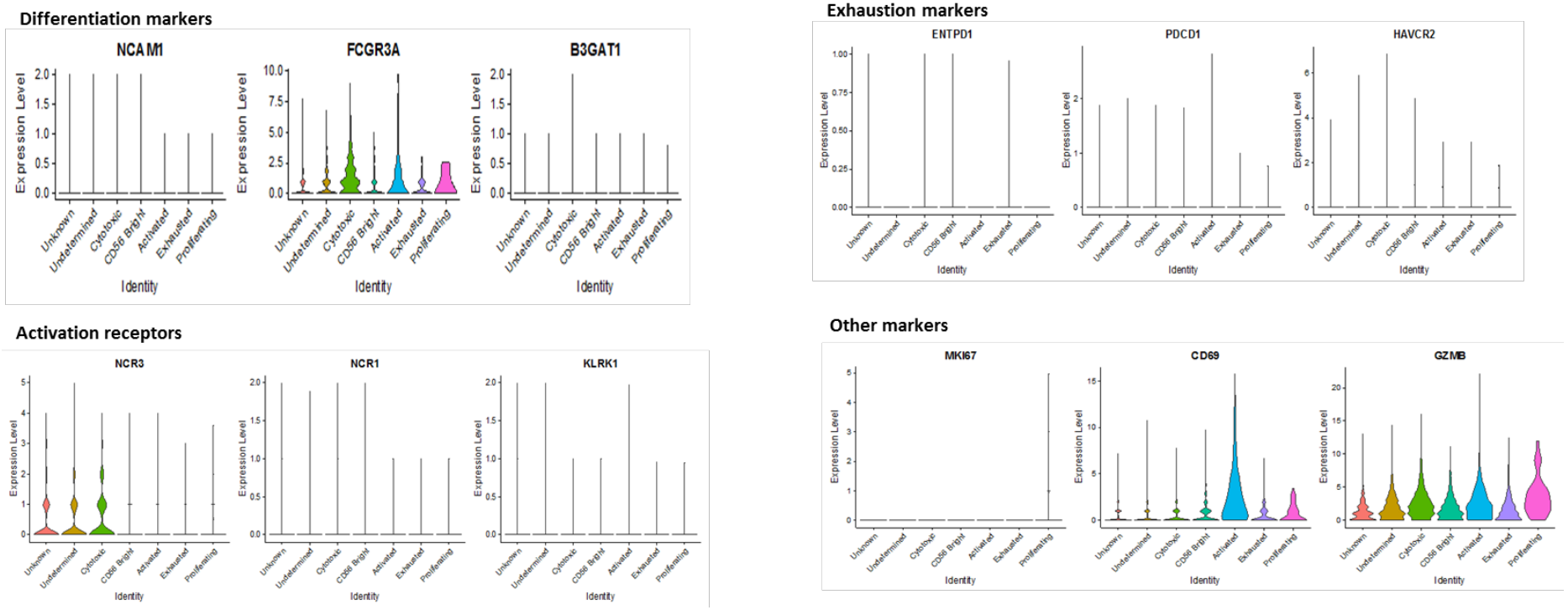

Figure 6.3 Violin plots demonstrate the differentiated gene transcription between 7 NK clusters.

Violin plots show the expression pattern of differntiation markers (CD56, CD16, CD57), activating receptors (NCRs, NKG2D), exhaustion markers (PD-1, CD39, Tim-3) and other important markers (Ki67, CD69, GZMB) between the 7 NK clusters. The y axis illustrates gene experssion level of each marker.

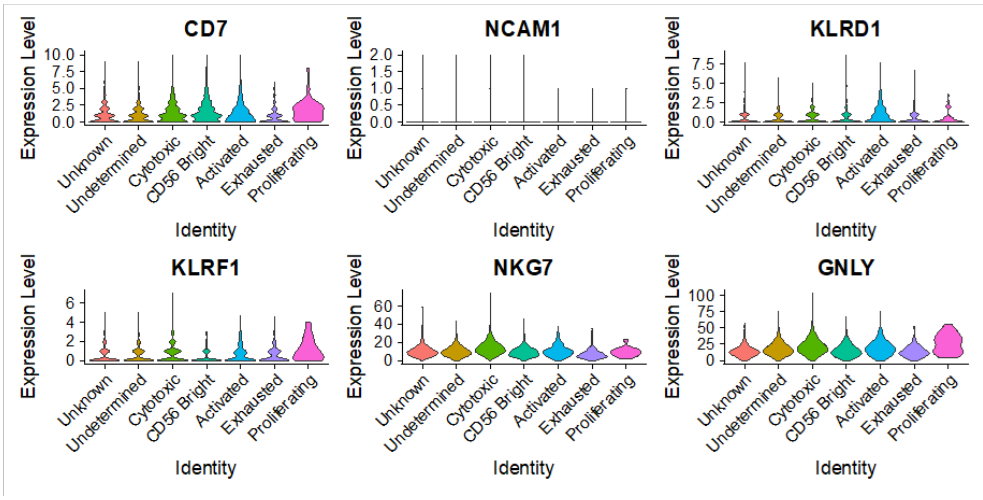

Figure 6.4 Violin plots demonstrate the global markers of NK cells.

Violin plots show the expression of six NK cell markers of each cluster. The y axis represents gene expression level.

Following the analysis of specific genes on each cluster, clusters were named based on the cell marker. After carful investigation, the first two clusters were determined as unknown and undetermined clusters. They might be transitional NK cells as they do not have specific functional and differentiated genes. In cluster #3 NK cells, the specific genes that associated with cytotoxic including *FCGR3A*/CD16, are strongly expressed. It has been identified as cytotoxicity NK subsets. Cluster #4 NK cells, have relatively high expression of *NCAM1*/CD56 and low expression of cytotoxic/highly differentiated markers *B3GAT1*/CD57, and *FCGR3A*, which indicates they are $CD56^{bright}$ NK cells. Cluster #5 NK cells have one major feature, which is the high expression of the activation receptor CD69. They were identified as activated NK subsets. There are relatively high expression of exhaustion marker *ENTPD1*/CD39 and low

expression of cytolytic receptor *FCGR3A*/CD16 in the cluster #6 NK cells. Thus, they were named exhausted NK subsets. Cluster #7 NK cells were determined as proliferative NK cells as it is the only cluster that has a high expression of proliferation genes *MKi67*/Ki67.

6.2.1.2 Differential gene expression on PD-1^{pos} vs PD-1^{neg} NK subsets through different clusters

The aim of this experiment in this study is to dissect the differentiated transcription profile between PD-1^{pos} and PD-1^{neg} NK cells. Therefore, the downstream analysis for determining the transcription profile of PD-1^{pos} vs PD-1^{neg} NK cells was carried out through all individual NK cell clusters based on PD-1^{pos} and PD-1^{neg} NK cells. The analysis will be focused more on the defined NK clusters (cytotoxic and activated) rather than unknown or undetermined clusters.

6.2.1.2.1 The transcriptomic profile of phenotypic markers for PD-1^{pos} NK cells in different NK clusters

To further investigate the essence of PD-1^{pos} NK cells in B-CLL patients, their transcription profile of phenotype and functional differences were determined and compared to flow cytometry. PD-1^{pos} NK cells have lower transcription of *NCAM-1*/CD56, *KLRC1*/NKG2A whilst high *B3GAT1*/CD57 in the majority of defined clusters, including the cytotoxicity, activated, and proliferating clusters (**Figure 6.5 panel a**). Identical observation was noticed by flow cytometry, as PD-1^{pos} NK cells have mature phenotype of CD56^{dim}CD57^{pos}NKG2A^{dim} **(Figure 6.5 panel b)**. Despite CD57 expression defines mature and functionally NK cells with greatest potential for cytotoxicity (Lopez-Vergès et al., 2010), there were no obvious

differences in terms of transcriptions for activating receptors observed on PD-1^{pos} NK cells vs PD-1^{neg} NK cells in NK clusters, particularly *NCR3*/NKp30, *NCR1*/NKp46 and *KLRK1*/NKG2D. Another interesting marker is the activation marker, CD69. The transcription is almost exclusively found within the activated NK cluster. In addition, transcription of *CD69* was only lower in PD-1^{pos} NK cells compared to PD-1^{neg} compartments within cytotoxic cluster (**Figure 6.6**)

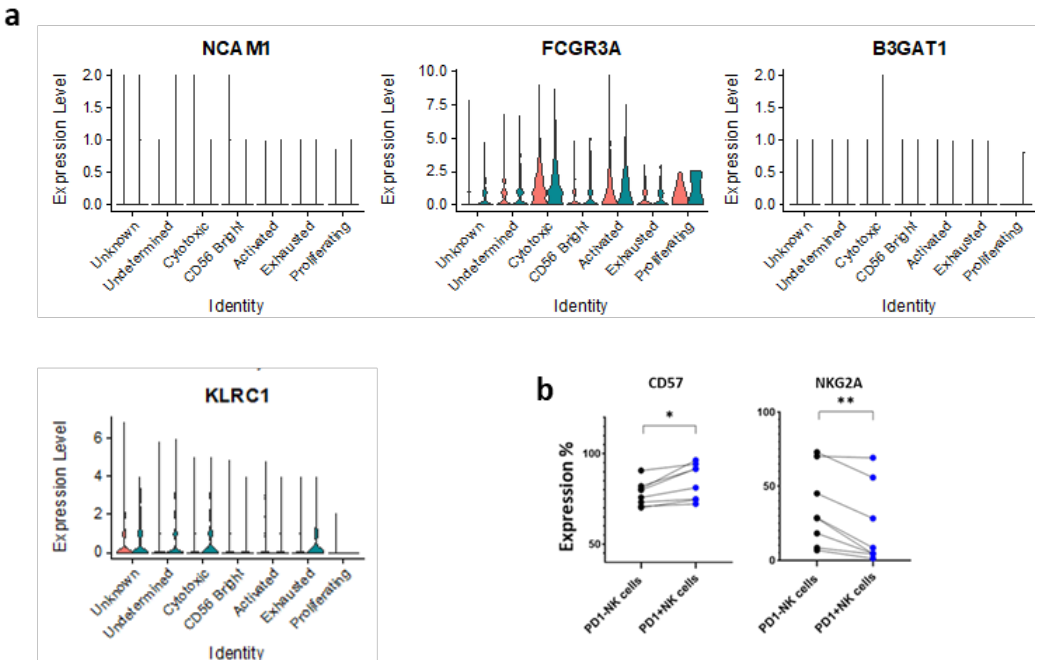

Figure 6.5 comparison of the transcription level of differentiation markers between PD-1^{pos} and PD-1^{neg} NK cell among the 7 NK clusters

(**a**) Violin plots demonstrate the transcription level of various genes related to NK cell differentiation, including CD56, CD16, CD57 and NKG2A from scRNA analysis. The orange plots represent PD-1^{neg} NK population, and green plots represent PD-1^{pos} NK population. (**b**) Flow plots comparing the percentage of surface expression of CD57 and NKG2A on PD-1^{pos} vs PD-1^{neg} NK cells.

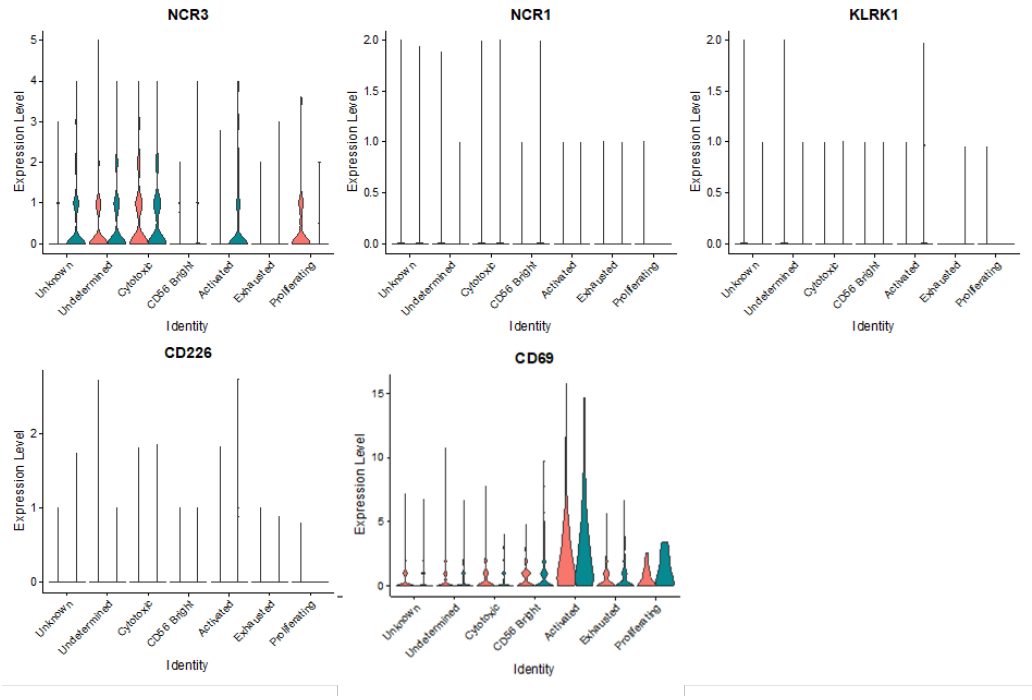

Figure 6.6 Comparison of the transcription level of activating receptors and CD69 between PD-1^{pos} and PD-1^{neg} NK cells among 7 NK clusters.

Violin plots demonstrate the transcription level of various genes related to activating receptors and activated markers, including NCRs, NKG2D, DNAM-1 and CD69 from scRNA analysis. The orange plots represent PD-1^{neg} NK population, and green plots represent PD-1^{pos} NK population.

Transcriptions of immune checkpoints were also present in almost all clusters, particularly the transcription of *HAVCR2*/TIM-3 was upregulated in PD-1^{pos} NK cells compared to PD-1^{neg} NK cells within cytotoxic clusters. However, *ENTPD1*/CD39 and *CTLA4* transcription were specifically found in PD-1^{neg} NK cells but not in PD-1^{pos} NK cells (**Figure 6.7**). CyTOF analysis revealed that CD39 was co-expressed with PD-1 on a fraction of cytotoxic NK cells (PD-1^{pos}CD56^{dim}CD16^{pos}), whereas low expression of CD39 was observed on PD-1^{neg} NK cells. No obvious difference for CD96 expression on both cell types was observed. This result indicates the discrepancy between the flow cytometry and scRNA-seq analysis, which measure either the protein level or RNA transcription level.

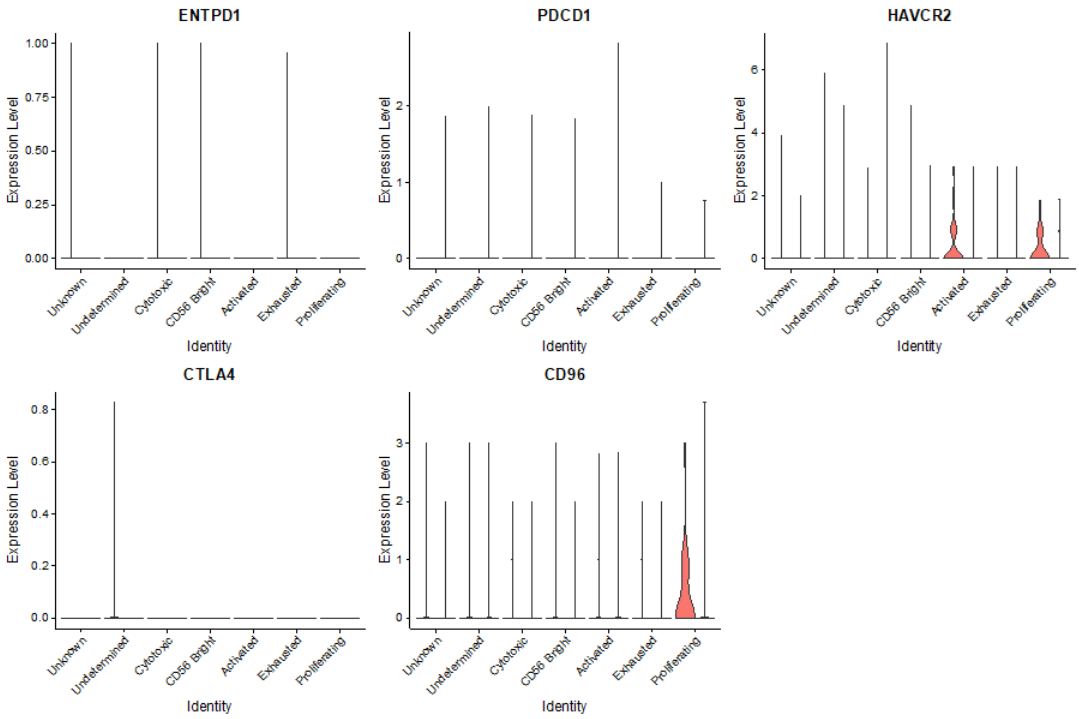

Figure 6.7 Comparison of the transcription level of checkpoint receptors between PD-1^{pos} and PD-1^{neg} NK cells among 7 NK clusters.

Violin plots demonstrate the transcription level of various genes related to checkpoint receptors in PD-1^{pos} vs PD-1^{neg} NK population, including CD39, PD-1, Tim-3, CTLA-4 and CD96 from scRNA analysis. The orange plots represent PD-1^{neg} NK population, and green plots represent PD-1^{pos} NK population.

Gene transcription of adhesion molecules was also investigated. Interestingly, the transcription of *ITGB2*/CD18 was higher in PD-1^{pos} NK cells compared to PD-1^{neg} NK cells, particularly in cytotoxic, activated, and exhausted clusters. At the protein level, surface expression of CD18 matched scRNA dataset, as CD18 expression was significantly up regulated and reached the highest percentage 98% on cytotoxic NK subsets (CD56^{dim} CD16^{pos}) (**Chapter 3, Figure 3.10 panel c**). CD18 has been reported to be involved in adhesion and transmigration of NK cells and other leukocytes in addition to contribution to NK cytotoxicity (Sadhu et al., 2007). On the other side, the transcription of *SPON2* gene, which codes for SPON2 protein was lower in PD-1^{pos} NK cells compared to PD-1^{neg} NK cells particularly in cytotoxic and activated clusters (**Figure 6.8**). SPON2 protein promotes cell adhesion through binding to integrin receptors and recruits other inflammatory immune cells (Y. Li et al., 2009).

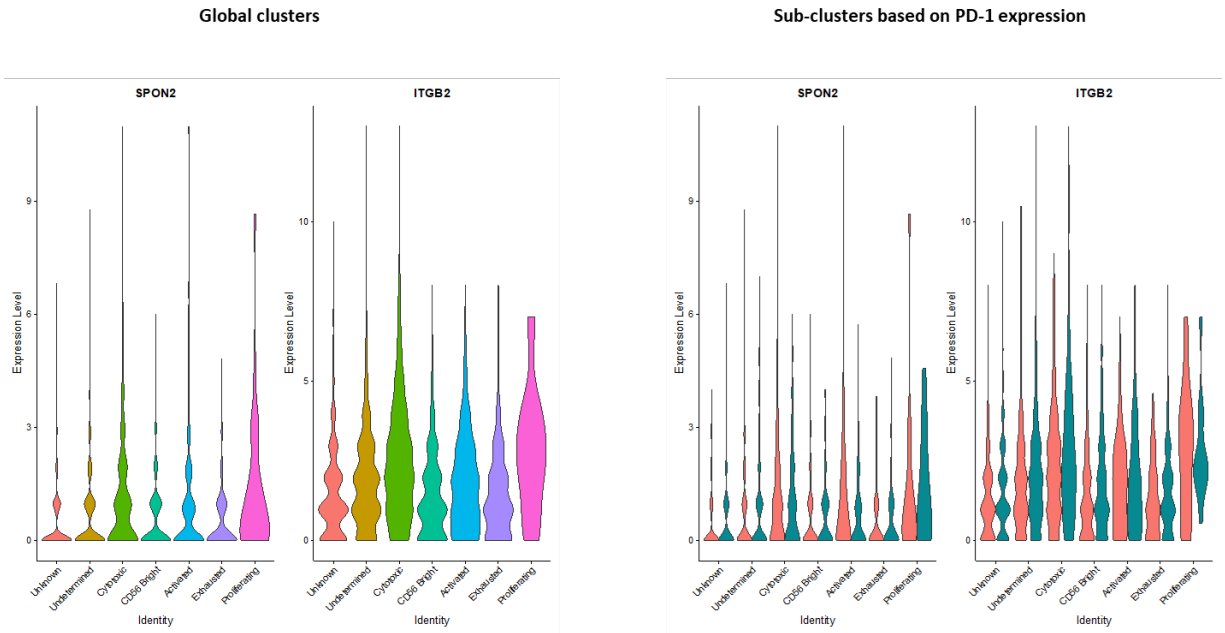

Figure 6.8 Comparison of the transcription level of adhesion molecules within the 7 NK clusters and between PD-1^{pos} and PD-1^{neg} NK population.

Violin plots demonstrate the transcription level of various genes related to adhesion molecules in the global 7 clusters and in PD-1^{pos} vs PD-1^{neg} NK population, including CD18 and SPON2 from scRNA analysis. The orange plots represent PD-1^{neg} NK population, and green plots represent PD-1^{pos} NK population.

6.2.1.2.2 The transcription profile of functional markers of PD-1^{pos} NK cells in different NK clusters.

Next, we investigated the transcription profile of PD-1^{pos} NK cells in comparison to PD-1^{neg} NK cells in terms of the functionality markers, which will be also focused on cytotoxic and activated NK clusters. Analysis of differentially expressed genes (DEG) revealed that the transcription of transcription factors and effector molecules were altered in PD-1^{pos} NK cells. DEG analysis indicated that cytotoxic and activated NK clusters have the highest level of gene expression of transcription factors including *TBx21*/T-box, *EOMES* and *ZNF683*/Hobit. However, PD-1^{pos} NK cells within the same clusters (particularly cytotoxic cluster) have low gene expression of transcription factor compared to PD-1^{neg} NK cells. The reduction of *EOMES* and *ZNF683* transcription were more obvious on cytotoxic NK clusters (**Figure 6.9**). Studies showed that EOMES, T-bet and Hobit transcription factors control the differentiation, proliferation, and effector functions of NK cells including expression of IFN-γ, perforin and granzyme B. In addition, impaired immune responses in cancer or other pathogens are linked to dysregulation of these transcription factors (Post et al., 2017; J. Zhang et al., 2018). This indicates that PD-1^{pos} NK cells have limited capacity of differentiation and proliferation compared to PD-1^{neg} counterparts.

NK cells release cytotoxic granules containing perforin and granzyme B to kill tumor and virally infected cells, which has been reported to be regulated by EOMES and T-bet transcription factors (Glimcher et al., 2004). Our data showed that the transcription level of perforin and granzyme B were highly expressed on activated NK cluster followed by cytotoxic clusters (**Figure 6.10**). However, although activated NK cluster has the highest transcription of granzyme B and perforin, the transcription of these two markers in PD-1^{pos} NK cells were

lower compared to PD-1^{neg} NK cells, and no difference seen within cytotoxic cluster. This indicates that there might be a compensatory role between transcription factors (Glimcher et al., 2004) that conserved perforin expression in PD-1^{pos} NK cells.

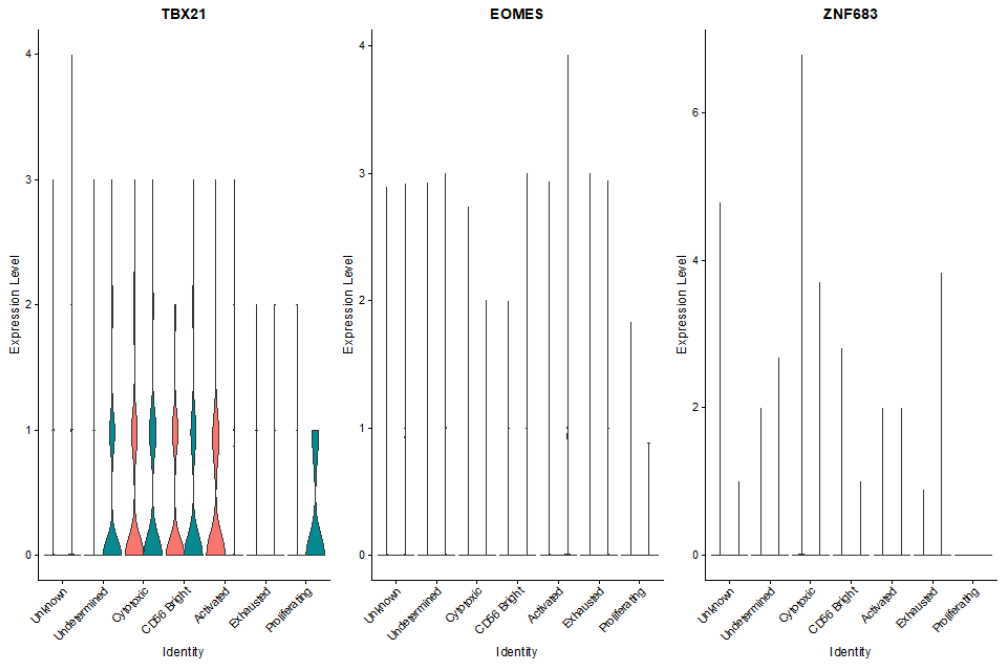

Figure 6.9 Comparison of the transcription level of transcription factors between PD-1^{pos} and PD-1^{neg} NK cells among the 7 NK clusters.

Violin plots demonstrate the transcription level of transcription factors in PD-1^{pos} vs PD-1^{neg} NK population, including T-box, Hobit, and EOMES from scRNA analysis. The orange plots represent PD-1^{neg} NK population, and green plots represent PD-1^{pos} NK population.

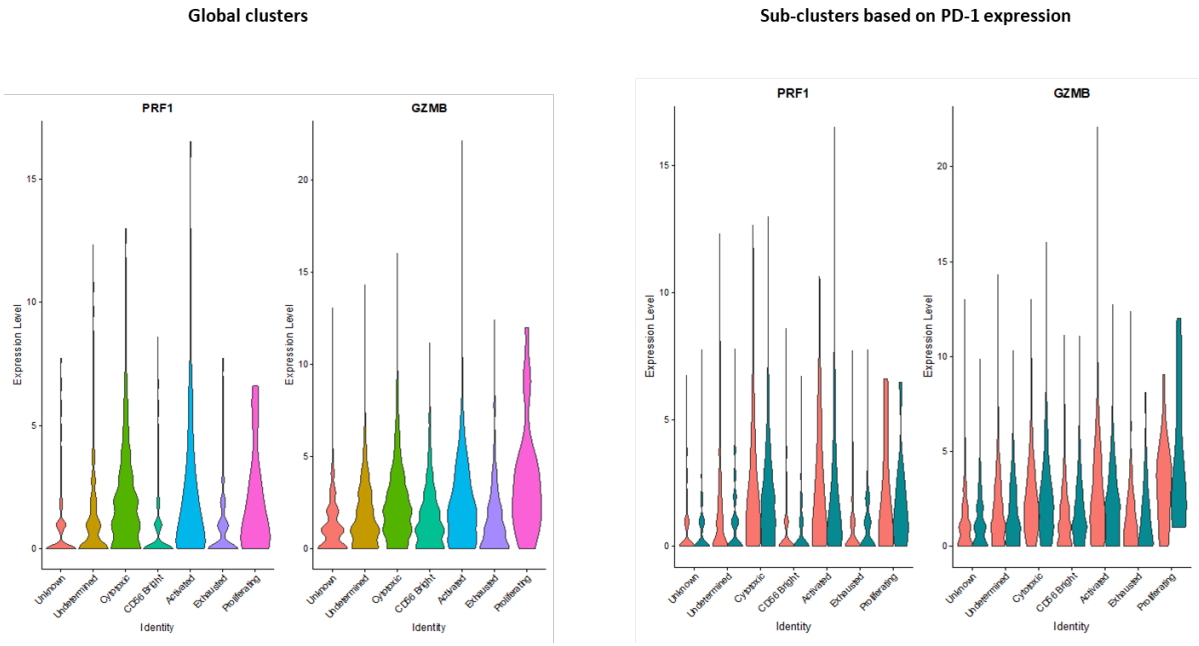

Figure 6.10 Comparison of the transcription level of cytolytic molecules within the 7 NK clusters and between PD-1^{pos} and PD-1^{neg} NK population.

Violin plots demonstrate the transcription level of cytolytic molecules in the global 7 clusters and in PD-1^{pos} vs PD-1^{neg} NK population, including Perforin and GZMB from scRNA analysis. The orange plots represent PD-1^{neg} NK population, and green plots represent PD-1^{pos} NK population.

6.2.1.3 Differentiated transcription profile of PD-1^{pos} versus PD-1^{neg} NK cells from whole NK population.

The downstream analyses of differentiated gene transcription in the previous section were based on PD-1^{pos} versus PD-1^{neg} within the specific NK clusters. Here, we focused the analysis of PD-1^{pos} versus PD-1^{neg} within whole NK population rather than specific NK clusters. Our data showed that the global PD-1^{pos} NK cells have altered transcription profile compared to PD-1^{neg} counterparts. Differential expression gene (DEG) analysis revealed that there were 302 genes differentially expressed on PD-1^{pos} NK cells compared to PD-1^{neg} NK cells ($p<0.05$). The heatmap was generated based on the gene list that fit in the criterial of FDR<0.01 and logFC>0.1 (**Figure 6.11**). Unfortunately, the PD-1pos and PD-1neg NK cells do not appear to be clustered separately. Nevertheless, the transcription profile of PD-1^{pos} NK cells compared with PD-1^{neg} NK cells was more distinct in the whole NK population than different 7 NK clusters. The transcription of *PDCD1*/PD-1 gene was solely present on PD-1^{pos} NK cells and not in PD-1^{neg} NK cells. Interestingly, our data showed that LAG-3 checkpoint transcription was upregulated on PD-1^{pos} NK cells, indicating that there is a gene co-expression of PD-1 with LAG-3 checkpoint. Moreover, transcription of *CCL5* chemokine was also upregulated on PD-1^{pos} NK cells. The transcription of activation markers *IL-32*, *CD3E* and cell cycle progression/differentiation *S100A4* were upregulated on PD-1^{pos} NK cells compared to PD-1^{neg} NK cells (**Figure 6.12**). Regarding CD3E expression, previous study showed that NK cells do express cytoplasmic CD3 epsilon but not on surface confirming the purity of our NK cell and CD3E not expressed by T or NKT cells (Lanier et al., 1992).

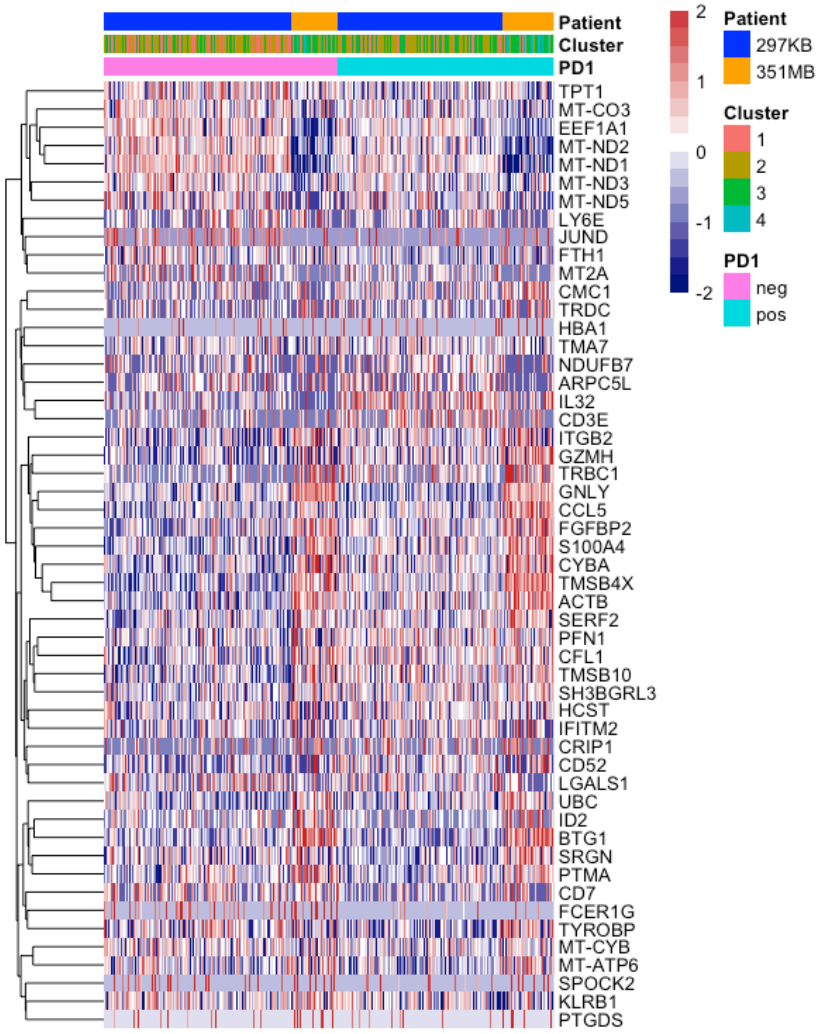

Figure 6.11 Heatmap to demonstrate the differentiated transcriptional profile of PD-1neg and PD-1pos NK cells.

Transcriptional profile of differentiated genes between PD-1^{pos} and PD-1^{neg} NK cells (FDR<0.01 and logFC>0.1).

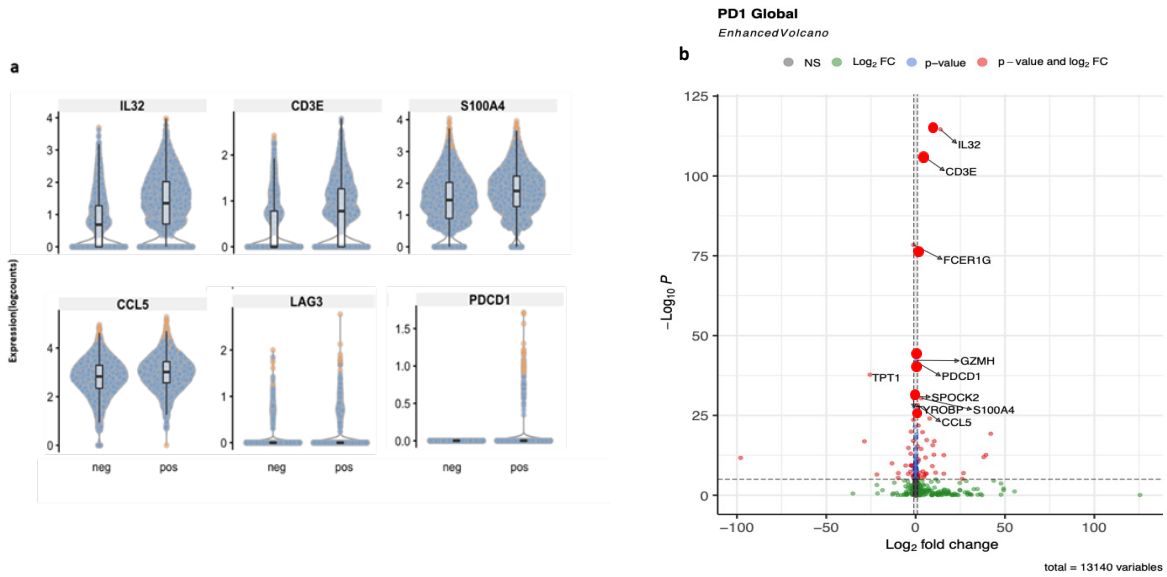

Figure 6.12 top modulated genes in the global PD-1^{pos} NK population.

(**a**) Representative violin plots to compare the transcription level of some genes from the top modulated genes list between PD-1^{pos} versus PD-1^{neg} NK cells, y axis is normalized log gene expression (left graphs). (**b**) Volcano plot to demonstrate the differential expression analysis results from PD-1^{pos} versus PD-1^{neg}NK cells. Genes labelled are those differentially upregulated or down regulated between PD-1^{pos} and PD-1^{neg} NK cells. X axis is the Log2 fold change of gene expression level and Y axis is the P value.

Interestingly, the transcription of genes that involved in negatively regulating cell motility and integrity of cytoskeleton structure, which are necessary for cytotoxic functions of NK cells (Schoppmeyer et al., 2017) were upregulated on PD-1^{pos} NK cells, these include *PFN1* and *ACTB* genes. This indicates the negative functional impact to NK cytotoxicity. Additionally, *PIK3R1* gene transcription which is important in NK metabolism by inducing glucose uptake was downregulated on PD-1^{pos} NK cells. In contrast and surprisingly, *KIR3DL2* and *KIR2DL3* gene transcriptions that code for KIRs inhibitory receptors were downregulated on PD-1^{pos} NK cells. In addition, CMV memory like marker of NK cells *KLRC2*/NKG2C expression was downregulated on PD-1^{pos} NK cells. This result is in line with surface expression of NKG2C on PD1-^{pos} NK cells. Another interesting finding is that *ID2* gene transcription was downregulated on PD-1^{pos} NK cells (**Figure 6.13**). ID2 deficiency will negatively regulates variety of cellular processes, including cellular growth, differentiation, and maturation, in addition to limiting NK functions such as IFN-γ production. (Z.-Y. Li et al., 2021).

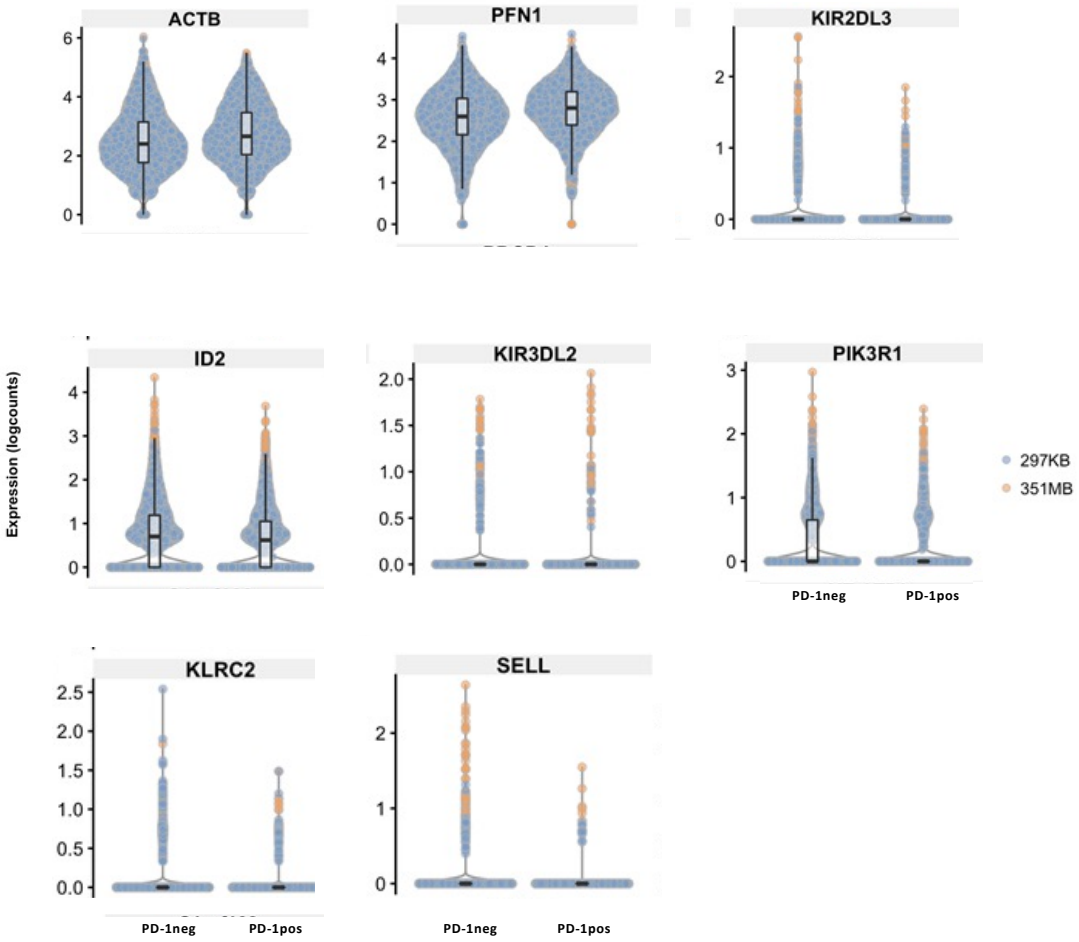

Figure 6.13 Top differentiated genes in the PD-1^{pos} NK population.

Violin plots to compare the transcription level of some genes from the top modulated genes list (up and down regulated genes) between PD-1^{pos} versus PD-1^{neg} NK cells form two B-CLL patients 297KB (blue dots), and 351MB (orang dots).

6.2.1.2.4 Pathway analysis of the differentiated transcription profile of PD-1^{pos} NK cells from the whole NK population.

Previously, the pattern of gene expression in PD-1^{pos} NK cells was determined and compared to the transcription profile of PD-1^{neg} NK cells. 302 genes (**Supplementary table 3**) were showed to be altered and upregulated on PD-1^{pos} NK cells. To determine how these genes biologically related to each other, 50 top up-regulated genes on PD-1^{pos} NK cells were analysed using DAVID functional annotation tool (https://david.ncifcrf.gov/summary.jsp) to annotate genes based on functional similarity. Gene Ontology term (GO TERM) was selected to identify gene sets that were enriched for biological process and cellular components of NK cells. 5 clusters were identified of GO term containing 15 genes that associated with T cell activation. 8 genes involved in initiating series of molecular signals by the cross linking of antigen – T cell receptor that augment T cell activation which includes *CD3E*, *GRAP2*, *LCK*, *TRBC1*, *LGALS1*, *PDCP1, UBC,* and *ZAP70.* In addition, another 3 genes associated with immune synapses were enriched in PD-1^{pos} NK cells. These synapses formed through associating of specific signalling and adhesion molecules between NK cells and target cells that associated with membrane rafts, and facilitate NK activation and killing target cells through release of effector granules and death pathways (Orange, 2008). Moreover, 3 genes coding for transmembrane receptor protein tyrosine kinase signalling pathways were also enriched in PD-1^{pos} NK cells. The initiation of these signals starts from binding extracellular ligand to its receptor with tyrosine activity on the cell surface and ends with regulation of cellular process such as gene transcription.

The next step was to determine the signalling pathways influenced by the pattern of differentiated transcription in PD-1^{pos} NK cells. KEGG pathway analysis tool (from DAVID

functional annotation tool) was used to identify enriched chemical pathways. There are at least 3 clusters of KEGG pathways, including T cell receptor signalling pathways (*CD3E, GRAP2, LCK, PDCD1, ZAP70*), regulation of actin cytoskeleton (*ACTB, ARPC5L, CFL, ITGB2, MYL12A, MYL12B, PFN1,PPP1CA, TMSB4X*), and primary immunodeficiency (*CD3E, LCK, ZAP70*) (**Figure 6.14**).

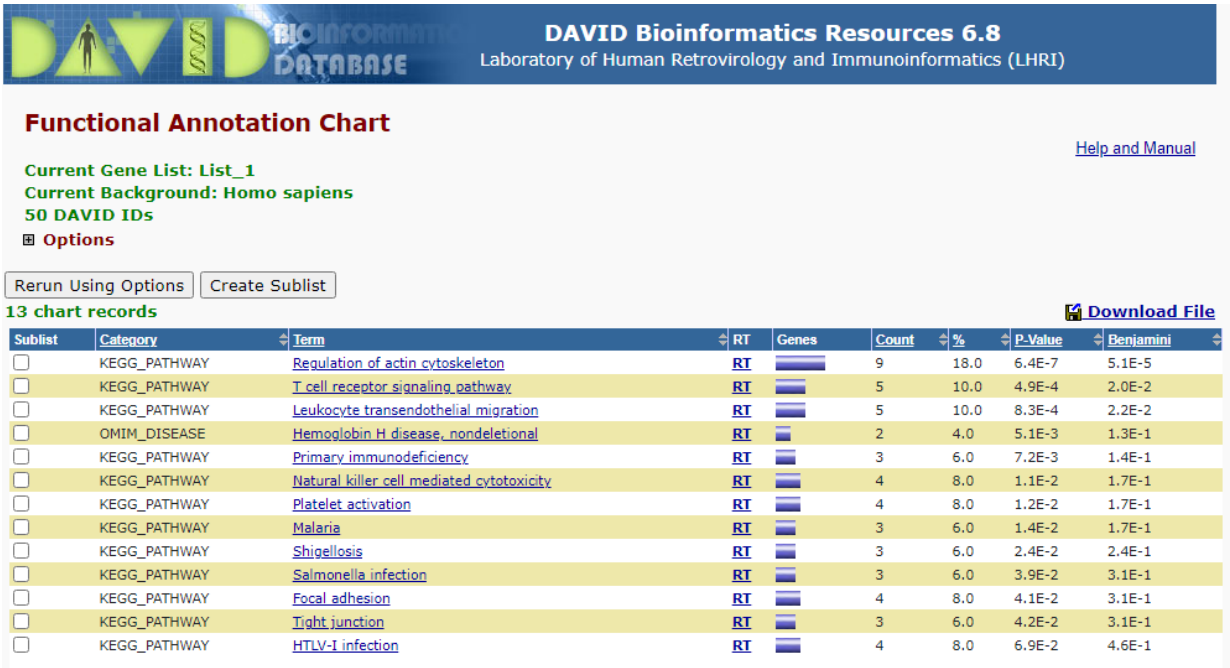

Sublist	Category	Term	RT	Genes	Count	%	P-Value	Benjamini
☐	KEGG_PATHWAY	Regulation of actin cytoskeleton	RT		9	18.0	6.4E-7	5.1E-5
☐	KEGG_PATHWAY	T cell receptor signaling pathway	RT		5	10.0	4.9E-4	2.0E-2
☐	KEGG_PATHWAY	Leukocyte transendothelial migration	RT		5	10.0	8.3E-4	2.2E-2
☐	OMIM_DISEASE	Hemoglobin H disease, nondeletional	RT		2	4.0	5.1E-3	1.3E-1
☐	KEGG_PATHWAY	Primary immunodeficiency	RT		3	6.0	7.2E-3	1.4E-1
☐	KEGG_PATHWAY	Natural killer cell mediated cytotoxicity	RT		4	8.0	1.1E-2	1.7E-1
☐	KEGG_PATHWAY	Platelet activation	RT		4	8.0	1.2E-2	1.7E-1
☐	KEGG_PATHWAY	Malaria	RT		3	6.0	1.4E-2	1.7E-1
☐	KEGG_PATHWAY	Shigellosis	RT		3	6.0	2.4E-2	2.4E-1
☐	KEGG_PATHWAY	Salmonella infection	RT		3	6.0	3.9E-2	3.1E-1
☐	KEGG_PATHWAY	Focal adhesion	RT		4	8.0	4.1E-2	3.1E-1
☐	KEGG_PATHWAY	Tight junction	RT		3	6.0	4.2E-2	3.1E-1
☐	KEGG_PATHWAY	HTLV-I infection	RT		4	8.0	6.9E-2	4.6E-1

Figure 6.14 KEGG pathway analysis of 50 top modulated genes in PD-1^{pos} NK population using DAVID functional annotation tool.

13 clusters of KEGG pathways were identified to be influenced by gene differentiated transcription in PD-1^{pos} NK cells.

6.2.2 Genome-wide chromatin accessibility study of PD-1^{pos}/PD-1^{neg} NK and whole NK cells from B-CLL/HC.

To investigate the landscape and dynamic of transcription regulatory machinery of particularly PD-1^{pos} NK cells, and whole NK cells from B-CLL, the assay of transposase accessible chromatin with sequencing (ATAC-seq) technique was applied. This assay is based on hyperactive Tn5 transposase (fragments and tags open regions of DNA) to assess chromatin accessibility. Sequencing reads from cells can reflect the accessible regions of chromatin (Y. Sun, Miao, et al., 2019). Whole NK population (CD56^{pos} CD3^{neg}) from B-CLL and HDs (n=3 each) were flow sorted. Also, we managed to sort enough cells from PD-1^{pos} CD56^{pos} CD3^{neg} NK cells in addition to PD-1^{neg} CD56^{pos} CD3^{neg} NK cells (50,000 cells each) from one B-CLL patient (297KB), followed by immediate DNA extraction, library preparation. Before Pool library was sent over to Genomic Birmingham department for sequencing, quality control of the ATAC-seq library was done to ensure that the library concentration meets the sequencing criteria (For full method refer to the material and methods). 75 cycle flow cell with 400M read capacity was used for sequencing using NextSeq 500 machine providing 50M reads per library, which is enough for the detection of open chromatin regions. FastQC analysis showed that ATAC-seq dataset was at high quality. Multiple bioinformatics analysis tools from R program were used for the analysis under the help from Dr Wayne Croft (not included in thesis). The spearman correlation analysis showed the read counts of each sample were similar to each other. In addition, spearman correlation of pairwise scatterplots of the average scores showed significant correlation between the variables (**Figure 6.15**).

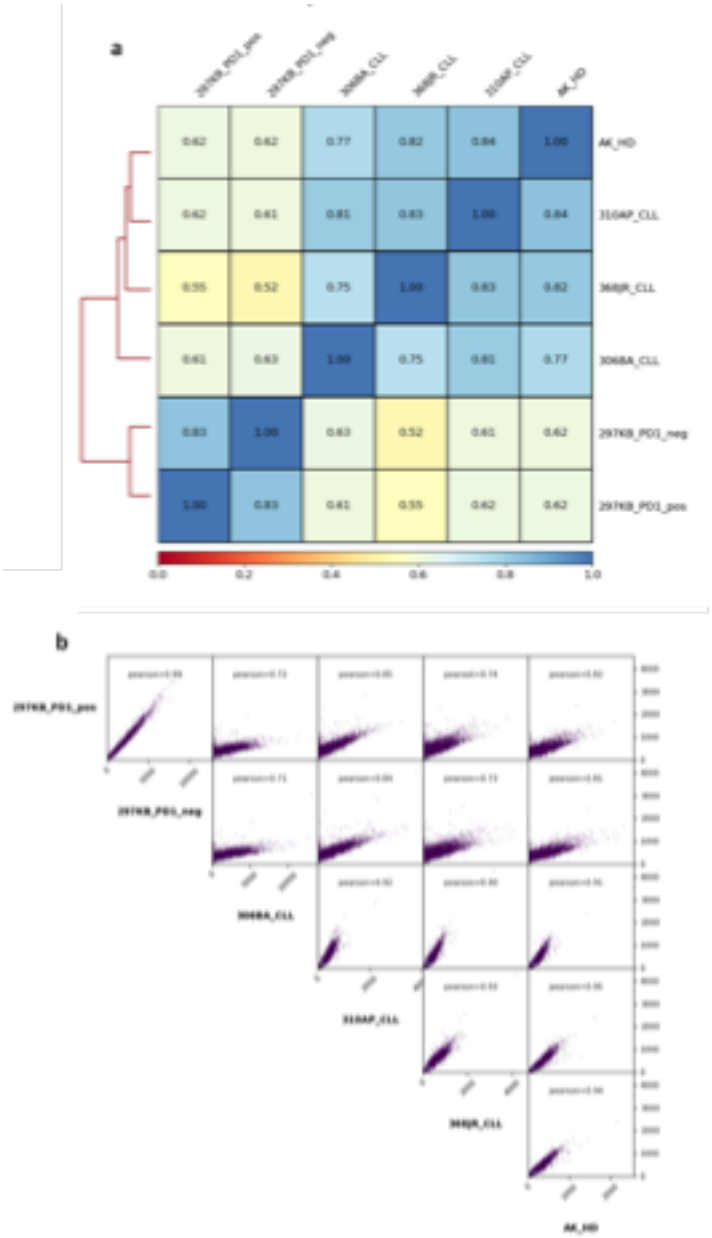

Figure 6.15 Correlation analysis on all CLL and HD samples

(**a**) Heatmap of the Pearson correlation coefficient of read counts of all samples with unsupervised clustering. Pairwise correlation can be detected by the variation in colour intensities and which sample's read counts are most similar to each other. (**b**) In addition to heatmap, pairwise scatterplots were generated for the average score of transcript with the Pearson correlation coefficient for each comparison.

6.2.2.1 The comparison of chromatin accessibility of PD-1^{pos} versus PD-1^{neg} NK cells and whole CLL-NK cells versus HC-NK cells.

We showed earlier that PD-1^{pos} NK cells have an altered transcription profile compared to PD-1^{neg} NK cells from B-CLL patients. To further investigate the gene expression regulatory of PD-1^{pos} vs PD-1^{neg} NK cells (n=1), chromatin accessibility was assessed for these NK cells. Interestingly, there is potentially increased read density close proximity to PD-1 promoter in PD-1^{pos} NK cells which may indicate increased accessibility of PD-1 sites (**Figure 6.16 green track**) compared to PD-1^{neg} NK cells (blue track). This indicates that there is potential correlation between PD-1 transcription and chromatin accessibility in PD-1^{pos} NK cells. However, as this data is only from one B-CLL patient, the conclusion that can be drawn from this assay is limited. Unfortunately, this experiment has to be stopped due to the COVID-19 pandemic. We plan to carry out the assay with at least 2 more donors to allow meaningful results in the future.

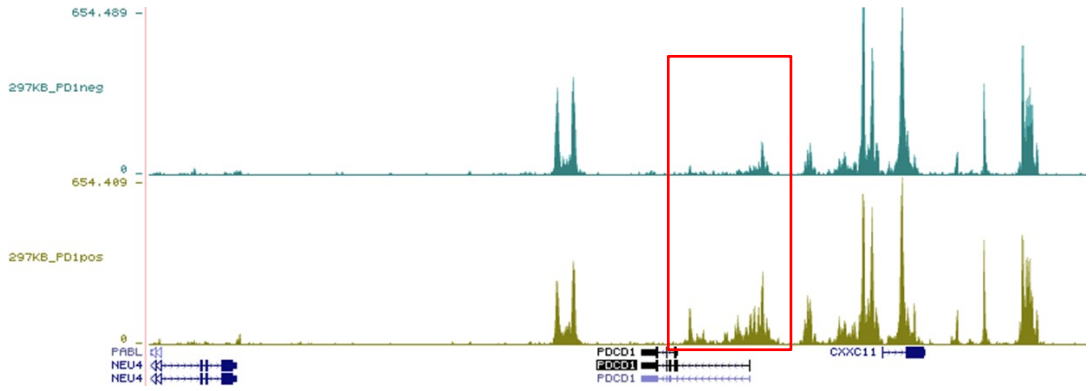

Figure 6.16 Chromatine accessibility of PD-1 promoter in PD-1^{pos} vs PD-1^{neg} NK cells

PD-1 open chromatin peaks shown in genome browser of PD-1^{pos} NK cells (grean peaks) vs PD-1^{neg} NK cells (blue peaks) from 297KB patient, y axis shows read counts.

We also looked at read densities of 86,742 regions in total NK population from CLL patients (n=3) and they were compared to age-matched of whole NK cells from HDs (n=3). Only 2 differential accessibility chromatin sites (DACs) were identified to be more accessible in NK cells from CLL patients based on the fold change (adjusted $p<0.05$). These sites were linked to the genes of *CYP4F11* and *SLC27A1*. Genes with promotors closest to DAC sites (*CYP4F11* and *SLC27A1*) have been shown to be involved in fatty acid metabolism and their oxygenated derivatives. (**Figure 6.18**). PCA and sample distance matrix clustering of these NK cells revealed two clusters of NK cells. Except one HD (AK), NK cells from CLL patients clustered far away from NK cells taken from HD (**Figure 6.17**), indicating the different chromatin accessibility between NK cells from B-CLL patients and NK cells from HDs. The analysis of this data is also ongoing.

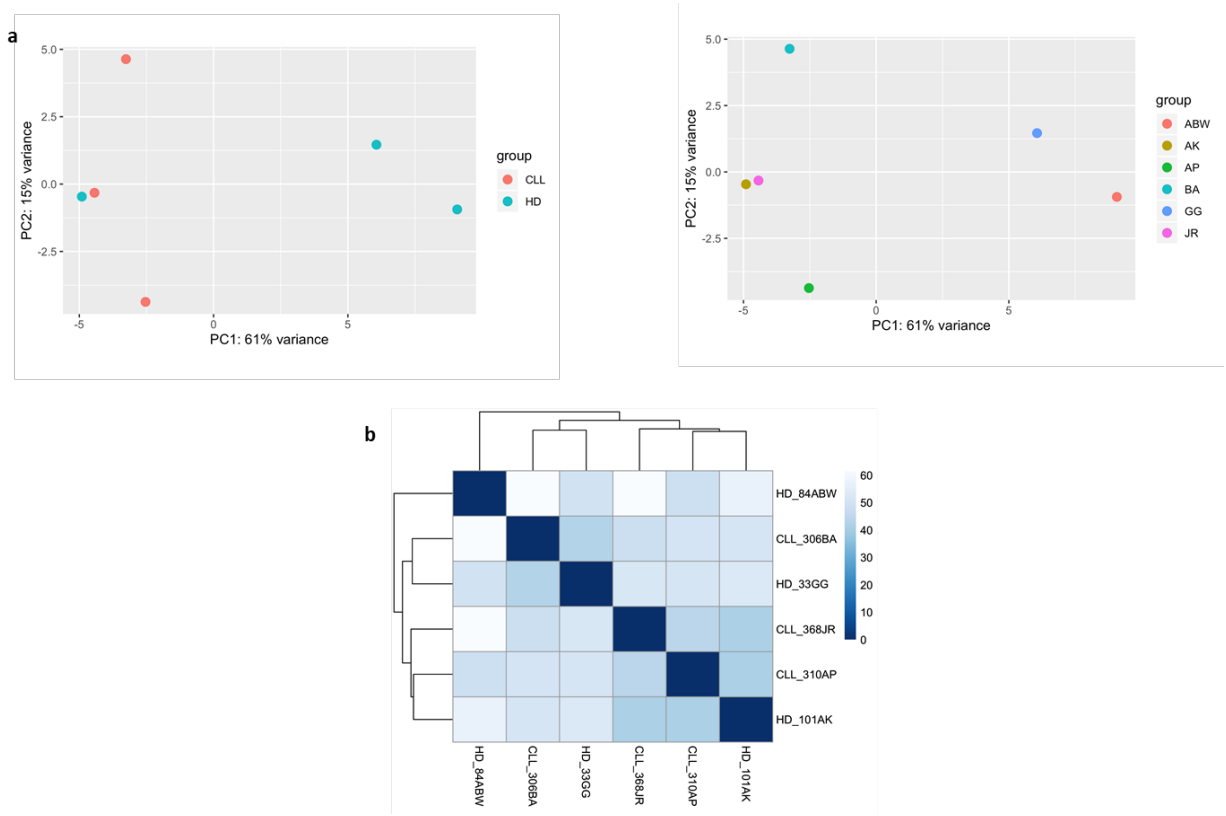

Figure 6.17 Comparisons of sample similarity of CLL-NK cells vs HD-NK cells

(**a**) PCA analysis of ATAC-seq samples from NK cells of CLL patients (n=3) and HDs (n=3), showing distinct separation of CLL samples vs HDs samples (left panel) and the ID label for each individaul donor (right panel). (**b**), Heatmap of the Pearson coefficiant correlation of all ATAC-seq samples.

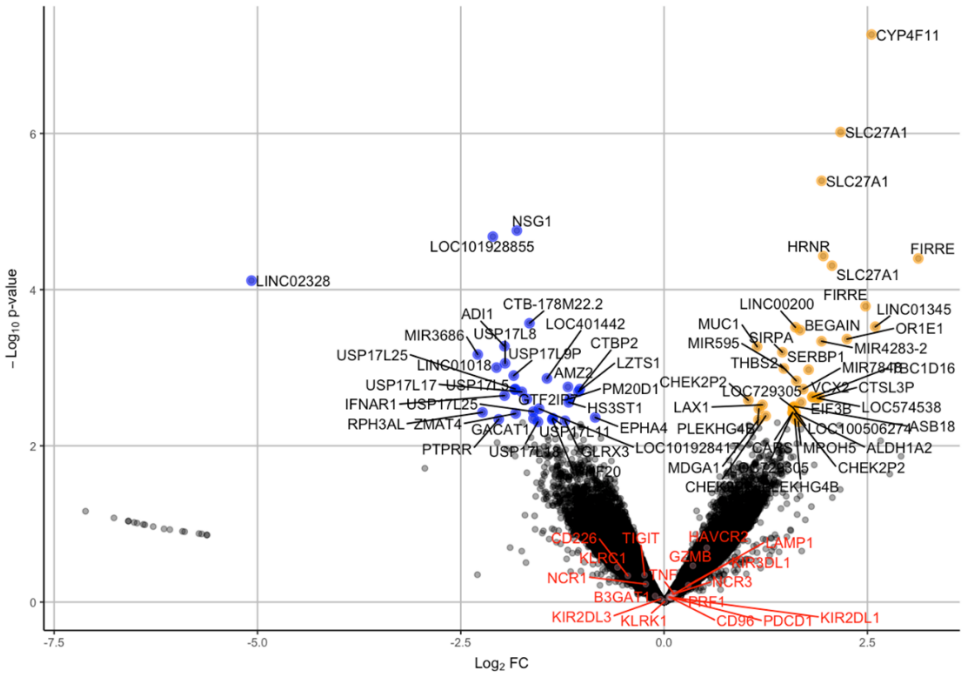

Figure 6.18 The differential accessible chromatin sites between CLL-NK and HD-NK cells using ATAC-seq.

Volcano plot to demonstrate the differential accessible chromatin sites between CLL-NK and HD-NK cells. Gene labelled in brown, and blue are those differentially upregulated or downregulated between CLL-NK cells and HC-NK cells. The gene labelled in red are the genes that are important for NK cell function. X axis is the Log2 fold change of read counts and Y axis is the P value.

6.3 Discussion

The previous chapters of this project have focused on the phenotypic and functional study between PD-1^{pos} and PD-1^{neg} NK cells from B-CLL patients. This chapter specifically aimed to explore the difference in terms of the transcription profile between PD-1^{pos} NK cells and PD-1^{neg} NK cells from B-CLL using scRNA-seq technology. This study can potentially reveal the underlying mechanism to explain the differences observed in phenotype and function of PD-1^{pos} NK cells. Also, this data can identify potential therapeutic targets to restore the PD-1^{pos} NK cells. In addition, the landscape of chromatin accessibility of PD-1^{pos} NK cells vs PD-1^{neg} NK cells and whole NK cells from CLL compared to whole NK cells from HD were investigated using ATAC-seq technology. scRNA-seq analysis showed seven distinct NK clusters. Based on the expression of known NK markers and transcription similarity, clusters were names as Cytotoxic, Activated, CD56^{bright}, Exhausted, Proliferating, Undetermined and Unknown. The analysis was carried out by two approaches. The first one is the analysis of PD-1^{pos} vs PD-1^{neg} NK cells within different clusters particularly cytotoxic and activated clusters. The second one is analysing PD-1^{pos} and PD-1^{neg} NK cells based on the whole NK population. The analysis showed that PD-1^{pos} NK cells exhibit altered transcription profile compared to PD-1^{neg} NK cells. This includes upregulation of gene transcription of some immune checkpoints such as LAG-3, adhesion molecules CD18, SPON2. On the other hand, the transcription of some important genes are downregulated, including activation marker CD69, transcription factors EOMES and ZNF683, and granzyme B. KEGG pathway analysis of modulated genes in PD-1^{pos} NK cells showed that there were 3 enriched pathways associated with T cell activation, regulation of actin cytoskeleton and primary immunodeficiency pathways.

ATAC-seq results has revealed minimal changes in chromatin accessibility sites between NK cells from B-CLL patients and HCs. Only 2 differential accessibility chromatin sites (DACs) were identified to be more accessible in NK cells from CLL patients compared to NK cells from HDs. These sites were linked to the genes of *CYP4F11* and *SLC27A1* which involved in the metabolism of fatty acids. The analysis of this data is ongoing, and more experiments will be needed.

6.3.1 scRNA-seq versus conventional RNA-seq

To further explore the potential mechanisms underlying PD-1expression and impaired functionality of PD-1^{pos} NK cells in B-CLL patients, transcription profile of PD-1^{pos} NK cells was investigated and compared to PD-1^{neg} counterparts. In contrast to conventional flow and CyTOF analysis that quantify maximum of 40 surface proteins, scRNA-seq enables genome-wide expression analysis at the transcription level. RNA-seq is a genome-wide approach, which allows us to detect and quantify the amount of mRNA molecules in the cellular samples. This will allow us to compare the transcription difference between different samples. RNA-seq analysis can be used to confirm the finding from phenotype and functional study and give far more information to explore the mechanism.

The amount of mRNA in a single cell is very low. Due to technique limitation, conventional RNA-seq was carried out using mixture of millions of cells to generate enough mRNA for analysis. This technology has been transformational for innovation research. However, the heterogeneity and complexity of cell population, even they probably identified as one single cell type like CD56^{pos}/CD3^{neg} NK cells are very much appreciated (Horowiz et al., 2013). Due to the technology development, the scRNA-seq allows us to analyse the transcriptomes from individual cell (Haque et al., 2017). The first scRNA-seq study was published in 2009 (Tang

et al., 2009). This will not only assess the differences of transcription profile among different single cells but also useful to identify potential rare populations. There have been many scRNA-seq studies on NK cells in recent years (Crinier et al., 2018; Yang et al., 2019). They revealed the heterogeneity of NK populations. From my knowledge, this study is the first scRNA-seq study on sorted PD-1^{pos} NK cells.

6.3.2 Transcription profile of immune checkpoints of PD-1^{pos} NK cells

From previous chapters, the data has revealed that PD-1^{pos} NK cells represent a phenotypically and functionally exhausted NK population. This scRNA-seq gives us another platform to study this impairment even further. PD-1 transcription was only present and elevated on PD-1^{pos} NK cells which confirm that PD-1 expression is real on NK cells and in line with conventional flow and CyTOF analysis. Various regulatory mechanisms control immune cell response including NK cells. Inhibitory checkpoints such as PD-1, CTLA-4 and LAG-3 play an important role in suppressing immune response (T cells) against tumor cells (Maruhashi et al., 2020). LAG-3 is not expressed on naïve T cells whilst their expression is induced upon stimulation and the inhibitory function induced by LAG-3 is strongly correlated to its expression on the cell surface (Maeda et al., 2019). Although LAG-3 is poorly investigated on NK cells, its expression has been observed on the mature NK subsets following exposure to IFN-α. LAG-3 expression has been linked to inhibition of cytokines production by NK cells which can be restored by LAG-3 blockade (Narayanan et al., 2020). We observed elevated gene transcription of LAG-3 on the PD-1^{pos} NK clusters from B-CLL patients, which indicated the co-expression of LAG-3 and PD-1 on PD-1^{pos} NK cells from B-CLL patients. They can both contribute to the functional impairment of PD-1^{pos} NK cells. In chapter 3, we have shown that LAG-3 surface expression was elevated on NK cells from B-CLL patients compared to NK cells from HCs using flow

cytometry (**Figure 3.7** in chapter 3). LAG-3 could be a potential therapeutic target to restore the dysfunction of NK population particularly PD-1^{pos} NK cells which need to be investigated in B-CLL patients.

Another important immune checkpoint CD39 that was shown to be increased on PD-1^{pos} NK cells from CyTOF data. However, its transcription was not observed on PD-1^{pos} NK clusters. The discrepancy of protein level and transcription level will need more investigation. This could be due to the post-transcription modification of CD39.

6.3.3 Transcription of effector molecules of PD-1pos NK cells

Transcription factors are important elements in the biology of NK cells. They have been found to regulate NK cell differentiation, effector, and memory response in a shared and unique way (Brillantes & Beaulieu, 2019). In CD8^{+} T cells and NK cells, EOMES and T-bet expression are broadly overlapping. Similar to what has been reported in T cells, EOMES and T-bet collectively regulate IFN-γ production in NK cells in a compensatory manner. They bind directly to the *ifng* promoter region and induce its transcription (Miller et al., 2010) . However, T-bet seems to have the main regulatory role in IFN-γ production, as its expression is indispensable during initiation phase of IFN-γ production. Moreover, T-bet appears to be a key regulatory of NK cytotoxicity activity by its ability to bind to *Gzmb* and *prf1* promotor regions of NK cells, whilst EOMES work as a cooperative factor with T-bet to augment cytotoxicity of NK cells (Simonetta et al., 2016).

In addition, PD-1^{pos} NK within activated cluster exhibited low transcription of GzmB. The cytotoxic pathway of GzmB/Perforin has been known to be a major mechanism by which NK and other lymphocytes used to eradicate virally infected and tumor cells (Boivin et al., 2009). In addition, EOMES has been identified as a key regulatory of GzmB and perforin expression, which control cytotoxic function of $CD8^+$ T cells. NK cell exhaustion is associated with dysfunctional phenotype which accompanied with downregulation of EOMES and T-bet in one study using the adoptively transferred murine NK cells. Interestingly, this exhausted state of NK cells can be partially reversed by forced overexpression of EOMES (Gill et al., 2012). Collectively, this data suggests that low EOMES transcription in PD-1pos NK cells within cytotoxic cluster at least partially play a role in the reduced cytokines production and cytotoxicity observed in PD-1^{pos} NK cells. In addition, EOMES can be a potential novel therapeutic target to restore PD-1^{pos} NK cells in B-CLL patients.

The transcription profile of PD-1^{pos} NK cells was also analysed using KEGG pathways. There was 14 genes grouped in 3 clusters which involved in T cell receptor signalling pathways (*CD3E, GRAP2, LCK, PDCD1, ZAP70*), regulation of actin cytoskeleton (*ACTB, ARPC5L, CFL, ITGB2, MYL12A, MYL12B, PFN1,PPP1CA, TMSB4X*), and more importantly primary immunodeficiency pathways (*CD3E, LCK, ZAP70*). These data indicate that PD-1^{pos} NK cells are activated, but actin cytoskeleton pathway might be dysfunctional and affect the formation of the immune synapse. The enriched immunodeficiency pathway fit in with the observation of defected killing function by PD-1^{pos} NK cells in this study.

Although this is the first study of scRNA-seq on PD-1^{pos} NK cells (as best of my knowledge), the analysis was very preliminary and still ongoing. This was due to the huge heterogeneity of NK cell population, time limitation to do more in-depth analysis and limitation in sample supply due to COVID-19 pandemic as the plan was to run minimum of 3 samples with high PD-1^{pos} NK cells. In addition, it's recommended to run CITE-seq along with these data to measure both cellular transcription and associated proteins as some important genes lack the expression in our data such as CD56 and genes for exhaustion markers .

6.4 Conclusion

In conclusion, the transcription profile of PD-1^{pos} NK cells was studied and compared with PD-1^{neg} NK cells in B-CLL patients using scRNA-seq. The data has revealed the heterogenicity of NK population. 7 distinct NK populations have been clustered based on the transcription profile. PD-1^{pos} NK cells exhibit altered transcription profile compared to PD-1^{neg} counterparts. This was more explicit particularly on cytotoxic and activated NK cells. 302 genes were identified to be differentially transcribed between PD-1^{pos} and PD-1^{neg} NK cells based on the whole NK population. There are upregulation of gene transcription of checkpoint receptors in PD-1^{pos} NK cells, like LAG-3. Also, the gene transcription of some important transcription factors and effector molecules, including ID-2, GzmB and EOMES are downregulated in PD-1^{pos} NK cells. This study has potentially identified a few novel therapeutic targets to reverse the impaired function of PD-1^{pos} NK cells in B-CLL patients.

CHAPTER 7: GENERAL DISCUSSION

7.1 discussion

NK cells play an important role in cancer immunosurveillance and function to supress tumor growth. They can recognise and directly kill tumor or virally infected cells. NK cells recognise target cells (tumor or infected cells) through a ray of activating receptors expressed on their surface and their cognate ligands on target cells, which activate NK cell receptors and induces cytotoxicity (Lodoen & Lanier, 2005). However, cancer cells have the ability to develop mechanisms to resist immune system including NK cells in order to proliferate and grow. Interaction of cancer cells and NK cell surveillance works on three stages, exclusion, or elimination stage, that NK cells completely wipe cancer cells, equilibrium stage that there is a balance of cancer cells and NK cells, and at last escape stage that NK cells unable to recognise, kill cancer cells and control their proliferation (Nouroz et al., 2016).

In my PhD project, I focused on the NK cell function in B-CLL patients. B-CLL is the most common form of adult leukaemia in western countries that characterised by clonal expansion of B-CLL cells. Despite the total number of NK cells in B-CLL patients are increased compared to age-matched HDs, NK cell cytotoxicity in B-CLL has been reported to be impaired since decade ago. This impairment leads to decreased anti-tumor surveillance and increase risk of infections (Forconi & Moss, 2015). However, full NK cell functions in B-CLL are not well understood, and data on NK phenotype and functionality are sometimes controversial (Katrinakis et al., 1996). The focus of this study was to explore the potential harness of NK cells as a novel immunotherapeutic strategy if their functions can be restored by sufficient and proper activation signal in B-CLL patients. (E. Liu et al., 2020).

In the present study, the frequency, extensive phenotyping, and functionality of NK cells from B-CLL patients were investigated. In particular, the study focused on PD-1^{pos} NK cells, including the phenotype, functionality, and transcription profile. In addition, PD-1 blockade was studied in restoring the anti-tumor activities of PD-1^{pos} NK cells from B-CLL patients. Moreover, DNAM-1 dependent NK cell cytotoxicity against tumor cell line was studies, including the checkpoint blockade with anti-TIGIT and/or CD96.

7.1.1 Overall phenotype and function impairment of NK cells in B-CLL patients

As discussed in chapter 1 and in agreement with previous studies (Hofland, Eldering, et al., 2019; Le Garff-Tavernier et al., 2011), our data showed that the frequency of total NK cells was significantly lower in B-CLL patients compared to age-matched healthy controls. In contrast, the frequency of NK subsets with cytotoxic potential CD56^{dim} CD16^{pos} and CD56^{bright} CD16^{pos} were significantly increased whilst the frequency of non-cytotoxic NK subsets CD56^{bright} CD16^{neg} and CD56^{dim} CD16^{neg} were substantially lower in B-CLL patients compared to HCs. We presume that the lower total NK cells in B-CLL patients is due to the high frequency of tumor B cells in those patients. Also, high cytotoxic NK subsets in B-CLL patients are induced by tumor microenvironment and B-CLL cells, as we found that the absolute count of cytotoxic potential NK subsets increased in line with tumour B-CLL cells count. However, we failed to perform the absolute count of total NK and NK subsets in age matched HCs to be compared with B-CLL patients due to COVID-19 pandemic and time limitation.

The phenotype and function of NK cells from B-CLL patients were extensively compared to HCs. The striking and novel findings in the current study are the up-regulation of some immune checkpoints on NK cells from B-CLL patients compared to HCs particularly PD-1,

CTLA-4, LAG-3 and CD96, whilst no significant changes in expression of TIGIT, TIM-3 and NKG2A receptors. Very interestingly, we found that the up-regulation of these checkpoints PD-1, CTLA-4, LAG-3 and CD96 were restricted on $CD56^{dim}$ NK subsets and more pronounced on cytotoxic $CD56^{dim}$ $CD16^{pos}$ NK cells. The exact role of these checkpoints on NK cells needs to be investigated in future studies as we only investigated the phenotype, functionality, and transcription profile of PD-1^{pos} NK cells in B-CLL patients. In addition, we report for the first time that the expression of some adhesion molecules is down regulated on NK cells from B-CLL patients compared with HCs, and this reduction was more pronounced on $CD56^{dim}$ $CD16^{neg}$ NK subsets compared with $CD56^{dim}$ $CD16^{neg}$ from HCs. Presumably, although this needs more investigation our data suggest that NK cells from B-CLL patients are less able to move and migrate towards target cells and have defects in cytotoxicity capacity, as adhesion molecules play an important role in these functions of NK cells.

NK cell is considered as one of the main components of the immune cells that produce considerable amounts of cytokines after stimulation. In my study, intracellular cytokine staining following stimulation with tumor cell line K562 showed that NK cells from B-CLL patients produce significantly lower IFN-γ compared to HCs. This reduction strongly correlated with the frequency of $CD56^{dim}$ $CD16^{neg}$ in the B-CLL patients. $CD56^{dim}$ $CD16^{neg}$ NK subset is the main producer of the cytokines after tumor cell line stimulation and are lower in B-CLL patients than in HCs. This indicates that lower IFN-γ production by NK cells from B-CLL patients is at least partially due to the reduced frequency of $CD56^{dim}$ $CD16^{neg}$ NK subsets. The limitation here is we were not able to do the absolute counting of $CD56^{dim}$ $CD16^{neg}$ NK subsets from particularly those B-CLL patients due to the stop of clinical samples because of COVID pandemic.

Moreover, NK cell cytotoxicity has been reported to be impaired in B-CLL patients, particularly NKG2D dependent NK cytotoxicity against tumor cell lines (Parry, et al., 2016; Veuillen et al., 2012). The lower cytotoxicity of NK cells is attributed to the lower expression of NKG2D activating receptor on NK cells from B-CLL patient. In this study we showed for the first time that DNAM-1 dependent NK cytotoxicity against tumor cell line was also significantly impaired compared to HCs. Our explanation of the impairment of DNAM-1 dependent NK killing in B-CLL patients is due to the lower expression of DNAM-1 and up-regulation of CD96 inhibitory receptor on NK cells, which competes with DNAM-1 for the same ligands on the target cells. The balance of DNAM-1/TIGIT/CD96 expression on NK cells from B-CLL patients shift to be more inhibitory phenotype. Interestingly, we also showed for the first time that blocking TIGIT and/or CD96 can robustly reverse the impairment of DNAM-1 dependent cytotoxicity of NK cells in B-CLL patients using *in vitro* model of CD-155 transduced CHO target cells. In addition, we observed that patients with high TIGIT positive NK cells were more responsive to TIGIT blockade compared to B-CLL patients with normal/low TIGIT positive NK cells. As such, these data indicate that TIGIT and CD96 receptors might be potential therapeutic targets to restore DNAM-1 cytotoxicity and reverse the inhibitory phenotype shift of DNAM-1/TIGIT/CD96 receptors on NK cells from B-CLL patients. In addition, CD155/CD112 expression on B-CLL cells are worth to be explored, as they are important factor in regulating NK/B-CLL tumor cell interaction.

7.1.2 Phenotype, functionality and transcription profile of PD-1^{pos} NK cells

One of the major observations of this study is the up-regulation of PD-1 on NK cells from B-CLL patients. Conventional flow and CyTOF data showed that PD-1 expression was confined on CD56^{dim} NK subset but minimal on CD56^{bright} NK subsets, and the expression was most

pronounced on $CD56^{dim}$ $CD16^{pos}$ subsets. Interestingly, our data showed that although PD-1^{pos} NK cells are fully mature NK cells by expressing high CD57 and low NKG2A, they express significantly lower activating receptors including NKG2D,DNAM-1 and NCRs compared with PD-1^{neg} counterparts. In addition, PD-1^{pos} NK cells exhibited more distinct phenotype compared to PD-1^{neg} NK cells by up-regulation of CD11c adhesion molecule and CCR7 chemokines, indicating the active migratory of these cells. Moreover, we observed co-expression of other inhibitory receptors with PD-1 on NK cells such as CD39 and TIGIT was evidently higher on PD-1^{pos} NK cells. This suggests that PD-1^{pos} NK cells represent the activated NK cells, but the long-term activation has driven the upregulation of other inhibitory receptors such as CD39 and lead to an exhausted phenotype.

As such, the anti-tumor activity of PD-1^{pos} NK cells was significantly lower compared to PD-1^{neg} NK cells. PD-1^{pos} NK cells produce substantially lower pro-inflammatory cytokines and show reduced degranulation after stimulation with tumor cell lines K562 or 721.221, and the impairment of cytokines production and the reduced degranulation were more profound after stimulation with 721.221. This indicates that PD-1expression on NK cells mediates suppression of NK cell function particularly after interaction with its ligands PDL1 and PDL2. However, we also demonstrated that blocking of PD-1/PDL1,2 interactions using anti PDL1 and PDL2 antibodies has partially restored the anti-tumor functions of NK cells. This observation seen specifically when 721.221 were used as target cells. As we showed from CyTOF analysis that PDL1 and PDL2 were expressed on other immune cells including $CD14^{pos}$ monocytes and NK cells themselves, this suggests that PD-1 blockade in B-CLL patients can potentially reinvigorate PD-1^{pos} NK cells to target tumor B CLL cells. One limitation of this study is that we could not perform the direct killing experiment by primary PD-1^{pos} NK cells from B-CLL patients due to the low viability and limited number of PD-1^{pos} NK cells after

FACS sorting and limited choice of patients with high PD-1^{pos} NK cells. However, the functionality of PD-1^{pos} NK cells including killing capacity was further validated by *in vitro* experiments using two PD-1 transduced NK cell line models, which showed lower degranulation and cytotoxicity capacity compared to wt-NK cell lines. In addition, PD-1/PDL1,2 blockade has also partially restored the degranulation and cytotoxicity of PD-1^{pos} NK-92 against 721.221 target cells.

As discussed in chapter 6, scRNA-seq was used to further investigate the underlying mechanisms of phenotypic and functional changes of PD-1^{pos} NK cells from B-CLL patients. Also, this analysis aims to identify potential therapeutic targets to restore the anti-tumor activity of PD-1^{pos} NK cells. Our analysis showed that PD-1^{pos} NK cells exhibited differentiated transcription profile compared to PD-1^{neg} counterparts. Transcription of some immune checkpoints were up-regulated in PD-1^{pos} NK cells such as LAG-3 in addition to PD-1. Also, surface expression of LAG-3 was observed to be significantly higher on the whole NK population from B-CLL patients compared to HCs, indicating the contribution of PD-1^{pos} NK cells in this overall increase of LAG-3 expression. In addition, the transcription of some important transcription factors and effector molecules were downregulated on PD-1^{pos} NK cells, including GzmB, EOMES and ID-2 which particularly might be potential therapeutic targets. For example, enhancing ID-2 expression on PD-1^{pos} NK cells should restore NK cell cytotoxicity function, as ID-2 is essential for NK maturation, expansion and function (Boos et al., 2007; Kee et al., 2019). ID-2 activator that increase the interaction between RNA polymerase and the promoter of ID-2 can be used to enhance the expression of ID-2 gene in PD-1^{pos} NK cells.

Due to the limitation in B-CLL samples (with high PD-1^{pos} NK cells) and time limitation of this study, we could not assess the transcription profile and cell behaviour of PD-1^{pos} NK cells after PD-1 blockade, therefore we recommend this in future studies. Another limitation of this study is that we used anti-PDL1 and PDL2 antibodies to block PD-1 signalling pathway. We could not block PD-1 itself in primary NK cells as PD-1 is the only identified marker for PD-1^{pos} NK cells and therefor these cells won't be stained with anti PD-1 antibody and identified during analysis. Potentially, PD-1 blockade probably would have been more efficient effect on the reversion of exhausted immune cells than blocking PD-1 ligands.

The therapeutic potential of PD-1 blockade to restore antitumor function of PD-1^{pos} NK cells in B-CLL patients cannot be ignored. Very recently, It has been shown that the up-regulation of PD-1 on intratumoral NK cells from non-small cell lung cancer (NSCLC) patients was correlated with the dysfunctional of these PD-1^{pos} NK cells. In addition, PD-1^{pos} NK cells from those patients express more inhibitory receptors compared to PD-1^{neg} NK cells. Also, It has been hypothesized that tumor cells expressing PDL1 suppressed the functionality of PD-1^{pos} NK cells leading to tumor cells escape NK cells mediated attack. However, PD-1 blockade has reversed the function of PD-1^{pos} NK cells, suggesting a therapeutic potential of PD-1^{pos} NK cells with immune checkpoint blockade (Trefny et al., 2020). One major finding in this study was up-regulation of PD-1 on NK cells from B-CLL patients. Moreover, PD-1 expression was co-expressed with other immune checkpoints, and its expression was correlated with the impairment of NK cell functions in B-CLL patients. Also, this study showed that by masking PD-1 signalling using PDL1, PDL2 specific blocking antibodies on the target cells can reverse the anti-tumor activity of PD-1^{pos} NK cells (primary and NK cell lines) including increased IFN-γ production, degranulation, and cytotoxicity.

B-CLL patients with high PD-1^{pos} NK cells might benefit from PD-1 blocking to activate NK cells against tumor B CLL cells, as PDL1 and PDL2 were expressed by other adjacent immune cells including monocytes and NK cells themselves within tumor microenvironment. Interaction of PD-1^{pos} NK cells with immune cells expressing PDL1 and PDL2 inhibits the function of PD-1^{pos} NK cells as demonstrated by *ex vivo* and *in vitro* assays. Although blocking PD-1 signalling has partially reversed the functionality of PD-1^{pos} NK cells, there is a possibility that PD-1^{pos} NK cells are still inhibited by other immune checkpoints such as LAG-3 and CD39. Therefore, blocking these immune checkpoints in combination with NK stimulating agents can be very effective strategies to fully unleash the functionality of PD-1^{pos} NK cells.

7.1.3 Future directions

The findings of this work have shown that the balance in activating and inhibitory receptors is broken on NK cells from B-CLL patients by upregulation of PD-1, CTLA-4, LAG-3 and CD96. In this project, the role of PD-1 expression on NK cells has been extensively investigated. As discussed previously that blocking PD-1 signalling through anti PDL1 and anti PDL2 antibodies has partially reversed the anti-tumor activity of PD-1^{pos} NK cells in B-CLL patients and PD-1 transduced NK-92 cell lines, therefore it is important to investigate other potential targets from scRNA-seq analysis that were downregulated or upregulated in PD-1^{pos} NK cells, such as ID2, and LAG-3 genes that potentially further improve the anti-tumor function of PD-1^{pos} NK cells. Also, this work has showed that there is a potential increase in read density close proximity to PD-1 promoter in PD-1^{pos} NK cells, which may indicate increased accessibility of PD-1 sites however this data was from only on B-CLL patient and would be interesting to do at least three other B-CLL patients with high percentage of PD-1^{pos}NK cells. In addition, as

mentioned previously blocking PD-1 signalling in NK cells has been performed using anti PDL1 and anti PDL2 antibodies, it is worth to investigate blocking PD-1 receptor itself as well as this might be more efficient in restoring PD-1^{pos} NK cells.

It will be also important to investigate the other checkpoints in terms of their role on NK cells and the beneficial of blocking these checkpoints that are upregulated on NK cells from B-CLL patients, including CTLA-4, LAG-3 and CD96. They might contribute to the overall suppression and functional impairment of NK cells in B-CLL patients. These checkpoints might be successful therapeutic targets to further restore the anti-tumor activity of NK cells in B-CLL patients.

7.2 Conclusion

In this study, overall phenotype and functionality of NK cells in B-CLL patients were extensively studied at first. The PD-1^{pos} NK cells were the focus of the second part of this study. For the overall NK population, we found that there is an increased frequency of cytotoxic potential NK subsets and non-cytotoxic potential NK subsets were decreased in B-CLL patients compared to age-matched HCs. Not only the frequency of NK cells was altered in those patients, phenotype and functionality of NK cells were significantly altered. The major finding of our study is the up-regulation of immune checkpoints such as PD-1, LAG-3, CTLA-4 and CD96, and down-regulation of activating receptors and adhesion molecules on NK cells from B-CLL patients including NKG2D, DNAM-1, NCRs and CD43, CD49d, CD49a respectively. This phenotype modification switches NK cells to be functionally inhibited particularly against tumor B CLL cells. This embedded in the impaired DNAM-1 dependent NK cytotoxicity capacity, which can be successfully reversed upon TIGIT and/or CD96 blockade. NK cells from B-CLL patients produce significantly lower IFN-γ compared to HCs and this reduction strongly correlated with the frequency of CD56^{dim} CD16^{neg} in B-CLL patients. We have demonstrated a significant up-regulation of PD-1 expression on NK cells from B-CLL patients for the first time. PD-1 expression was confined on the fully mature, cytotoxicity NK subset NKG2A^{low}CD57^{high}CD56^{dim} CD16^{pos}, the functionality of PD-1^{pos} NK cells was significantly impaired compared to the PD-1^{neg} counterparts. This observation was further pronounced after engagement of PD-1 with its respective ligands PDL1 and PDL2 on the target cells. The functional impairment of PD-1^{pos} NK cells was partially reversible by blocking PD-1/PD-1Ls interactions.

Altogether, our findings demonstrated that NK cells are dysfunctional in B-CLL patients and PD-1 expression is one of the mechanisms that can negatively regulate anti-tumor function of NK cells. Blocking PD-1signalling enhanced the anti-tumor function of PD-1^{pos} NK cells. Furthermore, as NK cells in B-CLL patients exhibited inhibitory phenotype, multiple immune checkpoints blockade including PD-1 in combination with NK stimulator agents are high likely to be successful therapeutic approach in B-CLL patients.

REFERENCES

Alberts, B., Johnson, A., Lewis, J., Raff, M., Roberts, K., & Walter, P. (2002). Innate Immunity. *Molecular Biology of the Cell. 4th Edition*. https://www.ncbi.nlm.nih.gov/books/NBK26846/

Chaplin, D. D. (2010). Overview of the immune response. *Journal of Allergy and Clinical Immunology*, *125*(2), S3–S23. https://doi.org/10.1016/j.jaci.2009.12.980

Georgountzou, A., & Papadopoulos, N. G. (2017). Postnatal Innate Immune Development: From Birth to Adulthood. *Frontiers in Immunology*, *8*. https://doi.org/10.3389/fimmu.2017.00957

Gasteiger, G., D'Osualdo, A., Schubert, D. A., Weber, A., Bruscia, E. M., & Hartl, D. (2017). Cellular Innate Immunity: An Old Game with New Players. *Journal of Innate Immunity*, *9*(2), 111–125. https://doi.org/10.1159/000453397

Marshall, J. S., Warrington, R., Watson, W., & Kim, H. L. (2018). An introduction to immunology and immunopathology. *Allergy, Asthma, and Clinical Immunology : Official Journal of the Canadian Society of Allergy and Clinical Immunology*, *14*(Suppl 2). https://doi.org/10.1186/s13223-018-0278-1

Huergo-Zapico, L., Acebes-Huerta, A., Gonzalez-Rodriguez, A. P., Contesti, J., Gonzalez-García, E., Payer, A. R., Villa-Alvarez, M., Fernández-Guizán, A., López-Soto, A., & Gonzalez, S. (2014). Expansion of NK Cells and Reduction of NKG2D Expression in Chronic Lymphocytic Leukaemia. Correlation with Progressive Disease. *PLOS ONE*, *9*(10), e108326. https://doi.org/10.1371/journal.pone.0108326

Palmer, S., Hanson, C. A., Zent, C. S., Porrata, L. F., LaPlant, B., Geyer, S. M., Markovic, S. N., Call, T. G., Bowen, D. A., Jelinek, D. F., Kay, N. E., & Shanafelt, T. D. (2008). The Prognostic Importance of T and NK-cells in a Consecutive Series of Newly Diagnosed Patients with Chronic Lymphocytic Leukaemia. *British Journal of Haematology*, *141*(5). https://doi.org/10.1111/j.1365-2141.2008.07070.x

Hofland, T., Endstra, S., Gomes, C. K. P., de Boer, R., de Weerdt, I., Bobkov, V., Riedl, J. A., Heukers, R., Smit, M. J., Eldering, E., Levin, M.-D., Kater, A. P., & Tonino, S. H. (2019). Natural Killer Cell Hypo-responsiveness in Chronic Lymphocytic Leukaemia can be Circumvented In Vitro by Adequate Activating Signaling. *HemaSphere*, *3*(6), e308. https://doi.org/10.1097/HS9.0000000000000308

Amand, M., Iserentant, G., Poli, A., Sleiman, M., Fievez, V., Sanchez, I. P., Sauvageot, N., Michel, T., Aouali, N., Janji, B., Trujillo-Vargas, C. M., Seguin-Devaux, C., & Zimmer, J. (2017). Human CD56dimCD16dim Cells As an Individualized Natural Killer Cell Subset. *Frontiers in Immunology*, *8*. https://doi.org/10.3389/fimmu.2017.00699

Béziat, V., Descours, B., Parizot, C., Debré, P., & Vieillard, V. (2010). NK Cell Terminal Differentiation: Correlated Stepwise Decrease of NKG2A and Acquisition of KIRs. *PLOS ONE*, *5*(8), e11966. https://doi.org/10.1371/journal.pone.0011966

Müller-Durovic, B., Grählert, J., Devine, O. P., Akbar, A. N., & Hess, C. (2019). CD56-negative NK cells with impaired effector function expand in CMV and EBV co-infected healthy donors with age. *Aging (Albany NY)*, *11*(2), 724–740. https://doi.org/10.18632/aging.101774

Le Garff-Tavernier, M., Decocq, J., de Romeuf, C., Parizot, C., Dutertre, C. A., Chapiro, E., Davi, F., Debré, P., Prost, J. F., Teillaud, J. L., Merle-Beral, H., & Vieillard, V. (2011). Analysis of CD16+CD56dim NK cells from CLL patients: Evidence supporting a therapeutic strategy with optimized anti-CD20 monoclonal antibodies. *Leukaemia*, *25*(1), 101–109. https://doi.org/10.1038/leu.2010.240

Caligiuri, M. A. (2008). Human natural killer cells. *Blood*, *112*(3), 461–469. https://doi.org/10.1182/blood-2007-09-077438

MacFarlane, A. W., Jillab, M., Smith, M. R., Alpaugh, R. K., Cole, M. E., Litwin, S., Millenson, M. M., Al-Saleem, T., Cohen, A. D., & Campbell, K. S. (2017). NK cell dysfunction in chronic lymphocytic leukemia is associated with loss of the mature cells expressing inhibitory killer cell Ig-like receptors. *Oncoimmunology*, *6*(7), e1330235. https://doi.org/10.1080/2162402X.2017.1330235

Cao, Y., Wang, X., Jin, T., Tian, Y., Dai, C., Widarma, C., Song, R., & Xu, F. (2020). Immune checkpoint molecules in natural killer cells as potential targets for cancer immunotherapy. *Signal Transduction and Targeted Therapy*, *5*(1), 1–19. https://doi.org/10.1038/s41392-020-00348-8

Zou, W. (2018). Mechanistic insights into cancer immunity and immunotherapy. *Cellular & Molecular Immunology*, *15*(5), 419–420. https://doi.org/10.1038/s41423-018-0011-5

Chiossone, L., Vienne, M., Kerdiles, Y. M., & Vivier, E. (2017). Natural killer cell immunotherapies against cancer: Checkpoint inhibitors and more. *Seminars in Immunology*, *31*, 55–63. https://doi.org/10.1016/j.smim.2017.08.003

Ntsethe, A., Dludla, P. V., Nyambuya, T. M., Ngcobo, S. R., & Nkambule, B. B. (2020). The impact of immune checkpoint inhibitors in patients with chronic lymphocytic leukemia (CLL). *Medicine*, *99*(28). https://doi.org/10.1097/MD.0000000000021167

Hannani, D., Vétizou, M., Enot, D., Rusakiewicz, S., Chaput, N., Klatzmann, D., Desbois, M., Jacquelot, N., Vimond, N., Chouaib, S., Mateus, C., Allison, J. P., Ribas, A., Wolchok, J. D., Yuan, J., Wong, P., Postow, M., Mackiewicz, A., Mackiewicz, J., … Zitvogel, L. (2015). Anticancer immunotherapy by CTLA-4 blockade: Obligatory contribution of IL-2 receptors and negative prognostic impact of soluble CD25. *Cell Research*, *25*(2), 208–224. https://doi.org/10.1038/cr.2015.3

Kim, N., & Kim, H. S. (2018). Targeting Checkpoint Receptors and Molecules for Therapeutic Modulation of Natural Killer Cells. *Frontiers in Immunology*, *9*. https://doi.org/10.3389/fimmu.2018.02041

Stojanovic, A., Fiegler, N., Brunner-Weinzierl, M., & Cerwenka, A. (n.d.). CTLA-4 Is Expressed by Activated Mouse NK Cells and Inhibits NK Cell IFN-g Production in Response to Mature Dendritic Cells. *The Journal of Immunology*, 9.

Taube, J. M., Anders, R. A., Young, G. D., Xu, H., Sharma, R., McMiller, T. L., Chen, S., Klein, A. P., Pardoll, D. M., Topalian, S. L., & Chen, L. (2012). Colocalization of Inflammatory Response with B7-H1 Expression in Human Melanocytic Lesions Supports an Adaptive Resistance Mechanism of Immune Escape. *Science Translational Medicine*, *4*(127), 127ra37-127ra37. https://doi.org/10.1126/scitranslmed.3003689

Blake, S. J., Stannard, K., Liu, J., Allen, S., Yong, M. C. R., Mittal, D., Aguilera, A. R., Miles, J. J., Lutzky, V. P., de Andrade, L. F., Martinet, L., Colonna, M., Takeda, K., Kühnel, F., Gurlevik, E., Bernhardt, G., Teng, M. W. L., & Smyth, M. J. (2016). Suppression of Metastases Using a New Lymphocyte Checkpoint Target for Cancer Immunotherapy. *Cancer Discovery*, *6*(4), 446–459. https://doi.org/10.1158/2159-8290.CD-15-0944

Benson, D. M., Bakan, C. E., Mishra, A., Hofmeister, C. C., Efebera, Y., Becknell, B., Baiocchi, R. A., Zhang, J., Yu, J., Smith, M. K., Greenfield, C. N., Porcu, P., Devine, S. M., Rotem-Yehudar, R., Lozanski, G., Byrd, J. C., & Caligiuri, M. A. (2010). The PD-1/PD-L1 axis modulates the natural killer cell versus multiple myeloma effect: A therapeutic target for CT-011, a novel monoclonal anti–PD-1 antibody. *Blood*, *116*(13), 2286–2294. https://doi.org/10.1182/blood-2010-02-271874

Narayanan, S., Ahl, P. J., Bijin, V. A., Kaliaperumal, N., Lim, S. G., Wang, C.-I., Fairhurst, A.-M., & Connolly, J. E. (2020). LAG3 is a Central Regulator of NK Cell Cytokine Production. *BioRxiv*, 2020.01.31.928200. https://doi.org/10.1101/2020.01.31.928200

Niu, C., Li, M., Zhu, S., Chen, Y., Zhou, L., Xu, D., Xu, J., Li, Z., Li, W., & Cui, J. (2020). PD-1-positive Natural Killer Cells have a weaker antitumor function than that of PD-1-negative Natural Killer Cells in Lung Cancer. *International Journal of Medical Sciences*, *17*(13), 1964–1973. https://doi.org/10.7150/ijms.47701

Mäenpää, A., Jääskeläinen, J., Carpén, O., Patarroyo, M., & Timonen, T. (1993). Expression of integrins and other adhesion molecules on NK cells; impact of IL-2 on short- and long-term cultures. *International Journal of Cancer*, *53*(5), 850–855. https://doi.org/10.1002/ijc.2910530524

Schneider, M. K. J., Strasser, M., Gilli, U. O., Kocher, M., Moser, R., & Seebach, J. D. (2002). Rolling adhesion of human NK cells to porcine endothelial cells mainly relies on CD49d-CD106 interactions. *Transplantation*, *73*(5), 789–796. https://doi.org/10.1097/00007890-200203150-00023

Aguado, E., Santamaría, M., Gallego, M. D., Peña, J., & Molina, I. J. (1999). Functional expression of CD43 on human natural killer cells. *Journal of Leukocyte Biology*, *66*(6), 923–929. https://doi.org/10.1002/jlb.66.6.923

Alfarra, H., Weir, J., Grieve, S., & Reiman, T. (2020). Targeting NK Cell Inhibitory Receptors for Precision Multiple Myeloma Immunotherapy. *Frontiers in Immunology*, *11*, 2936. https://doi.org/10.3389/fimmu.2020.575609

Alter, G., Malenfant, J. M., & Altfeld, M. (2004). CD107a as a functional marker for the identification of natural killer cell activity. *Journal of Immunological Methods*, *294*(1–2), 15–22. https://doi.org/10.1016/j.jim.2004.08.008

Amand, M., Iserentant, G., Poli, A., Sleiman, M., Fievez, V., Sanchez, I. P., Sauvageot, N., Michel, T., Aouali, N., Janji, B., Trujillo-Vargas, C. M., Seguin-Devaux, C., & Zimmer, J. (2017). Human CD56dimCD16dim Cells As an Individualized Natural Killer Cell Subset. *Frontiers in Immunology*, *8*. https://doi.org/10.3389/fimmu.2017.00699

Anderson, A. C., Joller, N., & Kuchroo, V. K. (2016). Lag-3, Tim-3, and TIGIT: Co-inhibitory Receptors with Specialized Functions in Immune Regulation. *Immunity*, *44*(5), 989–1004. https://doi.org/10.1016/j.immuni.2016.05.001

André, P., Denis, C., Soulas, C., Bourbon-Caillet, C., Lopez, J., Arnoux, T., Bléry, M., Bonnafous, C., Gauthier, L., Morel, A., Rossi, B., Remark, R., Breso, V., Bonnet, E., Habif, G., Guia, S., Lalanne, A. I., Hoffmann, C., Lantz, O., … Vivier, E. (2018). Anti-NKG2A mAb Is a Checkpoint Inhibitor that Promotes Anti-tumor Immunity by Unleashing Both T and NK Cells. *Cell*, *175*(7), 1731-1743.e13. https://doi.org/10.1016/j.cell.2018.10.014

Arruga, F., Guerra, G., Baev, D., Hoofd, C., Coscia, M., D'Arena, G. F., Gaidano, G., Furman, R. R., & Deaglio, S. (2019). Expression of the Tigit/CD226/CD155 Receptors/Ligand System in Chronic Lymphocytic Leukemia. *Blood*, *134*(Supplement_1), 5454–5454. https://doi.org/10.1182/blood-2019-128308

Bachanova, V., & Miller, J. S. (2014). NK cells in therapy of cancer. *Critical Reviews in Oncogenesis*, *19*(1–2), 133–141. https://doi.org/10.1615/critrevoncog.2014011091

Barrow, A. D., Martin, C. J., & Colonna, M. (2019). The Natural Cytotoxicity Receptors in Health and Disease. *Frontiers in Immunology*, *10*, 909. https://doi.org/10.3389/fimmu.2019.00909

Beldi-Ferchiou, A., & Caillat-Zucman, S. (2017). Control of NK Cell Activation by Immune Checkpoint Molecules. *International Journal of Molecular Sciences*, *18*(10), E2129. https://doi.org/10.3390/ijms18102129

Beldi-Ferchiou, A., Lambert, M., Dogniaux, S., Vély, F., Vivier, E., Olive, D., Dupuy, S., Levasseur, F., Zucman, D., Lebbé, C., Sène, D., Hivroz, C., & Caillat-Zucman, S. (2016). PD-1 mediates functional exhaustion of activated NK cells in patients with Kaposi sarcoma. *Oncotarget*, *7*(45), 72961–72977. https://doi.org/10.18632/oncotarget.12150

Bellora, F., Castriconi, R., Dondero, A., Reggiardo, G., Moretta, L., Mantovani, A., Moretta, A., & Bottino, C. (2010). The interaction of human natural killer cells with either unpolarized or polarized macrophages results in different functional outcomes. *Proceedings of the National Academy of Sciences of the United States of America*, *107*(50), 21659–21664. https://doi.org/10.1073/pnas.1007654108

Benson, D. M., Bakan, C. E., Mishra, A., Hofmeister, C. C., Efebera, Y., Becknell, B., Baiocchi, R. A., Zhang, J., Yu, J., Smith, M. K., Greenfield, C. N., Porcu, P., Devine, S. M., Rotem-Yehudar, R., Lozanski, G., Byrd, J. C., & Caligiuri, M. A. (2010). The PD-1/PD-L1 axis modulates the natural killer cell versus multiple myeloma effect: A therapeutic target for CT-011, a novel monoclonal anti–PD-1 antibody. *Blood*, *116*(13), 2286–2294. https://doi.org/10.1182/blood-2010-02-271874

Berahovich, R. D., Lai, N. L., Wei, Z., Lanier, L. L., & Schall, T. J. (2006). Evidence for NK cell subsets based on chemokine receptor expression. *Journal of Immunology (Baltimore, Md.: 1950)*, *177*(11), 7833–7840. https://doi.org/10.4049/jimmunol.177.11.7833

Bernatsky, S., Ramsey-Goldman, R., & Clarke, A. (2006). Malignancy and autoimmunity. *Current Opinion in Rheumatology*, *18*(2), 129–134. https://doi.org/10.1097/01.bor.0000209423.39033.94

Betrian, S., Ysebaert, L., Heider, K. H., Delord, J. P., Fournié, J. J., & Quillet-Mary, A. (2016). Idelalisib improves CD37 antibody BI 836826 cytotoxicity against chemo-resistant /relapse-initiating CLL cells: A rationale for combination treatment. *Blood Cancer Journal*, *6*(11), e496. https://doi.org/10.1038/bcj.2016.106

Bi, J., & Tian, Z. (2017). NK Cell Exhaustion. *Frontiers in Immunology*, *8*. https://doi.org/10.3389/fimmu.2017.00760

Binet, J. L., Auquier, A., Dighiero, G., Chastang, C., Piguet, H., Goasguen, J., Vaugier, G., Potron, G., Colona, P., Oberling, F., Thomas, M., Tchernia, G., Jacquillat, C., Boivin, P., Lesty, C., Duault, M. T., Monconduit, M., Belabbes, S., & Gremy, F. (1981). A new prognostic classification of chronic lymphocytic leukemia derived from a multivariate survival analysis. *Cancer*, *48*(1), 198–206. https://doi.org/10.1002/1097-0142(19810701)48:1<198::aid-cncr2820480131>3.0.co;2-v

Boddu, P., Kantarjian, H., Garcia-Manero, G., Allison, J., Sharma, P., & Daver, N. (2018). The emerging role of immune checkpoint based approaches in AML and MDS. *Leukemia & Lymphoma*, *59*(4), 790–802. https://doi.org/10.1080/10428194.2017.1344905

Boivin, W. A., Cooper, D. M., Hiebert, P. R., & Granville, D. J. (2009). Intracellular versus extracellular granzyme B in immunity and disease: Challenging the dogma. *Laboratory Investigation*, *89*(11), 1195–1220. https://doi.org/10.1038/labinvest.2009.91

Böning, M. A. L., Trittel, S., Riese, P., van Ham, M., Heyner, M., Voss, M., Parzmair, G. P., Klawonn, F., Jeron, A., Guzman, C. A., Jänsch, L., Schraven, B., Reinhold, A., & Bruder, D. (2019). ADAP Promotes Degranulation and Migration of NK Cells Primed During in vivo Listeria monocytogenes Infection in Mice. *Frontiers in Immunology*, *10*, 3144. https://doi.org/10.3389/fimmu.2019.03144

Boos, M. D., Yokota, Y., Eberl, G., & Kee, B. L. (2007). Mature natural killer cell and lymphoid tissue–inducing cell development requires Id2-mediated suppression of E protein activity. *Journal of Experimental Medicine*, *204*(5), 1119–1130. https://doi.org/10.1084/jem.20061959

Boross, P., & Leusen, J. H. W. (2012). Mechanisms of action of CD20 antibodies. *American Journal of Cancer Research*, *2*(6), 676–690.

Bösken, B., Hepner-Schefczyk, M., Vonderhagen, S., Dudda, M., & Flohé, S. B. (2020). An Inverse Relationship Between c-Kit/CD117 and mTOR Confers NK Cell Dysregulation Late After Severe Injury. *Frontiers in Immunology*, *11*, 1200. https://doi.org/10.3389/fimmu.2020.01200

Bouteiller, P. L., Barakonyi, A., Giustiniani, J., Lenfant, F., Marie-Cardine, A., Aguerre-Girr, M., Rabot, M., Hilgert, I., Mami-Chouaib, F., Tabiasco, J., Boumsell, L., & Bensussan, A. (2002). Engagement of CD160 receptor by HLA-C is a triggering mechanism used by circulating natural killer (NK) cells to mediate cytotoxicity. *Proceedings of the National Academy of Sciences*, *99*(26), 16963–16968. https://doi.org/10.1073/pnas.012681099

Brenchley, J. M., Karandikar, N. J., Betts, M. R., Ambrozak, D. R., Hill, B. J., Crotty, L. E., Casazza, J. P., Kuruppu, J., Migueles, S. A., Connors, M., Roederer, M., Douek, D. C., & Koup, R. A. (2003). Expression of CD57 defines replicative senescence and antigen-induced apoptotic death of CD8+ T cells. *Blood*, *101*(7), 2711–2720. https://doi.org/10.1182/blood-2002-07-2103

Brillantes, M., & Beaulieu, A. M. (2019). Transcriptional control of natural killer cell differentiation. *Immunology*, *156*(2), 111–119. https://doi.org/10.1111/imm.13017

Bruenke, J., Fischer, B., Barbin, K., Schreiter, K., Wachter, Y., Mahr, K., Titgemeyer, F., Niederweis, M., Peipp, M., Zunino, S. J., Repp, R., Valerius, T., & Fey, G. H. (2004). A recombinant bispecific single-chain Fv antibody against HLA class II and FcγRIII (CD16) triggers effective lysis of lymphoma cells. *British Journal of Haematology*, *125*(2), 167–179. https://doi.org/10.1111/j.1365-2141.2004.04893.x

Brusa, D., Serra, S., Coscia, M., Rossi, D., D'Arena, G., Laurenti, L., Jaksic, O., Fedele, G., Inghirami, G., Gaidano, G., Malavasi, F., & Deaglio, S. (2013). The PD-1/PD-L1 axis contributes to T-cell dysfunction in chronic lymphocytic leukemia. *Haematologica*, *98*(6), 953–963. https://doi.org/10.3324/haematol.2012.077537

Burger, J. A., Barr, P. M., Robak, T., Owen, C., Ghia, P., Tedeschi, A., Bairey, O., Hillmen, P., Coutre, S. E., Devereux, S., Grosicki, S., McCarthy, H., Simpson, D., Offner, F., Moreno, C., Dai, S., Lal, I., Dean, J. P., & Kipps, T. J. (2020). Long-term efficacy and safety of first-line ibrutinib treatment for patients with CLL/SLL: 5 years of follow-up from the phase 3 RESONATE-2 study. *Leukemia*, *34*(3), 787–798. https://doi.org/10.1038/s41375-019-0602-x

Bustamante, J., Boisson-Dupuis, S., Abel, L., & Casanova, J.-L. (2014). Mendelian susceptibility to mycobacterial disease: Genetic, immunological, and clinical features of inborn errors of IFN-γ immunity. *Seminars in Immunology*, *26*(6), 454–470. https://doi.org/10.1016/j.smim.2014.09.008

Caligiuri, M. A. (2008). Human natural killer cells. *Blood*, *112*(3), 461–469. https://doi.org/10.1182/blood-2007-09-077438

Calvo, T., Reina-Ortiz, C., Giraldos, D., Gascón, M., Woods, D., Asenjo, J., Marco-Brualla, J., Azaceta, G., Izquierdo, I., Palomera, L., Sánchez-Martínez, D., Marzo, I., Naval, J., Vilches, C., Villalba, M., & Anel, A. (2020). Expanded and activated allogeneic NK cells are cytotoxic against B-chronic lymphocytic leukemia (B-CLL) cells with sporadic cases of resistance. *Scientific Reports*, *10*, 19398. https://doi.org/10.1038/s41598-020-76051-z

Carlsten, M., Baumann, B. C., Simonsson, M., Jädersten, M., Forsblom, A.-M., Hammarstedt, C., Bryceson, Y. T., Ljunggren, H.-G., Hellström-Lindberg, E., & Malmberg, K.-J. (2010). Reduced DNAM-1

expression on bone marrow NK cells associated with impaired killing of CD34+ blasts in myelodysplastic syndrome. *Leukemia*, *24*(9), 1607–1616. https://doi.org/10.1038/leu.2010.149

Carrillo-Bustamante, P., Keşmir, C., & de Boer, R. J. (2016). The evolution of natural killer cell receptors. *Immunogenetics*, *68*(1), 3–18. https://doi.org/10.1007/s00251-015-0869-7

Catovsky, D., Richards, S., Matutes, E., Oscier, D., Dyer, M., Bezares, R. F., Pettitt, A. R., Hamblin, T., Milligan, D. W., Child, J. A., Hamilton, M. S., Dearden, C. E., Smith, A. G., Bosanquet, A. G., Davis, Z., Brito-Babapulle, V., Else, M., Wade, R., Hillmen, P., … NCRI Chronic Lymphocytic Leukaemia Working Group. (2007). Assessment of fludarabine plus cyclophosphamide for patients with chronic lymphocytic leukaemia (the LRF CLL4 Trial): A randomised controlled trial. *Lancet (London, England)*, *370*(9583), 230–239. https://doi.org/10.1016/S0140-6736(07)61125-8

Chan, C. J., Martinet, L., Gilfillan, S., Souza-Fonseca-Guimaraes, F., Chow, M. T., Town, L., Ritchie, D. S., Colonna, M., Andrews, D. M., & Smyth, M. J. (2014). The receptors CD96 and CD226 oppose each other in the regulation of natural killer cell functions. *Nature Immunology*, *15*(5), 431–438. https://doi.org/10.1038/ni.2850

Chauvin, J.-M., Pagliano, O., Fourcade, J., Sun, Z., Wang, H., Sander, C., Kirkwood, J. M., Chen, T. T., Maurer, M., Korman, A. J., & Zarour, H. M. (2015). TIGIT and PD-1 impair tumor antigen-specific $CD8^+$ T cells in melanoma patients. *The Journal of Clinical Investigation*, *125*(5), 2046–2058. https://doi.org/10.1172/JCI80445

Chauvin, J.-M., & Zarour, H. M. (2020). TIGIT in cancer immunotherapy. *Journal for ImmunoTherapy of Cancer*, *8*(2), e000957. https://doi.org/10.1136/jitc-2020-000957

Chen, X., Trivedi, P. P., Ge, B., Krzewski, K., & Strominger, J. L. (2007). Many NK cell receptors activate ERK2 and JNK1 to trigger microtubule organizing center and granule polarization and cytotoxicity. *Proceedings of the National Academy of Sciences*, *104*(15), 6329–6334. https://doi.org/10.1073/pnas.0611655104

Chitadze, G., Lettau, M., Bhat, J., Wesch, D., Steinle, A., Fürst, D., Mytilineos, J., Kalthoff, H., Janssen, O., Oberg, H.-H., & Kabelitz, D. (2013). Shedding of endogenous MHC class I-related chain molecules A and B from different human tumor entities: Heterogeneous involvement of the “a disintegrin and metalloproteases” 10 and 17. *International Journal of Cancer*, *133*(7), 1557–1566. https://doi.org/10.1002/ijc.28174

Cho, D., Shook, D. R., Shimasaki, N., Chang, Y.-H., Fujisaki, H., & Campana, D. (2010). Cytotoxicity of activated natural killer cells against pediatric solid tumors. *Clinical Cancer Research: An Official Journal of the American Association for Cancer Research*, *16*(15), 3901–3909. https://doi.org/10.1158/1078-0432.CCR-10-0735

Cho, M. M., Quamine, A. E., Olsen, M. R., & Capitini, C. M. (n.d.). Programmed cell death protein 1 on natural killer cells: Fact or fiction? *The Journal of Clinical Investigation*, *130*(6), 2816–2819. https://doi.org/10.1172/JCI137051

Choi, P. J., & Mitchison, T. J. (2013). Imaging burst kinetics and spatial coordination during serial killing by single natural killer cells. *Proceedings of the National Academy of Sciences of the United States of America*, *110*(16), 6488–6493. https://doi.org/10.1073/pnas.1221312110

Chow, K. U., Sommerlad, W. D., Boehrer, S., Schneider, B., Seipelt, G., Rummel, M. J., Hoelzer, D., Mitrou, P. S., & Weidmann, E. (2002). Anti-CD20 antibody (IDEC-C2B8, rituximab) enhances efficacy of cytotoxic drugs on neoplastic lymphocytes in vitro: Role of cytokines, complement, and caspases. *Haematologica*, *87*(1), 33–43. https://doi.org/10.3324/%x

Cifaldi, L., Doria, M., Cotugno, N., Zicari, S., Cancrini, C., Palma, P., & Rossi, P. (2019). DNAM-1 Activating Receptor and Its Ligands: How Do Viruses Affect the NK Cell-Mediated Immune Surveillance during the Various Phases of Infection? *International Journal of Molecular Sciences*, *20*, 3715. https://doi.org/10.3390/ijms20153715

Coaña, Y. P. de, Wolodarski, M., Àvila, I. van der H., Nakajima, T., Rentouli, S., Lundqvist, A., Masucci, G., Hansson, J., & Kiessling, R. (2020). PD-1 checkpoint blockade in advanced melanoma patients: NK cells, monocytic subsets and host PD-L1 expression as predictive biomarker candidates. *OncoImmunology*, *9*(1), 1786888. https://doi.org/10.1080/2162402X.2020.1786888

Concha-Benavente, F., Kansy, B., Moskovitz, J., Moy, J., Chandran, U., & Ferris, R. L. (2018). PD-L1 Mediates Dysfunction in Activated PD-1+ NK Cells in Head and Neck Cancer Patients. *Cancer Immunology Research*, *6*(12), 1548–1560. https://doi.org/10.1158/2326-6066.CIR-18-0062

Cooper, M. A., Fehniger, T. A., Turner, S. C., Chen, K. S., Ghaheri, B. A., Ghayur, T., Carson, W. E., & Caligiuri, M. A. (2001). Human natural killer cells: A unique innate immunoregulatory role for the CD56bright subset. *Blood*, *97*(10), 3146–3151. https://doi.org/10.1182/blood.V97.10.3146

Costello, R. T., Knoblauch, B., Sanchez, C., Mercier, D., Le Treut, T., & Sébahoun, G. (2012). Expression of natural killer cell activating receptors in patients with chronic lymphocytic leukaemia. *Immunology*, *135*(2), 151–157. https://doi.org/10.1111/j.1365-2567.2011.03521.x

Coupland, L. A., Chong, B. H., & Parish, C. R. (2012). Platelets and P-Selectin Control Tumor Cell Metastasis in an Organ-Specific Manner and Independently of NK Cells. *Cancer Research*, *72*(18), 4662–4671. https://doi.org/10.1158/0008-5472.CAN-11-4010

da Silva, I. P., Gallois, A., Jimenez-Baranda, S., Khan, S., Anderson, A. C., Kuchroo, V. K., Osman, I., & Bhardwaj, N. (2014). Reversal of NK-cell exhaustion in advanced melanoma by Tim-3 blockade. *Cancer Immunology Research*, *2*(5), 410–422. https://doi.org/10.1158/2326-6066.CIR-13-0171

Das, M., Zhu, C., & Kuchroo, V. K. (2017). Tim-3 and its role in regulating anti-tumor immunity. *Immunological Reviews*, *276*(1), 97–111. https://doi.org/10.1111/imr.12520

de Andrade, L. F., Smyth, M. J., & Martinet, L. (2014). DNAM-1 control of natural killer cells functions through nectin and nectin-like proteins. *Immunology and Cell Biology*, *92*(3), 237–244. https://doi.org/10.1038/icb.2013.95

De Maria, A., Bozzano, F., Cantoni, C., & Moretta, L. (2011). Revisiting human natural killer cell subset function revealed cytolytic CD56(dim)CD16+ NK cells as rapid producers of abundant IFN-gamma on activation. *Proceedings of the National Academy of Sciences of the United States of America*, *108*(2), 728–732. https://doi.org/10.1073/pnas.1012356108

Delahaye, N. F., Rusakiewicz, S., Martins, I., Ménard, C., Roux, S., Lyonnet, L., Paul, P., Sarabi, M., Chaput, N., Semeraro, M., Minard-Colin, V., Poirier-Colame, V., Chaba, K., Flament, C., Baud, V., Authier, H., Kerdine-Römer, S., Pallardy, M., Cremer, I., … Zitvogel, L. (2011). Alternatively spliced NKp30 isoforms affect the prognosis of gastrointestinal stromal tumors. *Nature Medicine*, *17*(6), 700–707. https://doi.org/10.1038/nm.2366

Ding, W., LaPlant, B. R., Call, T. G., Parikh, S. A., Leis, J. F., He, R., Shanafelt, T. D., Sinha, S., Le-Rademacher, J., Feldman, A. L., Habermann, T. M., Witzig, T. E., Wiseman, G. A., Lin, Y., Asmus, E., Nowakowski, G. S., Conte, M. J., Bowen, D. A., Aitken, C. N., … Ansell, S. M. (2017). Pembrolizumab in patients with CLL and Richter transformation or with relapsed CLL. *Blood*, *129*(26), 3419–3427. https://doi.org/10.1182/blood-2017-02-765685

Dougall, W. C., Kurtulus, S., Smyth, M. J., & Anderson, A. C. (2017). TIGIT and CD96: New checkpoint receptor targets for cancer immunotherapy. *Immunological Reviews*, *276*(1), 112–120. https://doi.org/10.1111/imr.12518

Dreger, P., Corradini, P., Kimby, E., Michallet, M., Milligan, D., Schetelig, J., Wiktor-Jedrzejczak, W., Niederwieser, D., Hallek, M., Montserrat, E., & Chronic Leukemia Working Party of the EBMT. (2007). Indications for allogeneic stem cell transplantation in chronic lymphocytic leukemia: The EBMT transplant consensus. *Leukemia*, *21*(1), 12–17. https://doi.org/10.1038/sj.leu.2404441

Drexler, H. G., & Matsuo, Y. (2000). Malignant hematopoietic cell lines: In vitro models for the study of natural killer cell leukemia–lymphoma. *Leukemia*, *14*(5), 777–782. https://doi.org/10.1038/sj.leu.2401778

Du, X., Almeida, P. de, Manieri, N., Nagata, D. de A., Wu, T. D., Bowles, K. H., Arumugam, V., Schartner, J., Cubas, R., Mittman, S., Javinal, V., Anderson, K. R., Warming, S., Grogan, J. L., & Chiang, E. Y. (2018). CD226 regulates natural killer cell antitumor responses via phosphorylation-mediated inactivation of transcription factor FOXO1. *Proceedings of the National Academy of Sciences*, *115*(50), E11731–E11740. https://doi.org/10.1073/pnas.1814052115

Dustin, M. L. (2019). Integrins and Their Role in Immune Cell Adhesion. *Cell*, *177*(3), 499–501. https://doi.org/10.1016/j.cell.2019.03.038

Eichhorst, B., Fink, A.-M., Bahlo, J., Busch, R., Kovacs, G., Maurer, C., Lange, E., Köppler, H., Kiehl, M., Sökler, M., Schlag, R., Vehling-Kaiser, U., Köchling, G., Plöger, C., Gregor, M., Plesner, T., Trneny, M., Fischer, K., Döhner, H., … German CLL Study Group (GCLLSG). (2016). First-line chemoimmunotherapy with bendamustine and rituximab versus fludarabine, cyclophosphamide, and rituximab in patients with advanced chronic lymphocytic leukaemia (CLL10): An international, open-label, randomised, phase 3, non-inferiority trial. *The Lancet. Oncology*, *17*(7), 928–942. https://doi.org/10.1016/S1470-2045(16)30051-1

El-Gazzar, A., Groh, V., & Spies, T. (2013). Immunobiology and conflicting roles of the human NKG2D lymphocyte receptor and its ligands in cancer. *Journal of Immunology (Baltimore, Md.: 1950)*, *191*(4), 1509–1515. https://doi.org/10.4049/jimmunol.1301071

Etzioni, A. (2009). Genetic etiologies of leukocyte adhesion defects. *Current Opinion in Immunology*, *21*(5), 481–486. https://doi.org/10.1016/j.coi.2009.07.005

Faria, J. R. de, Oliveira, J. S. R. de, Faria, R. M. D. de, Silva, M. R. R., Goihman, S., Yamamoto, M., & Kerbauy, J. (2000). Prognosis related to staging systems for chronic lymphocytic leukemia. *Sao Paulo Medical Journal*, *118*, 83–88. https://doi.org/10.1590/S1516-31802000000400002

Fathman, J. W., Bhattacharya, D., Inlay, M. A., Seita, J., Karsunky, H., & Weissman, I. L. (2011). Identification of the earliest natural killer cell-committed progenitor in murine bone marrow. *Blood*, *118*(20), 5439–5447. https://doi.org/10.1182/blood-2011-04-348912

Fauriat, C., Long, E. O., Ljunggren, H.-G., & Bryceson, Y. T. (2010). Regulation of human NK-cell cytokine and chemokine production by target cell recognition. *Blood*, *115*(11), 2167–2176. https://doi.org/10.1182/blood-2009-08-238469

Ferrajoli, A., Faderl, S., & Keating, M. J. (2006). Monoclonal antibodies in chronic lymphocytic leukemia. *Expert Review of Anticancer Therapy*, *6*(9), 1231–1238. https://doi.org/10.1586/14737140.6.9.1231

Fisher, D. T., Chen, Q., Skitzki, J. J., Muhitch, J. B., Zhou, L., Appenheimer, M. M., Vardam, T. D., Weis, E. L., Passanese, J., Wang, W.-C., Gollnick, S. O., Dewhirst, M. W., Rose-John, S., Repasky, E. A., Baumann, H., & Evans, S. S. (2011). IL-6 trans-signaling licenses mouse and human tumor

microvascular gateways for trafficking of cytotoxic T cells. *The Journal of Clinical Investigation*, *121*(10), 3846–3859. https://doi.org/10.1172/JCI44952

Forconi, F., & Moss, P. (2015). Perturbation of the normal immune system in patients with CLL. *Blood*, *126*(5), 573–581. https://doi.org/10.1182/blood-2015-03-567388

Freud, A. G., Yokohama, A., Becknell, B., Lee, M. T., Mao, H. C., Ferketich, A. K., & Caligiuri, M. A. (2006). Evidence for discrete stages of human natural killer cell differentiation in vivo. *The Journal of Experimental Medicine*, *203*(4), 1033–1043. https://doi.org/10.1084/jem.20052507

Fuchs, A., Cella, M., Giurisato, E., Shaw, A. S., & Colonna, M. (2004). Cutting edge: CD96 (tactile) promotes NK cell-target cell adhesion by interacting with the poliovirus receptor (CD155). *Journal of Immunology (Baltimore, Md.: 1950)*, *172*(7), 3994–3998. https://doi.org/10.4049/jimmunol.172.7.3994

Fuchs, A., & Colonna, M. (2006). The role of NK cell recognition of nectin and nectin-like proteins in tumor immunosurveillance. *Seminars in Cancer Biology*, *16*(5), 359–366. https://doi.org/10.1016/j.semcancer.2006.07.002

Gallois, A., Silva, I., Osman, I., & Bhardwaj, N. (2014). Reversal of natural killer cell exhaustion by TIM-3 blockade. *Oncoimmunology*, *3*(12), e946365. https://doi.org/10.4161/21624011.2014.946365

Geiger, T. L., & Sun, J. C. (2016). Development and maturation of natural killer cells. *Current Opinion in Immunology*, *39*, 82–89. https://doi.org/10.1016/j.coi.2016.01.007

Georgiev, H., Ravens, I., Papadogianni, G., & Bernhardt, G. (2018). Coming of Age: CD96 Emerges as Modulator of Immune Responses. *Frontiers in Immunology*, *9*, 1072. https://doi.org/10.3389/fimmu.2018.01072

Gill, S., Vasey, A. E., De Souza, A., Baker, J., Smith, A. T., Kohrt, H. E., Florek, M., Gibbs, K. D., Jr, Tate, K., Ritchie, D. S., & Negrin, R. S. (2012). Rapid development of exhaustion and down-regulation of eomesodermin limit the antitumor activity of adoptively transferred murine natural killer cells. *Blood*, *119*(24), 5758–5768. https://doi.org/10.1182/blood-2012-03-415364

Giuliani, M., Janji, B., & Berchem, G. (2017). Activation of NK cells and disruption of PD-L1/PD-1 axis: Two different ways for lenalidomide to block myeloma progression. *Oncotarget*, *8*(14), 24031–24044. https://doi.org/10.18632/oncotarget.15234

Glimcher, L. H., Townsend, M. J., Sullivan, B. M., & Lord, G. M. (2004). Recent developments in the transcriptional regulation of cytolytic effector cells. *Nature Reviews Immunology*, *4*(11), 900–911. https://doi.org/10.1038/nri1490

Golden-Mason, L., Palmer, B. E., Kassam, N., Townshend-Bulson, L., Livingston, S., McMahon, B. J., Castelblanco, N., Kuchroo, V., Gretch, D. R., & Rosen, H. R. (2009). Negative Immune Regulator Tim-3 Is Overexpressed on T Cells in Hepatitis C Virus Infection and Its Blockade Rescues Dysfunctional CD4+ and CD8+ T Cells. *Journal of Virology*, *83*(18), 9122–9130. https://doi.org/10.1128/JVI.00639-09

Gong, J. H., Maki, G., & Klingemann, H. G. (1994). Characterization of a human cell line (NK-92) with phenotypical and functional characteristics of activated natural killer cells. *Leukemia*, *8*(4), 652–658.

Gribben, J. G. (2010). How I treat CLL up front. *Blood*, *115*(2), 187–197. https://doi.org/10.1182/blood-2009-08-207126

Grutza, R., Moskorz, W., Senff, T., Bäcker, E., Lindemann, M., Zimmermann, A., Uhrberg, M., Lang, P. A., Timm, J., & Cosmovici, C. (2020). NKG2Cpos NK Cells Regulate the Expansion of Cytomegalovirus-

Specific CD8 T Cells. *Journal of Immunology (Baltimore, Md.: 1950)*, *204*(11), 2910–2917. https://doi.org/10.4049/jimmunol.1901281

Guillerey, C., Andrade, L. F. de, Vuckovic, S., Miles, K., Ngiow, S. F., Yong, M. C. R., Teng, M. W. L., Colonna, M., Ritchie, D. S., Chesi, M., Bergsagel, P. L., Hill, G. R., Smyth, M. J., & Martinet, L. (2015). Immunosurveillance and therapy of multiple myeloma are CD226 dependent. *The Journal of Clinical Investigation*, *125*(5), 2077–2089. https://doi.org/10.1172/JCI77181

Guillerey, C., Harjunpää, H., Carrié, N., Kassem, S., Teo, T., Miles, K., Krumeich, S., Weulersse, M., Cuisinier, M., Stannard, K., Yu, Y., Minnie, S. A., Hill, G. R., Dougall, W. C., Avet-Loiseau, H., Teng, M. W. L., Nakamura, K., Martinet, L., & Smyth, M. J. (2018). TIGIT immune checkpoint blockade restores CD8+ T-cell immunity against multiple myeloma. *Blood*, *132*(16), 1689–1694. https://doi.org/10.1182/blood-2018-01-825265

Guo, Y., Feng, X., Jiang, Y., Shi, X., Xing, X., Liu, X., Li, N., Fadeel, B., & Zheng, C. (2016). PD1 blockade enhances cytotoxicity of in vitro expanded natural killer cells towards myeloma cells. *Oncotarget*, *7*(30), 48360–48374. https://doi.org/10.18632/oncotarget.10235

Hadadi, L., Hafezi, M., Amirzargar, A. A., Sharifian, R. A., Abediankenari, S., & Asgarian-Omran, H. (2019). Dysregulated Expression of Tim-3 and NKp30 Receptors on NK Cells of Patients with Chronic Lymphocytic Leukemia. *Oncology Research and Treatment*, *42*(4), 202–208. https://doi.org/10.1159/000497208

Hallek, M., Cheson, B. D., Catovsky, D., Caligaris-Cappio, F., Dighiero, G., Döhner, H., Hillmen, P., Keating, M. J., Montserrat, E., Rai, K. R., & Kipps, T. J. (2008). Guidelines for the diagnosis and treatment of chronic lymphocytic leukemia: A report from the International Workshop on Chronic Lymphocytic Leukemia updating the National Cancer Institute–Working Group 1996 guidelines. *Blood*, *111*(12), 5446–5456. https://doi.org/10.1182/blood-2007-06-093906

Hanna, B. S., Yazdanparast, H., Demerdash, Y., Roessner, P. M., Schulz, R., Lichter, P., Stilgenbauer, S., & Seiffert, M. (2021). Combining ibrutinib and checkpoint blockade improves CD8+ T-cell function and control of chronic lymphocytic leukemia in Em-TCL1 mice. *Haematologica*, *106*(4), 968–977. https://doi.org/10.3324/haematol.2019.238154

Harjunpää, H., & Guillerey, C. (2020). TIGIT as an emerging immune checkpoint. *Clinical and Experimental Immunology*, *200*(2), 108–119. https://doi.org/10.1111/cei.13407

Harjunpää, H., Llort Asens, M., Guenther, C., & Fagerholm, S. C. (2019). Cell Adhesion Molecules and Their Roles and Regulation in the Immune and Tumor Microenvironment. *Frontiers in Immunology*, *10*, 1078. https://doi.org/10.3389/fimmu.2019.01078

Hassin, D., Garber, O. G., Meiraz, A., Schiffenbauer, Y. S., & Berke, G. (2011). Cytotoxic T lymphocyte perforin and Fas ligand working in concert even when Fas ligand lytic action is still not detectable. *Immunology*, *133*(2), 190–196. https://doi.org/10.1111/j.1365-2567.2011.03426.x

He, R., Ding, W., Viswanatha, D. S., Chen, D., Shi, M., Van Dyke, D., Tian, S., Dao, L. N., Parikh, S. A., Shanafelt, T. D., Call, T. G., Ansell, S. M., Leis, J. F., Mai, M., Hanson, C. A., & Rech, K. L. (2018). PD-1 Expression in Chronic Lymphocytic Leukemia/Small Lymphocytic Lymphoma (CLL/SLL) and Large B-cell Richter Transformation (DLBCL-RT): A Characteristic Feature of DLBCL-RT and Potential Surrogate Marker for Clonal Relatedness. *The American Journal of Surgical Pathology*, *42*(7), 843–854. https://doi.org/10.1097/PAS.0000000000001077

Hofland, T., Eldering, E., Kater, A. P., & Tonino, S. H. (2019). Engaging Cytotoxic T and NK Cells for Immunotherapy in Chronic Lymphocytic Leukemia. *International Journal of Molecular Sciences*, *20*(17), E4315. https://doi.org/10.3390/ijms20174315

Hofland, T., Endstra, S., Gomes, C. K. P., de Boer, R., de Weerdt, I., Bobkov, V., Riedl, J. A., Heukers, R., Smit, M. J., Eldering, E., Levin, M.-D., Kater, A. P., & Tonino, S. H. (2019). Natural Killer Cell Hyporesponsiveness in Chronic Lymphocytic Leukemia can be Circumvented In Vitro by Adequate Activating Signaling. *HemaSphere*, *3*(6), e308. https://doi.org/10.1097/HS9.0000000000000308

Hsu, J., Hodgins, J. J., Marathe, M., Nicolai, C. J., Bourgeois-Daigneault, M.-C., Trevino, T. N., Azimi, C. S., Scheer, A. K., Randolph, H. E., Thompson, T. W., Zhang, L., Iannello, A., Mathur, N., Jardine, K. E., Kirn, G. A., Bell, J. C., McBurney, M. W., Raulet, D. H., & Ardolino, M. (2018). Contribution of NK cells to immunotherapy mediated by PD-1/PD-L1 blockade. *The Journal of Clinical Investigation*, *128*(10), 4654–4668. https://doi.org/10.1172/JCI99317

Huang, R.-Y., Eppolito, C., Lele, S., Shrikant, P., Matsuzaki, J., & Odunsi, K. (2015). LAG3 and PD1 co-inhibitory molecules collaborate to limit CD8+ T cell signaling and dampen antitumor immunity in a murine ovarian cancer model. *Oncotarget*, *6*(29), 27359–27377. https://doi.org/10.18632/oncotarget.4751

Huergo-Zapico, L., Parodi, M., Cantoni, C., Lavarello, C., Fernández-Martínez, J. L., Petretto, A., DeAndrés-Galiana, E. J., Balsamo, M., López-Soto, A., Pietra, G., Bugatti, M., Munari, E., Marconi, M., Mingari, M. C., Vermi, W., Moretta, L., González, S., & Vitale, M. (2018). NK-cell Editing Mediates Epithelial-to-Mesenchymal Transition via Phenotypic and Proteomic Changes in Melanoma Cell Lines. *Cancer Research*, *78*(14), 3913–3925. https://doi.org/10.1158/0008-5472.CAN-17-1891

Humphries, J. D., Byron, A., & Humphries, M. J. (2006). Integrin ligands at a glance. *Journal of Cell Science*, *119*(Pt 19), 3901–3903. https://doi.org/10.1242/jcs.03098

Iwai, Y., Ishida, M., Tanaka, Y., Okazaki, T., Honjo, T., & Minato, N. (2002). Involvement of PD-L1 on tumor cells in the escape from host immune system and tumor immunotherapy by PD-L1 blockade. *Proceedings of the National Academy of Sciences of the United States of America*, *99*(19), 12293–12297. https://doi.org/10.1073/pnas.192461099

Jaglowski, S. M. (2014). Transplant for CLL: Still an option? *Blood*, *124*(26), 3835–3836. https://doi.org/10.1182/blood-2014-10-606871

Jaglowski, S. M., Alinari, L., Lapalombella, R., Muthusamy, N., & Byrd, J. C. (2010). The clinical application of monoclonal antibodies in chronic lymphocytic leukemia. *Blood*, *116*(19), 3705–3714. https://doi.org/10.1182/blood-2010-04-001230

Jakšić, B., Pejša, V., Ostojić-Kolonić, S., Kardum-Skelin, I., Bašić-Kinda, S., Coha, B., Gverić-Krečak, V., Vrhovac, R., Jakšić, O., Aurer, I., Sinčić-Petričević, J., Načinović-Duletić, A., & Nemet, D. (2018). Guidelines for Diagnosis and Treatment of Chronic Lymphocytic Leukemia. Krohem B-Cll 2017. *Acta Clinica Croatica*, *57*(1), 190–215. https://doi.org/10.20471/acc.2018.57.01.27

Jimbu, L., Mesaros, O., Popescu, C., Neaga, A., Berceanu, I., Dima, D., Gaman, M., & Zdrenghea, M. (2021). Is There a Place for PD-1-PD-L Blockade in Acute Myeloid Leukemia? *Pharmaceuticals*, *14*(4), 288. https://doi.org/10.3390/ph14040288

Jin, H.-S., & Park, Y. (2021). Hitting the complexity of the TIGIT-CD96-CD112R-CD226 axis for next-generation cancer immunotherapy. *BMB Reports*, *54*(1), 2–11.

Judge, S. J., Dunai, C., Aguilar, E. G., Vick, S. C., Sturgill, I. R., Khuat, L. T., Stoffel, K. M., Dyke, J. V., Longo, D. L., Darrow, M. A., Anderson, S. K., Blazar, B. R., Monjazeb, A. M., Serody, J. S., Canter, R. J., & Murphy, W. J. (2020). Minimal PD-1 expression in mouse and human NK cells under diverse conditions. *The Journal of Clinical Investigation*, *130*(6), 3051–3068. https://doi.org/10.1172/JCI133353

Judge, S. J., Dunai, C., Sturgill, I., Stoffel, K., Darrow, M., Canter, R., & Murphy, W. J. (2019). PD-1 is not expressed on highly activated Natural Killer cells in human and murine models. *The Journal of Immunology*, *202*(1 Supplement), 126.27-126.27.

Judge, S. J., Murphy, W. J., & Canter, R. J. (2020). Characterizing the Dysfunctional NK Cell: Assessing the Clinical Relevance of Exhaustion, Anergy, and Senescence. *Frontiers in Cellular and Infection Microbiology*, *10*, 49. https://doi.org/10.3389/fcimb.2020.00049

Jurczak, W., Zinzani, P. L., Gaidano, G., Goy, A., Provencio, M., Nagy, Z., Robak, T., Maddocks, K., Buske, C., Ambarkhane, S., Winderlich, M., Dirnberger-Hertweck, M., Korolkiewicz, R., & Blum, K. A. (2018). Phase IIa study of the CD19 antibody MOR208 in patients with relapsed or refractory B-cell non-Hodgkin's lymphoma. *Annals of Oncology: Official Journal of the European Society for Medical Oncology*, *29*(5), 1266–1272. https://doi.org/10.1093/annonc/mdy056

Kamiya, T., Seow, S. V., Wong, D., Robinson, M., & Campana, D. (n.d.). Blocking expression of inhibitory receptor NKG2A overcomes tumor resistance to NK cells. *The Journal of Clinical Investigation*, *129*(5), 2094–2106. https://doi.org/10.1172/JCI123955

Katrinakis, G., Kyriakou, D., Papadaki, H., Kalokyri, I., Markidou, F., & Eliopoulos, G. D. (1996). Defective Natural Killer Cell Activity in B-Cell Chronic Lymphocytic Leukaemia Is Associated with Impaired Release of Natural Killer Cytotoxic Factor(s) but Not of Tumour Necrosis Factor-α. *Acta Haematologica*, *96*(1), 16–23. https://doi.org/10.1159/000203709

Kawano, Y., Moschetta, M., Manier, S., Glavey, S., Görgün, G. T., Roccaro, A. M., Anderson, K. C., & Ghobrial, I. M. (2015). Targeting the bone marrow microenvironment in multiple myeloma. *Immunological Reviews*, *263*(1), 160–172. https://doi.org/10.1111/imr.12233

Kay, N. E., & Zarling, J. (1987). Restoration of impaired natural killer cell activity of B-chronic lymphocytic leukemia patients by recombinant interleukin-2. *American Journal of Hematology*, *24*(2), 161–167. https://doi.org/10.1002/ajh.2830240207

Kay, N. E., & Zarling, J. M. (1984). Impaired natural killer activity in patients with chronic lymphocytic leukemia is associated with a deficiency of azurophilic cytoplasmic granules in putative NK cells. *Blood*, *63*(2), 305–309.

Kee, B. L., Morman, R., Sun, M., & Li, Z.-Y. (2019). The transcription factor TCF1 is a critical target of ID2 that limits natural killer cell maturation. *The Journal of Immunology*, *202*(1 Supplement), 65.10-65.10.

Keir, M. E., Butte, M. J., Freeman, G. J., & Sharpe, A. H. (2008). PD-1 and Its Ligands in Tolerance and Immunity. *Annual Review of Immunology*, *26*(1), 677–704. https://doi.org/10.1146/annurev.immunol.26.021607.090331

Kelley, J., Walter, L., & Trowsdale, J. (2005). Comparative Genomics of Natural Killer Cell Receptor Gene Clusters. *PLOS Genetics*, *1*(2), e27. https://doi.org/10.1371/journal.pgen.0010027

Kellner, C., Bruenke, J., Horner, H., Schubert, J., Schwenkert, M., Mentz, K., Barbin, K., Stein, C., Peipp, M., Stockmeyer, B., & Fey, G. H. (2011). Heterodimeric bispecific antibody-derivatives against CD19 and CD16 induce effective antibody-dependent cellular cytotoxicity against B-lymphoid tumor cells. *Cancer Letters*, *303*(2), 128–139. https://doi.org/10.1016/j.canlet.2011.01.020

Kisielow, M., Kisielow, J., Capoferri-Sollami, G., & Karjalainen, K. (2005). Expression of lymphocyte activation gene 3 (LAG-3) on B cells is induced by T cells. *European Journal of Immunology*, *35*(7), 2081–2088. https://doi.org/10.1002/eji.200526090

Koch, J., Steinle, A., Watzl, C., & Mandelboim, O. (2013). Activating natural cytotoxicity receptors of natural killer cells in cancer and infection. *Trends in Immunology*, *34*(4), 182–191. https://doi.org/10.1016/j.it.2013.01.003

Konjević, G. M., Vuletić, A. M., Mirjačić Martinović, K. M., Larsen, A. K., & Jurišić, V. B. (2019). The role of cytokines in the regulation of NK cells in the tumor environment. *Cytokine*, *117*, 30–40. https://doi.org/10.1016/j.cyto.2019.02.001

Konjević, G., Vuletić, A., & Džodić, K. M. M. and R. (2017). The Role of Activating and Inhibitory NK Cell Receptors in Antitumor Immune Response. *Natural Killer Cells*. https://doi.org/10.5772/intechopen.69729

Kumar, S. (2018). Natural killer cell cytotoxicity and its regulation by inhibitory receptors. *Immunology*, *154*(3), 383–393. https://doi.org/10.1111/imm.12921

Kusnierczyk, P. (2013). Killer Cell Immunoglobulin-Like Receptor Gene Associations with Autoimmune and Allergic Diseases, Recurrent Spontaneous Abortion, and Neoplasms. *Frontiers in Immunology*, *4*, 8. https://doi.org/10.3389/fimmu.2013.00008

Kwon, H.-J., Kim, N., & Kim, H. S. (2017). Molecular checkpoints controlling natural killer cell activation and their modulation for cancer immunotherapy. *Experimental & Molecular Medicine*, *49*(3), e311. https://doi.org/10.1038/emm.2017.42

Labrijn, A. F., Janmaat, M. L., Reichert, J. M., & Parren, P. W. H. I. (2019). Bispecific antibodies: A mechanistic review of the pipeline. *Nature Reviews. Drug Discovery*, *18*(8), 585–608. https://doi.org/10.1038/s41573-019-0028-1

Lanier, L. L. (2008). Up on the tightrope: Natural killer cell activation and inhibition. *Nature Immunology*, *9*(5), 495–502. https://doi.org/10.1038/ni1581

Latchman, Y., Wood, C. R., Chernova, T., Chaudhary, D., Borde, M., Chernova, I., Iwai, Y., Long, A. J., Brown, J. A., Nunes, R., Greenfield, E. A., Bourque, K., Boussiotis, V. A., Carter, L. L., Carreno, B. M., Malenkovich, N., Nishimura, H., Okazaki, T., Honjo, T., … Freeman, G. J. (2001). PD-L2 is a second ligand for PD-1 and inhibits T cell activation. *Nature Immunology*, *2*(3), 261–268. https://doi.org/10.1038/85330

Le Garff-Tavernier, M., Decocq, J., de Romeuf, C., Parizot, C., Dutertre, C. A., Chapiro, E., Davi, F., Debré, P., Prost, J. F., Teillaud, J. L., Merle-Beral, H., & Vieillard, V. (2011). Analysis of CD16+CD56dim NK cells from CLL patients: Evidence supporting a therapeutic strategy with optimized anti-CD20 monoclonal antibodies. *Leukemia*, *25*(1), 101–109. https://doi.org/10.1038/leu.2010.240

Lee, A. J., Mian, F., Poznanski, S. M., Stackaruk, M., Chan, T., Chew, M. V., & Ashkar, A. A. (2019). Type I Interferon Receptor on NK Cells Negatively Regulates Interferon-γ Production. *Frontiers in Immunology*, *10*. https://doi.org/10.3389/fimmu.2019.01261

Lens, D., Dyer, M. J. S., Garcia-Marco, J. M., De Schouwer, P. J. J. C., Hamoudi, R. A., Jones, D., Farahat, N., Matutes, E., & Catovsky, D. (1997). P53 abnormalities in CLL are associated with excess of prolymphocytes and poor prognosis. *British Journal of Haematology*, *99*(4), 848–857. https://doi.org/10.1046/j.1365-2141.1997.4723278.x

Letestu, R., Lévy, V., Eclache, V., Baran-Marszak, F., Vaur, D., Naguib, D., Schischmanoff, O., Katsahian, S., Nguyen-Khac, F., Davi, F., Merle-Béral, H., Troussard, X., & Ajchenbaum-Cymbalista, F. (2010). Prognosis of Binet stage A chronic lymphocytic leukemia patients: The strength of routine parameters. *Blood*, *116*(22), 4588–4590. https://doi.org/10.1182/blood-2010-06-288274

Li, F., Wei, H., Wei, H., Gao, Y., Xu, L., Yin, W., Sun, R., & Tian, Z. (2013). Blocking the natural killer cell inhibitory receptor NKG2A increases activity of human natural killer cells and clears hepatitis B virus infection in mice. *Gastroenterology*, *144*(2), 392–401. https://doi.org/10.1053/j.gastro.2012.10.039

Li, J., Ni, L., & Dong, C. (2017). Immune checkpoint receptors in cancer: Redundant by design? *Current Opinion in Immunology*, *45*, 37–42. https://doi.org/10.1016/j.coi.2017.01.001

Li, M., Xia, P., Du, Y., Liu, S., Huang, G., Chen, J., Zhang, H., Hou, N., Cheng, X., Zhou, L., Li, P., Yang, X., & Fan, Z. (2014). T-cell Immunoglobulin and ITIM Domain (TIGIT) Receptor/Poliovirus Receptor (PVR) Ligand Engagement Suppresses Interferon-γ Production of Natural Killer Cells via β-Arrestin 2-mediated Negative Signaling. *The Journal of Biological Chemistry*, *289*(25), 17647–17657. https://doi.org/10.1074/jbc.M114.572420

Li, Y., Cao, C., Jia, W., Yu, L., Mo, M., Wang, Q., Huang, Y., Lim, J.-M., Ishihara, M., Wells, L., Azadi, P., Robinson, H., He, Y.-W., Zhang, L., & Mariuzza, R. A. (2009). Structure of the F-spondin domain of mindin, an integrin ligand and pattern recognition molecule. *The EMBO Journal*, *28*(3), 286–297. https://doi.org/10.1038/emboj.2008.288

Li, Z.-Y., Morman, R. E., Hegermiller, E., Sun, M., Bartom, E. T., Maienschein-Cline, M., Sigvardsson, M., & Kee, B. L. (2021). The transcriptional repressor ID2 supports natural killer cell maturation by controlling TCF1 amplitude. *Journal of Experimental Medicine*, *218*(6), e20202032. https://doi.org/10.1084/jem.20202032

Liu, E., Marin, D., Banerjee, P., Macapinlac, H. A., Thompson, P., Basar, R., Nassif Kerbauy, L., Overman, B., Thall, P., Kaplan, M., Nandivada, V., Kaur, I., Nunez Cortes, A., Cao, K., Daher, M., Hosing, C., Cohen, E. N., Kebriaei, P., Mehta, R., … Rezvani, K. (2020). Use of CAR-Transduced Natural Killer Cells in CD19-Positive Lymphoid Tumors. *The New England Journal of Medicine*, *382*(6), 545–553. https://doi.org/10.1056/NEJMoa1910607

Liu, F., Huang, J., He, F., Ma, X., Fan, F., Meng, M., Zhuo, Y., & Zhang, L. (2020). CD96, a new immune checkpoint, correlates with immune profile and clinical outcome of glioma. *Scientific Reports*, *10*(1), 10768. https://doi.org/10.1038/s41598-020-66806-z

Liu, G., Zhang, Q., Yang, J., Li, X., Xian, L., Li, W., Lin, T., Cheng, J., Lin, Q., Xu, X., Li, Q., Lin, Y., Zhou, M., & Shen, E. (2021). Increased TIGIT expressing NK cells with dysfunctional phenotype in AML patients correlated with poor prognosis. *Cancer Immunology, Immunotherapy: CII*. https://doi.org/10.1007/s00262-021-02978-5

Liu, H., Wang, S., Xin, J., Wang, J., Yao, C., & Zhang, Z. (2019). Role of NKG2D and its ligands in cancer immunotherapy. *American Journal of Cancer Research*, *9*(10), 2064–2078.

Liu, Y., Cheng, Y., Xu, Y., Wang, Z., Du, X., Li, C., Peng, J., Gao, L., Liang, X., & Ma, C. (2017). Increased expression of programmed cell death protein 1 on NK cells inhibits NK-cell-mediated anti-tumor function and indicates poor prognosis in digestive cancers. *Oncogene*, *36*(44), 6143–6153. https://doi.org/10.1038/onc.2017.209

Lodoen, M. B., & Lanier, L. L. (2005). Viral modulation of NK cell immunity. *Nature Reviews Microbiology*, *3*(1), 59–69. https://doi.org/10.1038/nrmicro1066

Long, E. O. (1999). Regulation of immune responses through inhibitory receptors. *Annual Review of Immunology*, *17*(1), 875–904. https://doi.org/10.1146/annurev.immunol.17.1.875

Long, E. O. (2008). Negative signaling by inhibitory receptors: The NK cell paradigm. *Immunological Reviews*, *224*(1), 70–84. https://doi.org/10.1111/j.1600-065X.2008.00660.x

Lopez-Vergès, S., Milush, J. M., Pandey, S., York, V. A., Arakawa-Hoyt, J., Pircher, H., Norris, P. J., Nixon, D. F., & Lanier, L. L. (2010). CD57 defines a functionally distinct population of mature NK cells

in the human CD56dimCD16+ NK-cell subset. *Blood*, *116*(19), 3865–3874. https://doi.org/10.1182/blood-2010-04-282301

Lozzio, B. B., & Lozzio, C. B. (1979). Properties and usefulness of the original K-562 human myelogenous leukemia cell line. *Leukemia Research*, *3*(6), 363–370. https://doi.org/10.1016/0145-2126(79)90033-X

Luo, Q., Li, X., Fu, B., Zhang, L., Deng, Z., Qing, C., Su, R., Xu, J., Guo, Y., Huang, Z., & Li, J. (2018). Decreased expression of TIGIT in NK cells correlates negatively with disease activity in systemic lupus erythematosus. *International Journal of Clinical and Experimental Pathology*, *11*(5), 2408–2418.

Ma, M., Wang, Z., Chen, X., Tao, A., He, L., Fu, S., Zhang, Z., Fu, Y., Guo, C., Liu, J., Han, X., Xu, J., Chu, Z., Ding, H., Shang, H., & Jiang, Y. (2017). NKG2C+NKG2A− Natural Killer Cells are Associated with a Lower Viral Set Point and may Predict Disease Progression in Individuals with Primary HIV Infection. *Frontiers in Immunology*, *8*. https://doi.org/10.3389/fimmu.2017.01176

Maas, R. J., Evert, J. S. H., Meer, J. M. V. der, Mekers, V., Rezaeifard, S., Korman, A. J., Jonge, P. K. de, Cany, J., Woestenenk, R., Schaap, N. P., Massuger, L. F., Jansen, J. H., Hobo, W., & Dolstra, H. (2020). TIGIT blockade enhances functionality of peritoneal NK cells with altered expression of DNAM-1/TIGIT/CD96 checkpoint molecules in ovarian cancer. *OncoImmunology*, *9*(1), 1843247. https://doi.org/10.1080/2162402X.2020.1843247

Mace, E. M., Monkley, S. J., Critchley, D. R., & Takei, F. (2009). A dual role for talin in NK cell cytotoxicity: Activation of LFA-1-mediated cell adhesion and polarization of NK cells. *Journal of Immunology (Baltimore, Md.: 1950)*, *182*(2), 948–956. https://doi.org/10.4049/jimmunol.182.2.948

MacFarlane, A. W., Jillab, M., Smith, M. R., Alpaugh, R. K., Cole, M. E., Litwin, S., Millenson, M. M., Al-Saleem, T., Cohen, A. D., & Campbell, K. S. (2017). NK cell dysfunction in chronic lymphocytic leukemia is associated with loss of the mature cells expressing inhibitory killer cell Ig-like receptors. *Oncoimmunology*, *6*(7), e1330235. https://doi.org/10.1080/2162402X.2017.1330235

Maeda, T. K., Sugiura, D., Okazaki, I., Maruhashi, T., & Okazaki, T. (2019). Atypical motifs in the cytoplasmic region of the inhibitory immune co-receptor LAG-3 inhibit T cell activation. *Journal of Biological Chemistry*, *294*(15), 6017–6026. https://doi.org/10.1074/jbc.RA119.007455

Magalhaes, I., Kalland, I., Kochenderfer, J. N., Österborg, A., Uhlin, M., & Mattsson, J. (2018). CD19 Chimeric Antigen Receptor T Cells From Patients With Chronic Lymphocytic Leukemia Display an Elevated IFN-γ Production Profile. *Journal of Immunotherapy (Hagerstown, Md.: 1997)*, *41*(2), 73–83. https://doi.org/10.1097/CJI.0000000000000193

Mah, A. Y., & Cooper, M. A. (2016). Metabolic Regulation of Natural Killer Cell IFN-γ Production. *Critical Reviews in Immunology*, *36*(2), 131–147. https://doi.org/10.1615/CritRevImmunol.2016017387

Malmberg, K.-J., Beziat, V., & Ljunggren, H.-G. (2012). Spotlight on NKG2C and the human NK-cell response to CMV infection. *European Journal of Immunology*, *42*(12), 3141–3145. https://doi.org/10.1002/eji.201243050

Mamessier, E., Sylvain, A., Thibult, M.-L., Houvenaeghel, G., Jacquemier, J., Castellano, R., Gonçalves, A., André, P., Romagné, F., Thibault, G., Viens, P., Birnbaum, D., Bertucci, F., Moretta, A., & Olive, D. (2011). Human breast cancer cells enhance self tolerance by promoting evasion from NK cell antitumor immunity. *The Journal of Clinical Investigation*, *121*(9), 3609–3622. https://doi.org/10.1172/JCI45816

Mandal, A., & Viswanathan, C. (2015). Natural killer cells: In health and disease. *Hematology/Oncology and Stem Cell Therapy*, *8*(2), 47–55. https://doi.org/10.1016/j.hemonc.2014.11.006

Marcon, F., Zuo, J., Pearce, H., Nicol, S., Margielewska-Davies, S., Farhat, M., Mahon, B., Middleton, G., Brown, R., Roberts, K. J., & Moss, P. (2020). NK cells in pancreatic cancer demonstrate impaired cytotoxicity and a regulatory IL-10 phenotype. *OncoImmunology*, *9*(1), 1845424. https://doi.org/10.1080/2162402X.2020.1845424

Marionneaux, S., Maslak, P., & Keohane, E. M. (2014). Morphologic identification of atypical chronic lymphocytic leukemia by digital microscopy. *International Journal of Laboratory Hematology*, *36*(4), 459–464. https://doi.org/10.1111/ijlh.12167

Mariotti, F. R., Quatrini, L., Munari, E., Vacca, P., Tumino, N., Pietra, G., Mingari, M. C., & Moretta, L. (2020). Inhibitory checkpoints in human natural killer cells: IUPHAR Review 28. *British Journal of Pharmacology*, *177*(13), 2889–2903. https://doi.org/10.1111/bph.15081

Martinet, L., & Smyth, M. (2015). Balancing natural killer cell activation through paired receptors. *Nature Reviews Immunology*. https://doi.org/10.1038/nri3799

Martínez-Lostao, L., Anel, A., & Pardo, J. (2015). How Do Cytotoxic Lymphocytes Kill Cancer Cells? *Clinical Cancer Research*, *21*(22), 5047–5056. https://doi.org/10.1158/1078-0432.CCR-15-0685

Maruhashi, T., Sugiura, D., Okazaki, I., & Okazaki, T. (2020). LAG-3: From molecular functions to clinical applications. *Journal for ImmunoTherapy of Cancer*, *8*(2), e001014. https://doi.org/10.1136/jitc-2020-001014

Matutes, E., & Polliack, A. (2000). Morphological and Immunophenotypic Features of Chronic Lymphocytic Leukemia. *Reviews in Clinical and Experimental Hematology*, *4*(1), 22–47. https://doi.org/10.1046/j.1468-0734.2000.00002.x

McEver, R. P., & Zhu, C. (2010). Rolling cell adhesion. *Annual Review of Cell and Developmental Biology*, *26*, 363–396. https://doi.org/10.1146/annurev.cellbio.042308.113238

McKechnie, J. L., Beltrán, D., Ferreira, A.-M. M., Vergara, R., Saenz, L., Vergara, O., Estripeaut, D., Araúz, A. B., Simpson, L. J., Holmes, S., López-Vergès, S., & Blish, C. A. (2020). Mass Cytometry Analysis of the NK Cell Receptor–Ligand Repertoire Reveals Unique Differences between Dengue-Infected Children and Adults. *ImmunoHorizons*, *4*(10), 634–647. https://doi.org/10.4049/immunohorizons.2000074

McWilliams, E. M., Mele, J. M., Cheney, C., Timmerman, E. A., Fiazuddin, F., Strattan, E. J., Mo, X., Byrd, J. C., Muthusamy, N., & Awan, F. T. (2016). Therapeutic CD94/NKG2A blockade improves natural killer cell dysfunction in chronic lymphocytic leukemia. *Oncoimmunology*, *5*(10), e1226720. https://doi.org/10.1080/2162402X.2016.1226720

Melero, I., Rouzaut, A., Motz, G. T., & Coukos, G. (2014). T-cell and NK-cell infiltration into solid tumors: A key limiting factor for efficacious cancer immunotherapy. *Cancer Discovery*, *4*(5), 522–526. https://doi.org/10.1158/2159-8290.CD-13-0985

Memmer, S., Weil, S., Beyer, S., Zöller, T., Peters, E., Hartmann, J., Steinle, A., & Koch, J. (2016). The Stalk Domain of NKp30 Contributes to Ligand Binding and Signaling of a Preassembled NKp30-CD3ζ Complex. *The Journal of Biological Chemistry*, *291*(49), 25427–25438. https://doi.org/10.1074/jbc.M116.742981

Meng, F., Li, L., Lu, F., Yue, J., Liu, Z., Zhang, W., & Fu, R. (2020). Overexpression of TIGIT in NK and T Cells Contributes to Tumor Immune Escape in Myelodysplastic Syndromes. *Frontiers in Oncology*. https://doi.org/10.3389/fonc.2020.01595

Michel, T., Poli, A., Cuapio, A., Briquemont, B., Iserentant, G., Ollert, M., & Zimmer, J. (2016). Human CD56bright NK Cells: An Update. *Journal of Immunology (Baltimore, Md.: 1950)*, *196*(7), 2923–2931. https://doi.org/10.4049/jimmunol.1502570

Miller, S. A., Mohn, S. E., & Weinmann, A. S. (2010). Jmjd3 and UTX play a demethylase-independent role in chromatin remodeling to regulate T-box family member-dependent gene expression. *Molecular Cell*, *40*(4), 594–605. https://doi.org/10.1016/j.molcel.2010.10.028

Mittal, D., Lepletier, A., Madore, J., Aguilera, A. R., Stannard, K., Blake, S. J., Whitehall, V. L. J., Liu, C., Bettington, M. L., Takeda, K., Long, G. V., Scolyer, R. A., Lan, R., Siemers, N., Korman, A., Teng, M. W. L., Johnston, R. J., Dougall, W. C., & Smyth, M. J. (2019). CD96 Is an Immune Checkpoint That Regulates CD8+ T-cell Antitumor Function. *Cancer Immunology Research*, *7*(4), 559–571. https://doi.org/10.1158/2326-6066.CIR-18-0637

Mlecnik, B., Tosolini, M., Charoentong, P., Kirilovsky, A., Bindea, G., Berger, A., Camus, M., Gillard, M., Bruneval, P., Fridman, W.-H., Pagès, F., Trajanoski, Z., & Galon, J. (2010). Biomolecular network reconstruction identifies T-cell homing factors associated with survival in colorectal cancer. *Gastroenterology*, *138*(4), 1429–1440. https://doi.org/10.1053/j.gastro.2009.10.057

Moore, T. I., Aaron, J., Chew, T.-L., & Springer, T. A. (2018). Measuring Integrin Conformational Change on the Cell Surface with Super-Resolution Microscopy. *Cell Reports*, *22*(7), 1903–1912. https://doi.org/10.1016/j.celrep.2018.01.062

Moretta, A., Bottino, C., Vitale, M., Pende, D., Cantoni, C., Mingari, M. C., Biassoni, R., & Moretta, L. (2001). Activating receptors and coreceptors involved in human natural killer cell-mediated cytolysis. *Annual Review of Immunology*, *19*, 197–223. https://doi.org/10.1146/annurev.immunol.19.1.197

Moretta, A., Marcenaro, E., Parolini, S., Ferlazzo, G., & Moretta, L. (2008). NK cells at the interface between innate and adaptive immunity. *Cell Death & Differentiation*, *15*(2), 226–233. https://doi.org/10.1038/sj.cdd.4402170

Nagasaki, J., Togashi, Y., Sugawara, T., Itami, M., Yamauchi, N., Yuda, J., Sugano, M., Ohara, Y., Minami, Y., Nakamae, H., Hino, M., Takeuchi, M., & Nishikawa, H. (2020). The critical role of CD4+ T cells in PD-1 blockade against MHC-II–expressing tumors such as classic Hodgkin lymphoma. *Blood Advances*, *4*(17), 4069–4082. https://doi.org/10.1182/bloodadvances.2020002098

Narayanan, S., Ahl, P. J., Bijin, V. A., Kaliaperumal, N., Lim, S. G., Wang, C.-I., Fairhurst, A.-M., & Connolly, J. E. (2020). *LAG3 is a Central Regulator of NK Cell Cytokine Production* [Preprint]. Immunology. https://doi.org/10.1101/2020.01.31.928200

Niu, C., Li, M., Zhu, S., Chen, Y., Zhou, L., Xu, D., Xu, J., Li, Z., Li, W., & Cui, J. (2020). PD-1-positive Natural Killer Cells have a weaker antitumor function than that of PD-1-negative Natural Killer Cells in Lung Cancer. *International Journal of Medical Sciences*, *17*(13), 1964–1973. https://doi.org/10.7150/ijms.47701

Noonan, K., & Borrello, I. (2011). The Immune Microenvironment of Myeloma. *Cancer Microenvironment*, *4*(3), 313–323. https://doi.org/10.1007/s12307-011-0086-3

Nouroz, F., Bibi, F., Noreen, S., & Masood, N. (2016). Natural killer cells enhance the immune surveillance of cancer. *Egyptian Journal of Medical Human Genetics*, *17*(2), 149–154. https://doi.org/10.1016/j.ejmhg.2015.08.006

Nückel, H., Switala, M., Sellmann, L., Horn, P. A., Dürig, J., Dührsen, U., Küppers, R., Grosse-Wilde, H., & Rebmann, V. (2010). The prognostic significance of soluble NKG2D ligands in B-cell chronic lymphocytic leukemia. *Leukemia*, *24*(6), 1152–1159. https://doi.org/10.1038/leu.2010.74

Ochoa, M. C., Minute, L., Rodriguez, I., Garasa, S., Perez-Ruiz, E., Inogés, S., Melero, I., & Berraondo, P. (2017). Antibody-dependent cell cytotoxicity: Immunotherapy strategies enhancing effector NK cells. *Immunology and Cell Biology*, *95*(4), 347–355. https://doi.org/10.1038/icb.2017.6

Ohmachi, K., Ogura, M., Suehiro, Y., Ando, K., Uchida, T., Choi, I., Ogawa, Y., Kobayashi, M., Fukino, K., Yokoi, Y., & Okamura, J. (2019). A multicenter phase I study of inebilizumab, a humanized anti-CD19 monoclonal antibody, in Japanese patients with relapsed or refractory B-cell lymphoma and multiple myeloma. *International Journal of Hematology*, *109*(6), 657–664. https://doi.org/10.1007/s12185-019-02635-9

Okazaki, T., & Honjo, T. (2006). Rejuvenating exhausted T cells during chronic viral infection. *Cell*, *124*(3), 459–461. https://doi.org/10.1016/j.cell.2006.01.022

Orange, J. S. (2008). Formation and function of the lytic NK-cell immunological synapse. *Nature Reviews. Immunology*, *8*(9), 713–725.

Palma, M., Gentilcore, G., Heimersson, K., Mozaffari, F., Näsman-Glaser, B., Young, E., Rosenquist, R., Hansson, L., Österborg, A., & Mellstedt, H. (2017). T cells in chronic lymphocytic leukemia display dysregulated expression of immune checkpoints and activation markers. *Haematologica*, *102*(3), 562–572. https://doi.org/10.3324/haematol.2016.151100

Papagno, L., Spina, C. A., Marchant, A., Salio, M., Rufer, N., Little, S., Dong, T., Chesney, G., Waters, A., Easterbrook, P., Dunbar, P. R., Shepherd, D., Cerundolo, V., Emery, V., Griffiths, P., Conlon, C., McMichael, A. J., Richman, D. D., Rowland-Jones, S. L., & Appay, V. (2004). Immune activation and CD8+ T-cell differentiation towards senescence in HIV-1 infection. *PLoS Biology*, *2*(2), E20. https://doi.org/10.1371/journal.pbio.0020020

Parodi, M., Favoreel, H., Candiano, G., Gaggero, S., Sivori, S., Mingari, M. C., Moretta, L., Vitale, M., & Cantoni, C. (2019). NKp44-NKp44 Ligand Interactions in the Regulation of Natural Killer Cells and Other Innate Lymphoid Cells in Humans. *Frontiers in Immunology*, *10*, 719. https://doi.org/10.3389/fimmu.2019.00719

Parry, H. M., Damery, S., Hudson, C., Maurer, M. J., Cerhan, J. R., Pachnio, A., Begum, J., Slager, S. L., Fegan, C., Man, S., Pepper, C., Shanafelt, T. D., Pratt, G., & Moss, P. A. H. (2016). Cytomegalovirus infection does not impact on survival or time to first treatment in patients with chronic lymphocytic leukemia. *American Journal of Hematology*, *91*(8), 776–781. https://doi.org/10.1002/ajh.24403

Parry, H. M., Stevens, T., Oldreive, C., Zadran, B., McSkeane, T., Rudzki, Z., Paneesha, S., Chadwick, C., Stankovic, T., Pratt, G., Zuo, J., & Moss, P. (2016). NK cell function is markedly impaired in patients with chronic lymphocytic leukaemia but is preserved in patients with small lymphocytic lymphoma. *Oncotarget*, *7*(42), 68513–68526. https://doi.org/10.18632/oncotarget.12097

Parry, R. V., Chemnitz, J. M., Frauwirth, K. A., Lanfranco, A. R., Braunstein, I., Kobayashi, S. V., Linsley, P. S., Thompson, C. B., & Riley, J. L. (2005). CTLA-4 and PD-1 receptors inhibit T-cell activation by distinct mechanisms. *Molecular and Cellular Biology*, *25*(21), 9543–9553. https://doi.org/10.1128/MCB.25.21.9543-9553.2005

Pauken, K. E., Godec, J., Odorizzi, P. M., Brown, K. E., Yates, K. B., Ngiow, S. F., Burke, K. P., Maleri, S., Grande, S. M., Francisco, L. M., Ali, M.-A., Imam, S., Freeman, G. J., Haining, W. N., Wherry, E. J., & Sharpe, A. H. (2020). The PD-1 Pathway Regulates Development and Function of Memory CD8+ T Cells following Respiratory Viral Infection. *Cell Reports*, *31*(13), 107827. https://doi.org/10.1016/j.celrep.2020.107827

Paul, S., & Lal, G. (2017). The Molecular Mechanism of Natural Killer Cells Function and Its Importance in Cancer Immunotherapy. *Frontiers in Immunology*, *8*. https://doi.org/10.3389/fimmu.2017.01124

Payandeh, Z., Noori, E., Khalesi, B., Mard-Soltani, M., Abdolalizadeh, J., & Khalili, S. (2018). Anti-CD37 targeted immunotherapy of B-Cell malignancies. *Biotechnology Letters*, *40*(11–12), 1459–1466. https://doi.org/10.1007/s10529-018-2612-6

Pegram, H. J., Andrews, D. M., Smyth, M. J., Darcy, P. K., & Kershaw, M. H. (2011). Activating and inhibitory receptors of natural killer cells. *Immunology and Cell Biology*, *89*(2), 216–224. https://doi.org/10.1038/icb.2010.78

Perez, O., Mitchell, D., Jager, G., South, S., Murriel, C. L., McBride, J., Herzenberg, L., Kinoshita, S., & Nolan, G. (2003). Leukocyte functional antigen 1 lowers T cell activation thresholds and signaling through cytohesin-1 and Jun-activating binding protein 1. *Nature Immunology*. https://doi.org/10.1038/ni1203-1254

Perez-Vilar, J., & Hill, R. L. (1999). The Structure and Assembly of Secreted Mucins * 210. *Journal of Biological Chemistry*, *274*(45), 31751–31754. https://doi.org/10.1074/jbc.274.45.31751

Pesce, S., Greppi, M., Tabellini, G., Rampinelli, F., Parolini, S., Olive, D., Moretta, L., Moretta, A., & Marcenaro, E. (2017). Identification of a subset of human natural killer cells expressing high levels of programmed death 1: A phenotypic and functional characterization. *Journal of Allergy and Clinical Immunology*, *139*(1), 335-346.e3. https://doi.org/10.1016/j.jaci.2016.04.025

Petrie, E. J., Clements, C. S., Lin, J., Sullivan, L. C., Johnson, D., Huyton, T., Heroux, A., Hoare, H. L., Beddoe, T., Reid, H. H., Wilce, M. C. J., Brooks, A. G., & Rossjohn, J. (2008). CD94-NKG2A recognition of human leukocyte antigen (HLA)-E bound to an HLA class I leader sequence. *The Journal of Experimental Medicine*, *205*(3), 725–735. https://doi.org/10.1084/jem.20072525

Post, M., Cuapio, A., Osl, M., Lehmann, D., Resch, U., Davies, D. M., Bilban, M., Schlechta, B., Eppel, W., Nathwani, A., Stoiber, D., Spanholtz, J., Casanova, E., & Hofer, E. (2017). The Transcription Factor ZNF683/HOBIT Regulates Human NK-Cell Development. *Frontiers in Immunology*, *8*. https://doi.org/10.3389/fimmu.2017.00535

Quatrini, L., Mariotti, F. R., Munari, E., Tumino, N., Vacca, P., & Moretta, L. (2020). The Immune Checkpoint PD-1 in Natural Killer Cells: Expression, Function and Targeting in Tumour Immunotherapy. *Cancers*, *12*(11). https://doi.org/10.3390/cancers12113285

Rafei, H., Daher, M., & Rezvani, K. (2021). Chimeric antigen receptor (CAR) natural killer (NK)-cell therapy: Leveraging the power of innate immunity. *British Journal of Haematology*, *193*(2), 216–230. https://doi.org/10.1111/bjh.17186

Raulet, D. (2004). Interplay of natural killer cells and their receptors with the adaptive immune response. *Nature Immunology*. https://doi.org/10.1038/ni1114

Rebmann, V., Schütt, P., Brandhorst, D., Opalka, B., Moritz, T., Nowrousian, M. R., & Grosse-Wilde, H. (2007). Soluble MICA as an independent prognostic factor for the overall survival and progression-free survival of multiple myeloma patients. *Clinical Immunology (Orlando, Fla.)*, *123*(1), 114–120. https://doi.org/10.1016/j.clim.2006.11.007

Reiners, K. S., Topolar, D., Henke, A., Simhadri, V. R., Kessler, J., Sauer, M., Bessler, M., Hansen, H. P., Tawadros, S., Herling, M., Krönke, M., Hallek, M., & Pogge von Strandmann, E. (2013). Soluble ligands for NK cell receptors promote evasion of chronic lymphocytic leukemia cells from NK cell anti-tumor activity. *Blood*, *121*(18), 3658–3665. https://doi.org/10.1182/blood-2013-01-476606

Reyfman, P. A., Walter, J. M., Joshi, N., Anekalla, K. R., McQuattie-Pimentel, A. C., Chiu, S., Fernandez, R., Akbarpour, M., Chen, C.-I., Ren, Z., Verma, R., Abdala-Valencia, H., Nam, K., Chi, M., Han, S., Gonzalez-Gonzalez, F. J., Soberanes, S., Watanabe, S., Williams, K. J. N., … Misharin, A. V. (2019). Single-Cell Transcriptomic Analysis of Human Lung Provides Insights into the Pathobiology of

Pulmonary Fibrosis. *American Journal of Respiratory and Critical Care Medicine*, *199*(12), 1517–1536. https://doi.org/10.1164/rccm.201712-2410OC

Robert, C. (2020). A decade of immune-checkpoint inhibitors in cancer therapy. *Nature Communications*, *11*(1), 3801. https://doi.org/10.1038/s41467-020-17670-y

Robert, C., Schachter, J., Long, G. V., Arance, A., Grob, J. J., Mortier, L., Daud, A., Carlino, M. S., McNeil, C., Lotem, M., Larkin, J., Lorigan, P., Neyns, B., Blank, C. U., Hamid, O., Mateus, C., Shapira-Frommer, R., Kosh, M., Zhou, H., … KEYNOTE-006 investigators. (2015). Pembrolizumab versus Ipilimumab in Advanced Melanoma. *The New England Journal of Medicine*, *372*(26), 2521–2532. https://doi.org/10.1056/NEJMoa1503093

Robertson, M. J., Caligiuri, M. A., Manley, T. J., Levine, H., & Ritz, J. (1990). Human natural killer cell adhesion molecules. Differential expression after activation and participation in cytolysis. *Journal of Immunology (Baltimore, Md.: 1950)*, *145*(10), 3194–3201.

Robertson, M. J., Cochran, K. J., Cameron, C., Le, J. M., Tantravahi, R., & Ritz, J. (1996). Characterization of a cell line, NKL, derived from an aggressive human natural killer cell leukemia. *Experimental Hematology*, *24*(3), 406–415.

Roda, J. M., Parihar, R., Magro, C., Nuovo, G. J., Tridandapani, S., & Carson, W. E. (2006). Natural Killer Cells Produce T Cell–Recruiting Chemokines in Response to Antibody-Coated Tumor Cells. *Cancer Research*, *66*(1), 517–526. https://doi.org/10.1158/0008-5472.CAN-05-2429

Rodrigues, C. A., Gonçalves, M. V., Ikoma, M. R. V., Lorand-Metze, I., Pereira, A. D., Farias, D. L. C. de, Chauffaille, M. de L. L. F., Schaffel, R., Ribeiro, E. F. O., Rocha, T. S. da, Buccheri, V., Vasconcelos, Y., Figueiredo, V. L. de P., Chiattone, C. S., Yamamoto, M., & Brazilian Group of Chronic Lymphocytic Leukemia. (2016). Diagnosis and treatment of chronic lymphocytic leukemia: Recommendations from the Brazilian Group of Chronic Lymphocytic Leukemia. *Revista Brasileira De Hematologia E Hemoterapia*, *38*(4), 346–357. https://doi.org/10.1016/j.bjhh.2016.07.004

Romee, R., Foley, B., Lenvik, T., Wang, Y., Zhang, B., Ankarlo, D., Luo, X., Cooley, S., Verneris, M., Walcheck, B., & Miller, J. (2013). NK cell CD16 surface expression and function is regulated by a disintegrin and metalloprotease-17 (ADAM17). *Blood*, *121*(18), 3599–3608. https://doi.org/10.1182/blood-2012-04-425397

Rose, D. M., Liu, S., Woodside, D. G., Han, J., Schlaepfer, D. D., & Ginsberg, M. H. (2003). Paxillin binding to the alpha 4 integrin subunit stimulates LFA-1 (integrin alpha L beta 2)-dependent T cell migration by augmenting the activation of focal adhesion kinase/proline-rich tyrosine kinase-2. *Journal of Immunology (Baltimore, Md.: 1950)*, *170*(12), 5912–5918. https://doi.org/10.4049/jimmunol.170.12.5912

Rosental, B., Brusilovsky, M., Hadad, U., Oz, D., Appel, M. Y., Afergan, F., Yossef, R., Rosenberg, L. A., Aharoni, A., Cerwenka, A., Campbell, K. S., Braiman, A., & Porgador, A. (2011). Proliferating cell nuclear antigen is a novel inhibitory ligand for the natural cytotoxicity receptor NKp44. *Journal of Immunology (Baltimore, Md.: 1950)*, *187*(11), 5693–5702. https://doi.org/10.4049/jimmunol.1102267

Rosmaraki, E., Douagi, I., Roth, C., Colucci, F., Cumano, A., & Di Santo, J. (2001). Identification of committed NK cell progenitors in the adult bone marrow. *European Journal of Immunology*, *31*, 1900–1909. https://doi.org/10.1002/1521-4141(200106)31:6<1900::aid-immu1900>3.0.co

Rudd, C. E., Taylor, A., & Schneider, H. (2009). CD28 and CTLA-4 coreceptor expression and signal transduction. *Immunological Reviews*, *229*(1), 12–26. https://doi.org/10.1111/j.1600-065X.2009.00770.x

Sanchez-Correa, B., Gayoso, I., Bergua, J. M., Casado, J. G., Morgado, S., Solana, R., & Tarazona, R. (2012). Decreased expression of DNAM-1 on NK cells from acute myeloid leukemia patients. *Immunology and Cell Biology*, *90*(1), 109–115. https://doi.org/10.1038/icb.2011.15

Sartor, W. M., Kyprianou, N., Fabian, D. F., & Lefor, A. T. (1995). Enhanced expression of ICAM-1 in a murine fibrosarcoma reduces tumor growth rate. *The Journal of Surgical Research*, *59*(1), 66–74. https://doi.org/10.1006/jsre.1995.1133

Schoppmeyer, R., Zhao, R., Cheng, H., Hamed, M., Liu, C., Zhou, X., Schwarz, E. C., Zhou, Y., Knörck, A., Schwär, G., Ji, S., Liu, L., Long, J., Helms, V., Hoth, M., Yu, X., & Qu, B. (2017). Human profilin 1 is a negative regulator of CTL mediated cell-killing and migration. *European Journal of Immunology*, *47*(9), 1562–1572. https://doi.org/10.1002/eji.201747124

Schroder, K., Hertzog, P. J., Ravasi, T., & Hume, D. A. (2004). Interferon-γ: An overview of signals, mechanisms and functions. *Journal of Leukocyte Biology*, *75*(2), 163–189. https://doi.org/10.1189/jlb.0603252

Scrivener, S., Goddard, R. V., Kaminski, E. R., & Prentice, A. G. (2003). Abnormal T-cell function in B-cell chronic lymphocytic leukaemia. *Leukemia & Lymphoma*, *44*(3), 383–389. https://doi.org/10.1080/1042819021000029993

Shannon, M. J., & Mace, E. M. (2021). Natural Killer Cell Integrins and Their Functions in Tissue Residency. *Frontiers in Immunology*, *12*, 647358. https://doi.org/10.3389/fimmu.2021.647358

Shimizu, Y., & DeMars, R. (1989). Production of human cells expressing individual transferred HLA-A,-B,-C genes using an HLA-A,-B,-C null human cell line. *Journal of Immunology (Baltimore, Md.: 1950)*, *142*(9), 3320–3328.

Simonetta, F., Pradier, A., & Roosnek, E. (2016). T-bet and Eomesodermin in NK Cell Development, Maturation, and Function. *Frontiers in Immunology*, *7*, 241. https://doi.org/10.3389/fimmu.2016.00241

Simula, L., Cancila, V., Antonucci, Y., Colamatteo, A., Procaccini, C., Matarese, G., Tripodo, C., & Campello, S. (2020). PD-1-induced T cell exhaustion is controlled by a Drp1-dependent mechanism. *BioRxiv*, 2020.07.14.200592. https://doi.org/10.1101/2020.07.14.200592

Sivori, S., Della Chiesa, M., Carlomagno, S., Quatrini, L., Munari, E., Vacca, P., Tumino, N., Mariotti, F. R., Mingari, M. C., Pende, D., & Moretta, L. (2020). Inhibitory Receptors and Checkpoints in Human NK Cells, Implications for the Immunotherapy of Cancer. *Frontiers in Immunology*, *11*. https://doi.org/10.3389/fimmu.2020.02156

Smyth, M. J., Cretney, E., Kelly, J. M., Westwood, J. A., Street, S. E. A., Yagita, H., Takeda, K., van Dommelen, S. L. H., Degli-Esposti, M. A., & Hayakawa, Y. (2005). Activation of NK cell cytotoxicity. *Molecular Immunology*, *42*(4), 501–510. https://doi.org/10.1016/j.molimm.2004.07.034

Sonar, S., & Lal, G. (2015). Role of Tumor Necrosis Factor Superfamily in Neuroinflammation and Autoimmunity. *Frontiers in Immunology*, *6*, 364. https://doi.org/10.3389/fimmu.2015.00364

Sordo-Bahamonde, C., Lorenzo-Herrero, S., González-Rodríguez, A. P., Payer, Á. R., González-García, E., López-Soto, A., & Gonzalez, S. (2021). LAG-3 Blockade with Relatlimab (BMS-986016) Restores Anti-Leukemic Responses in Chronic Lymphocytic Leukemia. *Cancers*, *13*(9), 2112. https://doi.org/10.3390/cancers13092112

Souza-Fonseca-Guimaraes, F., Cursons, J., & Huntington, N. (2019). The Emergence of Natural Killer Cells as a Major Target in Cancer Immunotherapy. *Trends in Immunology*. https://doi.org/10.1016/j.it.2018.12.003

Sportoletti, P., De Falco, F., Del Papa, B., Baldoni, S., Guarente, V., Marra, A., Dorillo, E., Rompietti, C., Adamo, F. M., Ruggeri, L., Di Ianni, M., & Rosati, E. (2021). NK Cells in Chronic Lymphocytic Leukemia and Their Therapeutic Implications. *International Journal of Molecular Sciences*, *22*(13), 6665. https://doi.org/10.3390/ijms22136665

Srivastava, R. M., Lee, S. C., Andrade Filho, P. A., Lord, C. A., Jie, H.-B., Davidson, H. C., López-Albaitero, A., Gibson, S. P., Gooding, W. E., Ferrone, S., & Ferris, R. L. (2013). Cetuximab-activated natural killer and dendritic cells collaborate to trigger tumor antigen-specific T-cell immunity in head and neck cancer patients. *Clinical Cancer Research: An Official Journal of the American Association for Cancer Research*, *19*(7), 1858–1872. https://doi.org/10.1158/1078-0432.CCR-12-2426

Stanietsky, N., Rovis, T. L., Glasner, A., Seidel, E., Tsukerman, P., Yamin, R., Enk, J., Jonjic, S., & Mandelboim, O. (2013). Mouse TIGIT inhibits NK-cell cytotoxicity upon interaction with PVR. *European Journal of Immunology*, *43*(8), 2138–2150. https://doi.org/10.1002/eji.201243072

Stanietsky, N., Simic, H., Arapovic, J., Toporik, A., Levy, O., Novik, A., Levine, Z., Beiman, M., Dassa, L., Achdout, H., Stern-Ginossar, N., Tsukerman, P., Jonjic, S., & Mandelboim, O. (2009). The interaction of TIGIT with PVR and PVRL2 inhibits human NK cell cytotoxicity. *Proceedings of the National Academy of Sciences*, *106*(42), 17858–17863. https://doi.org/10.1073/pnas.0903474106

Stanley, A. C., & Lacy, P. (2010). Pathways for Cytokine Secretion. *Physiology*, *25*(4), 218–229. https://doi.org/10.1152/physiol.00017.2010

Stojanovic, A., Fiegler, N., Brunner-Weinzierl, M., & Cerwenka, A. (2014). CTLA-4 is expressed by activated mouse NK cells and inhibits NK Cell IFN-γ production in response to mature dendritic cells. *Journal of Immunology (Baltimore, Md.: 1950)*, *192*(9), 4184–4191. https://doi.org/10.4049/jimmunol.1302091

Sun, C., Xu, J., Huang, Q., Huang, M., Wen, H., Zhang, C., Wang, J., Song, J., Zheng, M., Sun, H., Wei, H., Xiao, W., Sun, R., & Tian, Z. (2016). High NKG2A expression contributes to NK cell exhaustion and predicts a poor prognosis of patients with liver cancer. *Oncoimmunology*, *6*(1), e1264562. https://doi.org/10.1080/2162402X.2016.1264562

Sun, H., Huang, Q., Huang, M., Wen, H., Lin, R., Zheng, M., Qu, K., Li, K., Wei, H., Xiao, W., Sun, R., Tian, Z., & Sun, C. (2019). Human CD96 Correlates to Natural Killer Cell Exhaustion and Predicts the Prognosis of Human Hepatocellular Carcinoma. *Hepatology (Baltimore, Md.)*, *70*(1), 168–183. https://doi.org/10.1002/hep.30347

Sun, H., Liu, L., Huang, Q., Liu, H., Huang, M., Wang, J., Wen, H., Lin, R., Qu, K., Li, K., Wei, H., Xiao, W., Sun, R., Tian, Z., & Sun, C. (2019). Accumulation of Tumor-Infiltrating CD49a+ NK Cells Correlates with Poor Prognosis for Human Hepatocellular Carcinoma. *Cancer Immunology Research*, *7*(9), 1535–1546. https://doi.org/10.1158/2326-6066.CIR-18-0757

Sun, H., & Sun, C. (2019). The Rise of NK Cell Checkpoints as Promising Therapeutic Targets in Cancer Immunotherapy. *Frontiers in Immunology*, *10*, 2354. https://doi.org/10.3389/fimmu.2019.02354

Sun, Y., Miao, N., & Sun, T. (2019). Detect accessible chromatin using ATAC-sequencing, from principle to applications. *Hereditas*, *156*, 29. https://doi.org/10.1186/s41065-019-0105-9

Taghiloo, S., Allahmoradi, E., Ebadi, R., Tehrani, M., Hosseini-Khah, Z., Janbabaei, G., Shekarriz, R., & Asgarian-Omran, H. (2017). Upregulation of Galectin-9 and PD-L1 Immune Checkpoints Molecules in Patients with Chronic Lymphocytic Leukemia. *Asian Pacific Journal of Cancer Prevention : APJCP*, *18*(8), 2269–2274. https://doi.org/10.22034/APJCP.2017.18.8.2269

Tahara-Hanaoka, S., Shibuya, K., Onoda, Y., Zhang, H., Yamazaki, S., Miyamoto, A., Honda, S.-I., Lanier, L. L., & Shibuya, A. (2004). Functional characterization of DNAM-1 (CD226) interaction with its

ligands PVR (CD155) and nectin-2 (PRR-2/CD112). *International Immunology*, *16*(4), 533–538. https://doi.org/10.1093/intimm/dxh059

Tan, T.-T., & Coussens, L. M. (2007). Humoral immunity, inflammation and cancer. *Current Opinion in Immunology*, *19*(2), 209–216. https://doi.org/10.1016/j.coi.2007.01.001

Terra Junior, O. N., Maldonado, G. de C., Alfradique, G. R., Lisboa, V. da C., Arnóbio, A., de Lima, D. B., Diamond, H. R., & de Souza, M. H. F. O. (2016). Study of Natural Cytotoxicity Receptors in Patients with HIV/AIDS and Cancer: A Cross-Sectional Study. *The Scientific World Journal*, *2016*, 2085871. https://doi.org/10.1155/2016/2085871

Thielens, A., Vivier, E., & Romagné, F. (2012). NK cell MHC class I specific receptors (KIR): From biology to clinical intervention. *Current Opinion in Immunology*, *24*(2), 239–245. https://doi.org/10.1016/j.coi.2012.01.001

Topham, N. J., & Hewitt, E. W. (2009). Natural killer cell cytotoxicity: How do they pull the trigger? *Immunology*, *128*(1), 7–15. https://doi.org/10.1111/j.1365-2567.2009.03123.x

Trefny, M. P., Kaiser, M., Stanczak, M. A., Herzig, P., Savic, S., Wiese, M., Lardinois, D., Läubli, H., Uhlenbrock, F., & Zippelius, A. (2020). PD-1+ natural killer cells in human non-small cell lung cancer can be activated by PD-1/PD-L1 blockade. *Cancer Immunology, Immunotherapy*, *69*(8), 1505–1517. https://doi.org/10.1007/s00262-020-02558-z

Uhm, J. (2020). Recent advances in chronic lymphocytic leukemia therapy. *Blood Research*, *55*(0), S72–S82. https://doi.org/10.5045/br.2020.S012

van der Horst, H. J., Nijhof, I. S., Mutis, T., & Chamuleau, M. E. D. (2020). Fc-Engineered Antibodies with Enhanced Fc-Effector Function for the Treatment of B-Cell Malignancies. *Cancers*, *12*(10), 3041. https://doi.org/10.3390/cancers12103041

Velázquez, F., Grodecki-Pena, A., Knapp, A., Salvador, A. M., Nevers, T., Croce, K., & Alcaide, P. (2016). CD43 Functions as an E-Selectin Ligand for Th17 Cells In Vitro and Is Required for Rolling on the Vascular Endothelium and Th17 Cell Recruitment during Inflammation In Vivo. *Journal of Immunology (Baltimore, Md.: 1950)*, *196*(3), 1305–1316. https://doi.org/10.4049/jimmunol.1501171

Vendrame, E., Fukuyama, J., Strauss-Albee, D. M., Holmes, S., & Blish, C. A. (2017). Mass Cytometry Analytical Approaches Reveal Cytokine-Induced Changes in Natural Killer Cells. *Cytometry Part B: Clinical Cytometry*, *92*(1), 57–67. https://doi.org/10.1002/cyto.b.21500

Vesely, M. D., Kershaw, M. H., Schreiber, R. D., & Smyth, M. J. (2011). Natural innate and adaptive immunity to cancer. *Annual Review of Immunology*, *29*, 235–271. https://doi.org/10.1146/annurev-immunol-031210-101324

Veuillen, C., Aurran-Schleinitz, T., Castellano, R., Rey, J., Mallet, F., Orlanducci, F., Pouyet, L., Just-Landi, S., Coso, D., Ivanov, V., Carcopino, X., Bouabdallah, R., Collette, Y., Fauriat, C., & Olive, D. (2012). Primary B-CLL Resistance to NK Cell Cytotoxicity can be Overcome In Vitro and In Vivo by Priming NK Cells and Monoclonal Antibody Therapy. *Journal of Clinical Immunology*, *32*, 632–646. https://doi.org/10.1007/s10875-011-9624-5

Vey, N., Karlin, L., Sadot-Lebouvier, S., Broussais, F., Berton-Rigaud, D., Rey, J., Charbonnier, A., Marie, D., André, P., Paturel, C., Zerbib, R., Bennouna, J., Salles, G., & Gonçalves, A. (2018). A phase 1 study of lirilumab (antibody against killer immunoglobulin-like receptor antibody KIR2D; IPH2102) in patients with solid tumors and hematologic malignancies. *Oncotarget*, *9*(25), 17675–17688. https://doi.org/10.18632/oncotarget.24832

Vinay, D. S., Ryan, E. P., Pawelec, G., Talib, W. H., Stagg, J., Elkord, E., Lichtor, T., Decker, W. K., Whelan, R. L., Kumara, H. M. C. S., Signori, E., Honoki, K., Georgakilas, A. G., Amin, A., Helferich, W.

G., Boosani, C. S., Guha, G., Ciriolo, M. R., Chen, S., … Kwon, B. S. (2015). Immune evasion in cancer: Mechanistic basis and therapeutic strategies. *Seminars in Cancer Biology*, *35 Suppl*, S185–S198. https://doi.org/10.1016/j.semcancer.2015.03.004

Vivier, E., Nunès, J. A., & Vély, F. (2004). Natural killer cell signaling pathways. *Science (New York, N.Y.)*, *306*(5701), 1517–1519. https://doi.org/10.1126/science.1103478

Vivier, E., Raulet, D. H., Moretta, A., Caligiuri, M. A., Zitvogel, L., Lanier, L. L., Yokoyama, W. M., & Ugolini, S. (2011). Innate or Adaptive Immunity? The Example of Natural Killer Cells. *Science (New York, N.Y.)*, *331*(6013), 44–49. https://doi.org/10.1126/science.1198687

Vivier, E., Tomasello, E., Baratin, M., Walzer, T., & Ugolini, S. (2008). Functions of natural killer cells. *Nature Immunology*, *9*(5), 503–510. https://doi.org/10.1038/ni1582

Vivier, E., & Ugolini, S. (2011). Natural Killer Cells: From Basic Research to Treatments. *Frontiers in Immunology*, *2*, 18. https://doi.org/10.3389/fimmu.2011.00018

Vlachonikola, E., Stamatopoulos, K., & Chatzidimitriou, A. (2021). T Cells in Chronic Lymphocytic Leukemia: A Two-Edged Sword. *Frontiers in Immunology*, *11*, 3602. https://doi.org/10.3389/fimmu.2020.612244

Wang, F., Hou, H., Wu, S., Tang, Q., Liu, W., Huang, M., Yin, B., Huang, J., Mao, L., Lu, Y., & Sun, Z. (2015). TIGIT expression levels on human NK cells correlate with functional heterogeneity among healthy individuals. *European Journal of Immunology*, *45*(10), 2886–2897. https://doi.org/10.1002/eji.201545480

Wang, M., Zhang, C., Song, Y., Wang, Z., Wang, Y., Luo, F., Xu, Y., Zhao, Y., Wu, Z., & Xu, Y. (2017). Mechanism of immune evasion in breast cancer. *OncoTargets and Therapy*, *10*, 1561–1573. https://doi.org/10.2147/OTT.S126424

Wang, W., Erbe, A. K., Hank, J. A., Morris, Z. S., & Sondel, P. M. (2015). NK Cell-Mediated Antibody-Dependent Cellular Cytotoxicity in Cancer Immunotherapy. *Frontiers in Immunology*, *6*, 368. https://doi.org/10.3389/fimmu.2015.00368

Wang, W.-T., Zhu, H.-Y., Wu, Y.-J., Xia, Y., Wu, J.-Z., Wu, W., Liang, J.-H., Wang, L., Fan, L., Li, J.-Y., & Xu, W. (2018). Elevated absolute NK cell counts in peripheral blood predict good prognosis in chronic lymphocytic leukemia. *Journal of Cancer Research and Clinical Oncology*, *144*(3), 449–457. https://doi.org/10.1007/s00432-017-2568-2

Weinmann, A. S. (2021). Genome regulation in innate and adaptive immune cells. *Immunological Reviews*, *300*(1), 5–8. https://doi.org/10.1111/imr.12957

Wodnar-Filipowicz, A., & Kalberer, C. (2006). Function of natural killer cells in immune defence against human leukaemia. *Swiss Medical Weekly*.

Wolchok, J. D., Chiarion-Sileni, V., Gonzalez, R., Rutkowski, P., Grob, J.-J., Cowey, C. L., Lao, C. D., Wagstaff, J., Schadendorf, D., Ferrucci, P. F., Smylie, M., Dummer, R., Hill, A., Hogg, D., Haanen, J., Carlino, M. S., Bechter, O., Maio, M., Marquez-Rodas, I., … Larkin, J. (2017). Overall Survival with Combined Nivolumab and Ipilimumab in Advanced Melanoma. *The New England Journal of Medicine*, *377*(14), 1345–1356. https://doi.org/10.1056/NEJMoa1709684

Xia, Y., Jeffrey Medeiros, L., & Young, K. H. (2016). Signaling pathway and dysregulation of PD1 and its ligands in lymphoid malignancies. *Biochimica Et Biophysica Acta*, *1865*(1), 58–71. https://doi.org/10.1016/j.bbcan.2015.09.002

Xu-Monette, Z. Y., Zhou, J., & Young, K. H. (2018). PD-1 expression and clinical PD-1 blockade in B-cell lymphomas. *Blood*, *131*(1), 68–83. https://doi.org/10.1182/blood-2017-07-740993

Yang, Z.-Z., Kim, H. J., Villasboas, J. C., Chen, Y.-P., Price-Troska, T., Jalali, S., Wilson, M., Novak, A. J., & Ansell, S. M. (2017). Expression of LAG-3 defines exhaustion of intratumoral PD-1+ T cells and correlates with poor outcome in follicular lymphoma. *Oncotarget*, *8*(37), 61425–61439. https://doi.org/10.18632/oncotarget.18251

Young, H. A., Ortaldo, J. R., Herberman, R. B., & Reynolds, C. W. (1986). Analysis of T cell receptors in highly purified rat and human large granular lymphocytes (LGL): Lack of functional 1.3 kb beta-chain mRNA. *Journal of Immunology (Baltimore, Md.: 1950)*, *136*(7), 2701–2704.

Yu, J., Freud, A. G., & Caligiuri, M. A. (2013). Location and cellular stages of natural killer cell development. *Trends in Immunology*, *34*(12), 573–582. https://doi.org/10.1016/j.it.2013.07.005

Zafirova, B., Wensveen, F. M., Gulin, M., & Polić, B. (2011). Regulation of immune cell function and differentiation by the NKG2D receptor. *Cellular and Molecular Life Sciences: CMLS*, *68*(21), 3519–3529. https://doi.org/10.1007/s00018-011-0797-0

Zhang, H., Vijayan, D., Li, X.-Y., Robson, S. C., Geetha, N., Teng, M. W. L., & Smyth, M. J. (2019). The role of NK cells and CD39 in the immunological control of tumor metastases. *OncoImmunology*, *8*(6), e1593809. https://doi.org/10.1080/2162402X.2019.1593809

Zhang, J., Marotel, M., Fauteux-Daniel, S., Mathieu, A.-L., Viel, S., Marçais, A., & Walzer, T. (2018). T-bet and Eomes govern differentiation and function of mouse and human NK cells and ILC1. *European Journal of Immunology*, *48*(5), 738–750. https://doi.org/10.1002/eji.201747299

Zhang, K., & Chen, J. (2012). The regulation of integrin function by divalent cations. *Cell Adhesion & Migration*, *6*(1), 20–29. https://doi.org/10.4161/cam.18702

Zhang, Q., Bi, J., Zheng, X., Chen, Y., Wang, H., Wu, W., Wang, Z., Wu, Q., Peng, H., Wei, H., Sun, R., & Tian, Z. (2018). Blockade of the checkpoint receptor TIGIT prevents NK cell exhaustion and elicits potent anti-tumor immunity. *Nature Immunology*, *19*(7), 723–732. https://doi.org/10.1038/s41590-018-0132-0

Zitvogel, L., & Kroemer, G. (2012). Targeting PD-1/PD-L1 interactions for cancer immunotherapy. *Oncoimmunology*, *1*(8), 1223–1225. https://doi.org/10.4161/onci.21335

APPENDIX

Supplementary table 1, list of B-CLL patients recruited for this study

NO	Patients' code	CMV sero-status		NO	Patients' code	CMV sero-status
1	108RK	Positive		39	305PM	Negative
2	161SK	Negative		40	144BF	Positive
3	333LJ	Positive		41	176TR	Negative
4	357JF	Negative		42	338AB	Positive
5	14SP	Positive		43	69JS	Positive
6	259SB	Positive		44	279AB	Negative
7	57AC	Negative		45	158MH	Negative
8	84PS	Positive		46	CM345	Positive
9	183JN	Positive		47	299CW	Positive
10	219GR	Negative		48	306BA	Negative
11	258PH	Negative		49	174RW	Positive
12	265FM	Positive		50	272RH	Positive
13	266MC	Positive		51	217BS	Negative
14	330AR	Negative		52	114SP	Positive
15	302JH	Negative		53	234KW	Positive
16	310AP	Positive		54	157PS	Negative
17	370MH	Negative		55	56AT	Positive
18	IM332	Negative		56	303WP	Positive
19	PS374	Negative		57	323BC	Positive
20	314PS	Positive		58	226KM	Positive
21	286AB	Negative		59	229LH	Negative
22	288AP	Positive		60	241AP	Positive
23	SL290	Negative		61	328JG	Negative
24	261MY	Positive		62	MB351	Positive
25	309AM	Negative		63	MM352	Positive
26	178TS	Positive		64	335JT	Positive
27	65RG	Positive		65	184PW	Positive
28	JG235	Positive		66	368JR	Negative
29	263DJ	Positive		67	381PM	Negative
30	321AB	Positive		68	PL382	Negative
31	337CO	Negative		69	359CT	Positive
32	96TH	Negative		70	11JL	Negative
33	340TR	Positive		71	345LM	Negative
34	164FJ	Positive		72	274AM	Positive
35	375GM	Negative		73	313RB	Positive
36	283PJ	Positive		74	363EG	Negative
37	46AE	Negative		75	PH300	Negative
38	230YN	Positive				

Supplementary table 2 Healthy donors recruited for this study

NO	Donor code	CMV sero-status
1	8GT	Negative
2	59JH	Negative
3	63KM	Positive
4	6RC	Negative
5	30CC	Negative
6	SH	Negative
7	107JSC	Negative
8	26RE	Negative
9	33GG	Negative
10	84ABW	Negative
11	1AB	Negative
12	50DB	Positive
13	DA	Positive
14	PA	Positive
15	RB	Positive
16	GM	Positive
17	RA	Positive
18	DW	Positive
19	NH	Negative
20	TH	Negative
21	RP	Negative
22	SE	Negative
23	NC	Negative
24	EH	Negative
25	CDS	Positive

Supplementary table 3, list of 302 differentiated genes in PD-1^{pos} NK cells from scRNA-seq

Gene	Top	p.value	FDR	logFC.neg		Gene	Top	p.value	FDR	logFC.neg
IL32	1	1.96E-119	7.42E-116	0.602612		MYL12B	36	9.36E-10	9.87E-08	0.096569
CD3E	2	3.12E-85	5.91E-82	0.367826		TBC1D10C	37	1.93E-09	1.98E-07	0.059773
S100A4	3	7.30E-38	9.23E-35	0.255044		BLOC1S1	38	3.74E-09	3.73E-07	0.061719
GZMH	4	1.26E-36	1.20E-33	0.277754		ZAP70	39	5.13E-09	4.99E-07	0.057528
PFN1	5	1.05E-31	8.00E-29	0.210547		ANXA1	40	5.52E-09	5.24E-07	0.081165
TMSB4X	6	1.29E-31	8.19E-29	0.191444		IFITM2	41	6.26E-09	5.79E-07	0.107351
TMSB10	7	5.40E-31	2.93E-28	0.164334		HBA2	42	8.44E-09	7.62E-07	0.039426
TRBC1	8	3.87E-26	1.84E-23	0.168714		UBC	43	1.04E-08	9.18E-07	0.105093
B2M	9	5.42E-22	2.29E-19	0.083798		NKG7	44	1.25E-08	1.07E-06	0.064502
HBA1	10	1.16E-19	4.40E-17	0.110287		PPP1CA	45	1.70E-08	1.43E-06	0.062571
PDCD1	11	1.32E-19	4.56E-17	0.037309		ERP29	46	1.77E-08	1.46E-06	0.067314
CFL1	12	9.69E-19	3.06E-16	0.152511		KLRC1	47	2.59E-08	2.09E-06	0.014296
CCL5	13	1.70E-18	4.96E-16	0.201621		TECR	48	3.07E-08	2.42E-06	0.060684
SH3BGRL3	14	8.55E-18	2.32E-15	0.145842		GRAP2	49	3.33E-08	2.58E-06	0.027081
IFITM1	15	5.62E-17	1.42E-14	0.092091		MYL12A	50	4.00E-08	3.04E-06	0.095022
CMC1	16	6.33E-17	1.50E-14	0.220621		CORO1A	51	5.83E-08	4.34E-06	0.083057
CYBA	17	1.17E-16	2.61E-14	0.153877		C19orf24	52	8.19E-08	5.98E-06	0.042708
ACTB	18	6.23E-16	1.31E-13	0.205939		ATP5IF1	53	8.60E-08	6.16E-06	0.070719
ARPC5L	19	1.08E-15	2.17E-13	0.119956		SLC38A2	54	1.32E-07	9.28E-06	0.046477
CD52	20	2.88E-15	5.47E-13	0.132603		SIGIRR	55	1.55E-07	1.07E-05	0.050455
CRIP1	21	6.27E-15	1.13E-12	0.102811		PSMB9	56	1.59E-07	1.08E-05	0.05978
HCST	22	8.08E-15	1.39E-12	0.139391		PPP1R18	57	2.10E-07	1.40E-05	0.054887
LAG3	23	1.30E-14	2.15E-12	0.07068		SLC9A3R1	58	2.49E-07	1.63E-05	0.04759
PTMS	24	1.88E-14	2.97E-12	0.081107		PATL2	59	2.77E-07	1.78E-05	0.047345
ITGB2	25	6.71E-14	1.02E-11	0.127144		HSPA8	60	3.12E-07	1.93E-05	0.069519
NDUFB7	26	1.19E-13	1.74E-11	0.107417		DNAJB1	61	3.17E-07	1.93E-05	0.079146
LCK	27	2.53E-11	3.55E-09	0.090206		GZMA	62	3.19E-07	1.93E-05	0.096995
LGALS1	28	3.37E-11	4.54E-09	0.109628		PRSS57	63	3.20E-07	1.93E-05	0.045185
SERF2	29	3.47E-11	4.54E-09	0.103111		LYAR	64	3.41E-07	2.02E-05	0.071379
LSP1	30	6.68E-11	8.45E-09	0.097904		FCRL6	65	3.87E-07	2.26E-05	0.032762
TMA7	31	8.96E-11	1.10E-08	0.111088		ATP6V0E1	66	4.63E-07	2.66E-05	0.049856
TRDC	32	1.05E-10	1.25E-08	0.127158		LAIR2	67	4.88E-07	2.77E-05	0.04414
TSPO	33	1.71E-10	1.96E-08	0.065624		ARHGDIB	68	6.23E-07	3.48E-05	0.080615
KIF19	34	6.33E-10	7.06E-08	0.038878		PPP6R1	69	6.96E-07	3.83E-05	0.036036
FGFBP2	35	8.33E-10	9.04E-08	0.108978		MYL6	70	7.19E-07	3.90E-05	0.089386

FCGR3A	71	1.05E-06	5.61E-05	0.081018		LMF2	106	2.78E-05	0.000995	0.026325
C12orf75	72	1.12E-06	5.88E-05	0.086442		CUTA	107	3.40E-05	0.001207	0.050425
EFHD2	73	1.15E-06	5.96E-05	0.08831		TAF6L	108	3.64E-05	0.001277	0.021489
TRAPPC1	74	1.30E-06	6.68E-05	0.053658		CD2	109	4.13E-05	0.001438	0.050361
CCND3	75	1.33E-06	6.74E-05	0.041885		NCR3	110	4.32E-05	0.001489	0.040641
PFDN5	76	1.97E-06	9.79E-05	0.068104		CTSC	111	4.73E-05	0.001616	0.035557
CCDC107	77	1.99E-06	9.79E-05	0.031725		CD63	112	5.28E-05	0.001781	0.060657
DERL2	78	2.62E-06	0.000128	0.042896		TUBB	113	5.30E-05	0.001781	0.028079
FBXW5	79	3.73E-06	0.000179	0.040733		ARF5	114	6.26E-05	0.002083	0.031347
SPSB3	80	3.77E-06	0.000179	0.042939		NUBP2	115	6.54E-05	0.002158	0.022735
PSME1	81	4.03E-06	0.000189	0.065408		HSPB1	116	6.87E-05	0.002248	0.023837
ORMDL3	82	4.90E-06	0.000227	0.031936		MPPE1	117	7.10E-05	0.002295	0.032068
RHOH	83	5.88E-06	0.000265	0.050712		HSPA1A	118	7.14E-05	0.002295	0.04409
CD244	84	5.91E-06	0.000265	0.029849		SNHG25	119	7.25E-05	0.002295	0.045221
HDDC2	85	5.93E-06	0.000265	0.052895		EED	120	7.26E-05	0.002295	0.023403
S100A6	86	6.18E-06	0.00027	0.089405		MIEN1	121	7.67E-05	0.002405	0.035595
ATP5MD	87	6.23E-06	0.00027	0.053874		CTDSP1	122	7.78E-05	0.002419	0.030388
PET100	88	6.27E-06	0.00027	0.066622		POP4	123	8.32E-05	0.002568	0.028975
MLF1	89	6.87E-06	0.000293	0.019457		EMP3	124	8.59E-05	0.00263	0.049643
AGTRAP	90	8.21E-06	0.000346	0.029555		ATRAID	125	9.07E-05	0.002753	0.027772
RAC2	91	9.75E-06	0.000407	0.061239		BSG	126	9.19E-05	0.002769	0.045943
PRDX2	92	9.89E-06	0.000408	0.036133		TRG-AS1	127	9.50E-05	0.002838	0.024262
CASP1	93	1.03E-05	0.000418	0.031205		C1orf56	128	0.000101	0.003006	0.051439
TMEM258	94	1.28E-05	0.000513	0.05132		ARPC2	129	0.000102	0.003014	0.051861
MAPK1	95	1.28E-05	0.000513	0.044568		HNRNPA2B1	130	0.000104	0.003032	0.052986
OST4	96	1.35E-05	0.000533	0.05591		IKZF1	131	0.000106	0.00307	0.044273
DDB2	97	1.52E-05	0.000596	0.029023		YPEL3	132	0.000114	0.003275	0.050587
GTF3C1	98	1.78E-05	0.000687	0.05472		ISG20	133	0.00012	0.003434	0.048952
MRPL13	99	1.79E-05	0.000687	0.026122		GMFG	134	0.00013	0.003652	0.045515
TOX	100	1.82E-05	0.000689	0.020431		UQCR11	135	0.00013	0.003652	0.057245
PTPRA	101	2.00E-05	0.00075	0.030135		EOMES	136	0.000131	0.003652	0.041546
ATP5ME	102	2.19E-05	0.000814	0.064284		PSME2	137	0.000134	0.003726	0.042661
GADD45B	103	2.24E-05	0.000824	0.043037		NDUFB9	138	0.000139	0.003835	0.043336
MAP4K1	104	2.65E-05	0.000967	0.0264		SPCS1	139	0.000145	0.003969	0.043861
CAPN2	105	2.68E-05	0.000969	0.036748		ARRB2	140	0.000148	0.004015	0.029097

VPS28	141	0.000152	0.004082	0.033152		CD247	178	0.000493	0.010516	0.043208
TMEM273	142	0.000157	0.004169	0.018423		CYTOR	179	0.0005	0.010607	0.030286
PTGDR	143	0.000157	0.004169	0.021783		CELF2	180	0.000554	0.011679	0.028929
ATP5MC2	144	0.000158	0.004169	0.060922		CES1	181	0.000558	0.0117	0.009369
C1orf122	145	0.000175	0.004575	0.032999		PARK7	182	0.000566	0.011802	0.043784
SHKBP1	146	0.000177	0.004588	0.027418		GPAA1	183	0.000583	0.012083	0.026001
CYFIP2	147	0.000185	0.004765	0.02738		TMED9	184	0.000623	0.012842	0.026022
ARHGAP30	148	0.000186	0.004765	0.035058		KIF22	185	0.000677	0.01389	0.019919
ATP5F1E	149	0.000187	0.004775	0.066299		MAD2L2	186	0.000687	0.014016	0.029236
PRELID1	150	0.000191	0.004822	0.047971		AHNAK	187	0.0007	0.014169	0.029286
G6PD	151	0.000193	0.004846	0.029417		LLPH	188	0.000702	0.014169	0.025732
GTF2B	152	0.000202	0.005054	0.025783		NAA38	189	0.000717	0.014402	0.028961
DHRS7	153	0.000205	0.005096	0.041569		UFC1	190	0.000725	0.014454	0.04053
ATP5MG	154	0.000209	0.005147	0.052092		PPP1R15B	191	0.000727	0.014454	0.014335
SUN2	155	0.000216	0.005285	0.037116		CAP1	192	0.000761	0.015051	0.027381
TSC22D4	156	0.000223	0.005417	0.039886		ARHGAP25	193	0.000791	0.015555	0.021013
MYO1G	157	0.000225	0.005431	0.042219		CNPPD1	194	0.000796	0.015565	0.019209
SEM1	158	0.000233	0.005597	0.037093		AC103591.	195	0.000809	0.015743	0.0506
TRAF3IP3	159	0.000261	0.006222	0.036805		RAP1B	196	0.000824	0.015952	0.033242
TSTD1	160	0.000276	0.00651	0.030016		ASCL2	197	0.00084	0.016188	0.026551
RPUSD2	161	0.000276	0.00651	0.019885		ABCB1	198	0.000849	0.016271	0.017493
NPRL3	162	0.000319	0.007484	0.018019		IL2RG	199	0.000876	0.01671	0.020408
TAP1	163	0.000323	0.007494	0.023594		REX1BD	200	0.000883	0.016753	0.027785
FLNA	164	0.000324	0.007494	0.05629		IL10RA	201	0.00095	0.017906	0.030934
GPSM3	165	0.000344	0.007915	0.041199		C8orf59	202	0.000953	0.017906	0.027677
PTTG1	166	0.000382	0.008742	0.01792		MYH9	203	0.000966	0.018054	0.025371
BCL2	167	0.000389	0.008846	0.015815		TMEM59	204	0.000996	0.018532	0.033148
PRR13	168	0.000397	0.008929	0.047138		RAB11FIP5	205	0.001004	0.018536	0.018148
ANXA2	169	0.000398	0.008929	0.027176		DDX5	206	0.001006	0.018536	0.051973
CYC1	170	0.000411	0.009174	0.031275		NDUFB8	207	0.001022	0.018731	0.038704
MFSD10	171	0.000413	0.009174	0.034536		MAP2K2	208	0.001033	0.01884	0.028169
RBCK1	172	0.000452	0.009963	0.024697		PMPCA	209	0.001047	0.019018	0.016097
COX8A	173	0.000463	0.010162	0.051891		CD8B	210	0.001101	0.019893	0.011913
LAT	174	0.000468	0.010204	0.022452		AATF	211	0.001113	0.020026	0.018547
CD47	175	0.000476	0.010319	0.037849		MAP2K3	212	0.00113	0.020163	0.020866
LAMTOR1	176	0.000479	0.010319	0.036407		PEF1	213	0.001132	0.020163	0.018836
SNX17	177	0.000481	0.010319	0.021106		APBB1IP	214	0.001144	0.020294	0.013621

RHOB	215	0.001194	0.021076	0.025727		SVBP	252	0.002131	0.031987	0.019685
MYBL1	216	0.001219	0.02141	0.012055		HNRNPA0	253	0.002136	0.031987	0.037212
IRF3	217	0.001245	0.021772	0.019897		C11orf21	254	0.002141	0.031987	0.013146
MAGED2	218	0.001251	0.021781	0.009157		CNBP	255	0.00216	0.032144	0.043938
JAKMIP1	219	0.001272	0.022043	0.01608		LAMTOR4	256	0.002182	0.032234	0.034509
SELENOW	220	0.001301	0.022435	0.038332		SSBP4	257	0.002185	0.032234	0.027888
SH3BP1	221	0.001371	0.02355	0.020997		STX4	258	0.002197	0.032234	0.008999
IFNG	222	0.001385	0.023676	0.026263		MRPL34	259	0.0022	0.032234	0.020262
PRR7	223	0.001395	0.023686	0.015755		SPON2	260	0.002295	0.033424	0.006448
NDUFA2	224	0.001398	0.023686	0.034207		HNRNPD	261	0.002299	0.033424	0.028097
RCSD1	225	0.001418	0.023911	0.017857		VIM	262	0.002308	0.033438	0.031139
GLRX	226	0.001436	0.024106	0.025522		DGUOK	263	0.002342	0.033681	0.020743
DCK	227	0.001445	0.02415	0.017797		AP002387	264	0.002343	0.033681	0.020129
LSM14A	228	0.001474	0.024533	0.025616		PAXX	265	0.00238	0.034078	0.04122
FCMR	229	0.001524	0.025249	0.012957		SUB1	266	0.002525	0.036019	0.049462
NDUFA4	230	0.001534	0.025312	0.052094		COPE	267	0.002549	0.036228	0.020568
NDUFB10	231	0.001565	0.025559	0.033319		MAF	268	0.002561	0.036258	0.023665
GLUL	232	0.001571	0.025559	0.02187		FKBP8	269	0.002629	0.037087	0.028149
UQCR10	233	0.001575	0.025559	0.040571		TRBC2	270	0.002706	0.038029	0.034652
UBE2L6	234	0.00158	0.025559	0.025333		METTL23	271	0.002755	0.038313	0.020936
EIF2S2	235	0.001583	0.025559	0.015634		TERF2IP	272	0.002755	0.038313	0.02466
NPRL2	236	0.001601	0.025751	0.016323		POLR3GL	273	0.002756	0.038313	0.021398
ETNK1	237	0.00161	0.025788	0.019034		LSM5	274	0.002807	0.038878	0.021929
WDR55	238	0.001624	0.025872	0.016576		SLC2A4RG	275	0.002821	0.038923	0.016518
CETN2	239	0.001629	0.025872	0.013741		TAGLN2	276	0.002884	0.039437	0.024895
PSMD6	240	0.001642	0.025965	0.022477		CD74	277	0.002885	0.039437	0.061106
ARPP19	241	0.001687	0.026479	0.0295		NAA16	278	0.002889	0.039437	0.012265
COX7C	242	0.001688	0.026479	0.054564		TBX21	279	0.002962	0.040285	0.027123
ARPC1B	243	0.001708	0.026681	0.023587		EIF4A2	280	0.003098	0.041985	0.045198
ARID3B	244	0.001763	0.027383	0.017249		PRF1	281	0.003116	0.042034	0.004323
TBCB	245	0.001768	0.027383	0.026542		FASTK	282	0.003123	0.042034	0.02039
EIF3D	246	0.001801	0.027776	0.029266		ITGB2-AS1	283	0.003143	0.042146	0.016466
CCDC28A	247	0.001819	0.027954	0.016171		KLHDC2	284	0.00316	0.042233	0.017898
SNHG9	248	0.001832	0.028035	0.038664		PNRC2	285	0.003237	0.043097	0.033176
JPX	249	0.002021	0.030804	0.018961		MRPL57	286	0.003268	0.043361	0.029531
CTSW	250	0.002055	0.03119	0.06637		ATP5MC3	287	0.003426	0.045299	0.034975
IDH2	251	0.002073	0.031349	0.027356		RPP30	288	0.003467	0.0456	0.012125

PDIA6	289	0.003473	0.0456	0.025477		NAE1	296	0.003847	0.049321	0.019682
ZNF76	290	0.003488	0.045648	0.010874		ATP5F1B	297	0.003887	0.049633	0.027775
EIF1B	291	0.003556	0.046381	0.025863		ANAPC16	298	0.003899	0.049633	0.029001
H2AFZ	292	0.003584	0.046583	0.032107		HSPA6	299	0.003923	0.049633	0.010449
CKLF	293	0.003606	0.046703	0.019101		RAB11A	300	0.003924	0.049633	0.024263
CTBP1	294	0.003639	0.04697	0.018352		SYNGR1	301	0.003967	0.049964	0.009982
SNX6	295	0.003661	0.047095	0.011348		FBXO32	302	0.003976	0.049964	0.014393

Supplementary table 4. list of adapter 1 and adapters 2 (5' - 3') used for ATAC-seq library preparation

Ad1_noMX	AATGATACGGCGACCACCGAGATCTACACTCGTCGGCAGCGTCAGATGTG
Ad2.10_TAAGGCGA	CAAGCAGAAGACGGCATACGAGATCAGCCTCGGTCTCGTGGGCTCGGAGATGT
Ad2.17_TGCTGGGT	CAAGCAGAAGACGGCATACGAGATACCCAGCAGTCTCGTGGGCTCGGACATGT
Ad2.18_GAGGGGTT	CAAGCAGAAGACGGCATACGAGATAACCCCTCGTCTCGTGGGCTCGGAGATGT
Ad2.20_GTGTGGTG	CAAGCAGAAGACGGCATACGAGATCACCACACGTCTCGTGGGCTCGGAGATGT
Ad2.21_TGGGTTTC	CAAGCAGAAGACGGCATACGAGATGAAACCCAGTCTCGTGGGCTCGGAGATGT
Ad2.22_TGGTCACA	CAAGCAGAAGACGGCATACGAGATTGTGACCAGTCTCGTGGGCTCGGAGATGT
Ad2.23_TTGACCCT	CAAGCAGAAGACGGCATACGAGATAGGGTCAAGTCTCGTGGGCTCGGAGATGT
Ad2.24_CCACTCCT	CAAGCAGAAGACGGCATACGAGATAGGAGTGGGTCTCGTGGGCTCGGAGATGT

Supplementary Figure 1. Plasma TGF-β levels in B-CLL patients plasma vs Healthy controls